



**MONASH** University

---

# **THE ROLE OF FIBROBLAST GROWTH FACTOR RECEPTORS IN CANCER**

---

*Thesis in fulfilment of the requirement for the degree of*

**Doctor of Philosophy**



**NICOLE JING SIAN CHEW**

*B. Sc Biochemistry and Molecular Biology (First Class Honours)*

Department of Biochemistry and Molecular Biology

Biomedicine Discovery Institute

Faculty of Medicine, Nursing and Health Sciences

Monash University

December 2020

## **PREFACE**

---

**THIS PAGE HAS BEEN INTENTIONALLY LEFT BLANK**

## Copyright Notice

© Nicole Chew (2020). Except as provided in the Copyright Act 1968, this thesis may not be reproduced in any form without the written permission of the author.

I certify that I have made all reasonable efforts to secure copyright permissions for third-party content included in this thesis and have not knowingly added copyright content to my work without the owner's permission.

Nicole Jing Sian Chew

## General Declaration

This thesis is an original work of my research and contains no material which has been accepted for the award of any other degree or diploma at any university or equivalent institution and that, to the best of my knowledge and belief, this thesis contains no material previously published or written by another person, except where due reference is made in the text of the thesis.

*Signature:*

*Print Name:* Nicole Jing Sian Chew

*Date:* 11/12/2020



# Table of Contents

Title Page.....	i
Copyright Notice.....	iii
General Declaration.....	iv
Table of Contents.....	v
Declarations of Publication During Enrolment.....	vi
Acknowledgements.....	viii
Abstract.....	x
List of Publications.....	xiv
List of Figures.....	xv
List of Tables.....	xix
List of Abbreviations.....	xx

<b>Chapter 1:</b>	Literature Review .....	1
<b>Chapter 2:</b>	Materials and Methods .....	62
<b>Chapter 3:</b>	FGFR3 signaling and function in triple negative breast cancer .....	78
<b>Chapter 4:</b>	Evaluation of FGFR targeting in breast cancer through interrogation of patient-derived models .....	124
<b>Chapter 5:</b>	The FGFR4 signalling network and mechanisms of resistance to anti-FGFR4 therapy .....	166
<b>Chapter 6:</b>	Conclusions and Perspectives .....	206
<b>Appendix:</b>	Publication in Original Format .....	220

## Declarations of Publication During Enrolment

I hereby declare that this thesis contains no material which has been accepted for the award of any other degree or diploma at any university or equivalent institution and that, to the best of my knowledge and belief, this thesis contains no material previously published or written by another person, except where due reference is made in the text of the thesis.

This thesis includes 1 original paper published in a peer reviewed journal (Chapter 3) and 1 original paper ready for submission to peer reviewed journal (Chapter 4). The core theme of the thesis is FGFR signalling in cancer. The ideas, development and writing up of all the papers in the thesis were the principal responsibility of myself, the student, working within the Department of Biochemistry and Molecular Biology under the supervision of Prof. Roger Daly and Dr. Rachel Lee.

The inclusion of co-authors reflects the fact that the work came from active collaboration between researchers and acknowledges input into team-based research.

In the case of **Chapter 3**, my contribution to the **published** work involved the following:

Publication Title: FGFR3 signaling and function in triple negative breast cancer

Nature and % of student contribution	Co-author names, Nature and % of Co-author's contribution	Co-authors, Monash student Y/N
65%. Key ideas, experimental work, analysis of results, writing up	1) Elizabeth Nguyen, mass spectrometry analysis, 3% 2) Shih-Ping Su, assist with mass spectrometry, 1% 3) Karel Novy, assist with mass spectrometry, 2% 4) Howard Chan, cultured and harvested cells for mass spectrometry, 1% 5) Lan Nguyen, patient database analysis, 3% 6) Jennii Luu, advised on knockdown experiments, 1%	No

## PREFACE

---

	7) Kaylene Simpson, advised on knockdown experiments, 2%	
	8) Rachel Lee, supervision, 7%	
	9) Roger Daly, supervision, input into manuscript, 15%	

I have renumbered sections the published paper in order to generate a consistent presentation within the thesis.

**Student name:** Nicole Jing Sian Chew

**Student signature:**

**Date:** 11/12/2020

The undersigned hereby certify that the above declaration correctly reflects the nature and extent of the student's and co-authors' contributions to this work. In instances where I am not the responsible author, I have consulted with the responsible author to agree on the respective contributions of the authors.

**Main Supervisor name:** Roger Daly

**Main Supervisor signature:**

**Date:** 11/12/2020

## Acknowledgements

**This research was supported by a Departmental Scholarship.**

First and foremost, I would like to express my unending gratitude towards my supervisors Professor Roger Daly and Dr. Rachel Lee. Your guidance, knowledge, expertise, care and endearing support have made my PhD journey worthwhile. Thank you for the greatest opportunity of a lifetime, it has shaped me to be the person I am today. I am convinced that family surpasses blood relation and extends to the ones you hold dear.

To all the academics and staffs involved in my confirmation, mid-candidature and final review milestones: My sincerest thank you goes to Professor Colby Zaph, Associate Professor Peter Janes, Dr. Antonella Papa and Professor Mibel Aguilar, for your valuable input and time with the assessments.

To the post-docs, Ras, staff and students of the Daly: Dr. Hugh Ma, Dr. Mimi Nguyen, Dr. Kim Clark, Dr. Terry Lim, Dr. Brock Conley, Dr. Anderly Chueh, Mandy Theocharous, Ico Ma, Danielle Rika, Xue Yang, Jian Mei Hou, Yun Jian Wu, Chang Yuan Hu, Camila Ferezin, Sharon Varghese and Miguel Cruz. My deepest and warmest thank you goes to all of you for your guidance, knowledge and friendship. Our conversations and time spent together are the things I cherish the most. My heartfelt thank you to the lab members of Papa, Mitchell, Tiganis, Nguyen, Jans, Rosenbluh, Wong and Gras groups, for your friendship and love which tremendously brightened this whole experience.

To my loving family: Thank you for raising me, loving me, caring for me and supporting me through everything. I will never forget the great many sacrifices made to offer me a chance at a better life. I hope with all my heart that this thesis will bring you a sense of pride and joy.

To Shaun Ang, my partner, lover and best friend. Thank you for always believing in me and for comforting me especially during the times I felt the smallest. Thank you for your love,

## PREFACE

---

encouragement, patience, joyfulness, and invaluable support. Through it all, you were always by my side. I cannot imagine my life without you.

And above all, to my Lord and Saviour Jesus Christ, thank You for always making a way. I am forever in awe by Your mercy, grace, and faithfulness. You are the God who fights for me, the Lord of every victory. “For I know the plans I have for you, plans to prosper you and not to harm you, plans to give you hope and a future.” – *Jeremiah 29:11*

# Abstract

Cancer is a major global public health issue, presenting one of the largest clinical, social and economic burdens among all human diseases. Breast cancer accounts for a quarter of all cancers and ranks as the second most common cancer in the world. Breast cancer is a heterogeneous disease and global gene expression profiling has distinguished at least four intrinsic breast cancer subtypes that include luminal A, luminal B, HER2 enriched and basal-like, the latter also termed triple negative breast cancer (TNBC). TNBC accounts for 16% of breast cancers and represents an aggressive subtype that lacks targeted therapeutic options. As breast cancer research advances, new treatment strategies are being developed which include immunotherapy and other types of targeted therapy. In the TNBC subtype, there is a paucity of targeted treatments, currently limited to use of PARP inhibitors and immunotherapy for TNBC patients that exhibit mutant BRCA1 or are PD-L1 positive, respectively. Hence, new therapeutic targets need to be identified to build a platform for personalised treatment strategies to improve patient outcomes.

The fibroblast growth factor receptor (FGFR) family consists of four highly conserved transmembrane receptor tyrosine kinase members: FGFR1, FGFR2, FGFR3 and FGFR4. The investigation of FGFRs as oncogenic drivers and therapeutic targets in cancer made way for the development of therapeutic agents against the FGFR signalling pathway. Improved FGFR inhibitors have been developed to increase FGFR selectivity and minimise adverse side effects arising from multi-target kinase inhibitors. Despite successful outcomes of anti-FGFR therapy in patients, studies have identified the occurrence of resistance to anti-FGFR therapy over time.

Among the FGFR members, the roles of FGFR1 and FGFR2 in breast cancer have been investigated in considerable detail, while FGFR3 and FGFR4 remain poorly characterised in this setting. To thoroughly understand the role of FGFRs in breast cancer and implement new treatment strategies in the clinic, improved pre-clinical models are necessary. The use of breast cancer patient-derived models is a powerful tool to identify candidate therapeutic targets, as the tumour-stroma interactions and genetic and phenotypic heterogeneity of the primary

tumour is retained. Additionally, the identification of genetically altered FGFRs that are associated with drug response and novel targeted combinations involving FGFRs may improve patient outcomes.

In the first results chapter, the role of FGFR3 in TNBC was investigated in detail. Mass-spectrometry (MS)-based tyrosine phosphorylation profiling across a panel of TNBC cell lines was performed and identified aberrant activation of specific FGFRs, particularly FGFR3 in the SUM185PE cell line, which was evaluated as a potential therapeutic target. High FGFR3 expression and phosphorylation were detected in SUM185PE cells, which harboured both a FGFR3-TACC3 fusion and wildtype FGFR3. Low FGFR3 phosphorylation was detected in CAL51, MFM-223 and MDA-MB-231 cells. Characterisation of phosphorylated FGFR3 was performed using immunoprecipitation and Western blot analysis, which revealed that the FGFR3-TACC3 fusion protein contributed the majority of phosphorylated FGFR3. The localisation of FGFR3-TACC3 fusion and wildtype FGFR3 was also determined. Both FGFR3-TACC3 fusion and wildtype FGFR3 localised to the cytoplasm and plasma membrane, while the fusion also showed staining at the mitotic spindle in a small subset of cells. To characterise the functional role of FGFR3 *in vitro*, a selective FGFR1-3 inhibitor, PD173074 and siRNA knockdowns were used. Knockdown of the FGFR3-TACC3 fusion and wildtype FGFR3 in SUM185PE cells decreased phosphorylation of FRS2, AKT and ERK, and induced cell death, while knockdown of wildtype FGFR3 resulted in only a trend for decreased proliferation in these cells. Treatment with PD173074 significantly decreased FRS2, AKT and ERK activation, and reduced proliferation of SUM185PE cells. Additionally, phosphorylated-Rb and cyclin A were also decreased in PD173074-treated cells, while cleaved PARP was increased, indicating cell cycle arrest in G1 phases and apoptosis. In the CAL51, MFM-223 and MDA-MB-231 cells that exhibit low FGFR3 phosphorylation, knockdown of FGFR3 had no significant effect on cell proliferation. This suggests that marked FGFR3 activation is likely required to drive cancer progression, demonstrated in the SUM185PE cells. Lastly, the TCGA and METABRIC breast cancer patient datasets were interrogated to identify FGFR3 alterations and how they relate to breast cancer subtype and overall patient survival. The analysis revealed that increased FGFR3 expression in breast cancer was significantly associated with reduced overall survival, and that potentially oncogenic FGFR3 alterations, such as mutation and

amplification, occur in the TNBC and luminal subtypes, albeit rare. These results indicate that FGFR3-targeting may represent a therapeutic option for TNBC, however only for patients with oncogenic FGFR3 alterations, such as the FGFR3-TACC3 fusion.

The investigation of FGFRs was further expanded to breast cancer patient-derived models. In the second results chapter, global MS-based phosphotyrosine profiling was conducted across a panel comprising of 18 TNBC and 1 luminal B patient-derived xenografts (PDXs). This identified pronounced phosphorylation of specific FGFRs in particular PDXs. Western blotting analysis was also performed to characterise FGFR expression in the PDXs. In the TNBC group, PDX models ELX11-26 (high FGFR1 and FGFR2) and KCC\_P\_4043 (high FGFR2 activation) were selected for further interrogation with a FGFR-selective inhibitor, AZD4547. The HCI-009 luminal B PDX that exhibits high FGFR4 was also selected for interrogation with a FGFR4 inhibitor, BLU9931. An approach that integrated MS-based phosphoproteomics, RNA sequencing, whole exome sequencing and Western blotting was used to characterise the effects of specific FGFR inhibitors. Only the KCC\_P\_4043 PDX was extremely sensitive to AZD4547, and the integrated 'omic analysis revealed a novel FGFR2-SKI fusion that comprised the majority of FGFR2 fused to the C-terminal region of SKI. In HCI-009, treatment with BLU9931 significantly decreased tumour growth. Phosphoproteomic and transcriptomic analyses confirmed on-target action of AZD4547 and BLU9931 in the KCC\_P\_4043 and HCI-009 PDX models, respectively. Additionally, the TCGA and METABRIC breast cancer patient datasets were also interrogated. The analysis revealed that FGFR2 amplification, fusion or mutation occur in TNBC and other breast cancer subtypes, while FGFR4 overexpression and amplification occurred in all breast cancer subtypes, and is associated with poor prognosis. Lastly, a panel of patient-derived organoids (PDOs) was characterised and identified this a luminal A PDO, HBC22, that exhibited high FGFR4 expression. HBC22 was sensitive to BLU9931 treatment, which further highlights FGFR4 as a potential therapeutic target. In this chapter, the results highlight patient-derived models of human breast cancer as powerful platforms for therapeutic target identification and drug action analysis, and also specific FGFRs, including FGFR4, as targets for precision medicine.



## PREFACE

---

Continuing the focus on FGFR4, the final results chapter investigated how the FGFR4 signalling network is rewired and impacts sensitivity to FGFR4-selective inhibitors in TNBC and hepatocellular carcinoma (HCC). The TNBC cell line, MDA-MB-453, and HCC cell line, Hep3B were interrogated in this chapter. MDA-MB-453 cells express high levels of FGFR4 with activating FGFR4 mutation. Hep3B cells overexpress FGF19, the ligand of FGFR4, which is an oncogenic driver identified by genomic and functional analyses in HCC. MDA-MB-453 and Hep3B cells were treated with selective FGFR4 inhibitors BLU9931 and H3B-6527, respectively. The key aim of this chapter was to identify upregulated receptor tyrosine kinases (RTKs) in FGFR4-inhibitor resistant cells and suppress their activity to discover novel therapeutic combinations as improved strategies for targeted therapy. FGFR4-inhibitor resistant cells were generated by culturing cells in the presence of drug for at least 5 months, until resistant colonies formed. MDA-MB-453 and Hep3B cells were also treated short-term with their respective FGFR4 inhibitor to identify short-term resistance mechanisms. In the short-term FGFR4 inhibitor treatment setting, upregulation of activated signalling proteins AKT and ERK was identified in MDA-MB-453 and Hep3B cells, respectively. These results highlight that the FGFR4 signalling network is rewired to overcome inhibition of FGFR4. The corresponding combination treatments using a FGFR4 inhibitor and AKT or MEK inhibitors resulted in a greater decrease in cell proliferation, highlighting co-targeting FGFR4 and AKT/ERK as novel treatment strategies in TNBC and HCC. In terms of upregulated RTKs, ErbB2 exhibited a marked increase after long-term BLU9931 treatment in MDA-MB-453 cells and development of drug resistance. The subsequent co-targeting of FGFR4 and ErbB2 significantly decreased cell proliferation, suggesting a switch in receptor signalling. These results indicate that the identification and characterisation of upregulated RTKs occurring after inhibition of FGFR is important to reveal mechanisms of resistance to targeted therapy and highlights promising treatment strategies for clinical trials.

Overall, the findings in this thesis support targeting FGFRs as a precision medicine approach for specific cancers. Particularly, the identification of novel oncogenic FGFR alterations (e.g., FGFR2-SKI fusion) that drive cancer progression provide therapeutic targets and associated companion biomarkers, and identification of novel targeted combinations involving FGFR4 can provide potential treatment strategies for particular breast cancer subgroups and HCC.

## List of Publications

1. **Nicole J Chew**, Elizabeth V Nguyen, Shih-Ping Su, Karel Novy, Howard C Chan, Lan K Nguyen, Jennii Luu, Kaylene J Simpson, Rachel S Lee and Roger J Daly (2020) FGFR3 signaling and function in triple negative breast cancer, *Cell Communication and Signaling* 18(1): p. 13 (Impact Factor = 5.020)
2. Mona Tafreshi, Jyeswei Guan, Rebecca J Gorrell, **Nicole J Chew**, Yue Xin, Virginie Deswaerte, Manfred Rohde, Roger J Daly, Richard M Peek Jr, Brendan J Jenkins, Elizabeth M Davies, Terry Kwok (2018) Helicobacter pylori Type IV Secretion System and Its Adhesin Subunit, CagL, Mediate Potent Inflammatory Responses in Primary Human Endothelial Cells, *Frontiers in Cellular and Infection Microbiology* 8: p. 22 (Impact Factor = 4.300)

# List of Figures

## Chapter 1

Fig. 1.1	The hallmarks of cancer
Fig. 1.2	Cancer estimates according to GLOBOCAN 2012
Fig. 1.3	Current immunotherapeutic strategies against breast cancer
Fig. 1.4	An immunotherapy approach utilising immune checkpoint inhibitors
Fig. 1.5	Driver protein kinases identified by genomic studies and their corresponding genetic alterations in cancer
Fig. 1.6	PI3K-AKT signalling pathway
Fig. 1.7	MAPK-ERK signalling pathway
Fig. 1.8	JAK-STAT signalling pathway
Fig. 1.9	Schematic of FGFR structure
Fig. 1.10	The FGF ligand family
Fig. 1.11	FGFR1 phosphorylation sites
Fig. 1.12	FGFR structure and signalling pathways

## Chapter 3

Fig. 3.1	FGFR expression and phosphorylation signature in TNBC cell lines as determined by MS-based tyrosine phosphorylation profiling
Fig. 3.2	Characterisation of FGFR1-4 expression in a panel of 11 TNBC cell lines
Fig. 3.3	Schematic of FGFR3-TACC3 fusion protein adapted from Shaver <i>et al.</i> (2016)
Fig. 3.4	Characterisation of FGFR3 phosphorylation in the SUM185PE cell line
Fig. 3.5	Localisation of FGFR3-TACC3 fusion and wildtype FGFR3 by immunofluorescent staining in SUM185PE cells
Fig. 3.6	Immunofluorescent staining of mitotic SUM185PE cells with the FW FGFR3 antibody

Fig. 3.7	Effect of FGFR3 knockdown on downstream signalling in SUM185PE cells
Fig. 3.8	Effect of FGFR3 knockdown on SUM185PE cell proliferation
Fig. 3.9	Dose dependent effect of the FGFR inhibitor PD173074 on FGFR3 downstream signalling pathways in the SUM185PE cell line
Fig. 3.10	Effect of PD173074 on proliferation and apoptosis in SUM185PE cells
Fig. 3.11	Expression of FGFR3 in TNBC cell lines exhibiting low-moderate FGFR3 phosphorylation
Fig. 3.12	Function of FGFR3 in TNBC cell lines exhibiting low-moderate FGFR3 phosphorylation
Fig. 3.13	FGFR3 alterations in human breast cancer
Supp. Fig. 3.1	Interactions of proteins exhibiting specific tyrosine phosphorylation specific to SUM185PE cell line using STRING software

## Chapter 4

Fig. 4.1	FGFR expression and phosphorylation signature in TNBC cell lines as determined by MS-based tyrosine phosphorylation profiling
Fig. 4.2	Effect of FGFR1-3 inhibitor AZD4547 on the KCC_P_4043 PDX model
Fig. 4.3	Effect of FGFR1-3 inhibitor AZD4547 on the ELX11-26 PDX model
Fig. 4.4	Effect of FGFR1-3 inhibitor AZD4547 on the HCI-016 PDX model
Fig. 4.5	Identification of the FGFR2-SKI fusion in the KCC_P_4043 model
Fig. 4.6	Sanger sequencing of the KCC_P_4043 PDX model PCR product
Fig. 4.7	Characterisation of the FGFR2-SKI fusion in the KCC_P_4043 PDX model
Fig. 4.8	Effect of FGFR4 inhibitor BLU9931 on the HCI-009 PDX model
Fig. 4.9	FGFR2 and FGFR4 alterations in breast cancer patients.
Fig. 4.10	Immunohistochemical staining for FGFR4 on breast cancer specimens.
Fig. 4.11	The association of FGFR4 alterations with overall survival in breast cancer patients
Fig. 4.12	Characterization of FGFR4 expression in human breast cancer organoids.

Fig. 4.13	Effect of the FGFR4 inhibitor BLU9931 on organoid growth.
Supp. Fig. 4.1	Effects on site-selective protein phosphorylation as determined by MS-based phosphoproteomics
Supp. Fig. 4.2	Analysis of FGFR2 in the KCC_P_4043 using SNP arrays
Supp. Fig. 4.3	SNP arrays showing FGFR2 alterations in specific PDX
Supp. Fig. 4.4	SNP arrays showing FGFR1 alterations in specific PDX
Supp. Fig. 4.5	Effects on site-selective protein phosphorylation as determined by MS-based phosphoproteomics
Supp. Fig. 4.6	SNP arrays showing FGFR4 alterations in specific PDX

## **Chapter 5**

Fig. 5.1	Dose dependent effect of the FGFR4 inhibitor BLU9931 on FGFR4 downstream signalling pathways in the MDA-MB-453 cell line
Fig. 5.2	Effect of BLU9931 on proliferation in MDA-MB-453 and MDA-MB-468 cell lines
Fig. 5.3	Time course analysis of 10 nM FGFR4 inhibitor BLU9931 on FGFR4 downstream signalling pathways in the MDA-MB-453 cell line
Fig. 5.4	Time course analysis of 10 nM FGFR4 inhibitor H3B-6527 on FGFR4 downstream signalling pathways in the MDA-MB-453 cell line
Fig. 5.5	Dose dependent effect of PI3K- $\alpha$ inhibitor BYL719, pan-PI3K inhibitor BKM120 and AKT inhibitor MK2206 on AKT phosphorylation in the MDA-MB-453 cell line
Fig. 5.6	Dose dependent effect of the FGFR4 inhibitor BLU9931 in combination with PI3K- $\alpha$ inhibitor BYL719 or pan-PI3K inhibitor BKM120 on AKT phosphorylation in the MDA-MB-453 cell line
Fig. 5.7	Dose dependent effect of the FGFR4 inhibitor BLU9931 and AKT inhibitor MK2206 on AKT phosphorylation in the MDA-MB-453 cell line
Fig. 5.8	Effect of FGFR4 inhibitor BLU9931, in combination with PI3K- $\alpha$ inhibitor BYL719, pan-PI3K inhibitor BKM120 or AKT inhibitor MK2206 in parental MDA-MB-453 cells

Fig. 5.9	Effect of BLU9931 on parental MDA-MB-453 and long-term BLU9931-treated MDA-MB-453 cells
Fig. 5.10	Identification of upregulated RTKs in parental MDA-MB-453 after 24 h BLU9931 treatment and in long-term BLU9931 MDA-MB-453 cells
Fig. 5.11	Identification of upregulated RTKs in parental MDA-MB-453 cells after 24 h BLU9931 treatment and in long-term BLU9931 MDA-MB-453 cells
Fig. 5.12	Comparison of upregulated RTKs and downstream signalling in BLU9931-treated MDA-MB-453 parental cells and long-term BLU9931 cells
Fig. 5.13	Effect of co-targeting ErbB2 and FGFR4 on proliferation in long-term BLU9931 MDA-MB-453 cells using Lapatinib and BLU9931
Fig. 5.14	Effect of the FGFR4 inhibitor H3B-6527 on FGFR4 downstream signalling and proliferation in the Hep3B cell line
Fig. 5.15	Time course analysis of 50 nM FGFR4 inhibitor H3B-6527 on FGFR4 downstream signalling pathways in the Hep3B cell line
Fig. 5.16	Effect of FGFR4 inhibitor H3B-6527, in combination with MEK inhibitor Trametinib in parental Hep3B cells
Fig. 5.17	Effect of H3B-6527 on parental Hep3B and long-term H3B-6527 Hep3B cells
Fig. 5.18	Identification of upregulated RTKs in parental Hep3B after 24 h H3B-6527 treatment and in long-term H3B-6527 Hep3B cells
Fig. 5.19	Identification of upregulated RTKs in parental Hep3B treated with H3B-6527 for 24 h and H3B-6527-resistant Hep3B cells
Fig. 5.20	FGFR4 kinase domain analysis for gatekeeper mutations

## List of Tables

### Chapter 1

Table 1.1	Genetic alterations in FGFRs reported in human tumours
Table 1.2	Current FGFR inhibitors in clinical trials

### Chapter 2

Table 2.1	Commonly used buffers and solutions.
Table 2.2	Primary and secondary antibodies used in Western blotting.
Table 2.3	FGFR2-SKI fusion primers.
Table 2.4	FGFR4 kinase domain primers.
Table 2.5	Polymerase chain reaction conditions.

### Chapter 3

Supp. Table 3.1	Quantifiable FGFR tyrosine phosphorylated peptide expression (log2) identified across 24 TNBC cell lines
Supp. Table 3.2	Quantifiable tyrosine phosphorylated peptide expression (log2) specific to SUM185PE cell line

### Chapter 4

Table 4.1	Transcriptome analysis of enriched pathways downregulated in the AZD4547 treated KCC_P_4043 PDX using the KEGG and Reactome database
Supp. Table 4.1	SNVs in KCC_P_4043 tumour

## List of Abbreviations

ATCC	American Type Culture Collection
CAR-T	Chimeric antigen receptor T cell
CTL	Cytotoxic T lymphocytes
DDA	Data-dependent acquisition
DMEM	Dulbecco's modified eagle's medium
DMSO	Dimethyl sulfoxide
DSMZ	Deutsche Sammlung von Mikroorganismen und Zellkulturen
ECL	Enhanced chemiluminescence
EDTA	Ethylenediaminetetraacetic acid
EGFR	Epidermal growth factor receptor
ER	Estrogen receptor
ERK	Extracellular signal-regulated kinases
FDR	False discovery rate
FFPE	Formalin-fixed paraffin embedded
FGFR	Fibroblast growth factor receptor
FRS2	FGFR substrate 2
Gab	GRB2-associated binding protein
GRB2	Growth factor receptor-bound protein 2
HCC	Hepatocellular carcinoma
HER	Human epidermal growth factor receptor
HRM-DIA	Hyper-reaction monitoring data-independent acquisition
ICB	Immune checkpoint blockade
Ig	Immunoglobulin
IHC	Immunohistochemistry
IL	Interleukin
INF $\gamma$	Interferon gamma
IP3	Inositol triphosphate



---

## PREFACE

---

IR	Insulin receptor
iRT	indexed Retention Time
JAK	Janus kinase
LC-MS/MS	Liquid chromatography-tandem mass spectrometry
LT	Long-term
MAPK	Mitogen-activated protein kinase
METABRIC	Molecular Taxonomy of Breast Cancer International Consortium
MHC	Major histocompatibility complex
MKP3	MAPK phosphatase 3
MS	Mass spectrometry
NSCLC	Non-small cell lung carcinoma
NSG mouse	NOD scid gamma mouse
PARP	Poly ADP ribose polymerase
PBS	Phosphate-buffered saline
PD-1	Programmed cell death receptor 1
PDGFR	Platelet-derived growth factor receptor
PDK	Phosphoinositide-dependent kinase
PD-L1	Programmed cell death ligand 1
PDO	Patient-derived organoid
PDX	Patient derived-xenograft
PH	Pleckstrin homology
PI3K	Phosphoinositide 3-kinase
PIAS	Protein inhibitor of activated STAT
PIP2	Phosphatidylinositol-4,5-biphosphate
PIP3	Phosphatidylinositol-3,4,5-triphosphate
PKB	Protein kinase B
PKC	Protein kinase C
PLC- $\gamma$	Phospholipase C $\gamma$
PMSF	Phenylmethane sulfonyl fluoride
PR	Progesterone receptor

---

## PREFACE

---

PTB	Phosphotyrosine-binding
PTEN	Phosphatase and tensin homolog
PTPs	Protein tyrosine phosphatases
pY	Phosphorylated tyrosine
RPMI	Roswell Park Memorial Institute
RTK	Receptor tyrosine kinase
RT-PCR	Reverse transcription polymerase chain reaction
SDS-PAGE	Sodium dodecyl sulphate–polyacrylamide gel electrophoresis
Sef	Similar expression to FGF
Ser/Thr	Serine/threonine
SERD	Selective estrogen receptor downregulator
SERM	Selective estrogen receptor modulator
SH2	Src-homology 2
SNP	Single nucleotide polymorphism
SNP	Single nucleotide polymorphism
SOCS	Suppressors of cytokine signalling
ST	Short-term
STAT	Signal transducer and activation of transcription
SynDISCO	Synergistic Drug Combination Discovery
TACC	Transforming acidic coiled-coil containing protein
TBS	Tris-buffered saline
TBS-T	Tris-buffered saline with Tween 20
TCGA	The cancer genome atlas
TGF $\beta$	Transforming growth factor beta
TNBC	Triple negative breast cancer
TYK2	Tyrosine kinase 2
VEGFR	Vascular endothelial growth factor receptor
WB	Western blot
WES	Whole exome sequencing

---

# **CHAPTER 1**

## **LITERATURE REVIEW**

---

# Chapter 1: Literature Review

1.1 Overview of Cancer .....	3
1.2 Breast Cancer .....	4
1.2.1 Subtypes .....	5
1.3 Treatments for breast cancer .....	6
1.3.1 Surgery, radiotherapy and chemotherapy .....	6
1.3.2 Immunotherapy .....	7
1.3.3 Hormone therapy .....	10
1.3.4 Other types of targeted therapy .....	12
1.4 Signal Transduction via the Human Kinome in Cancer .....	13
1.4.1 Receptor Tyrosine Kinases .....	15
1.4.2 PI3K-AKT signalling pathway .....	15
1.4.3 MAPK-ERK signalling pathway .....	17
1.4.4 JAK-STAT signalling .....	19
1.5 Fibroblast growth factor receptors (FGFRs) .....	21
1.5.1 Structure of receptors and ligands .....	21
1.5.2 Regulation of FGFR signalling pathways .....	23
1.5.3 Aberrant FGFR signalling in cancer .....	27
1.5.4 Overview of FGFR inhibitors .....	31
1.5.5 Rewiring of FGFR signalling pathways .....	34
1.5.6 Combination drug therapy .....	34
1.6 Research Objectives .....	35
1.7 Thesis Outline .....	35
1.8 References .....	39

## **1.1 Overview of Cancer**

Cancer is a major global public health problem, representing one of the largest clinical, social and economic burden among all human diseases [1]. It is one of the main causes of death before the age of 70 years in 113 out of 172 countries, according to estimates from the World Health Organisation in 2015 [2]. The incidence and mortality of cancer are rapidly growing, with estimated worldwide numbers expected to increase to more than 9 million cases and at least 5 million deaths per year by 2030 due to the growth and aging of the population [3, 4]. Globally, lung cancer is the most commonly diagnosed cancer (2,093,876 cases, 11.6% of total cases), followed by breast cancer (11.5%), colorectal cancer (10.2%), prostate cancer (7.1%), and non-melanoma skin cancer (5.8%) [2]. Cancer survival is increasing as a result of progressing medical research and advances made in early detection and treatment [5]. Despite this improvement, there remain many issues yet to be addressed to improve cancer therapy.

Cancer is a genetic disease that stems from the accumulation of genetic aberrations that trigger the transformation of normal cells to become malignant [6]. Hanahan and Weinberg (2011) have provided a logical framework that constitutes the hallmarks of cancer for understanding the mechanisms underpinning this disease [7] (Fig. 1.1). These core hallmarks are: sustaining proliferative signalling, evading growth suppressors, enabling replicative immortality, activating invasion and metastasis, inducing angiogenesis, resisting cell death, deregulating cellular energetics and avoiding immune destruction; and enabling characteristics are tumour-promoting inflammation and genome instability and mutation [7] (Fig. 1.1).



**Figure 1.1: The hallmarks of cancer.** The illustration highlights the 10 biological tumour capabilities acquired during the development of human cancers. Reproduced from [7]. Copyright (2011) with permission from Elsevier.

## 1.2 Breast Cancer

Breast cancer accounts for 25% of all cancers and ranks as the second most common cancer in the world [3]. It is the most commonly diagnosed cancer in women, with more than 2 million new cases and more than 600,000 deaths in 2018 [8]. Breast cancer is the leading cause of cancer-related death among women in less developed regions but ranked second in more developed regions after lung cancer (Fig. 1.2) [3].

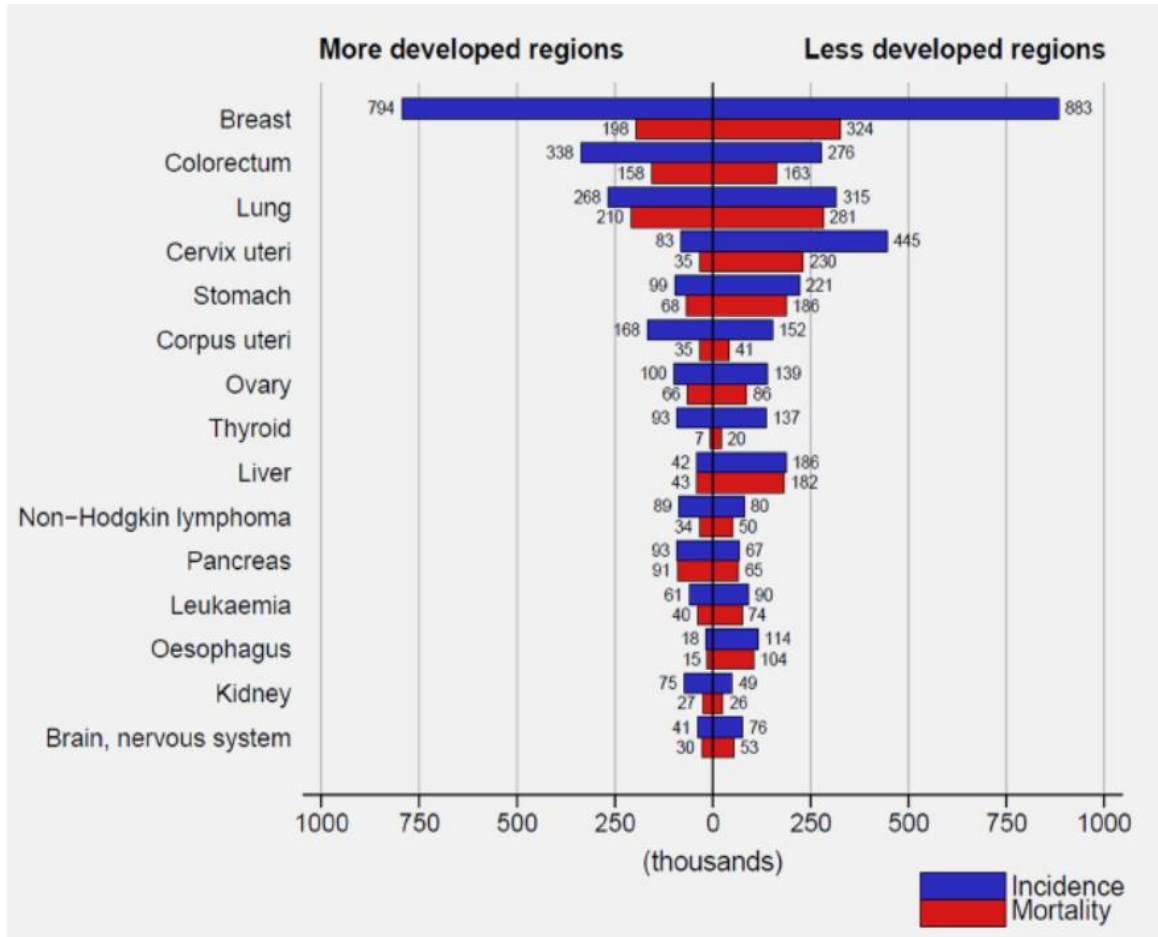


**Figure 1.2: Cancer estimates according to GLOBOCAN 2012.** Estimated numbers in thousands of new cancer cases (incidence) and deaths (mortality) in women in more developed and less developed regions of the world in 2012. Reproduced from [3]. Copyright (2015) with permission from John Wiley and Sons.

### 1.2.1 Subtypes

Breast cancer is a heterogenous disease and characterised into several subtypes, which is important to assess patient prognosis and stratification for effective targeted therapies [9]. The traditional approach of using immunohistochemistry (IHC) markers such as estrogen receptor (ER), progesterone receptor (PR) and human epidermal growth factor receptor 2 (HER2), with clinicopathological variables such as tumour size, tumour grade and nodal involvement are used for patient prognosis and management [10]. However, these classic parameters are not sufficient to effectively determine the best course of treatment for individual patients. Breast

cancer develops through accumulation of both genomic and epigenomic aberrations, resulting in cancer pathophysiology such as evading cell death, uncontrolled proliferation, increased motility and angiogenesis, all leading to its progression [11, 12]. Precision medicine can improve the prediction of patients' responses to therapy, where specific molecular or cellular features involved in cancer progression represent potential targets for treatment [13].

Global gene expression has distinguished at least four intrinsic breast cancer subtypes that include luminal A, luminal B, HER2 enriched and basal-like [10]. The luminal A and B groups are positive for ER but distinguishable primarily by better prognosis in the luminal A group and the expression of proliferation related genes such as Ki67 in the luminal B group [10, 14]. The HER2 enriched group is characterised by overexpression of HER2, while the basal-like group is characterised by the lack of ER, PR and HER2 expression, also known as “triple negative breast cancer” (TNBC) [15-17]. The luminal A group has the best prognosis, while the basal-like group has the worst prognosis among the 4 breast cancer subtypes [14]. In a cohort study of 1,601 breast cancer patients, the TNBC patient group displayed the poorest clinical outcome, showing worst overall survival, relapse-free survival and were more likely to experience early recurrence when compared to other subtypes of breast cancer [18].

## **1.3 Treatments for breast cancer**

Treatments for breast cancer aim to abolish cancer progression and reduce the risk of cancer metastasis and recurrence. The traditional treatment options for breast cancer patients include surgery, chemotherapy and radiotherapy. As breast cancer research progressed, new treatment strategies were developed which include immunotherapy, hormone therapy and other types of targeted therapy. These are administered to patients based on the breast cancer subtype, tumour stage and grade, as well as expression of specific predictive biomarkers.

### **1.3.1 Surgery, radiotherapy and chemotherapy**

At the present time, surgical removal of breast cancers has advanced to minimize the long-term cosmetic and functional sequelae of the treatment [19]. The standard two approaches of



either mastectomy or lumpectomy by an excision plus radiation, have demonstrated equivalent relapse-free and patient overall survival [20]. Additionally, axillary surgery, which is the removal of neighbouring lymph nodes are often performed during the breast cancer surgery to determine and remove potential metastasised cancer. Radiation therapy is often delivered to eliminate any remainder cancer cells after the surgery. Neoadjuvant chemotherapy was initially used to render locally advanced, inoperable breast tumour resectable [21]. Recently, the use of neoadjuvant chemotherapy has demonstrated an increased in the patient's eligibility for breast-conserving therapy without compromising long-term outcomes [22].

Chemotherapy is the use of a cocktail of cytotoxic drugs (e.g. Paclitaxel, Docetaxel and Doxorubicin) that eliminates highly proliferative cancer cells [23]. Chemotherapy is generally recommended to high-risk patients. In a meta-analysis, the strategy of utilising adjuvant chemotherapy reduced breast cancer recurrence and mortality, and of greater magnitude in hormone receptor-negative patients [24]. In some TNBC patients, the use of chemotherapy is only effective within the first 3 years of treatment before the patient develops chemoresistance [25]. Since chemotherapy targets all cells within the body, the side effects are inevitable. For example, Paclitaxel is a microtubule-interfering cancer drug that also results in severe neurotoxicity [26]. Other common side effects in chemotherapy-administered breast cancer patients include premature menopause (which increases risk of osteoporosis), cognitive dysfunction, chronic fatigue and increased likelihood to infections [27, 28]. Side effects of radiotherapy and surgery include lymphedema, tightness in the shoulders or chest wall, and chronic pain [29, 30].

### **1.3.2 Immunotherapy**

Specific cell types in the immune system, CD4<sup>+</sup> and CD8<sup>+</sup> T cells, eliminate tumours by recognising tumour antigens presented by the major histocompatibility complex (MHC) [31]. However, most tumours evolve to evade the immune system and inflammation, this being an additional hallmark of cancer progression [7]. Immunoediting is characterised by the evolving interaction between the tumour and the immune system [32]. In early breast tumour development, acute antitumour inflammatory responses result in the secretion of antitumour

cytokines interleukin-2 (IL-2) and interferon gamma (INF $\gamma$ ), and antitumour-directed B-cell-derived factors, immunoglobulins (Igs). These activate tumour inhibitory responses in innate immune cells and cytotoxic T lymphocytes (CTLs), leading to tumour rejection [33].

However, this imposed pressure leads to selection of tumour cell variants that escape the immune response. The immunoediting process reaches a state of equilibrium, followed by a switch from acute to chronic inflammation at the tumour site. This involves the accumulation of regulatory T cells, Th2 cells and activated B cells, and secretion of pro-growth cytokine factors (IL-4, IL-6, IL-10, IL-13, Igs and transforming growth factor beta; TGF $\beta$ ) that promotes pro-tumour responses in the innate immune cells and inactivation of CTL cytotoxicity, favouring tumour promotion [33]. This step establishes a complex tumour microenvironment consisting of suppressive immune cells and stromal cells, leading to tumour growth and metastasis that is unchecked by the immune system [33].

Immunotherapy is an approach that utilises cellular components of the immune system to stimulate and enhance the anti-tumour immune response. Current immunotherapeutic strategies include cancer vaccines, immune checkpoint blockade (ICB), adoptive cell therapies, chimeric antigen receptor T cell (CAR-T) therapy that involves genetic modification of T cells to better recognise tumour antigens, and combination therapy that involves chemotherapeutic agents combined with checkpoint inhibition (Fig. 1.3) [34]. Among these immunotherapy approaches, cancer vaccines, monoclonal antibodies and CAR-T are the most clinically advanced [35, 36].

Cancer vaccines composed of pathogen-associated molecular patterns and specific antigen are used to induce a specific T-cell response against the target cancer [35, 37]. The vaccine is injected into the patient's skin and activates resting dendritic cells, which migrate to lymph nodes and present antigens complexed to MHC for recognition, ultimately enhancing the anti-tumour response [37]. However, most cancer vaccines have failed to induce objective tumour shrinkage in patients, while more clinical success has been observed with blocking immune checkpoints.

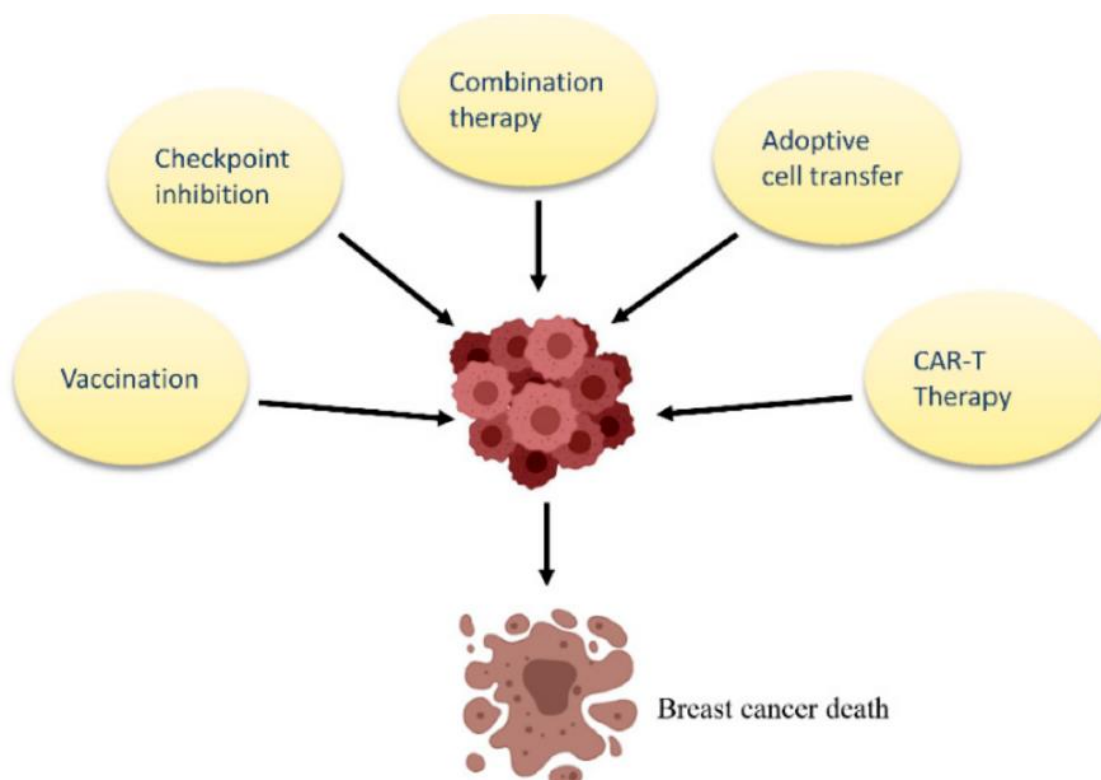


**Figure 1.3: Current immunotherapeutic strategies against breast cancer.** These include vaccination, checkpoint inhibition, combination therapy, adoptive cell transfer and CAR-T therapy. Adapted from [34]. Open access under the terms of the Creative Common CC BY license.

Immune checkpoints are down-regulators of the immune system to prevent over-exuberant responses [35]. In the chronic inflammation stage, immune checkpoint molecules are upregulated on tumour and immune cells, and immune-suppressive metabolic pathways are activated [38, 39]. Clinical trials of several cancer types showed that blocking immune checkpoint molecules with monoclonal antibodies is a viable clinical strategy to induce tumour shrinkage (Fig. 1.4) [40, 41]. Programmed cell death receptor 1 (PD-1) is an inhibitory immune checkpoint receptor expressed on immune cells such as activated T cells and its ligand PD-L1 is an immunosuppressive signal that is upregulated in tumour cells in response to proinflammatory signals such as IFN $\gamma$  (Fig. 1.4) [42].

Atezolizumab is an ICB, monoclonal antibody drug targeting PD-1, and the first immunotherapy approved by the FDA in combination with Paclitaxel for the treatment of

metastatic TNBC patients that are PD-L1 positive [43]. Another anti-PD-1 antibody, Pembrolizumab, was evaluated in a clinical trial and reported an objective response rate of 18.5% in TNBC patients [44]. Pembrolizumab has also recently received FDA-approval for locally recurrent, unresectable or metastatic TNBC (NCT02819518). Several clinical trials are currently investigating strategies to enhance the response to Atezolizumab in combination with chemotherapy (NCT03498716, NCT03371017) or radiotherapy to facilitate antigen release and tumour-specific immune responses [45, 46]. The HER2 and TNBC subtypes are more likely to harbour PD-L1 expression than the luminal subtypes [47, 48]. Therefore, the combination of ICB with targeted therapies such as Traztuzumab is also being investigated in HER2 metastatic breast cancer (NCT03199885).

### 1.3.3 Hormone therapy

The luminal A (ER+, PR+) and luminal B (ER+, PR-) subtypes represent approximately 50-60% and 15-20% of all breast cancer cases, respectively [49]. The treatments for ER+ breast cancer patients include selective estrogen receptor modulators (SERMs) such as Tamoxifen [50], selective estrogen receptor downregulators (SERDs) such as Fulvestrant [51], and aromatase inhibitors that block estrogen production [52].

Tamoxifen is a non-steroidal, ER antagonist that was FDA approved in the 1970s for premenopausal women with advanced metastatic breast cancer [53]. Since then, Tamoxifen has demonstrated effective treatment in early breast cancer, *in situ* ductal carcinoma and the chemoprevention of breast cancer [53]. Tamoxifen competitively binds at the ligand binding sites of ER, however, also has agonist properties that increases the risk of endometrial cancer [54, 55]. Despite many patients responding well to Tamoxifen, resistance may emerge [56], posing a serious clinical challenge. An alternative approach of utilising aromatase inhibitors (AIs) to block the production of estrogen was developed and demonstrated to be more effective and better tolerated than Tamoxifen [52, 57].

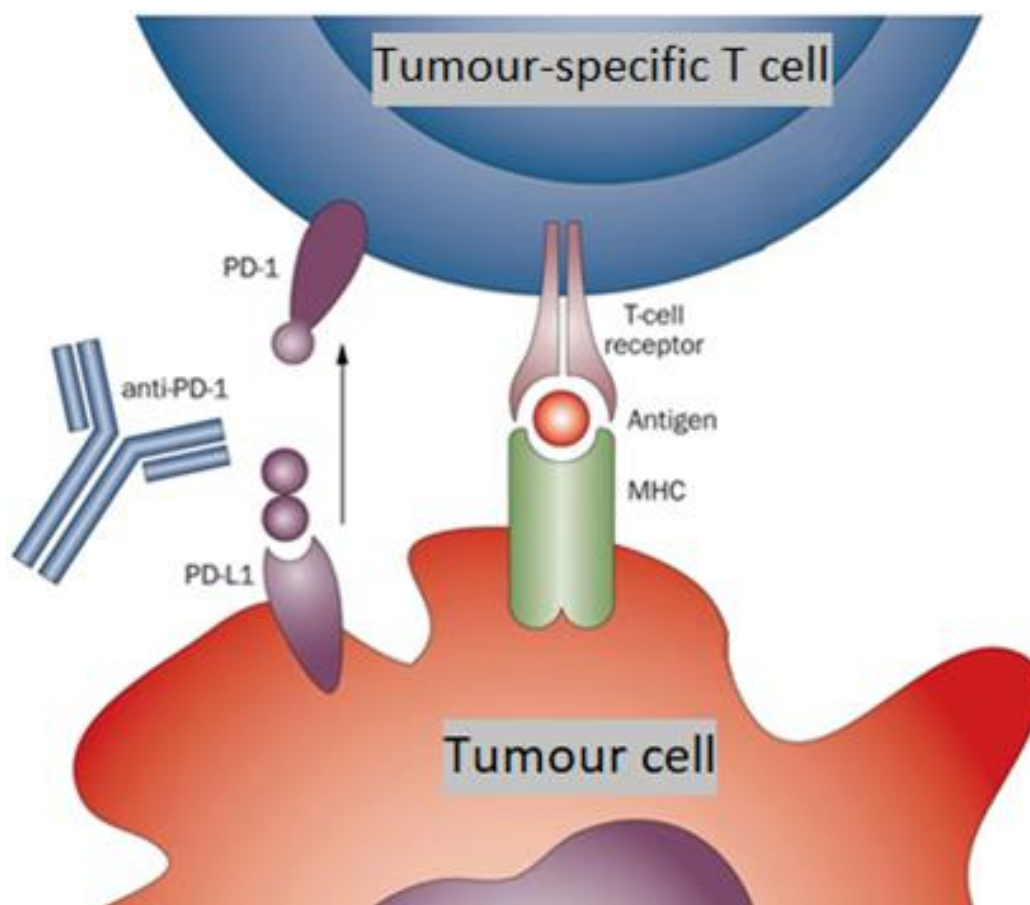


**Figure 1.4: An immunotherapy approach utilising immune checkpoint inhibitors.** The interaction of PD-1 on T cells binding to its ligand PD-L1 on tumour cells mediates a major immune checkpoint. Anti-PD-1 (e.g. Atezolizumab and Pembrolizumab) is used to inhibit PD-1 to reduce cancer progression. Reproduced from [35]. Copyright (2013) with permission from Springer Nature.

Anastrozole, Letrozole and Exemestane are three AIs that are FDA-approved for post-menopausal breast cancer patients in the adjuvant and metastatic settings [58]. However, the similar modes of action between SERMs and AIs have resulted in cross-resistance, hence new treatments through different mechanisms are required [59].

Fulvestrant is a steroidal antagonist of ER and one of the most widely used SERDs with no agonist effects [59]. It has a different chemical structure and a greater binding affinity than Tamoxifen to ER, and impairs receptor dimerisation and nuclear localisation [59]. Fulvestrant also accelerates the degradation of ER protein, leading to complete inhibition of estrogen

signalling [59]. Fulvestrant is approved for treatment in ER-positive metastatic breast cancer patients whose disease progressed following Tamoxifen or AIs [60, 61]. Currently, there are many ongoing clinical trials evaluating Fulvestrant as a single agent or in combination with immunotherapy agents (NCT03393845), other hormone therapy agents (NCT04214288) or targeted therapy (NCT04033172) in breast cancer.

### 1.3.4 Other types of targeted therapy

In addition to the ER and checkpoint receptors, other ‘actionable’ proteins are upregulated in cancer and represent potential therapeutic targets. This has led to the development of novel therapies to inhibit target activity or selectively kill cancer cells expressing the target and reduce cancer progression. Monoclonal antibodies and kinase inhibitors are common targeted therapies used in the treatment of cancer [62]. This will be visited in detail later in the chapter.

For example, the HER2 (also known as ErbB2) signalling pathway can be targeted using Herceptin, a recombinant humanised monoclonal antibody, approved by the FDA for HER2-positive metastatic breast cancers [63]. As HER2 is a kinase, it can also be targeted using kinase inhibitors such as Lapatinib, typically used to treat advanced breast cancer [64]. Another example is Alpelisib, a targeted inhibitor of the lipid kinase PI3K, encoded by PIK3CA. Alpelisib can be used in combination with Fulvestrant to treat post-menopausal women with advanced hormone receptor-positive breast cancer with a PIK3CA gene mutation [65].

In the TNBC subtype, there is a paucity of targeted treatments, currently limited to use of PARP inhibitors and immunotherapy for the 50% of TNBC patients that have mutant BRCA1 or are PD-L1 positive, respectively [66]. Therefore, it is important to identify oncogenic drivers involved in TNBC tumour progression as potential therapeutic targets for personalised treatment.

## 1.4 Signal Transduction via the Human Kinome in Cancer

Mammalian cells have the ability to respond appropriately to their environment by detecting external stimuli and transducing the signal into the cell to elicit relevant intracellular responses [67]. These mechanisms are important for normal cell regulation and are also dysregulated in diseases, such as cancer. Growth factors and cytokines are external signals that bind to cognate receptors, often transmembrane kinases on the cell surface, to initiate a cascade of intracellular signalling events to alter cell behaviour [67].

The human kinome consists of 535 proteins involved in regulating a wide range of biological processes [68]. Characterisation of the human kinome has provided crucial insights into how members of the protein kinase superfamily are deregulated in cancer by mutation, amplification, fusion and copy number alteration (Fig. 1.5) [69]. Oncogenic drivers of cancers are distributed throughout the 8 kinase groups and are most strongly represented in the tyrosine kinase group, accounting for approximately 40% of kinase drivers in the kinome tree (Fig. 1.5) [70]. Protein tyrosine kinases are enzymes that catalyse tyrosine phosphorylation reactions, by the transfer of the  $\gamma$ -phosphate of ATP to the hydroxyl group of a tyrosine in a protein substrate [71]. It is a form of reversible post-translational protein modification, that depending on the phosphorylation site, either positively or negatively regulates protein activity.



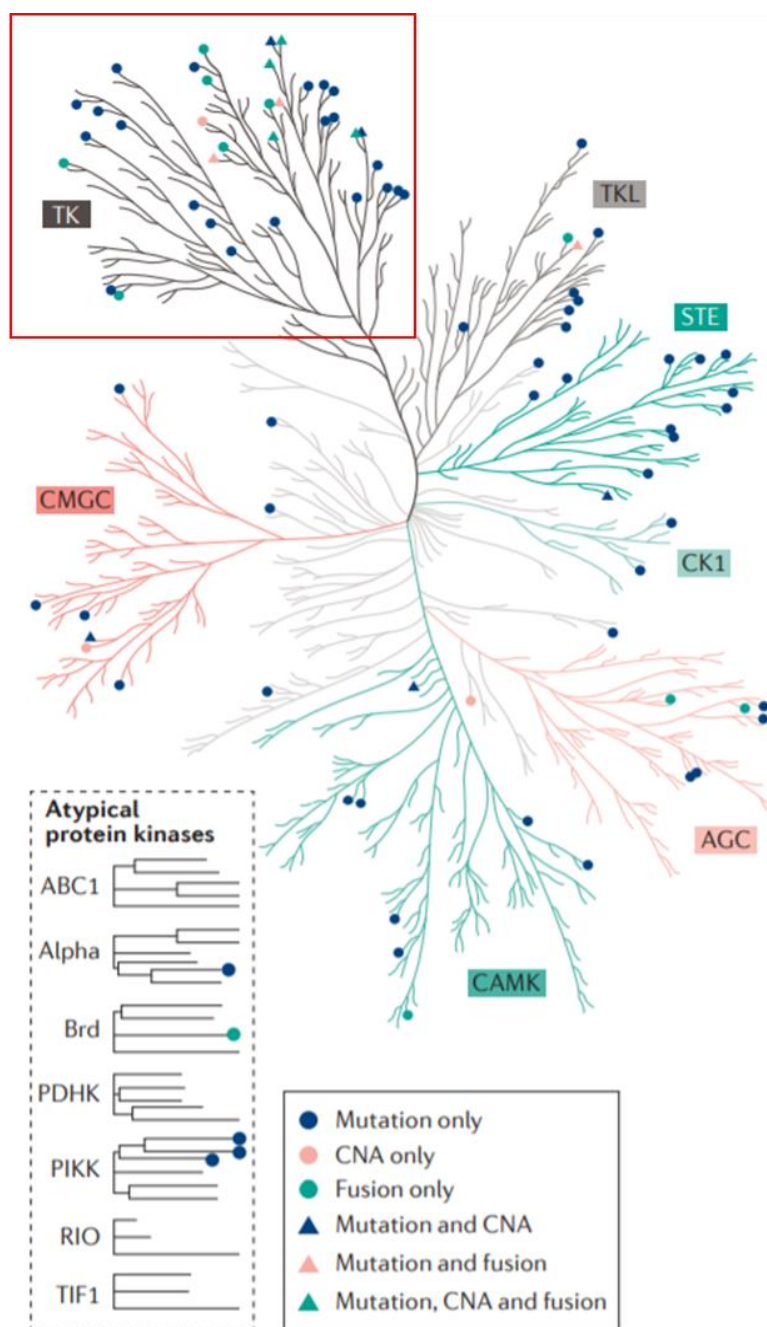


**Figure 1.5: Driver protein kinases identified by genomic studies and their corresponding genetic alterations in cancer.** The main 8 kinase groups are AGC (containing protein kinases A, G and C); CAMK (calcium/calmodulin-dependent protein kinase); CK1 (casein kinase 1); CMGC (containing cyclin-dependent kinase, MAPK, glycogen synthase kinase 3 and CDC2-like); STE (homologues of yeast sterile 7, sterile 11 and sterile 20); TK (tyrosine kinase); TKL (tyrosine kinase-like) and 'atypical'. Reproduced from [70]. Copyright (2016) with permission from Nature Reviews Cancer.



### **1.4.1 Receptor Tyrosine Kinases**

Receptor tyrosine kinases (RTKs) are a family of transmembrane glycoproteins that provide specific receptors for growth factors, cytokines, hormones and other extracellular signalling molecules [72]. RTKs dimerise and are phosphorylated upon ligand binding. These phosphorylated RTKs are then able to form complexes with cytoplasmic proteins that contain Src-homology 2 (SH2) or phosphotyrosine-binding (PTB) domains [73]. These cytoplasmic proteins that commonly interact with RTKs are often adaptor proteins and docking proteins. Adaptor proteins function as intermediaries to facilitate the interaction between two or more signalling proteins to create a signalling complex [74]. An example of an adaptor protein is growth factor receptor-bound protein 2 (GRB2). Docking proteins such as GRB2-associated binding proteins (Gab1 and Gab2) provide RTKs with additional tyrosine phosphorylation sites, therefore serving as docking sites for additional downstream signalling proteins [75].

RTKs activate a number of downstream signalling pathways within the cells (e.g. PI3K-AKT pathway, RAS-MAPK-ERK, JAK-STAT pathway) for signal transduction into the nucleus, leading to cell proliferation, differentiation, migration or metabolic changes [71, 72]. RTK subfamilies include, epidermal growth factor receptor (EGFR), fibroblast growth factor receptor (FGFR), vascular endothelial growth factor receptor (VEGFR), insulin receptor (IR) and platelet-derived growth factor receptor (PDGFR) [76]. In addition to the RTKs, a large family of non-RTKs also exists and includes Src, Abl and the Janus kinases (Jaks) [71]. The importance of tightly regulating the catalytic activity of RTKs is emphasized by the identification of many RTKs as oncogenic [77, 78].

### **1.4.2 PI3K-AKT signalling pathway**

Phosphatidylinositol-3 kinases, PI3Ks, are lipid kinases defined by the ability to phosphorylate the inositol ring 3'-OH group in inositol phospholipids [79]. Class-1 PI3Ks are heterodimers that are composed of a catalytic subunit (p110) and a regulatory subunit (p85) (Fig. 1.6) [80].

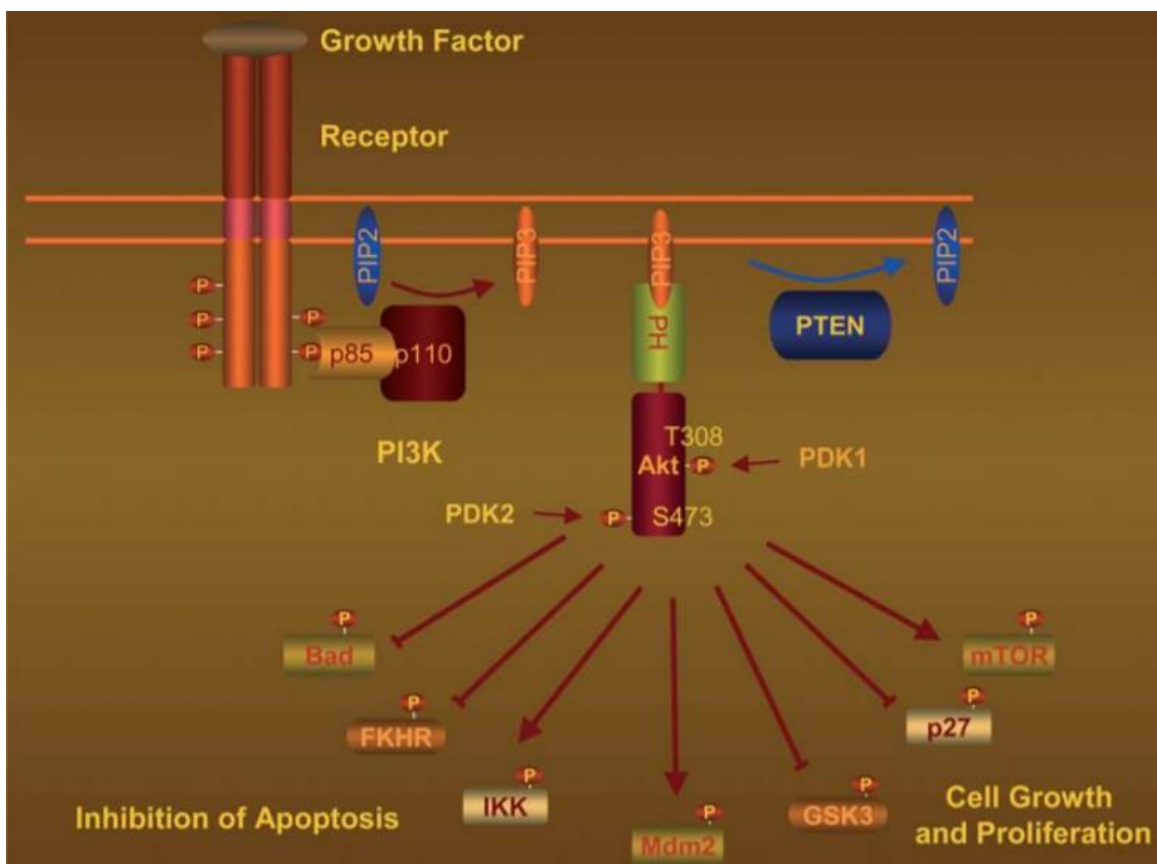


**Figure 1.6: PI3K-AKT signalling pathway.** Activation of growth factor receptor protein tyrosine kinases results in autophosphorylation on tyrosine residues and activation of the PI3K cascade. Reproduced from [80]. Copyright (2004) with permission from Elsevier.

The PI3K pathway is regulated by phosphorylation of the PI3K substrate phosphatidylinositol-4,5-bisphosphate (PIP<sub>2</sub>) to convert it to phosphatidylinositol-3,4,5-trisphosphate (PIP<sub>3</sub>), while phosphatase and tensin homolog (PTEN) is the phosphatase that dephosphorylates PIP<sub>3</sub> to PIP<sub>2</sub> (Fig. 1.6) [80]. AKT, also known as protein kinase B (PKB), is a serine/threonine (Ser/Thr) kinase involved in mediating a variety of cellular process including proliferation and survival [81]. AKT consist of a N-terminal pleckstrin homology (PH) domain, a kinase domain and a C-terminal regulatory domain (Fig. 1.6) [82] .

PI3Ks activate the AKT pathway by phosphorylating PIP<sub>2</sub> to PIP<sub>3</sub> at the cellular membrane, which in turn binds to AKT via the PH domain (Fig. 1.6) [80]. AKT is activated at two critical phosphorylate sites T308 and S473 by phosphoinositide-dependent kinase 1 and 2 (PDK1 and

PDK2 (also known as mTORC2)) (Fig. 1.6) [80]. AKT has many substrates and its phosphorylation of these substrates either has an activating or inhibiting effect [80]. Among the many substrates, Bad is a pro-apoptotic regulator that has direct implications in regulating cell survival (Fig. 1.6) [83]. When phosphorylated, Bad is not able to bind to other anti-apoptotic Bcl-2 family members, and remains in the cytosol through high-affinity binding with the cytoplasmic 14-3-3 molecule, effectively neutralising its pro-apoptotic activity [80, 83]. AKT can activate protein synthesis by stimulating the Rheb protein, which activates mTORC1, then S6K, leading to increased mRNA translation (Fig. 1.6) [83]. AKT regulates the cell cycle by inhibiting GSK3 and phosphorylating p27, which is a target gene of the transcription factor FOXO (Fig. 1.6) [83]. AKT promotes the interaction of FOXO with the scaffolding protein 14-3-3, preventing translocation of FOXO into the nucleus where FOXO can control gene expression [84, 85].

### **1.4.3 MAPK-ERK signalling pathway**

Mitogen-activated protein kinases (MAPKs) are a family of Ser/Thr specific kinases that are widely conserved among eukaryotes. The four major MAPK signalling cascades are ERK1/2, p38, JNK and ERK5 [86]. The main MAPK signalling cascade begins with Raf activating MEK1/2, which progresses downstream to activate ERK1/2 (Fig. 1.7) [86]. Many RTKs share this Raf-MEK-ERK signalling pathway, such as EGFR and FGFR (Fig. 1.7).

In the Raf-MEK-ERK MAPK signalling cascade, receptor dimerisation upon ligand binding induce activation of the kinase domain of the receptor (Fig. 1.7) [86]. Using EGFR as an example, the C-terminal tyrosine residues are phosphorylated, subsequently facilitating the recruitment and binding of adaptor proteins, Shc and GRB2, to EGFR residues pY1148 and pY1173; and pY1068, respectively (Fig. 1.7) [87]. GRB2 recruits the SOS protein, bringing SOS in close proximity to membrane-bound RAS proteins, where it promotes GDP to GTP nucleotide exchange, triggering RAS protein activation (Fig. 1.7) [88]. RAS proteins are a family of GTPases that propagate signal transduction from the activated RTK complex to the Raf-MEK-ERK signalling module [89]. Active RAS binds to Raf, initiating the phosphorylation of MEK, which phosphorylates ERK in a step-wise manner (Fig. 1.7) [86].

Activated ERK1/2 exhibits nuclear, cytosolic, membrane-associated and cytoskeletal substrates [86]. Notably, ERK translocates to the nucleus and phosphorylates transcription factors that regulate genes involved in proliferation and differentiation (Fig. 1.7) [89].

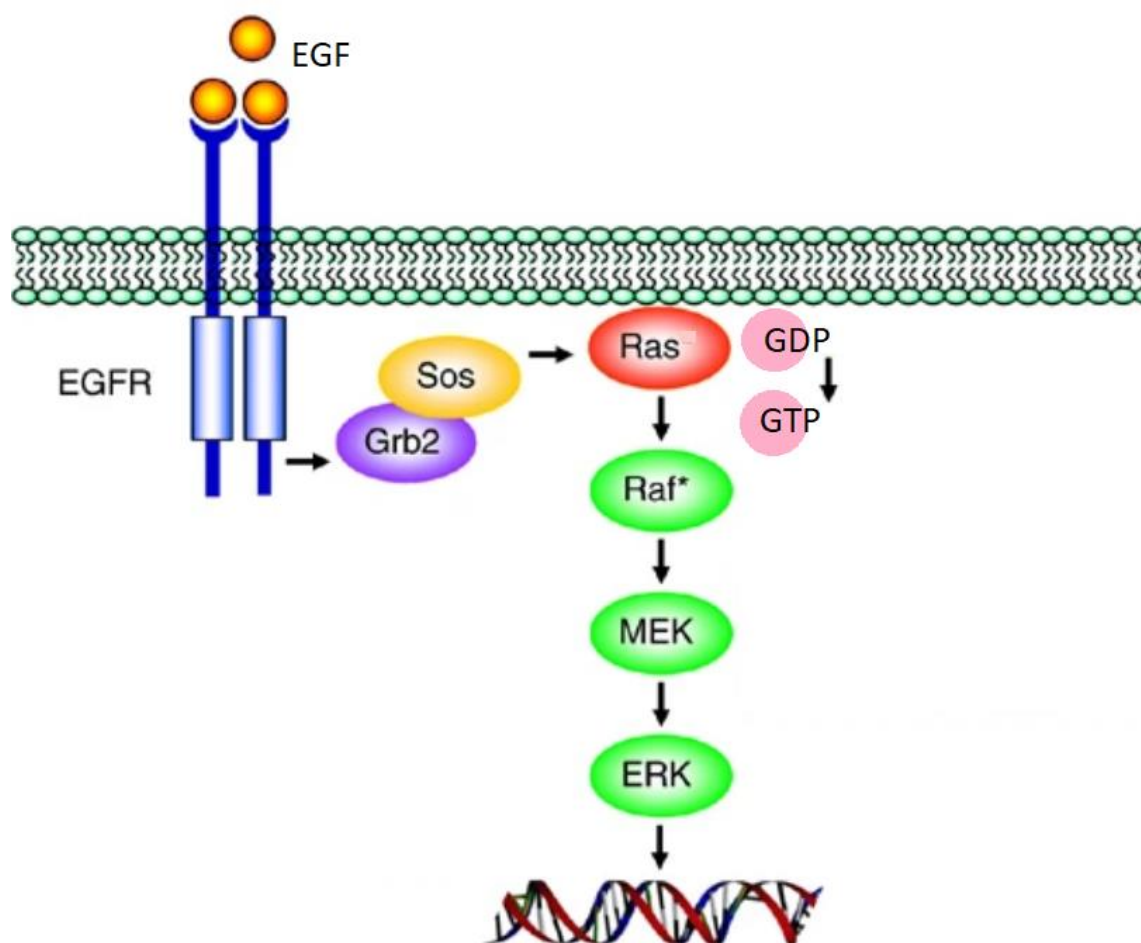


**Figure 1.7: MAPK-ERK signalling pathway.** The ligand epidermal growth factor (EGF) initiates the signal on the cell surface through binding to EGFR. The activated intracellular kinase portion of EGFR recruits GRB2 and SOS, which promotes GDP to GTP nucleotide exchange on RAS. RAS-GTP recruits Raf, which promotes the docking and activation of MEK, that phosphorylates ERK. The Raf-MEK-ERK signalling cascade generates a signal in the nucleus. Reproduced from [86]. Copyright (2007) with permission from Springer Nature.

### **1.4.4 JAK-STAT signalling**

Janus kinases (JAKs) are a family of cytosolic tyrosine kinases that phosphorylates signal transducer and activation of transcription (STAT) proteins. The mammalian JAK family consist of JAK1, JAK2, JAK3 and tyrosine kinase 2 (TYK2) [90]. The mammalian STAT family consist of seven members: STAT1, STAT2, STAT3, STAT4, STAT5A, STAT5B and STAT6 [91]. The JAK-STAT signalling pathway is often stimulated by cytokines, critical in the regulation of immune responses (Fig. 1.8) [92]. Cytokines can have an autocrine effect by binding to the receptors on the same cell that secretes them. Upon cytokine binding, cytokine receptors dimerise and facilitate the activation of associated JAKs through transphosphorylation (Fig. 1.8) [92]. Activated JAKs then recruit and phosphorylate their corresponding STATs (Fig. 1.8) [92]. Phosphorylated STATs dimerise and translocate into the nucleus to activate gene transcription (Fig. 1.8) [91, 93].

The JAK-STAT signalling pathway is negatively regulated by members of the suppressors of cytokine signalling (SOCS) proteins. The SH2 domain on SOCS1 directly binds to tyrosine phosphorylated JAKs, resulting in the inhibition of JAK activity [94, 95]. JAKs can also be negatively regulated by protein tyrosine phosphatases (PTPs) including SHP1, SHP2, CD45, PTP1B and T-cell PTP (TCPTP) [96], and ubiquitylation by the ubiquitin–proteasome pathway [92]. In regard to negatively regulating STAT, the protein inhibitor of activated STAT (PIAS) inhibits the transcriptional activity of STATs in the nucleus by blocking the DNA-binding activity [97].

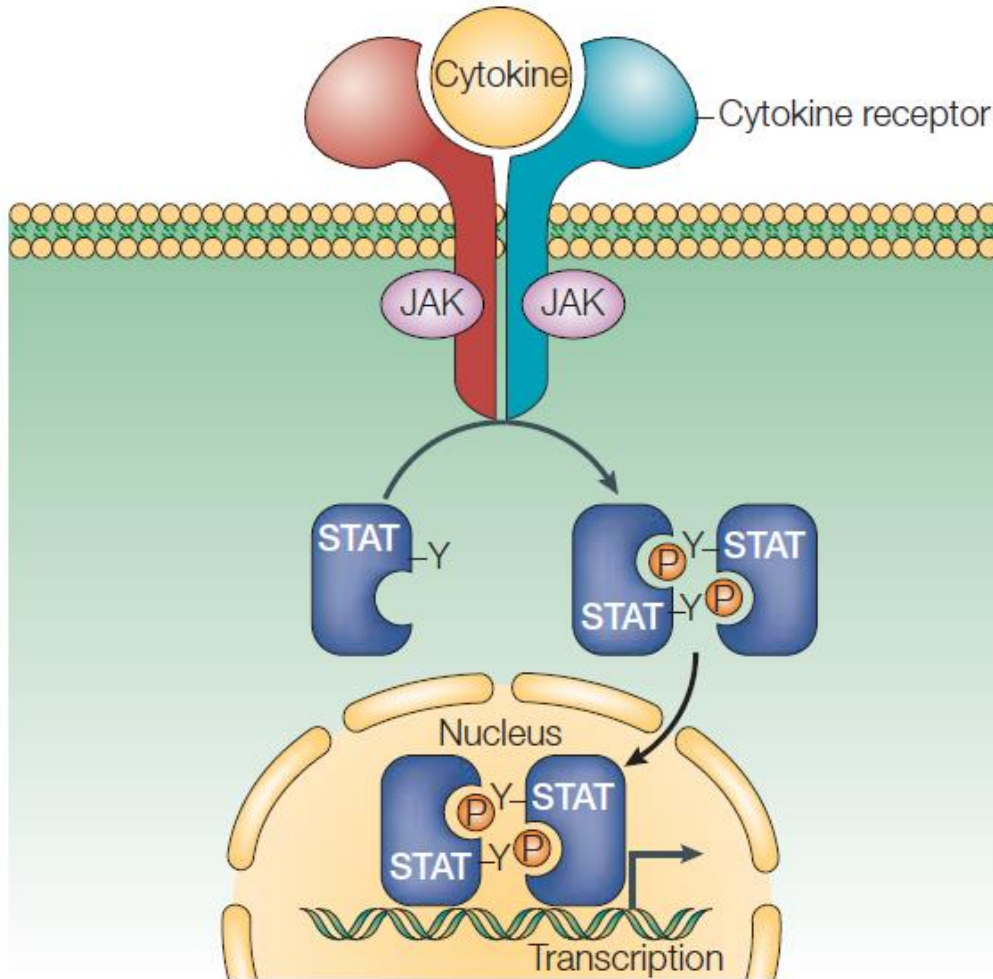


**Figure 1.8: JAK-STAT signalling pathway.** The JAK-STAT signalling cascade is induced by cytokines that bind to a specific receptor and allows the transactivation of the associated JAKs. Activated JAKs phosphorylate tyrosine residues on the intracellular domains of the receptor, which recruit STAT proteins. STATs are then translocated into the nucleus to activate gene transcription. Reproduced from [92]. Copyright (2003) with permission from Springer Nature.

## 1.5 Fibroblast growth factor receptors (FGFRs)

### 1.5.1 Structure of receptors and ligands

The FGFR family consist of four highly conserved transmembrane RTK members: FGFR1, FGFR2, FGFR3 and FGFR4. FGFRs structurally comprise of an extracellular ligand-binding domain made up of 3 immunoglobulin (Ig)-like domains (Ig-I, Ig-II, Ig-III) with an acidic, serine-rich region (between Ig-I and Ig-II, known as the acid box), a single-pass transmembrane domain and an intracellular tyrosine kinase domain (Fig. 1.9) [98-100]. The Ig-I and acid box are hypothesised to play a role in the auto-inhibition of the receptor, by, intramolecular contacts of Ig-I with Ig-II and Ig-III, and competitive binding of the acid box to the heparin binding site of Ig-II, respectively (Fig. 1.9) [101, 102]. Ig-II and Ig-III extracellular domains constitute the ligand-binding site where the FGF ligands can bind to multiple FGFRs with high affinity (Fig. 1.9) [103, 104]. The linker region between Ig-II and Ig-III domains regulates the specificity of ligand binding to the receptors [105]. FGFR1-3 have receptor splice variants due to alternative splicing that increases the complexity of the ligand-receptor binding, while this is absent in FGFR4 [103, 104]. The alternative splicing occurs in exons 8-9, which generates two different isoforms (IIIb or IIIc) of the Ig-III domain in FGFR1, FGFR2 and FGFR3 (Fig. 1.9) [106]. Differential expression of these two isoforms can be observed in specific tissues. The IIIb isoform is mostly expressed in epithelial tissues, particularly during tissue differentiation, while the IIIc isoform predominates in mesenchymal tissues [107]. The Ig-III domain of FGFR2 and FGFR3 is the most extensively studied, where the first half of Ig-III is encoded by an invariant exon (IIIa) and the second half spliced as IIIb or IIIc isoform, contributing to further ligand complexity and specificity [107]. Another potential FGFR member was identified, FGFR5, that can bind to FGFs with high affinity but lacks the intracellular tyrosine kinase domain [108].



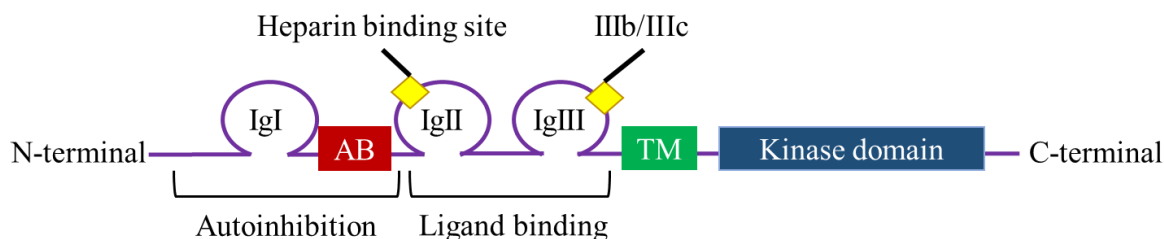


**Figure 1.9: Schematic of FGFR structure.** FGFRs are comprised of 3 immunoglobulin (Ig)-like domains, with the heparin binding site located on IgII. The location of the alternatively spliced IgIIIb or IgIIIc domain is indicated. The FGFR portions involved in receptor autoinhibition and FGF ligand binding are indicated. AB indicates acid box. TM indicates transmembrane. Adapted from [109].

The FGF ligand family consist of secreted FGFs (canonical or endocrine) that bind to their respective receptors and intracellular FGFs that function as cofactors for voltage gated sodium channels (Fig. 1.10) [105]. Secreted FGFs are expressed in most tissues and have essential roles in the early stages of embryonic development and during organogenesis [105]. In adult tissues, secreted FGFs serve important roles as homeostatic factors for tissue maintenance, repair, regeneration and metabolism [105]. Most secreted FGFs are canonical FGFs (Fig. 1.10) that act as autocrine or paracrine factors, controlling cell proliferation, differentiation and survival [99, 103, 107].

There are 22 known FGF ligands that bind to and activate receptor isoforms encoded by the 4 FGFRs (Fig. 1.10) [107, 110, 111]. Only 3 members of secreted FGFs function as endocrine factors (Fig. 1.10), which regulate phosphate, bile acid, carbohydrate and lipid metabolism [105]. Proteoglycan cofactors and extracellular binding proteins regulate the interaction of FGF ligands to the FGFRs (Fig. 1.10) [105]. FGFs are readily sequestered by heparan sulphate proteoglycans (HPSG) at the heparin binding site on the cell surface and the extracellular matrix (Fig. 1.9), that stabilise the FGF-FGFR interaction by shielding FGFs from degradation mediated by proteases [112]. Klotho family members associate with endocrine FGFs and act as cofactors for FGF-FGFR signalling (Fig. 1.10) [113].



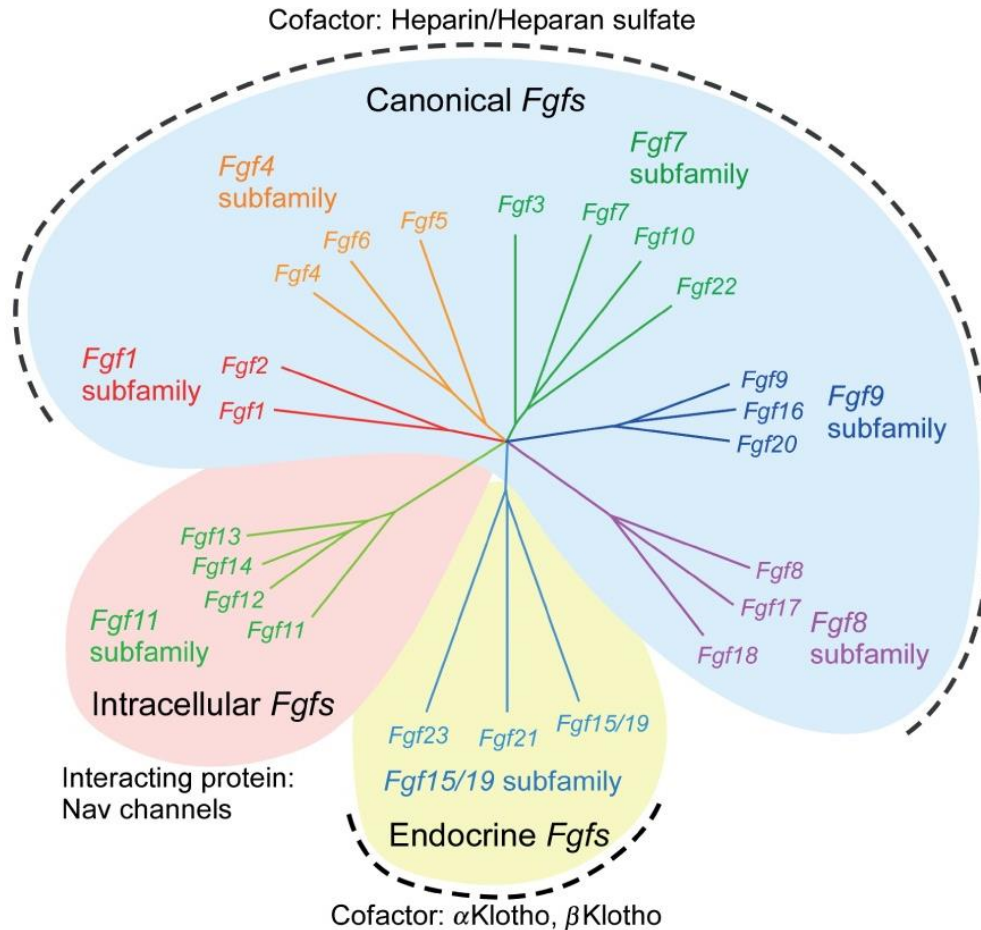


**Figure 1.10: The FGF ligand family.** The 22 FGF genes can be categorised into 7 subfamilies based on phylogenetic analysis. The secreted canonical FGF subgroup consists of the FGF1, FGF4, FGF7, FGF8 and FGF9 subfamilies and bind to FGFRs with heparin or heparan sulfate as cofactors. The endocrine FGF subgroup consists of FGF15/19 subfamily which bind to FGFRs with Klotho proteins as a cofactor. The intracellular FGF subgroup consists of the FGF11 subfamily, which are non-signalling proteins that serve as cofactors for voltage gated sodium channels. Reproduced from [105]. Copyright (2015) with permission from John Wiley and Sons.

### 1.5.2 Regulation of FGFR signalling pathways

FGFs bind to FGFRs to induce receptor dimerisation and initiate the trans-phosphorylation of FGFRs at key tyrosine residues in the intracellular activation loop of the FGFR tyrosine kinase domain and the C-terminus (Fig. 1.11) [113-115]. There are 8 FGFR phosphorylation sites that

are mostly conserved (75-92% homology) among the four FGFR members (Fig. 1.11) [116]. Using FGFR1 as an example, the phosphorylation sites are Y463 (juxtamembrane), Y583/Y585 (kinase insert), Y653/Y654 (the activation loop), Y730 (kinase domain) and Y766 (C-terminal tail) (Fig. 1.11) [117, 118]. An additional Y677 phosphorylation site allows the docking of STAT proteins (Fig. 1.11) [105].

The activation of the FGFR1 kinase is in three sequential steps: firstly, the activation loop Y653 is trans-phosphorylated, secondly the juxtamembrane region Y463, the kinase insert Y583/Y585 and the C-terminal tail Y766 are phosphorylated, followed by the final phosphorylation of the activation loop Y654, all which causes fold-activation of the kinase activity (Fig. 1.11) [119]. While FGFR3 lacks the equivalent Y463 and Y585 in FGFR1, and FGFR4 lacks Y583/Y585 and Y463, these dissimilarities may underlie the difference in the overall kinase activity and the specific effects mediated by the FGFR [114].

Once activated by FGF ligands, the phosphorylated FGFR tyrosine residues function as docking sites for various adaptor proteins such as the FGFR substrate 2 (FRS2) and the membrane-associated enzyme phospholipase C $\gamma$  (PLC- $\gamma$ ) (Fig. 1.12) [115]. FRS2 is an adaptor/scaffold protein particularly specific to FGFRs and is constitutively associated with the FGFR juxtamembrane domain through its PTB domains (Fig. 1.12) [114]. Phosphorylated FRS2 acts as a docking site for other adaptor proteins such as GRB2 and Gab1, and an exchange factor SOS, enabling further activation of downstream signalling pathways (Fig. 1.12) [107, 113, 114]. PLC- $\gamma$  binds to FGFR via its SH2 domain and becomes activated by phosphorylation (Fig. 1.12) [107]. PLC- $\gamma$  is activated for the catalysis of PIP2 to diacylglycerol (DAG) and inositol triphosphate (IP3) [120], which triggers the activation of calcium-dependent members of the protein kinase C (PKC) family for further activation of downstream signalling pathways (Fig. 1.12) [114]. FGFR-mediated signals are transduced in a step-wise manner through intracellular RAS-MAPK, JAK-STAT and PI3K-AKT downstream signalling pathways (Fig. 1.12) [99, 121].

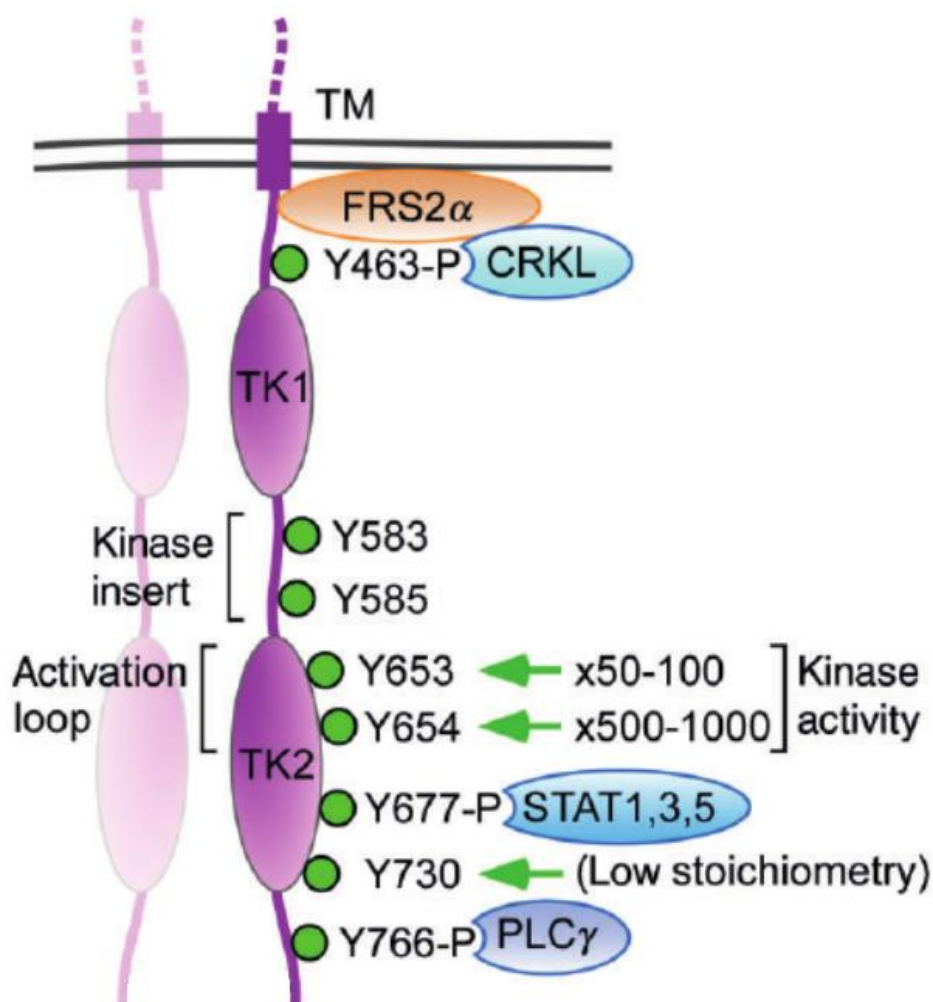


**Figure 1.11: FGFR1 phosphorylation sites.** FGFR1 dimerisation leads to sequential phosphorylation of tyrosine residues leading to increase kinase activity and phosphorylation of a specific site for PLC- $\gamma$  binding. FGFR phosphorylation starts at Y653 in the activation loop leading to 50-100 fold increase in kinase activity. The final phosphorylation step of Y654 in the activation loop results in an overall 500-1000 fold increase in kinase activity. The Y677 phosphorylation site allows the docking of STAT proteins. Reproduced from [105]. Copyright (2015) with permission from John Wiley and Sons.

The FGFR signalling pathway is strongly regulated by feedback mechanisms such as Sprouty (SPRY) that competes with GRB2 and MAPK phosphatase 3 (MKP3) that dephosphorylates ERK1 and ERK2 (Fig. 1.12) [122]. FGFR signalling is also negatively regulated by members of the “similar expression to FGF” (Sef) family by direct inhibition [123, 124] and by endocytosis followed by degradation of FGFR proteins in the lysosomes [115]. These complex

signalling cascades are involved in regulating a wide range of physiologic processes, such as cellular differentiation, cell growth, proliferation, survival, migration, embryonic development and angiogenesis [112, 125]. Specifically in embryonic development, the FGFR signalling pathway plays a fundamental role in mesenchymal-epithelial communication and in the organogenesis of the nervous system, midbrain, lungs, limbs and mammary glands [116].

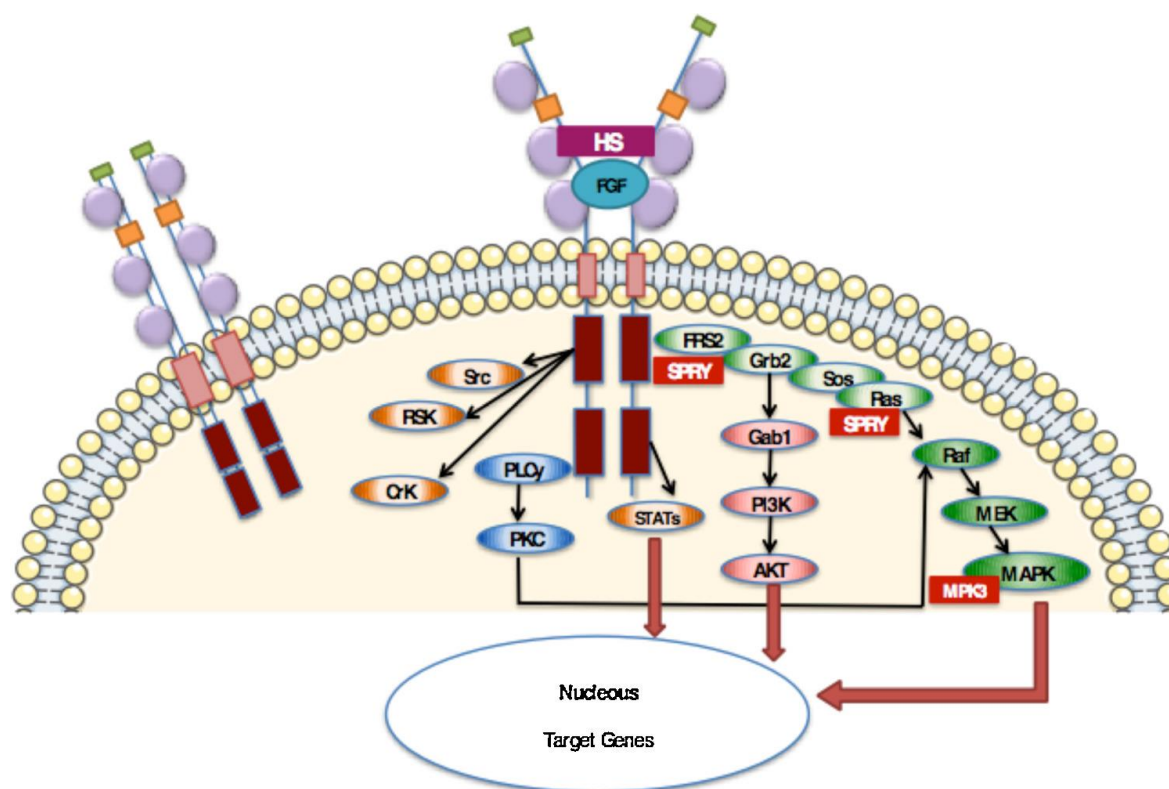


**Figure 1.12: FGFR structure and signalling pathway.** FGF ligand binds to FGFR between the IgII and IgIII domains, induce subsequent FGFR dimerisation and activates multiple signal transduction pathways: PLC- $\gamma$  pathway, PI3K-AKT pathway and the RAS-MAPK pathway. Negative regulators of FGFR such as the Sprouty protein (SPRY) compete with GRB2 or directly binds to Ras to prevent its activation. MAPK is also inhibited by the negative regulator MPK3. Reproduced [106]. Copyright (2017) with permission from Elsevier.

### **1.5.3 Aberrant FGFR signalling in cancer**

Genes implicated in cancer are classified as oncogenes when activated abnormally and contribute to the malignant transformation of cells. Changes in the expression and function of these genes and their protein products confer cells with uncontrolled growth and survival advantages that are the hallmarks of cancer. Deregulation of the FGFR signalling pathway frequently contributes to oncogenesis and progression across many cancer types [99, 100] and is reported in 7.1% of all cancers. Urothelial (23%) is the most commonly affected cancer, followed by breast (18%), endometrial (13%), squamous lung cancer (13%) and ovarian cancer (9%) [126]. Oncogenic FGFR signalling leading to pathway activation is mediated by genetic alterations (e.g. receptor amplification, mutations and chromosomal translocation), autocrine and/or paracrine signalling [127, 128]. Notably, several genetic alterations of FGFR signalling have been identified across many cancers (Table 1.1). In this thesis chapter, oncogenic FGFR signalling in breast cancer will be the main focus, with some additional cancer types included.

#### **FGFR amplification**

The FGFR1 gene, located on human chromosome 8p12, is amplified in 14% of hormone-receptor positive breast cancers, associated with poor prognosis and confers resistance to endocrine therapies [129-131]. FGFR1 amplification is found in 5% of TNBC [132] and its expression is an independent negative prognostic factor [133, 134]. Additionally, elevated FGFR1 mRNA is detected in 23 out of 103 (22%) breast tumour samples [135], and gene amplification is robustly associated with FGFR1 overexpression [129, 136]. In luminal and lobular breast carcinoma *in vitro* studies, FGFR1 silencing by small-interfering RNA (siRNA) and inhibition by a selective FGFR inhibitor PD173074 impaired the growth and oncogenic survival of FGFR1-amplified breast cancer cell lines [129, 131]. In other cancer types, FGFR1 amplification is found in 17% of squamous non-small cell lung carcinoma (NSCLC) and 6% of small-cell lung carcinoma cases [137-139], and is also an independent prognostic marker in the former [140].

**Table 1.1: Genetic alterations in FGFRs reported in human tumours.**

Gene	Genetic alteration	Tumour type (incidence)	Reference
FGFR1	Amplification	Luminal breast cancer (12-27%)	[128, 129, 141]
		TNBC (5%)	[132]
		Squamous cell lung carcinoma (9%)	[128]
Urothelial cancer (7%)		[128]	
Ovarian carcinoma (5%)		[128]	
Colorectal carcinoma (2%)		[128]	
	Mutation	Glioblastoma (10%)	[142]
	Translocation	Glioblastoma (1%)	[143]
FGFR2	Amplification	TNBC (4%)	[144]
		Gastric cancer (2-4%)	[145, 146]
	Mutation	Endometrial carcinoma (12%)	[147]
		Squamous cell lung carcinoma (3%)	[148]
	Translocation	Intrahepatic cholangiocarcinoma (16%)	[149, 150]
Breast cancer		[150]	
FGFR3	Amplification	Urothelial cancer (3%)	[128]
	Mutation	Bladder cancer (60%)	[150, 151]
		Cervical cancer (5%)	[152]
	Translocation	Glioblastoma (3%)	[143]
		Bladder cancer (3%)	[150, 153]
		Nasopharyngeal carcinoma (2.5%)	[154]
Squamous cell lung carcinoma (3%)		[155]	
Cervical cancer (2%)	[156]		
FGFR4	Amplification	Breast cancer (2.3%)	[128]
	Mutation	Breast cancer (11%)	[112, 157]
		Lung adenocarcinoma (8%)	[158]
		Rhabdomyosarcoma (6-8%)	[112]



FGFR2 gene amplification on 10q26, is found in 2% of breast cancer cases and in 4% of TNBC [144, 159-161]. Increased FGFR2 expression is associated with poor prognosis, overall survival and disease-free survival in breast cancer patients [162]. Breast cancer cell lines with high FGFR2 amplification are extremely sensitive to selective FGFR inhibitors and siRNA silencing significantly reduced cell survival [144, 163]. These results were also observed in gastric cancers, implicating that cancers with amplified FGFR2 are addicted to the FGFR signalling pathway for oncogenic growth [160, 164, 165]. FGFR3 and FGFR4 amplification are rarely reported as the oncogenic activation of these receptors are often linked to mutation or ligand amplification [127, 128]. For example, FGFR4 overexpression was detected in a TNBC cell line MDA-MB-453, arising from an activating mutation Y367C that causes constitutive activation of receptor activity [166].

### **FGFR mutations or polymorphisms**

Single nucleotide polymorphisms (SNPs) and somatic activating mutations are detected in FGFR members in breast cancer. For example, SNPs in intron 2 of FGFR2 have been identified in ER-positive tumours [167-169]. One of the FGFR2 SNPs, rs2981578, increases FGFR2 expression through increased Oct-1/Runx2 and C/EBP $\beta$  transcription factor binding [167]. Other FGFR2 SNPs identified (e.g. rs1219648, rs2420946) were associated with increased risk of developing breast cancer [168, 170]. In FGFR4, a SNP involving the conversion of glycine (Gly) to arginine (Arg), Gly388Arg, was identified in breast cancer and demonstrated to be associated with increased cell motility *in vitro* [169]. Increased tumour formation and tumour progression through degradation of the extracellular matrix involving epithelial-to-mesenchymal transition *in vivo* are also effects of the Gly388Arg SNP [171, 172]. FGFR4 Gly388Arg is also correlated with significantly reduced disease-free survival [157]. Point mutations in breast cancer are rare, though S125L in FGFR1 and R203C in FGFR2 were reported in breast tumours, and the aforementioned activating mutation Y367C in FGFR4 was detected in MDA-MB-453 cells [166, 173].

### **FGFR fusion**

Oncogenic fusions have more recently been discovered across many cancers but at low prevalence. Fusion genes involve the rearrangement of independent genes and play an

important role in the development and progression of cancer. Most fusion partners of FGFR contain dimerisation domains that induce ligand-independent receptor dimerisation, oncogenic activation of downstream signalling pathways or loss of genomic regulators [143, 150, 153]. Fusion partners of FGFR1-3 have been reported but not of FGFR4.

FGFR3 fusions are relatively common, including a fusion between FGFR3 and transforming acidic coiled-coil containing protein 3 (TACC3), detected in a TNBC tumour specimen and cell line, and more frequently reported in glioblastoma and bladder cancer [174, 175]. In the FGFR3-TACC3 fusion protein, the C-terminal region of FGFR3 is removed and replaced with the C-terminal portion of TACC3, with the coiled-coil domain of TACC3 mediating protein oligomerisation and driving the activation of the fusion receptor and ligand-independent signalling [150]. FGFR2 also has several fusion partners that can fuse at either the C-terminal or N-terminal of FGFR2, for example FGFR2-AFF3 or SLC45A3-FGFR2 [150]. FGFR2 fusion partners reported in breast cancer are AFF3, CASP7 and CCDC6 [150, 176]. Other fusion partners reported in other cancers include TACC and KIAA family members, PPHLN1, NTRK1, BICC1, AHCYL1, OFD1 and SLC45A3 [149, 150, 177, 178]. In regard to fusions involving FGFR1, the FGFR1-TACC1 fusion was found in glioblastoma [143] and the ERLIN2-FGFR1 fusion found in breast cancer [150].

### **Autocrine/paracrine signalling**

Most of the genetic alterations described lead to constitutive activation of the receptor, downstream signalling and ligand-independent signalling. Additionally, ligand-dependent signalling from abnormal FGF expression may also contribute to cancer increasing cell survival and angiogenesis [179]. Pre-clinical studies across various cancer types including in TNBC have demonstrated that the expression of FGFs stimulate cancer cells and stromal cells through autocrine and paracrine signalling, respectively [180, 181]. Overall, in understanding the mechanisms of aberrant FGFR signalling in breast cancer, appropriate strategies can be developed to target specific FGFRs to improve treatment.



### **1.5.4 Overview of FGFR inhibitors**

The investigation of FGFRs as oncogenic drivers and therapeutic targets in cancer made way for the development of therapeutic agents against the FGFR signalling pathway. Studies on FGFR targeting has exponentially advanced over the years, allowing the development of novel agents that inhibit FGFRs or FGF ligands, including, small molecule tyrosine kinase inhibitors, monoclonal antibodies and FGF ligand traps (Table 1.2) [100].

#### **Small molecule tyrosine kinase inhibitors**

Small molecule tyrosine kinase inhibitors directly inhibit receptor kinase activity by interfering with the binding of ATP or substrates to the cytoplasmic tyrosine kinase domain [182]. These can be further categorised into non-selective and selective FGFR inhibitors (Table 1.2). Successful pre-clinical demonstration of the efficacy of FGFR targeting utilising small molecule inhibitors has led to the evaluation of such approaches in human clinical trials. For example, an inhibitor of FGFR1-4, Erdafitinib was FDA-approved for patients with metastatic urothelial carcinoma exhibiting FGFR gene alterations and resistance to chemotherapy, based on results from a phase II clinical trial [183]. Many clinical trials are currently underway to identify novel approaches and treatment strategies (Table 1.2).

Non-selective FGFR inhibitors are multi-target inhibitors that mainly target other RTKs such as VEGFR and PDGFR (Table 1.2), but also exert activity against FGFRs due to structure similarity of the kinase domains [184]. In the context of FGFR-overexpressed tumours, the lack of bioactivity against FGFRs may limit drug efficacy and the inhibition of multiple RTKs may increase undesirable side effects [179]. For example, Dovitinib has high inhibitory activity against c-KIT, VEGFRs, PDGFRs and FGFRs, and can inhibit the activity of FGFR1-3 in FGFR-amplified breast cancer patients [159]. Lenvatinib is another multikinase inhibitor that also inhibits FGFR1-4, VEGFRs, KIT and PDGFRs (Table 1.2) [185]. Lenvatinib demonstrated significant growth inhibition in TNBC xenograft models and blocked the development of lung and lymph node metastasis [186]. Moreover, Lenvatinib is in a phase II clinical trial as a single therapeutic agent for breast cancer (NCT03168074) and in clinical

trials as part of combination treatment with immunotherapy in hormone receptor positive breast cancer and TNBC (NCT02562118, NCT04427293) (Table 1.2).

Selective FGFR inhibitors were developed to increase FGFR selectivity and minimise adverse side effects arising from multi-target kinase inhibitors. AZD4547 is a selective inhibitor of FGFR1-3 with *in vitro* IC<sub>50</sub> values of 0.2 – 2.5 nM, and 165 nM for FGFR4 [187]. In a translational clinical trial, 12.5% and 33% of gastric cancers exhibiting FGFR1- and FGFR2 amplification respectively, exhibited responses to the FGFR1-3 inhibitor AZD4547 [165]. Erdafitinib is another selective FGFR1-4 inhibitor and is currently being evaluated in a clinical trial for FGFR-amplified metastatic breast cancer (NCT03238196) (Table 1.2). Most FGFR1-3 selective inhibitors have lower affinity to FGFR4 due to the unique cysteine residue (Cys552) within the ATP binding pocket of FGFR4 [127, 188]. Specific FGFR4 inhibitors such as BLU9931 and H3B-6527 have demonstrated significant anti-tumour activity in breast cancer and hepatocellular carcinoma (HCC) overexpressing FGF19 [189, 190]. Other selective FGFR inhibitors being evaluated in clinical trials for many solid tumours including breast cancer are described in Table 1.2.

### **Monoclonal antibodies**

Monoclonal antibodies bind to the FGFR extracellular domain and compete with FGFs, thereby blocking the FGF-FGFR binding and receptor dimerisation [179]. These were originally developed against cancer with deregulated FGFR signalling to reduce adverse side effects associated with multiple RTK inhibition. For example, the monoclonal antibody GP369 that targets the extracellular Ig-IIIb isoform of FGFR, has demonstrated potent suppression of proliferation in FGFR2-amplified cancer cells and in patient xenografts harbouring activated FGFR2 signalling [191].

### **FGF ligand traps**

FGF ligand trap such as FP-1039 was developed to bind and neutralise FGF ligands, preventing their binding to the receptor [179]. Particularly, FP-1039 selectively blocks canonical FGFs, and inhibits lung cancer cell proliferation and angiogenesis [192]. Another FGF ligand trap NSC12 also inhibited FGFR signalling, cell proliferation and tumour growth in models of

FGF-dependent lung cancer *in vitro* and *in vivo* [193]. Clinical trials utilising FGF ligand traps in breast cancer patients with aberrant FGFR signalling have yet to be designed.

**Table 1.2: Current FGFR inhibitors in clinical trials.**

Inhibitor name	Kinase Target	Cancer type
FGFR-selective		
Infgratinib (BGJ398)	FGFR1-3	Advanced breast cancer (NCT04504331)
Erdafitinib (JNJ-42756493)	FGFR1-3	Metastatic breast cancer (NCT03238196)
Pemigatinib	FGFR1-3	Multiple advanced malignancies including breast cancer (NCT02393248, NCT04591431)
H3B-6527	FGFR4	HCC patients with high FGF19 (NCT02834780)
Fisogatinib (BLU-554)	FGFR4	HCC (NCT04194801)
TAS120	FGFR1-4	Metastatic breast cancer (NCT04024436) Advanced cholangiocarcinoma (NCT04507503)
Non-selective/ Multi-kinase		
Ponatinib	FLT3, FGFR, SRC, KIT, RET, PDGFR, FLT1	Multiple advanced malignancies including breast cancer (NCT03878524, NCT04591431)
Lenvatinib	VEGFR, PDGFR, FGFR, KIT and RET	Hormone receptor positive breast cancer and TNBC in combination with immunotherapy (NCT02562118, NCT04427293) Breast cancer (NCT03168074)

### **1.5.5 Rewiring of FGFR signalling pathways**

Despite successful outcomes of anti-FGFR therapy in cancer, studies have identified the occurrence of resistance to anti-FGFR therapy over time [127]. For example the TNBC cell line MDA-MB-453, which displays aberrant FGFR4 signalling, developed resistance to a FGFR4 antagonistic monoclonal antibody, 10F10 [166]. In a HCC cell line, Hep3B, the treatment of FGFR4 inhibitor H3B-6527 showed recovery of downstream protein ERK after initial inhibition [194]. This perturbation of ERK signalling suggests rewiring of the FGFR4 signalling network, which can limit the efficacy of the targeted therapy. Crosstalk between the FGFR signalling pathway and other oncogenic pathways may also contribute to pathway rewiring and resistance to anti-FGFR therapy. In two FGFR-dependent basal-like breast cancer tumour xenografts, high levels of pEGFR and pErbB2 were detected after FGFR inhibition [195]. Subsequently, combination treatment using a pan-ErbB inhibitor and Dovitinib reduced tumour growth and metastasis in these PDXs [195]. This highlights the potential of combination treatments involving FGFR inhibitors as novel therapeutic strategies.

### **1.5.6 Combination drug therapy**

Further pre-clinical investigations on the role of aberrant FGFR signalling in patients that may respond to anti-FGFR therapy and the potential use of combination therapy would assist in improving the efficacy of anti-FGFR therapies in cancer. This highlights the importance of identifying upregulated targets for combination treatment with FGFR inhibition. For example, pre-clinical studies demonstrated that the combination of Dovitinib with a PI3K or HER2/VEGFR2 inhibitor blocked metastasis and cell growth in breast cancer models *in vivo* [195]. Co-targeting FGFR4 and ER resulted in a greater decrease in cell growth in invasive lobular breast carcinoma cells [196]. These studies suggest that combination treatments may increase the efficacy of FGFR inhibitors in certain settings.

Consequently, the literature indicates a promising outlook for with targeting FGFRs in cancer. However, much is still uncertain regarding the nature and role of alterations to specific FGFRs in particular cancer types, predicting the response of individual patients to anti-FGFR therapy

and understanding development of resistance to anti-FGFR therapy over time. Further research in these areas is necessary to optimise anti-FGFR treatments and apply them in precision oncology approaches.

## **1.6 Research Objectives**

The original research objective of this doctoral thesis was to investigate the role of FGFR signalling in TNBC. As the project progressed, the investigation expanded and covered luminal B breast cancer and HCC.

The specific research aims which are addressed in the experimental chapters in this thesis are:

1. To characterise the signalling and function of FGFR3 in TNBC
2. To interrogate breast cancer patient-derived models to evaluate specific FGFRs as therapeutic targets.
3. To characterise the regulation of FGFR4 signalling pathways in cancer to develop combination therapy strategies in the context of resistance to FGFR4-selective therapy.

## **1.7 Thesis Outline**

The thesis consists of three experimental chapters, with the first results chapter already published, the second results chapter ready for submission and the third results chapter in preparation for submission. The published paper was reformatted to ensure a consistent presentation throughout the thesis while its content remains unchanged. The original publication is also provided in the Appendix. The full thesis structure and outline is elaborate here.

### **Chapter 1: Literature Review**

This chapter provides background knowledge to the reader pertaining to breast cancer and the treatment strategies available. It introduces the key concept of signal transduction in

mammalian cells and how abnormal signalling can lead to cancer with a specific focus on the FGFR family. This is followed by a thorough review on the drugs that are currently being evaluated in the clinical setting and potential treatment strategies to improve drug efficacy. The chapter concludes with research objectives and thesis outline.

### **Chapter 2: Materials and Methods**

This chapter describes the methodology undertaken for the experiments in this thesis.

### **Chapter 3: FGFR3 signaling and function in triple negative breast cancer**

*Nicole J Chew, Elizabeth V Nguyen, Shih-Ping Su, Karel Novy, Howard C Chan, Lan K Nguyen, Jennii Luu, Kaylene J Simpson, Rachel S Lee and Roger J Daly (2020) FGFR3 signaling and function in triple negative breast cancer*

*[Manuscript published in Cell Communication and Signaling (Impact Factor = 5.020)]*

This chapter investigates the role of FGFR3 and FGFR3-TACC3 fusion in TNBC. The chapter first identified potential therapeutic targets in TNBC by applying mass-spectrometry based tyrosine phosphorylation profiling across a comprehensive TNBC cell line panel. This identified aberrant activation of specific FGFRs, in particular FGFR3, which had not been previously characterised in this context before. Importantly, one cell line expressed a FGFR3-TACC3 fusion, as well as the wildtype FGFR3. This is followed by a detailed characterisation of the signalling and functional role of these two receptor forms. This chapter also identified the FGFR3-TACC3 fusion as the major oncogenic driver and revealed the subcellular localisation of the fusion protein, which has been a controversial issue in the literature. Additionally, in TNBC cell lines with moderate FGFR3 expression/phosphorylation, FGFR3 did not contribute to cell proliferation, suggesting that marked activation, due to genetic alterations is likely required. Public datasets (TCGA and METABRIC) were interrogated and revealed that FGFR3 mutation and amplification, while rare, do occur in TNBC/basal and in the luminal subtypes. Lastly, the increased FGFR3 expression in breast cancer was significantly associated with reduced overall survival. Overall, these data indicate that

targeting FGFR3 may represent a therapeutic option for TNBC, but only for a select group of patients with oncogenic FGFR3 alterations.

### **Chapter 4: Evaluation of FGFR targeting in breast cancer through interrogation of patient-derived models**

*Nicole J Chew, Terry C C Lim Kam Sian, Elizabeth V Nguyen, Sung-Young Shin, Jessica Yang, Mun N Hui, Niantao Deng, Catriona A McLean, Alana L Welm, Elgene Lim, Peter Gregory, Tim Nottle, Tali Lang, Melissa Vereker, Gary Richardson, Genevieve Kerr, Diana Micati, Thierry Jardé, Helen E Abud, Rachel S Lee, Alex Swarbrick and Roger J Daly*  
*[Manuscript to be submitted to Breast Cancer Research]*

This chapter applied an integrated multi-omic approach across panels of breast cancer patient-derived models in order to identify candidate therapeutic targets, with a major focus on specific FGFRs. Mass-spectrometry based phosphoproteomics, RNA sequencing, whole exome sequencing and Western blotting were used to characterise aberrantly activated FGFRs and the effects of specific FGFR inhibitors. Phosphoproteomic profiling across 18 TNBC and 1 luminal B PDX revealed a third of PDX exhibited enhanced phosphorylation of FGFR1, FGFR2 or FGFR4. The TNBC PDX with high FGFR2 activation was extremely sensitive to AZD4547, and integrated ‘omic analysis revealed a novel FGFR2-SKI fusion. In a luminal B PDX with high FGFR4 phosphorylation, treatment with a FGFR4 inhibitor BLU9931 significantly decreased tumour growth. Additionally, interrogation of public datasets revealed FGFR2 amplification, fusion or mutation occur in TNBC and other breast cancer subtypes, while FGFR4 overexpression and amplification occurred in all breast cancer subtypes and was associated with poor prognosis. Lastly, characterisation of a patient-derived organoid (PDO) panel identified a luminal A PDO with high FGFR4 expression that was sensitive to BLU9931 treatment, further highlighting FGFR4 as a potential therapeutic target. Overall, this chapter highlights how patient-derived models of human breast cancer provide powerful platforms for therapeutic target identification and analysis of drug action, and also the potential specific FGFRs, including FGFR4, as targets for precision treatment.

### **Chapter 5: The FGFR4 signalling network and mechanisms of resistance to anti-FGFR4 therapy**

This chapter investigates how the FGFR4 signalling network is rewired and impacts sensitivity to FGFR4-selective inhibitors in TNBC and HCC. A key aim of the chapter is to identify upregulated RTKs in FGFR4-inhibitor resistant cells and suppress the activity of upregulated RTKs to discover novel therapeutic combinations as improved strategies for targeted therapy. Upregulation of activated signalling proteins AKT and ERK was identified in response to short-term FGFR4 inhibitor treatment of a TNBC and HCC cell line respectively, highlighting that the FGFR4 network is rewired to overcome the FGFR4 inhibition. In these models, corresponding combination treatment with a FGFR4 inhibitor and AKT or MEK inhibitors resulted in a greater decrease in cell proliferation, highlighting co-targeting FGFR4 and AKT/ERK as novel treatment strategies to reduce tumour progression *in vivo*. In the TNBC cell line, ErbB2 exhibited a marked increase after long-term FGFR4 inhibition and development of drug resistance, and co-targeting FGFR4 and ErbB2 significantly decreased cell proliferation, suggesting a switch in receptor signalling. Overall, the identification and characterisation of upregulated RTKs post-FGFR inhibition is important to reveal mechanisms of resistance to targeted therapy, including the switch in receptor dependency and highlights promising treatment strategies for clinical trials.

### **Chapter 6: Discussion**

This chapter summarises the work conducted and highlights the key results. The main conclusions from each chapter are noted. Future directions and perspectives of the work are discussed.



## 1.8 References

1. **Mattiuzzi, C. and G. Lippi**, *Current Cancer Epidemiology*. Journal of epidemiology and global health, 2019. 9(4): p. 217-222.
2. **Bray, F., J. Ferlay, I. Soerjomataram, R.L. Siegel, L.A. Torre, and A. Jemal**, *Global cancer statistics 2018: GLOBOCAN estimates of incidence and mortality worldwide for 36 cancers in 185 countries*. CA Cancer Journal for Clinicians, 2018. 68(6): p. 394-424.
3. **Ferlay, J., I. Soerjomataram, R. Dikshit, S. Eser, C. Mathers, M. Rebelo, D.M. Parkin, D. Forman, and F. Bray**, *Cancer incidence and mortality worldwide: Sources, methods and major patterns in GLOBOCAN 2012*. International Journal of Cancer, 2015. 136(5): p. E359-E386.
4. **Torre, L.A., F. Islami, R.L. Siegel, E.M. Ward, and A. Jemal**, *Global cancer in women: Burden and trends*. Cancer Epidemiology Biomarkers and Prevention, 2017. 26(4): p. 444-457.
5. **Miller, K.D., R.L. Siegel, C.C. Lin, A.B. Mariotto, J.L. Kramer, J.H. Rowland, K.D. Stein, R. Alteri, and A. Jemal**, *Cancer treatment and survivorship statistics, 2016*. CA Cancer Journal for Clinicians, 2016. 66(4): p. 271-289.
6. **Cooper, G.M. and R.E. Hausman**, *The development and causes of cancer*. The cell: A molecular approach, 2000. 2.
7. **Hanahan, D. and R.A. Weinberg**, *Hallmarks of cancer: the next generation*. cell, 2011. 144(5): p. 646-674.
8. **Ferlay, J., M. Colombet, I. Soerjomataram, C. Mathers, D.M. Parkin, M. Piñeros, A. Znaor, and F. Bray**, *Estimating the global cancer incidence and mortality in 2018: GLOBOCAN sources and methods*. International Journal of Cancer, 2019. 144(8): p. 1941-1953.
9. **Kao, J., K. Salari, M. Bocanegra, Y.L. Choi, L. Girard, J. Gandhi, K.A. Kwei, T. Hernandez-Boussard, P. Wang, A.F. Gazdar, J.D. Minna, and J.R. Pollack**, *Molecular profiling of breast cancer cell lines defines relevant tumor models and provides a resource for cancer gene discovery*. PLoS ONE, 2009. 4(7).

10. **Guido, L.P. and C. Gomez-Fernandez**, *Advances in the Molecular Taxonomy of Breast Cancer*. Archives of Medical Research, 2020.
11. **Sørli, T., C.M. Perou, R. Tibshirani, T. Aas, S. Geisler, H. Johnsen, T. Hastie, M.B. Eisen, M. Van De Rijn, S.S. Jeffrey, T. Thorsen, H. Quist, J.C. Matese, P.O. Brown, D. Botstein, P.E. Lønning, and A.L. Børresen-Dale**, *Gene expression patterns of breast carcinomas distinguish tumor subclasses with clinical implications*. Proceedings of the National Academy of Sciences of the United States of America, 2001. 98(19): p. 10869-10874.
12. **Chin, K., S. DeVries, J. Fridlyand, P.T. Spellman, R. Roydasgupta, W.L. Kuo, A. Lapuk, R.M. Neve, Z. Qian, T. Ryder, F. Chen, H. Feiler, T. Tokuyasu, C. Kingsley, S. Dairkee, Z. Meng, K. Chew, D. Pinkel, A. Jain, B.M. Ljung, L. Esserman, D.G. Albertson, F.M. Waldman, and J.W. Gray**, *Genomic and transcriptional aberrations linked to breast cancer pathophysiologies*. Cancer Cell, 2006. 10(6): p. 529-541.
13. **Malone, E.R., M. Oliva, P.J. Sabatini, T.L. Stockley, and L.L. Siu**, *Molecular profiling for precision cancer therapies*. Genome medicine, 2020. 12(1): p. 8.
14. **Dai, X., T. Li, Z. Bai, Y. Yang, X. Liu, J. Zhan, and B. Shi**, *Breast cancer intrinsic subtype classification, clinical use and future trends*. American journal of cancer research, 2015. 5(10): p. 2929.
15. **Liedtke, C. and A. Rody**, *New treatment strategies for patients with triple-negative breast cancer*. Current Opinion in Obstetrics and Gynecology, 2015. 27(1): p. 77-84.
16. **Reis-Filho, J.S. and A.N.J. Tutt**, *Triple negative tumours: A critical review*. Histopathology, 2008. 52(1): p. 108-118.
17. **Burstein, M.D., A. Tsimelzon, G.M. Poage, K.R. Covington, A. Contreras, S.A.W. Fuqua, M.I. Savage, C.K. Osborne, S.G. Hilsenbeck, J.C. Chang, G.B. Mills, C.C. Lau, and P.H. Brown**, *Comprehensive genomic analysis identifies novel subtypes and targets of triple-negative breast cancer*. Clinical Cancer Research, 2015. 21(7): p. 1688-1698.
18. **Dent, R., M. Trudeau, K.I. Pritchard, W.M. Hanna, H.K. Kahn, C.A. Sawka, L.A. Lickley, E. Rawlinson, P. Sun, and S.A. Narod**, *Triple-negative breast cancer:*

- Clinical features and patterns of recurrence*. Clinical Cancer Research, 2007. 13(15): p. 4429-4434.
19. **Waks, A.G. and E.P. Winer**, *Breast cancer treatment: a review*. Jama, 2019. 321(3): p. 288-300.
  20. **Fisher, B., S. Anderson, J. Bryant, R.G. Margolese, M. Deutsch, E.R. Fisher, J.-H. Jeong, and N. Wolmark**, *Twenty-year follow-up of a randomized trial comparing total mastectomy, lumpectomy, and lumpectomy plus irradiation for the treatment of invasive breast cancer*. New England Journal of Medicine, 2002. 347(16): p. 1233-1241.
  21. **Moo, T.-A., R. Sanford, C. Dang, and M. Morrow**, *Overview of breast cancer therapy*. PET clinics, 2018. 13(3): p. 339-354.
  22. **Asselain, B., W. Barlow, J. Bartlett, J. Bergh, E. Bergsten-Nordström, J. Bliss, F. Boccardo, C. Boddington, J. Bogaerts, and G. Bonadonna**, *Long-term outcomes for neoadjuvant versus adjuvant chemotherapy in early breast cancer: meta-analysis of individual patient data from ten randomised trials*. The Lancet Oncology, 2018. 19(1): p. 27-39.
  23. **Galluzzi, L., J. Humeau, A. Buqué, L. Zitvogel, and G. Kroemer**, *Immunostimulation with chemotherapy in the era of immune checkpoint inhibitors*. Nature Reviews Clinical Oncology, 2020: p. 1-17.
  24. **Group, E.B.C.T.C.**, *Comparisons between different polychemotherapy regimens for early breast cancer: meta-analyses of long-term outcome among 100 000 women in 123 randomised trials*. The Lancet, 2012. 379(9814): p. 432-444.
  25. **Dean, M., J. Boland, M. Yeager, K.M. Im, L. Garland, M. Rodriguez-Herrera, M. Perez, J. Mitchell, D. Roberson, K. Jones, H.J. Lee, R. Eggebeen, J. Sawitzke, S. Bass, X. Zhang, V. Robles, C. Hollis, C. Barajas, E. Rath, C. Arentz, J.A. Figueroa, D.D. Nguyen, and Z. Nahleh**, *Addressing health disparities in Hispanic breast cancer: accurate and inexpensive sequencing of BRCA1 and BRCA2*. GigaScience, 2015. 4: p. 50.
  26. **Schmidt, S., L. Schneider, F. Essmann, I.C. Cirstea, F. Kuck, A. Kletke, R.U. Jänicke, C. Wiek, H. Hanenberg, M.R. Ahmadian, K. Schulze-Osthoff, B. Nürnberg, and R.P. Piekorz**, *The centrosomal protein TACC3 controls paclitaxel*

- sensitivity by modulating a premature senescence program. Oncogene, 2010. 29(46): p. 6184-6192.*
27. **Howard-Anderson, J., P.A. Ganz, J.E. Bower, and A.L. Stanton,** *Quality of life, fertility concerns, and behavioral health outcomes in younger breast cancer survivors: A systematic review. Journal of the National Cancer Institute, 2012. 104(5): p. 386-405.*
  28. **Pinto, A.C. and E. De Azambuja,** *Improving quality of life after breast cancer: Dealing with symptoms. Maturitas, 2011. 70(4): p. 343-348.*
  29. **DiSipio, T., S. Rye, B. Newman, and S. Hayes,** *Incidence of unilateral arm lymphoedema after breast cancer: A systematic review and meta-analysis. The Lancet Oncology, 2013. 14(6): p. 500-515.*
  30. **Desantis, C.E., C.C. Lin, A.B. Mariotto, R.L. Siegel, K.D. Stein, J.L. Kramer, R. Alteri, A.S. Robbins, and A. Jemal,** *Cancer treatment and survivorship statistics, 2014. CA Cancer Journal for Clinicians, 2014. 64(4): p. 252-271.*
  31. **Huppa, J.B. and M.M. Davis,** *T-cell-antigen recognition and the immunological synapse. Nature Reviews Immunology, 2003. 3(12): p. 973-983.*
  32. **Smyth, M.J., G.P. Dunn, and R.D. Schreiber,** *Cancer immunosurveillance and immunoediting: the roles of immunity in suppressing tumor development and shaping tumor immunogenicity. Advances in immunology, 2006. 90: p. 1-50.*
  33. **DeNardo, D.G. and L.M. Coussens,** *Inflammation and breast cancer. Balancing immune response: crosstalk between adaptive and innate immune cells during breast cancer progression. Breast Cancer Research, 2007. 9(4): p. 212.*
  34. **Edechi, C.A., N. Ikeogu, J.E. Uzonna, and Y. Myal,** *Regulation of immunity in breast cancer. Cancers, 2019. 11(8): p. 1080.*
  35. **Drake, C.G., E.J. Lipson, and J.R. Brahmer,** *Breathing new life into immunotherapy: review of melanoma, lung and kidney cancer. Nature reviews Clinical oncology, 2014. 11(1): p. 24.*
  36. **Brown, C.E. and C.L. Mackall,** *CAR T cell therapy: inroads to response and resistance. Nature Reviews Immunology, 2019. 19(2): p. 73.*
  37. **Lee, C., M. Lee, and I. Rhee,** *Distinct features of dendritic cell-based immunotherapy as cancer vaccines. Clinical and experimental vaccine research, 2018. 7(1): p. 16-23.*

38. **Ribas, A.**, *Adaptive immune resistance: how cancer protects from immune attack*. Cancer discovery, 2015. 5(9): p. 915-919.
39. **Allard, B., P.A. Beavis, P.K. Darcy, and J. Stagg**, *Immunosuppressive activities of adenosine in cancer*. Current opinion in pharmacology, 2016. 29: p. 7-16.
40. **Brahmer, J.R., S.S. Tykodi, L.Q. Chow, W.-J. Hwu, S.L. Topalian, P. Hwu, C.G. Drake, L.H. Camacho, J. Kauh, and K. Odunsi**, *Safety and activity of anti-PD-L1 antibody in patients with advanced cancer*. New England Journal of Medicine, 2012. 366(26): p. 2455-2465.
41. **Topalian, S.L., F.S. Hodi, J.R. Brahmer, S.N. Gettinger, D.C. Smith, D.F. McDermott, J.D. Powderly, R.D. Carvajal, J.A. Sosman, and M.B. Atkins**, *Safety, activity, and immune correlates of anti-PD-1 antibody in cancer*. New England Journal of Medicine, 2012. 366(26): p. 2443-2454.
42. **Topalian, S.L., C.G. Drake, and D.M. Pardoll**, *Targeting the PD-1/B7-H1 (PD-L1) pathway to activate anti-tumor immunity*. Current opinion in immunology, 2012. 24(2): p. 207-212.
43. **Cyprian, F.S., S. Akhtar, Z. Gatalica, and S. Vranic**, *Targeted immunotherapy with a checkpoint inhibitor in combination with chemotherapy: A new clinical paradigm in the treatment of triple-negative breast cancer*. Bosnian journal of basic medical sciences, 2019. 19(3): p. 227.
44. **Nanda, R., L.Q. Chow, E.C. Dees, R. Berger, S. Gupta, R. Geva, L. Pusztai, K. Pathiraja, G. Aktan, and J.D. Cheng**, *Pembrolizumab in patients with advanced triple-negative breast cancer: phase Ib KEYNOTE-012 study*. Journal of Clinical Oncology, 2016. 34(21): p. 2460.
45. **Galluzzi, L., A. Buqué, O. Kepp, L. Zitvogel, and G. Kroemer**, *Immunogenic cell death in cancer and infectious disease*. Nature Reviews Immunology, 2017. 17(2): p. 97.
46. **Demaria, S., E.B. Golden, and S.C. Formenti**, *Role of local radiation therapy in cancer immunotherapy*. JAMA oncology, 2015. 1(9): p. 1325-1332.
47. **Savas, P., R. Salgado, C. Denkert, C. Sotiriou, P.K. Darcy, M.J. Smyth, and S. Loi**, *Clinical relevance of host immunity in breast cancer: from TILs to the clinic*. Nature reviews Clinical oncology, 2016. 13(4): p. 228.

48. **Cimino-Mathews, A., E. Thompson, J.M. Taube, X. Ye, Y. Lu, A. Meeker, H. Xu, R. Sharma, K. Lecksell, and T.C. Cornish**, *PD-L1 (B7-H1) expression and the immune tumor microenvironment in primary and metastatic breast carcinomas*. Human pathology, 2016. 47(1): p. 52-63.
49. **Yersal, O. and S. Barutca**, *Biological subtypes of breast cancer: Prognostic and therapeutic implications*. World journal of clinical oncology, 2014. 5(3): p. 412.
50. **Fisher, B., J.P. Costantino, D.L. Wickerham, C.K. Redmond, M. Kavanah, W.M. Cronin, V. Vogel, A. Robidoux, N. Dimitrov, and J. Atkins**, *Tamoxifen for prevention of breast cancer: report of the National Surgical Adjuvant Breast and Bowel Project P-1 Study*. JNCI: Journal of the National Cancer Institute, 1998. 90(18): p. 1371-1388.
51. **Walker, A.J., S. Wedam, L. Amiri-Kordestani, E. Bloomquist, S. Tang, R. Sridhara, W. Chen, T.R. Palmby, J.F. Zirkelbach, and W. Fu**, *FDA approval of palbociclib in combination with fulvestrant for the treatment of hormone receptor–positive, HER2-negative metastatic breast cancer*. Clinical Cancer Research, 2016. 22(20): p. 4968-4972.
52. **Smith, I.E. and M. Dowsett**, *Aromatase inhibitors in breast cancer*. New England Journal of Medicine, 2003. 348(24): p. 2431-2442.
53. **Clemons, M., S. Danson, and A. Howell**, *Tamoxifen ('Nolvadex'): a review: Antitumour treatment*. Cancer treatment reviews, 2002. 28(4): p. 165-180.
54. **Nilsson, S. and J.Å. Gustafsson**, *Estrogen receptors: therapies targeted to receptor subtypes*. Clinical Pharmacology & Therapeutics, 2011. 89(1): p. 44-55.
55. **Fisher, B., J.P. Costantino, C.K. Redmond, E.R. Fisher, D.L. Wickerham, W.M. Cronin, and N. contributors**, *Endometrial cancer in tamoxifen-treated breast cancer patients: findings from the National Surgical Adjuvant Breast and Bowel Project (NSABP) B-14*. JNCI: Journal of the National Cancer Institute, 1994. 86(7): p. 527-537.
56. **Group, E.B.C.T.C.**, *Relevance of breast cancer hormone receptors and other factors to the efficacy of adjuvant tamoxifen: patient-level meta-analysis of randomised trials*. The lancet, 2011. 378(9793): p. 771-784.
57. **Johnston, S.R. and M. Dowsett**, *Aromatase inhibitors for breast cancer: lessons from the laboratory*. Nature Reviews Cancer, 2003. 3(11): p. 821-831.

58. **Chumsri, S., T. Howes, T. Bao, G. Sabnis, and A. Brodie**, *Aromatase, aromatase inhibitors, and breast cancer*. The Journal of steroid biochemistry and molecular biology, 2011. 125(1-2): p. 13-22.
59. **Osborne, C., A. Wakeling, and R. Nicholson**, *Fulvestrant: an oestrogen receptor antagonist with a novel mechanism of action*. British journal of cancer, 2004. 90(1): p. S2-S6.
60. **Robertson, J.F., K.-L. Cheung, S. Noguchi, Z. Shao, A. Degboe, J. Lichfield, J. Thirlwell, M. Fazal, and M.J. Ellis**, *Health-related quality of life from the FALCON phase III randomised trial of fulvestrant 500 mg versus anastrozole for hormone receptor-positive advanced breast cancer*. European Journal of Cancer, 2018. 94: p. 206-215.
61. **Robertson, J.F., Z. Jiang, A. Di Leo, S. Ohno, K.I. Pritchard, M. Ellis, I. Bradbury, and C. Campbell**, *A meta-analysis of clinical benefit rates for fulvestrant 500 mg vs. alternative endocrine therapies for hormone receptor-positive advanced breast cancer*. Breast Cancer, 2019. 26(6): p. 703-711.
62. **Nielsen, D.L., M. Andersson, and C. Kamby**, *HER2-targeted therapy in breast cancer. Monoclonal antibodies and tyrosine kinase inhibitors*. Cancer treatment reviews, 2009. 35(2): p. 121-136.
63. **Nahta, R., D. Yu, M.-C. Hung, G.N. Hortobagyi, and F.J. Esteva**, *Mechanisms of disease: understanding resistance to HER2-targeted therapy in human breast cancer*. Nature clinical practice Oncology, 2006. 3(5): p. 269-280.
64. **Azuma, K., J. Tsurutani, K. Sakai, H. Kaneda, Y. Fujisaka, M. Takeda, M. Watatani, T. Arao, T. Satoh, I. Okamoto, T. Kurata, K. Nishio, and K. Nakagawa**, *Switching addictions between HER2 and FGFR2 in HER2-positive breast tumor cells: FGFR2 as a potential target for salvage after lapatinib failure*. Biochemical and Biophysical Research Communications, 2011. 407(1): p. 219-224.
65. **Mayer, I.A., V.G. Abramson, L. Formisano, J.M. Balko, M.V. Estrada, M.E. Sanders, D. Juric, D. Solit, M.F. Berger, and H.H. Won**, *A phase Ib study of alpelisib (BYL719), a PI3K $\alpha$ -specific inhibitor, with letrozole in ER+/HER2- metastatic breast cancer*. Clinical cancer research, 2017. 23(1): p. 26-34.



66. **Azim, H.A., M. Ghosn, K. Oualla, and L. Kassem**, *Personalized treatment in metastatic triple-negative breast cancer: The outlook in 2020*. Breast Journal, 2020. 26(1): p. 69-80.
67. **Alberts, B., A. Johnson, J. Lewis, M. Raff, K. Roberts, and P. Walter**, *General principles of cell communication*, in *Molecular Biology of the Cell*. 4th edition. 2002, Garland Science.
68. **Wilson, L.J., A. Linley, D.E. Hammond, F.E. Hood, J.M. Coulson, D.J. MacEwan, S.J. Ross, J.R. Slupsky, P.D. Smith, and P.A. Eyers**, *New perspectives, opportunities, and challenges in exploring the human protein kinome*. Cancer research, 2018. 78(1): p. 15-29.
69. **Ha, J.R., P.M. Siegel, and J. Ursini-Siegel**, *The Tyrosine Kinome Dictates Breast Cancer Heterogeneity and Therapeutic Responsiveness*. Journal of Cellular Biochemistry, 2016: p. 1971-1990.
70. **Fleuren, E.D.G., L. Zhang, J. Wu, and R.J. Daly**, *The kinome 'at large' in cancer*. Nature Reviews Cancer, 2016. 16(2): p. 83-98.
71. **Hubbard, S.R. and J.H. Till**, *Protein tyrosine kinase structure and function*. Annual review of biochemistry, 2000. 69(1): p. 373-398.
72. **Regad, T.**, *Targeting RTK signaling pathways in cancer*. Cancers, 2015. 7(3): p. 1758-1784.
73. **Schlessinger, J. and M.A. Lemmon**, *SH2 and PTB domains in tyrosine kinase signaling*. Science's STKE, 2003. 2003(191): p. re12-re12.
74. **Pawson, T. and J.D. Scott**, *Signaling through scaffold, anchoring, and adaptor proteins*. Science, 1997. 278(5346): p. 2075-2080.
75. **Wöhrle, F.U., R.J. Daly, and T. Brummer**, *Function, regulation and pathological roles of the Gab/DOS docking proteins*. Cell Communication and Signaling, 2009. 7(1): p. 22.
76. **Hubbard, S.R. and W.T. Miller**, *Receptor tyrosine kinases: mechanisms of activation and signaling*. Current Opinion in Cell Biology, 2007. 19(2): p. 117-123.
77. **Hunter, T.**, *Oncoprotein networks*. Cell, 1997. 88(3): p. 333-346.
78. **Robinson, D.R., Y.-M. Wu, and S.-F. Lin**, *The protein tyrosine kinase family of the human genome*. Oncogene, 2000. 19(49): p. 5548-5557.



79. **Fruman, D.A., R.E. Meyers, and L.C. Cantley**, *Phosphoinositide kinases*. 1998, Annual Reviews 4139 El Camino Way, PO Box 10139, Palo Alto, CA 94303-0139, USA.
80. **Vara, J.Á.F., E. Casado, J. de Castro, P. Cejas, C. Belda-Iniesta, and M. González-Barón**, *PI3K/Akt signalling pathway and cancer*. Cancer treatment reviews, 2004. 30(2): p. 193-204.
81. **Manning, B.D. and L.C. Cantley**, *AKT/PKB signaling: navigating downstream*. Cell, 2007. 129(7): p. 1261-1274.
82. **Song, G., G. Ouyang, and S. Bao**, *The activation of Akt/PKB signaling pathway and cell survival*. Journal of cellular and molecular medicine, 2005. 9(1): p. 59-71.
83. **Franke, T.**, *PI3K/Akt: getting it right matters*. Oncogene, 2008. 27(50): p. 6473-6488.
84. **Zhang, X., N. Tang, T.J. Hadden, and A.K. Rishi**, *Akt, FoxO and regulation of apoptosis*. Biochimica et Biophysica Acta (BBA)-Molecular Cell Research, 2011. 1813(11): p. 1978-1986.
85. **Brunet, A., A. Bonni, M.J. Zigmond, M.Z. Lin, P. Juo, L.S. Hu, M.J. Anderson, K.C. Arden, J. Blenis, and M.E. Greenberg**, *Akt promotes cell survival by phosphorylating and inhibiting a Forkhead transcription factor*. cell, 1999. 96(6): p. 857-868.
86. **Roberts, P.J. and C.J. Der**, *Targeting the Raf-MEK-ERK mitogen-activated protein kinase cascade for the treatment of cancer*. Oncogene, 2007. 26(22): p. 3291-3310.
87. **Jorissen, R.N., F. Walker, N. Pouliot, T.P. Garrett, C.W. Ward, and A.W. Burgess**, *Epidermal growth factor receptor: mechanisms of activation and signalling, in The EGF receptor family*. 2003, Elsevier. p. 33-55.
88. **De Luca, A., M.R. Maiello, A. D'Alessio, M. Pergameno, and N. Normanno**, *The RAS/RAF/MEK/ERK and the PI3K/AKT signalling pathways: role in cancer pathogenesis and implications for therapeutic approaches*. Expert opinion on therapeutic targets, 2012. 16(sup2): p. S17-S27.
89. **Kolch, W.**, *Coordinating ERK/MAPK signalling through scaffolds and inhibitors*. Nature reviews Molecular cell biology, 2005. 6(11): p. 827-837.

90. **Stark, G.R., I.M. Kerr, B.R. Williams, R.H. Silverman, and R.D. Schreiber**, *How cells respond to interferons*. 1998, Annual Reviews 4139 El Camino Way, PO Box 10139, Palo Alto, CA 94303-0139, USA.
91. **Darnell, J.E.**, *STATs and gene regulation*. Science, 1997. 277(5332): p. 1630-1635.
92. **Shuai, K. and B. Liu**, *Regulation of JAK–STAT signalling in the immune system*. Nature Reviews Immunology, 2003. 3(11): p. 900-911.
93. **Levy, D.E. and J. Darnell**, *Stats: transcriptional control and biological impact*. Nature reviews Molecular cell biology, 2002. 3(9): p. 651-662.
94. **Starr, R., T.A. Willson, E.M. Viney, L.J. Murray, J.R. Rayner, B.J. Jenkins, T.J. Gonda, W.S. Alexander, D. Metcalf, and N.A. Nicola**, *A family of cytokine-inducible inhibitors of signalling*. Nature, 1997. 387(6636): p. 917-921.
95. **Endo, T.A., M. Masuhara, M. Yokouchi, R. Suzuki, H. Sakamoto, K. Mitsui, A. Matsumoto, S. Tanimura, M. Ohtsubo, and H. Misawa**, *A new protein containing an SH2 domain that inhibits JAK kinases*. Nature, 1997. 387(6636): p. 921-924.
96. **Neel, B.G.** *Structure and function of SH2-domain containing tyrosine phosphatases*. in *Seminars in cell biology*. 1993. Elsevier.
97. **Shuai, K. and B. Liu**, *Regulation of gene-activation pathways by PIAS proteins in the immune system*. Nature Reviews Immunology, 2005. 5(8): p. 593-605.
98. **Chell, V., K. Balmanno, A.S. Little, M. Wilson, S. Andrews, L. Blockley, M. Hampson, P.R. Gavine, and S.J. Cook**, *Tumour cell responses to new fibroblast growth factor receptor tyrosine kinase inhibitors and identification of a gatekeeper mutation in FGFR3 as a mechanism of acquired resistance*. Oncogene, 2013. 32(25): p. 3059-3070.
99. **Turner, N. and R. Grose**, *Fibroblast growth factor signalling: From development to cancer*. Nature Reviews Cancer, 2010. 10(2): p. 116-129.
100. **Brooks, A.N., E. Kilgour, and P.D. Smith**, *Molecular pathways: Fibroblast growth factor signaling: A new therapeutic opportunity in cancer*. Clinical Cancer Research, 2012. 18(7): p. 1855-1862.
101. **Olsen, S.K., O.A. Ibrahimi, A. Raucci, F. Zhang, A.V. Eliseenkova, A. Yayon, C. Basilico, R.J. Linhardt, J. Schlessinger, and M. Mohammadi**, *Insights into the molecular basis for fibroblast growth factor receptor autoinhibition and ligand-*

- binding promiscuity*. Proceedings of the National Academy of Sciences, 2004. 101(4): p. 935-940.
102. **Kalinina, J., K. Dutta, D. Ilghari, A. Beenken, R. Goetz, A.V. Eliseenkova, D. Cowburn, and M. Mohammadi**, *The alternatively spliced acid box region plays a key role in FGF receptor autoinhibition*. Structure, 2012. 20(1): p. 77-88.
103. **Itoh, N. and D.M. Ornitz**, *Fibroblast growth factors: From molecular evolution to roles in development, metabolism and disease*. Journal of Biochemistry, 2011. 149(2): p. 121-130.
104. **Brady, N.J., P. Chuntova, L.K. Bade, and K.L. Schwertfeger**, *The FGF/FGF receptor axis as a therapeutic target in breast cancer*. Expert Review of Endocrinology and Metabolism, 2013. 8(4): p. 391-402.
105. **Ornitz, D.M. and N. Itoh**, *The fibroblast growth factor signaling pathway*. Wiley Interdisciplinary Reviews: Developmental Biology, 2015. 4(3): p. 215-266.
106. **Porta, R., R. Borea, A. Coelho, S. Khan, A. Araújo, P. Reclusa, T. Franchina, N. Van Der Steen, P. Van Dam, and J. Ferri**, *FGFR a promising druggable target in cancer: Molecular biology and new drugs*. Critical Reviews in Oncology/Hematology, 2017. 113: p. 256-267.
107. **Eswarakumar, V.P., I. Lax, and J. Schlessinger**, *Cellular signaling by fibroblast growth factor receptors*. Cytokine and Growth Factor Reviews, 2005. 16(2 SPEC. ISS.): p. 139-149.
108. **Gong, S.G.**, *Isoforms of receptors of fibroblast growth factors*. Journal of cellular physiology, 2014. 229(12): p. 1887-1895.
109. **Mohammadi, M., S.K. Olsen, and O.A. Ibrahimi**, *Structural basis for fibroblast growth factor receptor activation*. Cytokine & growth factor reviews, 2005. 16(2): p. 107-137.
110. **André, F. and J. Cortés**, *Rationale for targeting fibroblast growth factor receptor signaling in breast cancer*. Breast Cancer Research and Treatment, 2015. 150(1): p. 1-8.
111. **Gallo, L.H., K.N. Nelson, A.N. Meyer, and D.J. Donoghue**, *Functions of Fibroblast Growth Factor Receptors in cancer defined by novel translocations and mutations*. Cytokine and Growth Factor Reviews, 2015. 26(4): p. 425-449.

112. **Touat, M., E. Ileana, S. Postel-Vinay, F. André, and J.C. Soria**, *Targeting FGFR signaling in cancer*. Clinical Cancer Research, 2015. 21(12): p. 2684-2694.
113. **Beenken, A. and M. Mohammadi**, *The FGF family: biology, pathophysiology and therapy*. Nature reviews Drug discovery, 2009. 8(3): p. 235-253.
114. **Ahmad, I., T. Iwata, and H.Y. Leung**, *Mechanisms of FGFR-mediated carcinogenesis*. Biochimica et Biophysica Acta (BBA)-Molecular Cell Research, 2012. 1823(4): p. 850-860.
115. **Knights, V. and S.J. Cook**, *De-regulated FGF receptors as therapeutic targets in cancer*. Pharmacology & therapeutics, 2010. 125(1): p. 105-117.
116. **Powers, C., S. McLeskey, and A. Wellstein**, *Fibroblast growth factors, their receptors and signaling*. Endocrine-related cancer, 2000. 7(3): p. 165-197.
117. **Mohammadi, M., A. Honegger, D. Rotin, R. Fischer, F. Bellot, W. Li, C. Dionne, M. Jaye, M. Rubinstein, and J. Schlessinger**, *A tyrosine-phosphorylated carboxy-terminal peptide of the fibroblast growth factor receptor (Flg) is a binding site for the SH2 domain of phospholipase C-gamma 1*. Molecular and cellular biology, 1991. 11(10): p. 5068-5078.
118. **Mohammadi, M., I. Dikic, A. Sorokin, W. Burgess, M. Jaye, and J. Schlessinger**, *Identification of six novel autophosphorylation sites on fibroblast growth factor receptor 1 and elucidation of their importance in receptor activation and signal transduction*. Molecular and cellular biology, 1996. 16(3): p. 977-989.
119. **Furdui, C.M., E.D. Lew, J. Schlessinger, and K.S. Anderson**, *Autophosphorylation of FGFR1 kinase is mediated by a sequential and precisely ordered reaction*. Molecular cell, 2006. 21(5): p. 711-717.
120. **Dailey, L., D. Ambrosetti, A. Mansukhani, and C. Basilico**, *Mechanisms underlying differential responses to FGF signaling*. Cytokine & growth factor reviews, 2005. 16(2): p. 233-247.
121. **Wesche, J., K. Haglund, and E.M. Haugsten**, *Fibroblast growth factors and their receptors in cancer*. Biochemical Journal, 2011. 437(2): p. 199-213.
122. **Lax, I., A. Wong, B. Lamothe, A. Lee, A. Frost, J. Hawes, and J. Schlessinger**, *The docking protein FRS2 $\alpha$  controls a MAP kinase-mediated negative feedback mechanism for signaling by FGF receptors*. Molecular Cell, 2002. 10(4): p. 709-719.

123. **Fürthauer, M., W. Lin, S.-L. Ang, B. Thisse, and C. Thisse**, *Sef is a feedback-induced antagonist of Ras/MAPK-mediated FGF signalling*. Nature cell biology, 2002. 4(2): p. 170-174.
124. **Tsang, M., R. Friesel, T. Kudoh, and I.B. Dawid**, *Identification of Sef, a novel modulator of FGF signalling*. Nature cell biology, 2002. 4(2): p. 165-169.
125. **Haugsten, E.M., A. Wiedlocha, S. Olsnes, and J. Wesche**, *Roles of fibroblast growth factor receptors in carcinogenesis*. Molecular Cancer Research, 2010. 8(11): p. 1439-1452.
126. **Perez-Garcia, J., E. Muñoz-Couselo, J. Soberino, F. Racca, and J. Cortes**, *Targeting FGFR pathway in breast cancer*. Breast, 2018. 37: p. 126-133.
127. **Babina, I.S. and N.C. Turner**, *Advances and challenges in targeting FGFR signalling in cancer*. Nature Reviews Cancer, 2017. 17(5): p. 318-332.
128. **Helsten, T., S. Elkin, E. Arthur, B.N. Tomson, J. Carter, and R. Kurzrock**, *The FGFR landscape in cancer: Analysis of 4,853 tumors by next-generation sequencing*. Clinical Cancer Research, 2016. 22(1): p. 259-267.
129. **Turner, N., A. Pearson, R. Sharpe, M. Lambros, F. Geyer, M.A. Lopez-Garcia, R. Natrajan, C. Marchio, E. Iorns, A. Mackay, C. Gillett, A. Grigoriadis, A. Tutt, J.S. Reis-Filho, and A. Ashworth**, *FGFR1 amplification drives endocrine therapy resistance and is a therapeutic target in breast cancer*. Cancer Research, 2010. 70(5): p. 2085-2094.
130. **Elbauomy Elsheikh, S., A.R. Green, M.B. Lambros, N.C. Turner, M.J. Grainge, D. Powe, I.O. Ellis, and J.S. Reis-Filho**, *FGFR1 amplification in breast carcinomas: a chromogenic in situ hybridisation analysis*. Breast cancer research : BCR, 2007. 9(2).
131. **Reis-Filho, J.S., P.T. Simpson, N.C. Turner, M.B. Lambros, C. Jones, A. Mackay, A. Grigoriadis, D. Sarrio, K. Savage, T. Dexter, M. Iravani, K. Fenwick, B. Weber, D. Hardisson, F.C. Schmitt, J. Palacios, S.R. Lakhani, and A. Ashworth**, *FGFR1 emerges as a potential therapeutic target for lobular breast carcinomas*. Clinical Cancer Research, 2006. 12(22): p. 6652-6662.
132. **Lee, H.J., A.N. Seo, S.Y. Park, J.Y. Kim, J.Y. Park, J.H. Yu, J.H. Ahn, and G. Gong**, *Low prognostic implication of fibroblast growth factor family activation in*

- triple-negative breast cancer subsets*. Annals of Surgical Oncology, 2014. 21(5): p. 1561-1568.
133. **Chang, J., X. Liu, S. Wang, Z. Zhang, Z. Wu, X. Zhang, and J. Li**, *Prognostic value of FGFR gene amplification in patients with different types of cancer: A systematic review and meta-analysis*. PLoS ONE, 2014. 9(8).
  134. **Cheng, C.L., A.A. Thike, S.Y.J. Tan, P.J. Chua, B.H. Bay, and P.H. Tan**, *Expression of FGFR1 is an independent prognostic factor in triple-negative breast cancer*. Breast Cancer Research and Treatment, 2015. 151(1): p. 99-111.
  135. **Penault-Llorca, F., F. Bertucci, J. Adelaide, P. Parc, F. Coulier, J. Jacquemier, D. Birnbaum, and O. DeLapeyriere**, *Expression of FGF and FGF receptor genes in human breast cancer*. International Journal of Cancer, 1995. 61(2): p. 170-176.
  136. **Andre, F., B. Job, P. Dessen, A. Tordai, S. Michiels, C. Liedtke, C. Richon, K. Yan, B. Wang, and G. Vassal**, *Molecular characterization of breast cancer with high-resolution oligonucleotide comparative genomic hybridization array*. Clinical cancer research, 2009. 15(2): p. 441-451.
  137. **Weiss, J., M.L. Sos, D. Seidel, M. Peifer, T. Zander, J.M. Heuckmann, R.T. Ullrich, R. Menon, S. Maier, A. Soltermann, H. Moch, P. Wagener, F. Fischer, S. Heynck, M. Koker, J. Schöttle, F. Leenders, F. Gabler, I. Dabow, S. Querings, L.C. Heukamp, H. Balke-Want, S. Ansén, D. Rauh, I. Baessmann, J. Altmüller, Z. Wainer, M. Conron, G. Wright, P. Russell, B. Solomon, E. Brambilla, C. Brambilla, P. Lorimier, S. Sollberg, O.T. Brustugun, W. Engel-Riedel, C. Ludwig, I. Petersen, J. Sängler, J. Clement, H. Groen, W. Timens, H. Sietsma, E. Thunnissen, E. Smit, D. Heideman, F. Cappuzzo, C. Ligorio, S. Damiani, M. Hallek, R. Beroukhi, W. Pao, B. Klebl, M. Baumann, R. Buettner, K. Ernestus, E. Stoelben, J. Wolf, P. Nürnberg, S. Perner, and R.K. Thomas**, *Frequent and focal FGFR1 amplification associates with therapeutically tractable FGFR1 dependency in squamous cell lung cancer*. Science Translational Medicine, 2010. 2(62).
  138. **Peifer, M., L. Fernández-Cuesta, M.L. Sos, J. George, D. Seidel, L.H. Kasper, D. Plenker, F. Leenders, R. Sun, and T. Zander**, *Integrative genome analyses identify key somatic driver mutations of small-cell lung cancer*. Nature genetics, 2012. 44(10): p. 1104-1110.

139. **Yang, W., Y.-W. Yao, J.-L. Zeng, W.-J. Liang, L. Wang, C.-Q. Bai, C.-H. Liu, and Y. Song**, *Prognostic value of FGFR1 gene copy number in patients with non-small cell lung cancer: a meta-analysis*. Journal of thoracic disease, 2014. 6(6): p. 803.
140. **Cihoric, N., S. Savic, S. Schneider, I. Ackermann, M. Bichsel-Naef, R. Schmid, D. Lardinois, M. Gugger, L. Bubendorf, and I. Zlobec**, *Prognostic role of FGFR1 amplification in early-stage non-small cell lung cancer*. British journal of cancer, 2014. 110(12): p. 2914-2922.
141. **Fumagalli, D., T.R. Wilson, R. Salgado, X. Lu, J. Yu, C. O'Brien, K. Walter, L.Y. Huw, C. Criscitiello, I. Laios, V. Jose, D.N. Brown, F. Rothé, M. Maetens, D. Zardavas, P. Savas, D. Larsimont, M.J. Piccart-Gebhart, S. Michiels, M.R. Lackner, C. Sotiriou, and S. Loi**, *Somatic mutation, copy number and transcriptomic profiles of primary and matched metastatic estrogen receptor-positive breast cancers*. Annals of Oncology, 2016. 27(10): p. 1860-1866.
142. **Rand, V., J. Huang, T. Stockwell, S. Ferriera, O. Buzko, S. Levy, D. Busam, K. Li, J.B. Edwards, and C. Eberhart**, *Sequence survey of receptor tyrosine kinases reveals mutations in glioblastomas*. Proceedings of the National Academy of Sciences, 2005. 102(40): p. 14344-14349.
143. **Singh, D., J.M. Chan, P. Zoppoli, F. Niola, R. Sullivan, A. Castano, E.M. Liu, J. Reichel, P. Porra, S. Pellegatta, K. Qiu, Z. Gao, M. Ceccarelli, R. Riccardi, D.J. Brat, A. Guha, K. Aldape, J.G. Golfinos, D. Zagzag, T. Mikkelsen, G. Finocchiaro, A. Lasorella, R. Rabadan, and A. Iavarone**, *Transforming fusions of FGFR and TACC genes in human glioblastoma*. Science, 2012. 337(6099): p. 1231-1235.
144. **Turner, N., M.B. Lambros, H.M. Horlings, A. Pearson, R. Sharpe, R. Natrajan, F.C. Geyer, M. Van Kouwenhove, B. Kreike, A. MacKay, A. Ashworth, M.J. Van De Vijver, and J.S. Reis-Filho**, *Integrative molecular profiling of triple negative breast cancers identifies amplicon drivers and potential therapeutic targets*. Oncogene, 2010. 29(14): p. 2013-2023.
145. **Matsumoto, K., T. Arao, T. Hamaguchi, Y. Shimada, K. Kato, I. Oda, H. Taniguchi, F. Koizumi, K. Yanagihara, and H. Sasaki**, *FGFR2 gene amplification and clinicopathological features in gastric cancer*. British journal of cancer, 2012. 106(4): p. 727-732.



146. **Xie, L., X. Su, L. Zhang, X. Yin, L. Tang, X. Zhang, Y. Xu, Z. Gao, K. Liu, and M. Zhou,** *FGFR2 gene amplification in gastric cancer predicts sensitivity to the selective FGFR inhibitor AZD4547*. *Clinical cancer research*, 2013. 19(9): p. 2572-2583.
147. **Dutt, A., H.B. Salvesen, T.-H. Chen, A.H. Ramos, R.C. Onofrio, C. Hatton, R. Nicoletti, W. Winckler, R. Grewal, and M. Hanna,** *Drug-sensitive FGFR2 mutations in endometrial carcinoma*. *Proceedings of the National Academy of Sciences*, 2008. 105(25): p. 8713-8717.
148. **Liao, R.G., J. Jung, J. Tchaicha, M.D. Wilkerson, A. Sivachenko, E.M. Beauchamp, Q. Liu, T.J. Pugh, C.S. Peadamallu, and D.N. Hayes,** *Inhibitor-sensitive FGFR2 and FGFR3 mutations in lung squamous cell carcinoma*. *Cancer research*, 2013. 73(16): p. 5195-5205.
149. **Sia, D., B. Losic, A. Moeini, L. Cabellos, K. Hao, K. Revill, D. Bonal, O. Miltiadous, Z. Zhang, Y. Hoshida, H. Cornella, M. Castillo-Martin, R. Pinyol, Y. Kasai, S. Roayaie, S.N. Thung, J. Fuster, M.E. Schwartz, S. Waxman, C. Cordon-Cardo, E. Schadt, V. Mazzaferro, and J.M. Llovet,** *Massive parallel sequencing uncovers actionable FGFR2–PPHLN1 fusion and ARAF mutations in intrahepatic cholangiocarcinoma*. *Nature Communications*, 2015. 6(1): p. 6087.
150. **Wu, Y.M., F. Su, S. Kalyana-Sundaram, N. Khazanov, B. Ateeq, X. Cao, R.J. Lonigro, P. Vats, R. Wang, S.F. Lin, A.J. Cheng, L.P. Kunju, J. Siddiqui, S.A. Tomlins, P. Wyngaard, S. Sadis, S. Roychowdhury, M.H. Hussain, F.Y. Feng, M.M. Zalupski, M. Talpaz, K.J. Pienta, D.R. Rhodes, D.R. Robinson, and A.M. Chinnaiyan,** *Identification of targetable FGFR gene fusions in diverse cancers*. *Cancer Discovery*, 2013. 3(6): p. 636-647.
151. **van Rhijn, B.W., I. Lurkin, F. Radvanyi, W.J. Kirkels, T.H. van der Kwast, and E.C. Zwarthoff,** *The fibroblast growth factor receptor 3 (FGFR3) mutation is a strong indicator of superficial bladder cancer with low recurrence rate*. *Cancer research*, 2001. 61(4): p. 1265-1268.
152. **Rosty, C., M.-H. Aubriot, D. Cappellen, J. Bourdin, I. Cartier, J.P. Thiery, X. Sastre-Garau, and F. Radvanyi,** *Clinical and biological characteristics of cervical neoplasias with FGFR3 mutation*. *Molecular cancer*, 2005. 4(1): p. 15.



153. **Williams, S.V., C.D. Hurst, and M.A. Knowles,** *Oncogenic FGFR3 gene fusions in bladder cancer.* Human Molecular Genetics, 2013. 22(4): p. 795-803.
154. **Yuan, L., Z.H. Liu, Z.R. Lin, L.H. Xu, Q. Zhong, and M.S. Zeng,** *Recurrent FGFR3-TACC3 fusion gene in nasopharyngeal carcinoma.* Cancer Biology and Therapy, 2014. 15(12): p. 1613-1621.
155. **Wang, R., L. Wang, Y. Li, H. Hu, L. Shen, X. Shen, Y. Pan, T. Ye, Y. Zhang, X. Luo, Y. Zhang, B. Pan, B. Li, H. Li, J. Zhang, W. Pao, H. Ji, Y. Sun, and H. Chen,** *FGFR1/3 tyrosine kinase fusions define a unique molecular subtype of non-small cell lung cancer.* Clinical Cancer Research, 2014. 20(15): p. 4107-4114.
156. **Tamura, R., K. Yoshihara, T. Saito, R. Ishimura, J.E. Martínez-Ledesma, H. Xin, T. Ishiguro, Y. Mori, K. Yamawaki, and K. Suda,** *Novel therapeutic strategy for cervical cancer harboring FGFR3-TACC3 fusions.* Oncogenesis, 2018. 7(1): p. 1-12.
157. **Bange, J., D. Prechtel, Y. Cheburkin, K. Specht, N. Harbeck, M. Schmitt, T. Knyazeva, S. Müller, S. Gärtner, and I. Sures,** *Cancer progression and tumor cell motility are associated with the FGFR4 Arg388 allele.* Cancer research, 2002. 62(3): p. 840-847.
158. **Spinola, M., V. Leoni, C. Pignatiello, B. Conti, F. Ravagnani, U. Pastorino, and T.A. Dragani,** *Functional FGFR4 Gly388Arg polymorphism predicts prognosis in lung adenocarcinoma patients.* Journal of clinical oncology, 2005. 23(29): p. 7307-7311.
159. **André, F., T. Bachelot, M. Campone, F. Dalenc, J.M. Perez-Garcia, S.A. Hurvitz, N. Turner, H. Rugo, J.W. Smith, S. Deudon, M. Shi, Y. Zhang, A. Kay, D.G. Porta, A. Yovine, and J. Baselga,** *Targeting FGFR with dovitinib (TKI258): Preclinical and clinical data in breast cancer.* Clinical Cancer Research, 2013. 19(13): p. 3693-3702.
160. **Guagnano, V., A. Kauffmann, S. Wöhrle, C. Stamm, M. Ito, L. Barys, A. Pornon, Y. Yao, F. Li, Y. Zhang, Z. Chen, C.J. Wilson, V. Bordas, M. Le Douget, L. Alex Gaither, J. Borawski, J.E. Monahan, K. Venkatesan, T. Brümmendorf, D.M. Thomas, C. Garcia-Echeverria, F. Hofmann, W.R. Sellers, and D. Graus-Porta,** *FGFR genetic alterations predict for sensitivity to NVP-BGJ398, a selective Pan-FGFR inhibitor.* Cancer Discovery, 2012. 2(12): p. 1118-1133.

161. **Kim, S., A. Dubrovskaya, R.J. Salamone, J.R. Walker, K.B. Grandinetti, G.M. Bonamy, A.P. Orth, J. Elliott, D.G. Porta, and C. Garcia-Echeverria, *FGFR2 promotes breast tumorigenicity through maintenance of breast tumor-initiating cells. PloS one*, 2013. 8(1): p. e51671.**
162. **Sun, S., Y. Jiang, G. Zhang, H. Song, X. Zhang, Y. Zhang, X. Liang, Q. Sun, and D. Pang, *Increased expression of fibroblastic growth factor receptor 2 is correlated with poor prognosis in patients with breast cancer. Journal of surgical oncology*, 2012. 105(8): p. 773-779.**
163. **Campbell, J., C.J. Ryan, R. Brough, I. Bajrami, H.N. Pemberton, I.Y. Chong, S. Costa-Cabral, J. Frankum, A. Gulati, H. Holme, R. Miller, S. Postel-Vinay, R. Rafiq, W. Wei, C.T. Williamson, D.A. Quigley, J. Tym, B. Al-Lazikani, T. Fenton, R. Natrajan, S.J. Strauss, A. Ashworth, and C.J. Lord, *Large-Scale Profiling of Kinase Dependencies in Cancer Cell Lines. Cell Reports*, 2016. 14(10): p. 2490-2501.**
164. **Su, X., P. Zhan, P.R. Gavine, S. Morgan, C. Womack, X. Ni, D. Shen, Y.J. Bang, S.A. Im, W. Ho Kim, E.J. Jung, H.I. Grabsch, and E. Kilgour, *FGFR2 amplification has prognostic significance in gastric cancer: Results from a large international multicentre study. British Journal of Cancer*, 2014. 110(4): p. 967-975.**
165. **Pearson, A., E. Smyth, I.S. Babina, M.T. Herrera-Abreu, N. Tarazona, C. Peckitt, E. Kilgour, N.R. Smith, C. Geh, C. Rooney, R. Cutts, J. Campbell, J. Ning, K. Fenwick, A. Swain, G. Brown, S. Chua, A. Thomas, S.R.D. Johnston, M. Ajaz, K. Sumpter, A. Gillbanks, D. Watkins, I. Chau, S. Popat, D. Cunningham, and N.C. Turner, *High-level clonal FGFR amplification and response to FGFR inhibition in a translational clinical trial. Cancer Discovery*, 2016. 6(8): p. 838-851.**
166. **Roidl, A., P. Foo, W. Wong, C. Mann, S. Bechtold, H.J. Berger, S. Streit, J.E. Ruhe, S. Hart, A. Ullrich, and H.K. Ho, *The FGFR4 Y367C mutant is a dominant oncogene in MDA-MB453 breast cancer cells. Oncogene*, 2010. 29(10): p. 1543-1552.**
167. **Meyer, K.B., A.-T. Maia, M. O'Reilly, A.E. Teschendorff, S.-F. Chin, C. Caldas, and B.A. Ponder, *Allele-specific up-regulation of FGFR2 increases susceptibility to breast cancer. PLoS Biol*, 2008. 6(5): p. e108.**
168. **Easton, D.F., K.A. Pooley, A.M. Dunning, P.D. Pharoah, D. Thompson, D.G. Ballinger, J.P. Struwing, J. Morrison, H. Field, and R. Luben, *Genome-wide***

- association study identifies novel breast cancer susceptibility loci.* Nature, 2007. 447(7148): p. 1087-1093.
169. **Stacey, S.N., A. Manolescu, P. Sulem, S. Thorlacius, S.A. Gudjonsson, G.F. Jonsson, M. Jakobsdottir, J.T. Bergthorsson, J. Gudmundsson, and K.K. Aben,** *Common variants on chromosome 5p12 confer susceptibility to estrogen receptor–positive breast cancer.* Nature genetics, 2008. 40(6): p. 703-706.
  170. **Hunter, D.J., P. Kraft, K.B. Jacobs, D.G. Cox, M. Yeager, S.E. Hankinson, S. Wacholder, Z. Wang, R. Welch, and A. Hutchinson,** *A genome-wide association study identifies alleles in FGFR2 associated with risk of sporadic postmenopausal breast cancer.* Nature genetics, 2007. 39(7): p. 870-874.
  171. **Seitzer, N., T. Mayr, S. Streit, and A. Ullrich,** *A single nucleotide change in the mouse genome accelerates breast cancer progression.* Cancer research, 2010. 70(2): p. 802-812.
  172. **Sugiyama, N., M. Varjosalo, P. Meller, J. Lohi, M. Hyytiäinen, S. Kilpinen, O. Kallioniemi, S. Ingvarsen, L.H. Engelholm, and J. Taipale,** *Fibroblast growth factor receptor 4 regulates tumor invasion by coupling fibroblast growth factor signaling to extracellular matrix degradation.* Cancer research, 2010. 70(20): p. 7851-7861.
  173. **Greenman, C., P. Stephens, R. Smith, G.L. Dalgliesh, C. Hunter, G. Bignell, H. Davies, J. Teague, A. Butler, C. Stevens, S. Edkins, S. O'Meara, I. Vastrik, E.E. Schmidt, T. Avis, S. Barthorpe, G. Bhamra, G. Buck, B. Choudhury, J. Clements, J. Cole, E. Dicks, S. Forbes, K. Gray, K. Halliday, R. Harrison, K. Hills, J. Hinton, A. Jenkinson, D. Jones, A. Menzies, T. Mironenko, J. Perry, K. Raine, D. Richardson, R. Shepherd, A. Small, C. Tofts, J. Varian, T. Webb, S. West, S. Widaa, A. Yates, D.P. Cahill, D.N. Louis, P. Goldstraw, A.G. Nicholson, F. Brasseur, L. Looijenga, B.L. Weber, Y.E. Chiew, A. DeFazio, M.F. Greaves, A.R. Green, P. Campbell, E. Birney, D.F. Easton, G. Chenevix-Trench, M.H. Tan, S.K. Khoo, B.T. Teh, S.T. Yuen, S.Y. Leung, R. Wooster, P.A. Futreal, and M.R. Stratton,** *Patterns of somatic mutation in human cancer genomes.* Nature, 2007. 446(7132): p. 153-158.

174. **Nelson, K.N., A.N. Meyer, A. Siari, A.R. Campos, K. Motamedchaboki, and D.J. Donoghue**, *Oncogenic gene fusion FGFR3-TACC3 Is regulated by tyrosine phosphorylation*. *Molecular Cancer Research*, 2016. 14(5): p. 458-469.
175. **Shaver, T.M., B.D. Lehmann, J.S. Beeler, C.I. Li, Z. Li, H. Jin, T.P. Stricker, Y. Shyr, and J.A. Pietenpol**, *Diverse, biologically relevant, and targetable gene rearrangements in triple-negative breast cancer and other malignancies*. *Cancer Research*, 2016. 76(16): p. 4850-4860.
176. **De Luca, A., D. Frezzetti, M. Gallo, and N. Normanno**, *FGFR-targeted therapeutics for the treatment of breast cancer*. *Expert Opinion on Investigational Drugs*, 2017. 26(3): p. 303-311.
177. **Ross, J.S., K. Wang, L. Gay, R. Al-Rohil, J.V. Rand, D.M. Jones, H.J. Lee, C.E. Sheehan, G.A. Otto, G. Palmer, R. Yelensky, D. Lipson, D. Morosini, M. Hawryluk, D.V.T. Catenacci, V.A. Miller, C. Churi, S. Ali, and P.J. Stephens**, *New routes to targeted therapy of intrahepatic cholangiocarcinomas revealed by next-generation sequencing*. *The oncologist*, 2014. 19(3): p. 235-242.
178. **Arai, Y., Y. Totoki, F. Hosoda, T. Shiota, N. Hama, H. Nakamura, H. Ojima, K. Furuta, K. Shimada, and T. Okusaka**, *Fibroblast growth factor receptor 2 tyrosine kinase fusions define a unique molecular subtype of cholangiocarcinoma*. *Hepatology*, 2014. 59(4): p. 1427-1434.
179. **Chae, Y.K., K. Ranganath, P.S. Hammerman, C. Vaklavas, N. Mohindra, A. Kalyan, M. Matsangou, R. Costa, B. Carneiro, and V.M. Villaflor**, *Inhibition of the fibroblast growth factor receptor (FGFR) pathway: the current landscape and barriers to clinical application*. *Oncotarget*, 2017. 8(9): p. 16052.
180. **Sharpe, R., A. Pearson, M.T. Herrera-Abreu, D. Johnson, A. Mackay, J.C. Welti, R. Natrajan, A.R. Reynolds, J.S. Reis-Filho, A. Ashworth, and N.C. Turner**, *FGFR signaling promotes the growth of triple-negative and basal-like breast cancer cell lines both in vitro and in vivo*. *Clinical Cancer Research*, 2011. 17(16): p. 5275-5286.
181. **Fillmore, C.M., P.B. Gupta, J.A. Rudnick, S. Caballero, P.J. Keller, E.S. Lander, and C. Kuperwasser**, *Estrogen expands breast cancer stem-like cells through paracrine FGF/Tbx3 signaling*. *Proceedings of the National Academy of Sciences*, 2010. 107(50): p. 21737-21742.

182. **Jiao, Q., L. Bi, Y. Ren, S. Song, Q. Wang, and Y.-s. Wang,** *Advances in studies of tyrosine kinase inhibitors and their acquired resistance.* Molecular cancer, 2018. 17(1): p. 1-12.
183. **Loriot, Y., A. Necchi, S.H. Park, J. Garcia-Donas, R. Huddart, E. Burgess, M. Fleming, A. Rezazadeh, B. Mellado, S. Varlamov, M. Joshi, I. Duran, S.T. Tagawa, Y. Zakharia, B. Zhong, K. Stuyckens, A. Santiago-Walker, P. De Porre, A. O'Hagan, A. Avadhani, and A.O. Siefker-Radtke,** *Erdaftinib in Locally Advanced or Metastatic Urothelial Carcinoma.* New England Journal of Medicine, 2019. 381(4): p. 338-348.
184. **Baselga, J.,** *Targeting tyrosine kinases in cancer: the second wave.* Science, 2006. 312(5777): p. 1175-1178.
185. **Matsui, J., Y. Yamamoto, Y. Funahashi, A. Tsuruoka, T. Watanabe, T. Wakabayashi, T. Uenaka, and M. Asada,** *E7080, a novel inhibitor that targets multiple kinases, has potent antitumor activities against stem cell factor producing human small cell lung cancer H146, based on angiogenesis inhibition.* International journal of cancer, 2008. 122(3): p. 664-671.
186. **Matsui, J., Y. Funahashi, T. Uenaka, T. Watanabe, A. Tsuruoka, and M. Asada,** *Multi-kinase inhibitor E7080 suppresses lymph node and lung metastases of human mammary breast tumor MDA-MB-231 via inhibition of vascular endothelial growth factor-receptor (VEGF-R) 2 and VEGF-R3 kinase.* Clinical Cancer Research, 2008. 14(17): p. 5459-5465.
187. **Gavine, P.R., L. Mooney, E. Kilgour, A.P. Thomas, K. Al-Kadhimi, S. Beck, C. Rooney, T. Coleman, D. Baker, M.J. Mellor, A.N. Brooks, and T. Klinowska,** *AZD4547: An orally bioavailable, potent, and selective inhibitor of the fibroblast growth factor receptor tyrosine kinase family.* Cancer Research, 2012. 72(8): p. 2045-2056.
188. **Fairhurst, R.A., T. Knoepfel, C. Leblanc, N. Buschmann, C. Gaul, J. Blank, I. Galuba, J. Trappe, C. Zou, and J. Voshol,** *Approaches to selective fibroblast growth factor receptor 4 inhibition through targeting the ATP-pocket middle-hinge region.* MedChemComm, 2017. 8(8): p. 1604-1613.

189. **Hagel, M., C. Miduturu, M. Sheets, N. Rubin, W. Weng, N. Stransky, N. Bifulco, J.L. Kim, B. Hodous, N. Brooijmans, A. Shutes, C. Winter, C. Lengauer, N.E. Kohl, and T. Guzi,** *First selective small molecule inhibitor of FGFR4 for the treatment of hepatocellular carcinomas with an activated FGFR4 signaling pathway.* Cancer Discovery, 2015. 5(4): p. 424-437.
190. **Zhao, X., F. Xu, N.P. Dominguez, Y. Xiong, Z. Xiong, H. Peng, C. Shay, and Y. Teng,** *FGFR4 provides the conduit to facilitate FGF19 signaling in breast cancer progression.* Molecular Carcinogenesis, 2018. 57(11): p. 1616-1625.
191. **Bai, A., K. Meetze, N.Y. Vo, S. Kollipara, E.K. Mazsa, W.M. Winston, S. Weiler, L.L. Poling, T. Chen, and N.S. Ismail,** *GP369, an FGFR2-IIIb-specific antibody, exhibits potent antitumor activity against human cancers driven by activated FGFR2 signaling.* Cancer research, 2010. 70(19): p. 7630-7639.
192. **Harding, T.C., L. Long, S. Palencia, H. Zhang, A. Sadra, K. Hestir, N. Patil, A. Levin, A.W. Hsu, and D. Charych,** *Blockade of nonhormonal fibroblast growth factors by FP-1039 inhibits growth of multiple types of cancer.* Science translational medicine, 2013. 5(178): p. 178ra39-178ra39.
193. **Castelli, R., A. Giacomini, M. Anselmi, N. Bozza, F. Vacondio, S. Rivara, S. Matarazzo, M. Presta, M. Mor, and R. Ronca,** *Synthesis, structural elucidation, and biological evaluation of NSC12, an orally available fibroblast growth factor (FGF) ligand trap for the treatment of FGF-dependent lung tumors.* Journal of Medicinal Chemistry, 2016. 59(10): p. 4651-4663.
194. **Joshi, J.J., H. Coffey, E. Corcoran, J. Tsai, C.L. Huang, K. Ichikawa, S. Prajapati, M.H. Hao, S. Bailey, J. Wu, V. Rimkunas, C. Karr, V. Subramanian, P. Kumar, C. MacKenzie, R. Hurley, T. Satoh, K. Yu, E. Park, N. Rioux, A. Kim, W.G. Lai, L. Yu, P. Zhu, S. Buonamici, N. Larsen, P. Fekkes, J. Wang, M. Warmuth, D.J. Reynolds, P.G. Smith, and A. Selvaraj,** *H3B-6527 Is a potent and selective inhibitor of FGFR4 in FGF19-Driven hepatocellular carcinoma.* Cancer Research, 2017. 77(24): p. 6999-7013.
195. **Issa, A., J.W. Gill, M.R. Heideman, O. Sahin, S. Wiemann, J.H. Dey, and N.E. Hynes,** *Combinatorial targeting of FGF and ErbB receptors blocks growth and metastatic spread of breast cancer models.* Breast Cancer Research, 2013. 15(1).

196. Levine KM, C.J., Sikora MJ, Tasdemir N, Priedigkeit N, Tseng GC, Puhalla SL, Jankowitz RC, Dabbs DJ, McAuliffe PF, Lee AV, Oesterreich S, *Combination FGFR4 and ER-targeted therapy for invasive lobular carcinoma*. Cancer Research, 2017.

---

## **CHAPTER 2**

### **MATERIALS AND METHODS**

---



# Chapter 2: Materials and Methods

2.1 Cell culture .....	64
2.1.1 Cell lines .....	64
2.1.2 Inhibitors .....	64
2.2 Organoid Culture .....	65
2.2.1 Organoid Passaging .....	65
2.2.2 Organoid drug treatments .....	66
2.3 Patient-derived xenograft lysate preparation .....	66
2.3.1 PDX lysate preparation .....	67
2.4 Western blot .....	67
2.4.1 Cell lysis .....	67
2.4.2 Immunoprecipitation .....	68
2.4.3 Sodium Dodecyl Sulphate-Polyacrylamide Gel Electrophoresis (SDS-PAGE), immunoblotting and detection .....	69
2.5 Immunofluorescence and cell synchronization .....	71
2.6 Immunohistochemistry (IHC) .....	72
2.7 siRNA knockdown .....	72
2.8 Inhibitor treatment and cell viability assays .....	73
2.8.1 Inhibitor treatment .....	73
2.8.2 Cell viability assays .....	73
2.9 Generation of FGFR4 inhibitor resistant cells .....	74
2.10 Reverse transcription and polymerase chain reaction (PCR) .....	75
2.10.1 DNA and RNA isolation .....	75
2.10.2 Whole exome sequencing and RNA sequencing .....	75
2.10.3 RT-PCR and Sanger sequencing .....	75
2.11 Statistical analysis .....	77

## **2.1 Cell culture**

### **2.1.1 Cell lines**

The BT549, BT20, DU4475, HCC38, HCC70, HCC1500, HCC1569, HCC1954, HCC1806, HCC1143, HCC1937, HS578T, MDA-MB-157, MDA-MB-436, MDA-MB-453, MDA-MB-231 and MDA-MB-468 cell lines were purchased from the American Type Culture Collection (ATCC). CAL51, CAL148 and CAL851 cells were obtained from Deutsche Sammlung von Mikroorganismen und Zellkulturen (DSMZ) and CAL120 cells were a gift from Professor Elgene Lim (Garvan Institute of Medical Research, Darlinghurst, NSW 2010, Australia). MFM223 cells were purchased from Sigma Aldrich. SUM185PE and SUM149PT cells were purchased from Asterand Bioscience. All breast cancer cell lines were cultured in RPMI 1640 (Gibco) supplemented with 10% (v/v) FBS, 10 µg/mL Actrapid penfill insulin (Clifford Hallam Healthcare) and 20 mM HEPES (Thermoscientific). Hepatocellular carcinoma cell line Hep3B was also purchased from ATCC. The Hep3B cell line was cultured in EMEM (USbio) supplemented with 10% (v/v) FBS and 1 mM sodium pyruvate (Thermofisher). All cell lines were used for experiments from passage 2 to 10. To passage cells, cells were washed once with 1x phosphate buffered saline (PBS), detached from plates with 0.05% (w/v) trypsin/ethylenediaminetetraacetic acid (EDTA) (Gibco) at 37°C in a 5% CO<sub>2</sub> atmosphere. Trypsin was then inhibited with complete media.

### **2.1.2 Inhibitors**

The FGFR1-3 inhibitor PD173074 was purchased from Apex Biotech. The following inhibitors were purchased from Selleckchem: FGFR4 inhibitor BLU9931 and H3B-6527, ErbB family inhibitor Lapatinib, PI3K $\alpha$  inhibitor BYL719, pan-PI3K inhibitor BKM120, AKT inhibitor MK2206 and MEK inhibitor Trametinib. All inhibitors were reconstituted in DMSO.

## **2.2 Organoid Culture**

Studies on patient-derived xenografts (PDO) were conducted in accordance with the Declaration of Helsinki, and the protocol was approved by the Cabrini Human Research Ethics Committee (CHREC 05-26-03-18) and the Monash Human Research Ethics Committee (MHREC 2018-13673-18220). Breast tumours were obtained from treatment naïve breast cancer patients undergoing surgical resection at Cabrini Health, Brighton, Australia. All subjects provided written informed consent. Derivation of human breast cancer organoids was performed by the Monash BDI Organoid Program. I acknowledge the collaboration with Dr. Peter Gregory (Cabrini Health, Brighton, Australia), Dr. Tim Nottle (TissuPath, Mount Waverley, Australia), Dr. Tali Lang, Melissa Vereker and Prof. Gary Richardson from Cabrini Institute, Malvern, Australia.

### **2.2.1 Organoid Passaging**

Organoids in Matrigel (Corning, 356231) were mechanically scraped and collected into a tube with cold advanced DMEM/F12 (Gibco). Organoids were then centrifuged at 1500 rpm at 4 °C for 5 min and the medium removed. The cell pellet was resuspended with TrypLE Express (ThermoFisher) and incubated at 37 °C for 6 min, followed by the addition of advanced DMEM/F12 and centrifugation at 1500 rpm at 4 °C for 5 min. The supernatant was removed, and the cell pellet resuspended in growth factor reduced Matrigel and 50 µL seeded per well in a 24 well plate. After the Matrigel polymerized at 37 °C for 10 min, the Matrigel was overlaid with 500 µL of complete culture medium composed of adDF+ (advanced DMEM/F12 media, 1x Glutamax, 10 mM HEPES and 50 µg/mL primocin) supplemented with 1x B27 (Gibco, 17504044), 5 ng/mL recombinant human EGF (Peprotech, AF-100-15), 5 ng/ml FGF7 (Peprotech, 00-19-100), 20 ng/ml FGF10 (Peprotech, 100-26-100), 5 nM Neuregulin 1 (Peprotech, 100-03-100), 50 ng/ml IGF (BioLegends, 590908), 500 nM A83-01 (Tocris Bioscience, 2939), 1.25 mM N-acetylcysteine (Sigma, A9165), 5 mM nicotinamide (Sigma, N0636), 10% Noggin conditioned media and 10% R-spondin1 conditioned media. Following initial seeding of the cultures, 5 µM Y-27632 dihydrochloride kinase inhibitor (MedChem Express, HY-10583) was also added to the media for 2–3 days. Organoids were maintained in

a 37°C humidified atmosphere under 5% CO<sub>2</sub>. The culture medium was replaced with fresh medium every 2-3 days.

### **2.2.2 Organoid drug treatments**

For inhibitor experiments, organoids were mechanically passaged and 5000 organoid fragments per well were replated in 10 µL Matrigel in a 96 well plate. Organoid fragments were cultured in complete medium described above. After 2 d, the culture medium was replaced with fresh complete medium containing fresh 10 nM BLU9931 or DMSO as vehicle control and the process repeated every 2 days. Organoid growth was determined using CellTitre-Glo Luminescent cell viability assay (Promega) on day 5, 8, 10, 12 and 15 according to the manufacturer's protocol. Absorbance was determined using the PHERAstar microplate reader (BMG Labtech).

## **2.3 Patient-derived xenograft lysate preparation**

PDX propagation, drug testing and tissue collection was performed by A/Prof Alex Swarbrick's group at the Garvan Institute of Medical Research, Sydney. PDX models were provided by the Brocade consortium (<https://www.petermac.org/research/research-cohort-studies/brocade>) and 2 models were previously published [35]. Viably frozen PDX tumour tissue was first propagated and expanded into 3 immunodeficient mice per PDX model. Briefly, 1 mm<sup>3</sup> tumour pieces were implanted into the fourth mammary fat pad of NSG mice. Twice weekly standard monitoring and tumour measurement were conducted, and once tumours reached appropriate size, ~1000 mm<sup>3</sup>, mice were sacrificed by cervical dislocation under deep, isoflurane-induced anaesthesia. Tumours were harvested and cryopreserved prior to passaging into mice for drug studies. Mice were enrolled for drug or vehicle control treatment when tumours reached 200 mm<sup>3</sup> for the short-term studies, and 100 mm<sup>3</sup> for the long-term studies. Mice were subjected to either 12.5 mg/kg AZD4547 (Selleckchem, S2801) or 100 mg/kg BLU9931 (Selleckchem, S7819) treatment by oral gavage. Vehicle control mice were given 1% (v/v) Tween-80 with 0.5% (w/v) carboxymethylcellulose.

For the short-term AZD4547 (ST AZD) study, mice were dosed once a day for 5 d and harvested 6 h after the last dose. Some mice were harvested at 4 d of treatment due to the tumour shrinking rapidly. For the long-term AZD4547 (LT AZD) study, mice were dosed once a day for 28 d and harvested 6 h after the last dose. For the short-term BLU9931 (ST BLU) study, mice were dosed twice a day for 5 d and harvested 6 h after the last dose. For the long-term BLU9931 (LT BLU) study, mice were dosed twice a day for 5 d, then 2 d without drug, weekly for 4 weeks. Mice were euthanized using isoflurane with cervical dislocation. The tumours were resected, diced and processed by either snap freezing in liquid nitrogen or fixed in 10% neutral buffered formalin solution for subsequent paraffin embedding.

### **2.3.1 PDX lysate preparation**

PDX samples were homogenised in tubes containing zirconia beads (Biospec) and RIPA buffer supplemented with additives (Table 2.1) using a bead ruptor 12 homogeniser (Omni International). Fully homogenised PDX samples were collected and clarified by centrifugation at 21130 x *g* at 4°C for 10 min, then the protein concentration was determined using a Pierce BCA protein assay kit (Thermoscientific) according to the manufacturer's protocol.

## **2.4 Western blot**

### **2.4.1 Cell lysis**

For harvesting, cells at 80% confluency were washed twice with ice cold 1x PBS then lysed with RIPA buffer supplemented with additives prior to use (Table 2.1). Lysed cells were collected and clarified by centrifugation at 21130 x *g* at 4°C for 20 min, then the protein concentration was determined using a Pierce BCA protein assay kit (Thermoscientific) and absorbance measured at 562 nm with PHERAstar (BMG Labtech).

**Table 2.1: Commonly used buffers and solutions.**

Solution	Composition
RIPA lysis buffer	0.5% (w/v) sodium deoxycholate, 150 mM NaCl, 1% (v/v) NP40, 50 mM Tris-HCl pH 8.0, 0.1% (w/v) sodium dodecyl sulphate (SDS), 10% (v/v) glycerol, 5 mM EDTA and 20 mM NaF
Protease and phosphatase inhibitors (additives) added to RIPA lysis buffer prior to use	10 µg/mL aprotinin, 1 mM phenylmethane sulfonyl fluoride (PMSF), 10 µg/mL leupeptin, 1 mM sodium orthovanadate, 2.5 mM sodium pyrophosphate and 2.5 mM β-glycerophosphate
5X SDS-PAGE loading buffer	50% (v/v) glycerol, 0.3 M Tris-HCl pH 6.8, 10% (w/v) SDS, 0.25% (v/v) β-mercapethanol and 0.4% (w/v) bromophenol blue
SDS-PAGE running buffer	0.25 M Tris-HCl pH 8.3, 0.19 M glycine and 0.1% (w/v) SDS
Transfer buffer	0.25 M Tris-HCl pH 8.3, 0.19M glycine and 10% (v/v) ethanol
TBS-T	50 mM Tris-buffered saline (TBS) pH 7.5, 150 mM NaCl, 0.1% (v/v) Tween 20 (TBS-T)
BSA blocking buffer	5% (w/v) bovine serum albumin reconstituted in 50 mM TBS pH 7.5, 0.02% (v/v) sodium azide, phenol red
Skim milk blocking buffer	5% (w/v) skim milk powder reconstituted in TBS-T

### 2.4.2 Immunoprecipitation

Protein lysates (2.5 mg) were incubated with 10 µg of the indicated antibodies overnight at 4°C with gentle rotation. 40 µL of recombinant protein G-Sepharose 4B conjugate beads (Life Technologies) were equilibrated in RIPA buffer (Table 2.1), added to samples and incubated for 3 h at 4°C with gentle rotation. Samples were centrifuged at 500 x g for 1 min at 4°C and the unbound fraction transferred to a fresh microfuge tube. Beads were the washed thrice with

RIPA buffer and centrifuged for 1 min at 500 x *g* at 4°C and the supernatant removed. Immunoprecipitated proteins were then eluted using 2x sample loading buffer.

### **2.4.3 Sodium Dodecyl Sulphate-Polyacrylamide Gel Electrophoresis (SDS-PAGE), immunoblotting and detection**

Protein lysates (25-40 µg) were resolved by SDS-PAGE on a 4% (v/v) stacking gel and 8% (v/v) separating gel in SDS-PAGE running buffer (Table 2.1). Resolved proteins were wet transferred onto polyvinylidene difluoride membranes (PVDF) Immobilon-P membranes (Millipore) in transfer buffer (Table 2.1). After the transfer, membranes were blocked in 5% (w/v) skim milk in Tris buffered saline (TBS; Table 2.1) or in 5% (w/v) BSA-TBS blocking buffer depending on the antibody datasheet for 1 h at room temperature, then incubated in primary antibody (Table 2.2) diluted accordingly in 5% (w/v) skim milk in TBS-T or in 5% (w/v) BSA-TBS rolling overnight at 4°C. Following primary incubation, membranes were washed thrice for 10 min with TBS-T on a shaker, then probed with secondary antibody (Table 2.2) diluted 1:3000 in 5% (w/v) skim milk for 1 h at room temperature. Membranes were washed thrice for 10 min with TBS-T before signal detection by Western Lightning enhanced-chemiluminescence (ECL; Perkin Elmer) or Luminata Forte Western HRP substrate (Millipore) and images acquired with ChemiDoc Touch Imaging system (Bio-Rad).

Densitometry analysis was performed on the detected bands using ImageLab, version 5.2.1 (Bio-Rad).  $\beta$ -actin or  $\alpha$ -tubulin were used as the loading controls. The intensity of each band was normalised against the intensity of their corresponding loading control. Bands correlating to phospho-proteins were further normalised to the bands of corresponding total protein levels.

**Table 2.2: Primary and secondary antibodies used in Western blotting.**

Antibody	Dilution	Source	Product #	Manufacturer
FGFR1	1:1000 (skim milk)	Rabbit	9740	CST
FGFR2	1:500 (skim milk)	Mouse	sc-6930	SCBT
FGFR3 (B-9)	1:500 (skim milk)	Mouse	sc-13121	SCBT
FGFR3 (C-15)	1:200 (skim milk)	Rabbit	sc-123	SCBT
FGFR4	1:1000 (skim milk)	Mouse	sc-136988	SCBT
pan-phosFGFR (Tyr653/654)	1:500 (BSA)	Rabbit	3471	CST
pFGFR3 (Tyr724)	1:500 (BSA)	Rabbit	sc-33041	SCBT
TACC3	1:1000 (skim milk)	Rabbit	8069	CST
PARP	1:1000 (skim milk)	Mouse	9546	CST
Rb	1:1000 (skim milk)	Rabbit	9313	CST
pRb (Ser780)	1:1000 (BSA)	Rabbit	3590	CST
AKT	1:1000 (skim milk)	Rabbit	4685	CST
pAKT (Ser473)	1:1000 (BSA)	Rabbit	4058	CST
ERK; p44/42 MAPK	1:1000 (skim milk)	Rabbit	4695	CST
pERK; p44/42 MAPK (Thr202/Tyr204)	1:2000 (BSA)	Rabbit	4370	CST
FRS2	1:500 (skim milk)	Rabbit	05-502	Sigma Aldrich
pFRS2 (Tyr436)	1:500 (BSA)	Rabbit	3861	CST
ALK	1:1000 (skim milk)	Rabbit	3333	CST
pALK (Tyr1096)	1:1000 (BSA)	Rabbit	4143	CST
pALK (Tyr1282/Tyr1283)	1:1000 (skim milk)	Rabbit	9687	CST
pALK (Tyr1078)	1:1000 (skim milk)	Rabbit	4144	CST
ErbB2	1:1000 (skim milk)	Rabbit	2165	CST
pErbB2 (Tyr1248)	1:1000 (BSA)	Rabbit	2247	CST
ErbB3	1:1000 (skim milk)	Rabbit	4754	CST
pErbB3 (Tyr1328)	1:1000 (BSA)	Rabbit	8017	CST



**Table 2.2: Primary and secondary antibodies used in Western blotting (continued).**

Antibody	Dilution	Source	Product #	Manufacturer
IRS-1	1:1000 (skim milk)	Rabbit	6248	Upstate
pIRS-1 (Tyr612)	1:1000 (BSA)	Rabbit	44-816G	Biosource
IGF-1R	1:1000 (skim milk)	Rabbit	9750	CST
pIGF-1R	1:1000 (BSA)	Rabbit	44-804G	Biosource
GSK	1:1000 (skim milk)	Rabbit	5676	CST
pGSK (Tyr216/Tyr279)	1:1000 (BSA)	Rabbit	ab4797-50	Abcam
$\alpha$ -tubulin	1:2000 (skim milk)	Mouse	T5168	Sigma Aldrich
$\beta$ -actin	1:5000 (skim milk)	Mouse	sc-69879	SCBT
Goat anti-rabbit IgG (H+L)-HRP Conjugate	1:3000		1706515	Bio-Rad
Goat anti-mouse IgG (H+L)-HRP Conjugate	1:3000		1706516	Bio-Rad

## 2.5 Immunofluorescence and cell synchronization

SUM185PE cells seeded onto coverslips were fixed and permeabilized with PTEMF buffer (20 mM PIPES pH 6.8, 0.2% (v/v) Triton X 100, 10 mM EGTA, 1 mM MgCl<sub>2</sub>, 4% (v/v) PFA) 24 h post seeding for 20 min. The samples were then blocked with 1% (w/v) bovine serum albumin for 1 h then immunostained with the indicated primary antibodies for 2 h followed by either anti-mouse Alexa Fluor 488 (Life Technologies, A21202) or anti-rabbit Alexa Fluor 555 (Life Technologies, A21428) for 1 h. All antibody incubations were performed at RT. Coverslips were mounted onto microscope slides with ProLong Gold Antifade Mountant with DAPI (Invitrogen). Cells were imaged 48 h later by immunofluorescence using a Nikon inverted confocal microscope. For cell synchronization, SUM185PE cells were synchronized at G1/S phase by 3 mM thymidine block for 18 h then released into media for 9 h. Next, the cells were then subjected to 3 mM thymidine block for another 15 h, released into media for 45 h and imaging was undertaken as above. Mitotic spindles were visualized by staining with rabbit anti- $\alpha$ -tubulin (Abcam, 6046) or mouse anti- $\alpha$ -tubulin (Sigma-Aldrich, T5168).

## **2.6 Immunohistochemistry (IHC)**

Immunohistochemistry was completed by the Monash Histology Platform at Monash University. Formalin-fixed paraffin embedded (FFPE) blocks from PDX tumours or breast cancer organoids were sectioned at 4  $\mu\text{m}$  onto Superfrost Plus slides. Immunohistochemistry was carried out using the DAKO Autostainer Link 48. Sections underwent dewaxing, heat induced antigen retrieval using DAKO Target Retrieval Solution (S1699) at 98°C for 30 min, endogenous peroxidases were quenched by applying Dako Real Peroxidase Blocking solution (S2023) for 10 min, followed by Dako Serum Free Protein Block (X0909) for 30 min. Then, primary antibody incubation using FGFR4 (sc-136988, Santa Cruz Biotechnology, 1:300 dilution) or Ki-67 antibody (9027, Cell Signaling Technology, 1:300 dilution) was followed by the Dako Envision+ System – HRP Labelled Polymer Anti-Rabbit (K4003) secondary antibody incubation system. Lastly, sections were counterstained with Dako Automation Hematoxylin Histological Staining Reagent (S3301).

## **2.7 siRNA knockdown**

In 96 well plate format, 7000 SUM185PE cells were reverse transfected with 0.15  $\mu\text{L}$  of DharmaFECT1 (Dharmacon RNAi Technologies, Horizon Discovery). Media were changed 24 h later, replaced again at 96 h and the experiment ended at 144 h post transfection. 8000 CAL51 cells were reverse transfected with 0.1  $\mu\text{L}$  of lipofectamine 3000 (Thermofisher Scientific), 5000 MDA-MB-231 cells with 0.1  $\mu\text{L}$  of DharmaFECT4 (Dharmacon RNAi Technologies, Horizon Discovery) and 10,000 MFM-223 cells with 0.1  $\mu\text{L}$  of DharmaFECT3 (Dharmacon RNAi Technologies, Horizon Discovery). Media were changed 24 h later and the experiment ended at 96 h post transfection. In 6 well plate format, 360,000 SUM185PE cells, 300,000 CAL51 cells, 300,000 MFM-223 cells and 90,000 MDA-MB-231 cells were reverse transfected with 3  $\mu\text{L}$  of the corresponding lipid as previously mentioned. Media were changed 24 h later and the experiment ended at 72 h post transfection.

The FGFR3-TACC3 fusion and wildtype FGFR3 were knocked down together using ON-TARGETplus human FGFR3 set of 4 individual siRNAs labelled as FW 1–4 (Dharmacon RNAi Technologies, Horizon Discovery, Q-003133-00). Wildtype FGFR3 expression was knocked down using 3 individual custom FGFR3 siRNAs from Bioneer with the following sequence: GAGGAAAAGGCUGGUACAA (W1), CACAUGUCCAGCACCUUGU (W2) and GAUGCUGUGUAUAUGGUAU (W3). The ON-TARGETplus non-targeting SMARTpool (siOTP) was used as the control (Dharmacon RNAi Technologies, Horizon Discovery, D-001810-10). All siRNAs were used at a final concentration of 20 nM.

## **2.8 Inhibitor treatment and cell viability assays**

### **2.8.1 Inhibitor treatment**

Cells were seeded into culture plates and cultured for the indicated days with an 80% end point confluence for all the cell lines. After 24 h, media was replaced with complete media with DMSO (vehicle control) or freshly made inhibitors at the indicated concentration. This process was repeated every 48 h.

### **2.8.2 Cell viability assays**

For assays with PD173074 treatment, cell viability was determined by direct cell counting. SUM185PE cells and MDA-MB-468 cells were seeded into 6 well plates and cultured for 7 days with an 80% end point confluence. Cells were washed with 1x PBS then trypsinised at 37°C in a 5% CO<sub>2</sub> atmosphere until detachment. Trypsinised cells were then resuspended thoroughly in complete media to inhibit trypsin. Cells were stained with Trypan blue (EVS-1000, NanoTek), then transferred to an EVE cell counting slide (EVS-1000, NanoTek) and counted with the EVE automatic cell counter (EVE-MC-DEMO, NanoTek) according to the manufacturer's protocol.

For MTS proliferation assays, 3000 – 5000 cells were seeded into 96 well plates and cultured for the indicated days with an 80% end point confluence for all the cell lines. Cell viability was determined using CellTiter 96 Aqueous One Solution Cell Proliferation Assay (Promega) according to the manufacturer's protocol. 20  $\mu$ L of solution was added into wells and incubated at 37°C in a 5% CO<sub>2</sub> atmosphere for 45 mins. Absorbance was determined using the PHERAstar microplate reader (BMG LABTECH).

For assays with siRNAs knockdown, SUM185PE cells were seeded into 96 well plates and cultured for 6 days, while CAL51, MFM223 and MDA-MB-231 were cultured for 4 days, with an 80% end point confluence for all the cell lines. Cell viability was determined using CellTiter96 Aqueous One Solution Cell Proliferation Assay (Promega) according to the manufacturer's protocol. 20  $\mu$ L of solution was added into wells and incubated at 37°C in a 5% CO<sub>2</sub> atmosphere for 45 mins. Absorbance was determined using the PHERAstar microplate reader (BMG LABTECH).

## **2.9 Generation of FGFR4 inhibitor resistant cells**

MDA-MB-453 or Hep3B cells were seeded into 10 cm plates at a density of 500 cells. After 48 h, cells were treated with DMSO (as vehicle control) or FGFR4 inhibitor (BLU9931 or H3B6527) for at least 3 months. Culture medium was replaced twice a week with fresh complete medium containing DMSO or the respective FGFR4 inhibitor. When cells formed colonies visible to the naked eye, small pieces of sterile filter paper soaked in trypsin were used to detach cells by placing on top of visible colonies and collected for further maintenance in DMSO or FGFR4 inhibitor. These cells were termed long-term BLU9931 MDA-MB-453 cells and long-term H3B-6527 Hep3B cells in this thesis.

For identification of upregulated RTKs in the long-term FGFR4 inhibitor cells, lysates were immunoblotted using a proteome profile human phospho-RTK array kit (RND systems) following the manufacturer's protocol.

## **2.10 Reverse transcription polymerase chain reaction (RT-PCR)**

### **2.10.1 DNA and RNA isolation**

Genomic DNA was isolated from PDX KCC\_P\_4043 using a genomic DNA purification kit (Promega) according to the manufacturer's protocol. DNA was quantified using a Nanodrop ND-1000 (Nanodrop Technologies). Total RNA was isolated from the PDX KCC\_P\_4043, parental MDA-MB-453, long-term BLU9931 MDA-MB-453 cells, parental Hep3B and long-term H3B-6527 Hep3B cells with a RNeasy mini kit (Qiagen) following the manufacturer's protocol. RNA was quantified using a Nanodrop ND-1000 (NanoDrop Technologies).

### **2.10.2 Whole exome sequencing and RNA sequencing**

DNA and RNA of PDX model KCC\_P\_4043 was subjected to whole exome sequencing and RNA sequencing. DNA and RNA of KCC\_P\_4043 were dried down in specialised DNA and RNA tubes and shipped at room temperature to GENEWIZ, Suzhou, China for sequencing.

### **2.10.3 RT-PCR and Sanger sequencing**

RNAs were reverse transcribed using a high capacity cDNA reverse transcription kit (Thermoscientific). Subsequently, cDNA was amplified by PCR to identify the FGFR2-SKI fusion or gatekeeper mutations in the FGFR4 kinase domain using forward primers and reverse primers (Table 2.3 & 2.4). The PCR products were resolved by gel electrophoresis, and the bands at the predicted product size were excised and purified with a gel and PCR clean-up system (Promega). Sanger sequencing was completed by the Micromon facility at Monash University. Reactions were repeated on two biological replicates.

PCR was performed by addition of the reaction mixture described in Table 2.5a and performed under the conditions described in Table 2.5b.

**Table 2.3: FGFR2-SKI fusion primers.**

Primer	Primer sequence (5' to 3')	T <sub>m</sub> (°C)
A forward	GTTGCTTTGGGCAAGTGGTC	59
A reverse	CTTGTCCTTTTCGGAAGGCG	58
B forward	AACAACACGCCTCTCTTCAACG	60
B reverse	TTTTGGGTCTTATGGAGGCCG	59
C forward	CTTCTTGGAGCCTGCACACA	59
C reverse	AGCCCAGGCTCTTATTGGAA	56

**Table 2.4: FGFR4 kinase domain primers.**

Primer	Primer sequence (5' to 3')	T <sub>m</sub> (°C)
1F	AGATGCTCAAAGACAACGCC	58
1R	AGATACTGCATGCCTCGGG	59
2F	CACTGTGCAGAAGCTCTCCC	59
2R	AAGGTCGAGCACTGTGTCAG	59
3F	TCTCGACCCACTATGGGAGT	59
3R	TTGTCCTCAGTCACCAGCAC	59
4F	GCCGGCCTCGTGAGTCTA	59
4R	TACACTTCCGGGACTCCAGAT	59
5F	CAGAAGCTCTCCCGCTTCC	59
5R	CCGAGCAGAACCCTGACATT	59

**Table 2.5: Polymerase chain reaction conditions.**

A	PCR reaction mixture	
	Component	Final Concentration
	Template DNA	900 ng
	Forward primer (10 $\mu$ M)	0.5 $\mu$ M
	Reverse primer (10 $\mu$ M)	0.5 $\mu$ M
	10 mM dNTPs	200 $\mu$ M
	5X Q5 reaction buffer	1X
	Q5 high-fidelity DNA polymerase	0.02U/ $\mu$ L
	RNAse-free water	variable
	Total volume	25 $\mu$ L

B	PCR cycling conditions			
	Step	Temperature ( $^{\circ}$ C)	Time (s)	Cycles
	Initial denaturation	98	30	1
	Denaturation	98	10	35
	Annealing	68	30	
	Extension	72	30	
	Final extension	72	120	1

## 2.11 Statistical analysis

Immunohistochemistry quantification was performed using NIS-Elements Viewer 4.50 and ImageJ. Quantification of western blots by densitometry was performed using ImageLab version 5.2.1 (Bio-Rad) and statistical t-tests were performed using GraphPad Prism 8 and Microsoft-Excel.

---

## **CHAPTER 3**

### **FGFR3 SIGNALLING AND FUNCTION IN TRIPLE NEGATIVE BREAST CANCER**

---



# Chapter 3: FGFR3 signalling and function in triple negative breast cancer

Published (2020) in Cell Communication and Signaling.

3.1 Abstract .....	81
3.2 Background .....	83
3.2 Materials and Methods .....	85
3.2.1 Cell lines, cell culture and reagents .....	85
3.2.2 Tyrosine phosphorylation profiling by mass spectrometry .....	86
3.2.3 Mass spectrometry analysis .....	86
3.2.4 HRM-DIA data analysis .....	87
3.2.5 Cell lysis .....	88
3.2.6 Western blotting .....	88
3.2.7 Immunoprecipitation .....	88
3.2.8 Immunofluorescence and cell synchronisation.....	89
3.2.9 Cell viability assays .....	89
3.2.10 PD173074 treatment .....	90
3.2.11 siRNA knockdown .....	90
3.2.12 Quantification and statistical analysis .....	91
3.3 Results .....	91
3.3.1 Expression and phosphorylation of FGFRs and FGFR3-TACC3 fusion protein in TNBC cell lines .....	91
3.3.2 Tyrosine phosphorylation of wildtype FGFR3 and the FGFR3-TACC3 fusion in SUM185PE cells.....	95
3.3.3 The FGFR3-TACC3 fusion predominantly localises to the cytoplasm and plasma membrane .....	97
3.3.4 Wildtype FGFR3 and the FGFR3-TACC3 fusion exhibit contrasting functional roles in SUM185PE cells .....	101

## CHAPTER 3

---

3.3.5 Functional role of FGFR3 in TNBC cell lines with low to moderate levels of FGFR3 phosphorylation .....	105
3.3.6 Evaluation of FGFR3 alterations in breast cancer patients using public datasets	107
3.4 Discussion .....	109
3.5 Conclusion.....	111
3.6 Supplementary Materials.....	112
3.7 References .....	115

# FGFR3 signalling and function in triple negative breast cancer

Published (2020) in Cell Communication and Signaling.

Nicole J Chew<sup>1,2</sup>, Elizabeth V Nguyen<sup>1,2</sup>, Shih-Ping Su<sup>1,2</sup>, Karel Novy<sup>1,2</sup>, Howard C Chan<sup>1,2</sup>, Lan K Nguyen<sup>1,2</sup>, Jennii Luu<sup>3,4</sup>, Kaylene J Simpson<sup>3,4</sup>, Rachel S Lee<sup>1,2</sup> and Roger J Daly<sup>1,2</sup>

1 Cancer Program, Biomedicine Discovery Institute, Monash University, VIC 3800, Australia.

2 Department of Biochemistry and Molecular Biology, Monash University, VIC 3800, Australia.

3 Sir Peter MacCallum Department of Oncology, The University of Melbourne, VIC 3010, Australia.

4 Victorian Centre for Functional Genomics, Peter MacCallum Cancer Centre, VIC 3000, Australia.

## 3.1 Abstract

**Background:** Triple negative breast cancer (TNBC) accounts for 16% of breast cancers and represents an aggressive subtype that lacks targeted therapeutic options. In this study, mass spectrometry (MS)-based tyrosine phosphorylation profiling identified aberrant FGFR3 activation in a subset of TNBC cell lines. This kinase was therefore evaluated as a potential therapeutic target.

**Methods:** MS-based tyrosine phosphorylation profiling was undertaken across a panel of 24 TNBC cell lines. Immunoprecipitation and Western blot were used to further characterise FGFR3 phosphorylation. Indirect immunofluorescence and confocal microscopy were used to determine FGFR3 localisation. The selective FGFR1-3 inhibitor, PD173074 and siRNA

knockdowns were used to characterise the functional role of FGFR3 *in vitro*. The TCGA and METABRIC breast cancer datasets were interrogated to identify FGFR3 alterations and how they relate to breast cancer subtype and overall patient survival.

**Results:** High FGFR3 expression and phosphorylation were detected in SUM185PE cells, which harbor a FGFR3-TACC3 gene fusion. Low FGFR3 phosphorylation was detected in CAL51, MFM-223 and MDA-MB-231 cells. In SUM185PE cells, the FGFR3-TACC3 fusion protein contributed the majority of phosphorylated FGFR3, and largely localised to the cytoplasm and plasma membrane, with staining at the mitotic spindle in a small subset of cells. Knockdown of the FGFR3-TACC3 fusion and wildtype FGFR3 in SUM185PE cells decreased FRS2, AKT and ERK phosphorylation, and induced cell death. Knockdown of wildtype FGFR3 resulted in only a trend for decreased proliferation. PD173074 significantly decreased FRS2, AKT and ERK activation, and reduced SUM185PE cell proliferation. Cyclin A and pRb were also decreased in the presence of PD173074, while cleaved PARP was increased, indicating cell cycle arrest in G1 phase and apoptosis. Knockdown of FGFR3 in CAL51, MFM-223 and MDA-MB-231 cells had no significant effect on cell proliferation. Interrogation of public datasets revealed that increased FGFR3 expression in breast cancer was significantly associated with reduced overall survival, and that potentially oncogenic FGFR3 alterations (eg mutation and amplification) occur in the TNBC/basal, luminal A and luminal B subtypes, but are rare.

**Conclusions:** These results indicate that targeting FGFR3 may represent a therapeutic option for TNBC, but only for patients with oncogenic FGFR3 alterations, such as the FGFR3-TACC3 fusion.

**Keywords:** Receptor tyrosine kinase, Fibroblast growth factor receptor, Oncogene, Targeted therapy, Signal transduction

## **3.2 Background**

Breast cancer accounts for 25% of all cancer and ranks as the second most common cancer in the world [1]. Triple negative breast cancer (TNBC) is the most aggressive subtype that represents approximately 10-20% of breast cancers and its oncogenic drivers are poorly understood [2, 3]. TNBC lacks expression of estrogen receptor (ER), progesterone receptor (PR) and human epidermal growth factor receptor-2 (HER-2) resulting in clinical resistance to endocrine and trastuzumab therapy [4]. Chemotherapy remains the only treatment option since targeted treatment strategies are lacking [5]. TNBC is associated with higher tumour grade, larger tumour size, higher metastasis rate, lymph node involvement and a median survival of 13 months after relapse [6-8]. To improve patient outcomes, we need to identify new therapeutic targets to build a platform for personalized treatment strategies.

Fibroblast growth factor receptors (FGFRs) are a family of four highly conserved transmembrane receptor tyrosine kinases (RTKs), comprising of FGFR1, FGFR2, FGFR3 and FGFR4 [9]. Activated FGFRs initiate intracellular signalling cascades involved in regulating a wide range of physiological processes such as cellular differentiation, proliferation, survival and migration, embryonic development and angiogenesis [10]. Aberrant FGFR signalling has been reported in many human cancers including breast cancer, colorectal carcinoma and endometrial carcinoma, and contributes to oncogenesis, tumour progression and resistance to anticancer therapies [11-13]. FGFR alterations have been reported in approximately 7.1% of cancers (most commonly in urothelial and breast cancer), with gene amplification being the most frequent FGFR aberration (66%), followed by mutation (26%) and rearrangement (8%) [14].

Given the oncogenic potential of FGFRs and their ‘druggability’, there has been considerable interest in developing targeted cancer therapies directed towards these receptors. Dovitinib, a multi-tyrosine kinase inhibitor with FGFR-inhibiting activity, induced tumour regression in patient-derived xenograft models exhibiting gene sets related to the FGFR signalling pathway, highlighting the latter as potential predictors for Dovitinib sensitivity [15]. Dovitinib is currently in phase 2 clinical trials and has demonstrated modest efficacy against lung squamous

cell carcinomas harbouring FGFR1 amplification [16]. BGJ398, a highly potent and selective pan-FGFR kinase inhibitor in clinical trials, has demonstrated antitumour activity in advanced cholangiocarcinoma patients with FGFR2 alterations [17] and promoted tumour reductions in FGFR1-amplified breast cancer patients [18]. Erdafitinib, an inhibitor of FGFR1-4, resulted in tumour shrinkage in an adrenal carcinoma patient with the FGFR3-TACC3 fusion [19]. Pemigatinib is another selective FGFR inhibitor that is currently under evaluation for its efficacy and safety in patients with urothelial carcinoma (NCT03011372).

FGFRs represent potential therapeutic targets in many human malignancies including breast cancer [20]. FGFR1 amplification on chromosome 8p11-12 is the most common FGFR1 alteration [21, 22], occurring in 14% of breast cancers and 16-27% of luminal B breast cancer, where it is associated with poor prognosis, shorter overall survival and resistance to endocrine therapies [23-25]. FGFR1 amplification is also an independent negative prognostic factor in gastric cancer, lung squamous cell carcinoma and TNBC [26-28]. Knockdown of FGFR1 expression in a FGFR1-overexpressing TNBC cell line MDA-MB-231 significantly reduced cell migration [28] and knock-out of FGFR1 reduced primary tumour growth and metastasis in a mouse mammary tumour model [29]. FGFR2 amplification is also a common FGFR aberration, occurring in 5-10% of breast cancers and 4% of TNBCs, and FGFR2 signalling drives resistance to Tamoxifen in ER+ disease [30, 31]. Knockdown of FGFR2 significantly reduced cell survival in the TNBC cell line MFM223 and this cell line also showed substantial sensitivity to the FGFR inhibitor PD173074 [30]. In breast cancer, high FGFR2 expression is significantly associated with tumour size and metastasis, shorter overall survival and lower disease-free survival rates [32]. Expression of autocrine FGF2 is associated with the basal/TNBC subtype of breast cancer cell lines and primary breast cancers, and in the former, confers sensitivity to PD173074 [33].

While the roles of FGFR1 and FGFR2 in breast cancer have been studied in considerable detail, FGFR3 remains poorly characterised in this setting. Molecular screening via segmental transcript analysis identified a FGFR3-TACC3 fusion in a primary TNBC specimen and TNBC cell line, SUM185PE [34]. In this fusion, the FGFR3 kinase domain is fused to the upstream region of the coiled-coil domain of transforming acidic coiled-coil 3 (TACC3) protein [34, 35].

FGFR3-TACC3 fusions also occur in other cancers, such as glioblastoma (3 out of 97 tumours examined, 3.1%), bladder cancer (2 of 43 bladder cancer cell lines, 4.7%) and nasopharyngeal carcinoma (4 out of 159 patients, 2.5%) [35-37]. The presence of the coiled-coil domain of TACC3 enhances dimerization of the fusion protein, thus activating the FGFR3 tyrosine kinase [38]. The presence of the FGFR3-TACC3 fusion increases cell proliferation and tumour formation *in vivo* [35], but confers sensitivity to specific FGFR inhibitors, indicating an oncogenic addiction to the fusion [37, 39, 40].

Previously, we utilised MS to compare the tyrosine phosphorylation profiles of luminal breast cancer and TNBC cell lines. This identified a prominent Src family kinase signalling network in TNBC and highlighted multiple kinases for further evaluation as therapeutic targets and biomarkers [41]. In this study, we applied this approach to a large panel of TNBC cell lines to interrogate this disease subtype in more detail and identify targets for personalized treatment. One potential target that emerged was FGFR3, and this was characterised in detail in this study.

## **3.2 Materials and Methods**

### **3.2.1 Cell lines, cell culture and reagents**

The BT549, BT20, DU4475, HCC38, HCC70, HCC1500, HCC1569, HCC1954, HCC1806, HCC1143, HCC1937, HS578T, MDA-MB-157, MDA-MB-436, MDA-MB-453, MDA-MB-231 and MDA-MB-468 cell lines were purchased from the American Type Culture Collection (ATCC; Manassas, VA, USA). CAL51, CAL148 and CAL851 cells were obtained from Deutsche Sammlung von Mikroorganismen und Zellkulturen (DSMZ) and CAL120 cells were a gift from Professor Elgene Lim from the Garvan Institute of Medical Research, Darlinghurst, NSW 2010, Australia. MFM223 cells were purchased from Sigma Aldrich. SUM185PE and SUM149PT cells were purchased from Asterand Bioscience. Cells were cultured in RPMI 1640 (Gibco) supplemented with 10% (v/v) FBS, 10 µg/mL insulin and 20 mM HEPES.

### **3.2.2 Tyrosine phosphorylation profiling by mass spectrometry**

To harvest proteins for mass spectrometry (MS) analysis, TNBC cell lines were cultured until 80% confluent, washed twice with ice cold phosphate-buffered saline (PBS), and lysed directly in the dish with lysis buffer (6 M guanidine hydrochloride, 50 mM Tris-HCl, 1 mM sodium orthovanadate, 2.5 mM sodium pyrophosphate, 1 mM b-glycerophosphate). Approximately 20 mg of lysate protein was reduced with 5 mM TCEP at 37°C for 1 h and alkylated with iodoacetamide in the dark for 1 h. The samples were then diluted 1:4 with ammonium bicarbonate (25 mM) before digestion with a 1:200 LysC (Worthington) at room temperature (RT) for 4 h. Samples were further diluted 10x from the original volume before digested with a 1:100 trypsin (Promega) at 37°C for 18 h. Tryptic digests were acidified with 10%TFA to pH 3 before desalting on a C18 column (Thermo Fisher Scientific) and elution with 0.1% TFA/40% ACN. Peptides were dried in a SpeedVac and reconstituted in 1.8ml of IAP wash buffer (1% n-octyl- $\beta$ -D-glucopyranoside, 50 mM Tris-HCl, 150 mM NaCl, pH 7.4). 50  $\mu$ g each of P-Tyr-1000 (Cell Signalling Technology, 8954), P-Tyr-100 (Cell Signalling Technology, 9411), and P-Tyr-20 (BD Biosciences, 610000) antibodies were coupled to 60  $\mu$ L of sepharose beads slurry (Rec-Protein G, Zymed) and incubated overnight with peptide samples at 4°C with gentle shaking. Immobilized antibody beads were washed three times with IAP buffer and further washed three times with water before elution with 110  $\mu$ L of 0.15% TFA. Samples were then desalted on a C18 column (as described above) and evaporated to dryness in a SpeedVac. The dried peptides were reconstituted in 2% ACN/0.5% FA.

### **3.2.3 Mass spectrometry analysis**

Samples were analyzed on an UltiMate 3000 RSLC nano LC system (Thermo Fisher Scientific) coupled to an LTQ-Orbitrap mass spectrometer (LTQ-Orbitrap, Thermo Fisher Scientific). Peptides were loaded via an Acclaim PepMap 100 trap column (100  $\mu$ m x 2 cm, nanoViper, C18, 5  $\mu$ m, 100 Å, Thermo Fisher Scientific) and subsequent peptide separation was on an Acclaim PepMap RSLC analytical column (75  $\mu$ m x 50 cm, nanoViper, C18, 2  $\mu$ m, 100 Å, Thermo Fisher Scientific). For each liquid chromatography-tandem mass spectrometry (LC-MS/MS) analysis, 1  $\mu$ g of peptides as measured by a nanodrop 1000 spectrophotometer



(Thermo Fisher Scientific) was loaded on the pre-column with microliter pickup. Peptides were eluted using a 2 h linear gradient of 80% ACN/0.1% FA at a flow rate of 250 nL/min using a mobile phase gradient of 2.5-42.5% ACN. The eluting peptides were interrogated with an Orbitrap mass spectrometer. The HRM DIA method consisted of a survey scan (MS1) at 35,000 resolution (automatic gain control target 5e6 and maximum injection time of 120 ms) from 400 to 1,220 m/z followed by tandem MS/MS scans (MS2) through 19 overlapping DIA windows increasing from 30 to 222 Da. MS/MS scans were acquired at 35,000 resolution (automatic gain control target 3e6 and auto for injection time). Stepped collision energy was 22.5%, 25%, 27.5% and a 30 m/z isolation window. The spectra were recorded in profile type.

### **3.2.4 HRM-DIA data analysis**

The DIA data were analyzed with Spectronaut 8, a mass spectrometer vendor-independent software from Biognosys. The default settings were used for the Spectronaut search. Retention time prediction type was set to dynamic indexed Retention Time (iRT; correction factor for window 1). Decoy generation was set to scrambled (no decoy limit). Interference correction on MS2 level was enabled. The false discovery rate (FDR) was set to 1% at peptide level. A peptide identification required at least 3 transitions in quantification. Quantification was based on the top 3 proteotypic peptides for each protein, normalized with the default settings, and exported as an excel file with Spectronaut 8 software [42]. For generation of the spectral libraries, DDA measurements of each sample were performed. The DDA spectra were analyzed with the MaxQuant Version 1.5.2.8 analysis software using default settings. Enzyme specificity was set to Trypsin/P, minimal peptide length of 6, and up to 3 missed cleavages were allowed. Search criteria included carbamidomethylation of cysteine as a fixed modification; oxidation of methionine; acetyl (protein N terminus); and phosphorylation of serine, threonine, and tyrosine as variable modifications. The mass tolerance for the precursor was 4.5 ppm and for the fragment ions was 20 ppm. The DDA files were searched against the human UniProt fasta database (v2015-08, 20,210 entries) and the Biognosys HRM calibration peptides. The identifications were filtered to satisfy FDR of 1% on peptide and protein level. The spectral library was generated in Spectronaut and normalized to iRT peptides.

### **3.2.5 Cell lysis**

Cells at 80% confluency were washed twice with ice cold 1x PBS then lysed with RIPA buffer (0.5% (w/v) sodium deoxycholate, 150 mM NaCl, 1% (v/v) NP40, 50 mM Tris-HCl pH 8.0, 0.1% (w/v) sodium dodecyl sulphate (SDS), 10% (v/v) glycerol, 5 mM EDTA and 20 mM NaF), supplemented with 10 µg/mL aprotinin, 1 mM phenylmethane sulfonyl fluoride (PMSF), 10 µg/mL leupeptin, 1 mM sodium orthovanadate, 2.5 mM sodium pyrophosphate and 2.5 mM β-glycerophosphate prior to use. Lysed cells were collected and clarified by centrifugation at 21130 x g at 4°C for 10 min, then the protein concentration was determined using a Pierce BCA protein assay kit (Thermoscientific) according to the manufacturer's protocol.

### **3.2.6 Western blotting**

Protein lysates were subjected to Western blot analysis with antibodies. The following antibodies were purchased from Cell Signalling Technology: FGFR1 (9740), wildtype FGFR3 (4574), pan-phosFGFR (Y653, Y654) (3471), TACC3 (8069), AKT (4685), ERK (4695), pAKT (S473) (4058), pERK (T202, Y204) (4370), pFRS2 (Y436) (3861), PARP (9546), Rb (9313) and pRb (S780) (3590). The following antibodies were purchased from Santa Cruz Biotechnology: FGFR2 (sc-6930), FW FGFR3 (sc-13121), FGFR4 (sc-136988), pFGFR3 (Y724) (sc-33041), FRS2 (sc-17841), cyclin A (sc-53227) and β-actin (sc-69879). Two α-tubulin antibodies were purchased from Sigma-Aldrich (T5168) and from Abcam (ab6046).

### **3.2.7 Immunoprecipitation**

Protein lysates (2.5 mg) were incubated with 10 µg of the indicated antibodies overnight at 4°C with gentle rotation. 40 µL of recombinant protein G-Sepharose 4B conjugate beads (Life Technologies, 101242) was equilibrated in RIPA buffer were added to samples and incubated for 3 h at 4°C with gentle rotation. Samples were centrifuged at 500 x g for 1 min at 4°C and the unbound fraction transferred to a fresh microfuge tube. Beads were the washed thrice with RIPA buffer and centrifuged for 1 min at 500 x g at 4°C and the supernatant removed. Immunoprecipitated proteins were then eluted using 2x sample loading buffer.

### **3.2.8 Immunofluorescence and cell synchronisation**

SUM185PE cells seeded onto coverslips were fixed and permeabilized with PTEMF buffer (20 mM PIPES pH 6.8, 0.2% (v/v) Triton X 100, 10 mM EGTA, 1 mM MgCl<sub>2</sub>, 4% (v/v) PFA) 24 h post seeding for 20 mins. The samples were then blocked with 1% (w/v) bovine serum albumin for 1 h then immunostained with the indicated primary antibodies for 2 h followed by either anti-mouse Alexa Fluor 488 (Life Technologies, A21202) or anti-rabbit Alexa Fluor 555 (Life Technologies, A21428) for 1 h. All antibody incubations were performed at RT. Coverslips were mounted onto microscope slides with ProLong Gold Antifade Mountant with DAPI (Invitrogen). Cells were imaged 48 h later by immunofluorescence using a Nikon inverted confocal microscope. For cell synchronization, SUM185PE cells were synchronized at G1/S phase by 3 mM thymidine block for 18 h then released into media for 9 h. Next, the cells were then subjected to 3 mM thymidine block for another 15 h, released into media for 45 h and imaging was undertaken as above. Mitotic spindles were visualized by staining with rabbit anti- $\alpha$ -tubulin (Abcam, 6046) or mouse anti- $\alpha$ -tubulin (Sigma-Aldrich, T5168).

### **3.2.9 Cell viability assays**

For assays with siRNAs knockdown, SUM185PE cells were seeded into 96 well plates and cultured for 6 days, while CAL51, MFM223 and MDA-MB-231 were cultured for 4 days, with an 80% end point confluence for all the cell lines. Cell viability was determined using CellTiter96 Aqueous One Solution Cell Proliferation Assay (Promega) according to the manufacturer's protocol. Absorbance was determined using the PHERAstar microplate reader (BMG LABTECH).

For assays with PD173074 treatment, SUM185PE cells and MDA-MB-468 cells were seeded into 6 well plates and cultured for 7 days with an 80% end point confluence. Cell numbers were obtained via direct cell counting. Cells were washed with 1x PBS then trypsinised at 37°C in a 5% CO<sub>2</sub> atmosphere until detachment. Trypsinised cells were then resuspended thoroughly in complete media to inhibit trypsin. Cells were stained with Trypan blue (EVS-1000, NanoTek), then transferred to an EVE cell counting slide (EVS-1000, NanoTek) and

counted with the EVE automatic cell counter (EVE-MC-DEMO, NanoTek) according to the manufacturer's protocol.

### **3.2.10 PD173074 treatment**

The selective small molecule inhibitor of FGFR1-3, PD173074 (Apex Biotech), was reconstituted in DMSO. For Western blotting, cells were treated with 5 – 1000 nM PD173074 for the indicated time before lysing in RIPA buffer. For viability assays, cells were treated with PD173074 24 h post seeding and viability determined at the indicated days.

### **3.2.11 siRNA knockdown**

In 96 well plate format, 7000 SUM185PE cells were reverse transfected with 0.15  $\mu$ L of DharmaFECT1 (Dharmacon RNAi Technologies, Horizon Discovery). Media were changed 24 h later, replaced again at 96 h and the experiment ended at 144 h post transfection. 8000 CAL51 cells were reverse transfected with 0.1  $\mu$ L of lipofectamine 3000 (ThermoFisher Scientific), 5000 MDA-MB-231 cells with 0.1  $\mu$ L of DharmaFECT4 (Dharmacon RNAi Technologies, Horizon Discovery) and 10 000 MFM223 cells with 0.1  $\mu$ L of DharmaFECT3 (Dharmacon RNAi Technologies, Horizon Discovery). Media were changed 24 h later and the experiment ended at 96 h post transfection. In 6 well plate format, 360 000 SUM185PE cells, 300 000 CAL51 cells, 300 000 MFM223 cells and 90 000 MDA-MB-231 cells were reverse transfected with 3  $\mu$ L of the corresponding lipid as previously mentioned. Media were changed 24 h later and the experiment ended at 72 h post transfection.

The FGFR3-TACC3 fusion and wildtype FGFR3 were knocked down together using ON-TARGETplus human FGFR3 set of 4 individual siRNAs labelled as FW 1 – 4 (Dharmacon RNAi Technologies, Horizon Discovery, Q-003133-00). Wildtype FGFR3 expression was knocked down using 3 individual custom FGFR3 siRNAs from Bioneer with the following sequence: GAGGAAAAGGCUGGUACAA (W1), CACAUGUCCAGCACCUUGU (W2) and GAUGCUGUGUAUAUGGUAU (W3). The ON-TARGETplus non-targeting

SMARTpool (siOTP-NT) was used as the control (Dharmacon RNAi Technologies, Horizon Discovery, D-001810-10). All siRNAs were used at a final concentration of 20 nM.

### **3.2.12 Quantification and statistical analysis**

Quantification by densitometry was performed using ImageLab version 5.2.1 (Bio-Rad) and statistical t-tests were performed using GraphPad Prism 8 and Microsoft-Excel.

## **3.3 Results**

### **3.3.1 Expression and phosphorylation of FGFRs and FGFR3-TACC3 fusion protein in TNBC cell lines**

To identify potential therapeutic targets in TNBC, global MS-based phosphotyrosine profiling was undertaken. First, a data-dependent acquisition (DDA) workflow was used to generate a spectral library, with 2287 phosphotyrosine sites identified across the 24 TNBC cell lines. Then a hyper-reaction monitoring data-independent acquisition (HRM-DIA) workflow was utilized to quantitatively profile tyrosine phosphorylation patterns across this panel. Since FGFRs are implicated in cancer, including breast cancer, and represent candidate therapeutic targets, we extracted data for specific FGFR phosphorylation sites from this dataset (Fig. 3.1, Supplementary Table 3.1). In addition, a panel of 11 TNBC cell lines was selected and subjected to Western blot analysis using selective FGFR antibodies (Fig. 3.2). FGFRs resolve as a doublet (FGFR2 and FGFR4) or a triplet (FGFR1 and FGFR3) upon SDS-PAGE due to post-translational modifications (Fig. 3.2). Overall, the results revealed high activation and expression of specific FGFRs, highlighting them as potential oncogenic drivers and therapeutic targets in TNBC.

Moderate FGFR1 phosphorylation was observed in BT549, CAL51, HS578T and MFM223 cells, and low phosphorylation in an additional 5 cell lines (Fig. 3.1). High FGFR1 expression was detected by Western blotting in CAL120 cells and low to moderate levels in a further 6

cell lines (Fig. 3.2). The results for the CAL120 cell line indicate that high FGFR1 expression may not be accompanied by detectable tyrosine phosphorylation (Fig. 3.1-3.2).

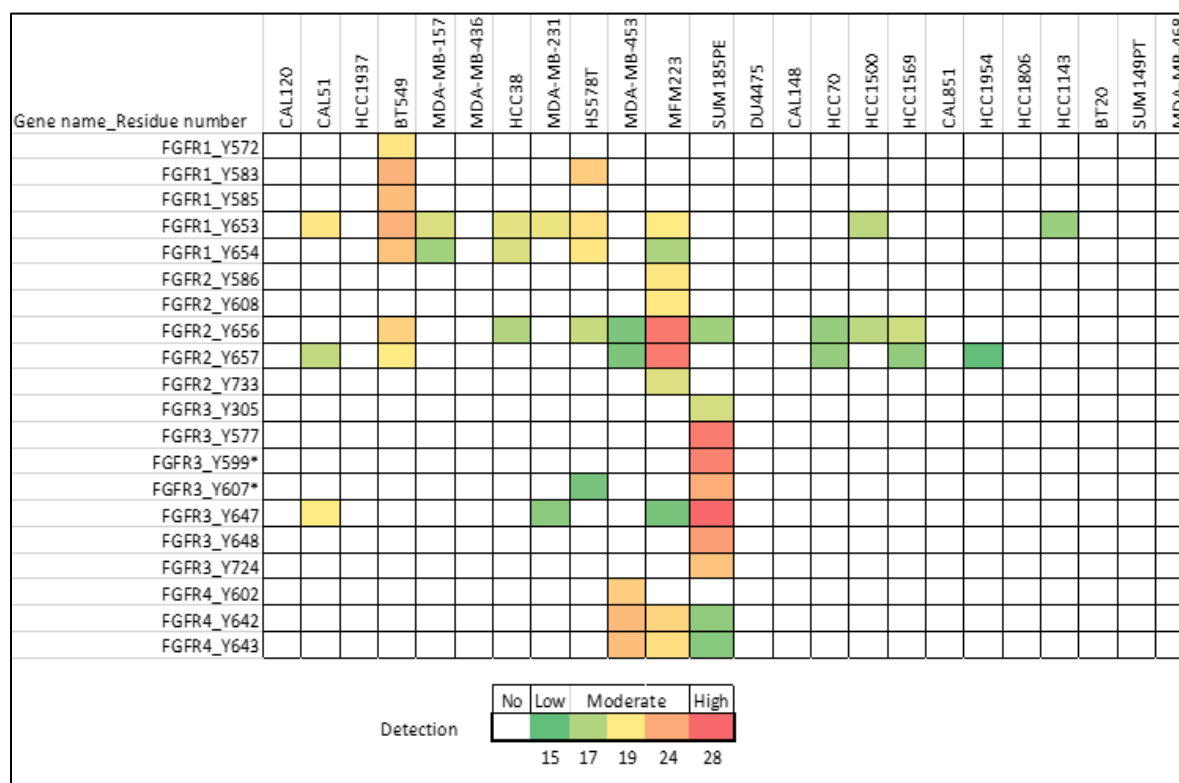


**Figure 3.1: FGFR expression and phosphorylation signature in TNBC cell lines as determined by MS-based tyrosine phosphorylation profiling.** Relative normalized abundance of FGFR1 – 4 phosphorylated tyrosine (pY) residues based on z-score across a panel of 24 TNBC cell lines. The z-scores of detectable tyrosine-phosphosites were obtained by subtracting the mean of all pY sites across the 24 TNBC cell line panel from the value for the pY site, and then dividing by the standard deviation of all 24 TNBC cell lines. The white box represents a non-detectable pY site. The asterisks indicate that FGFR3\_Y599 is identical to FGFR1 (Y605) while FGFR3\_Y607 is identical to FGFR2 (Y616), but the FGFR3 assignment is more likely given relative receptor expression levels.

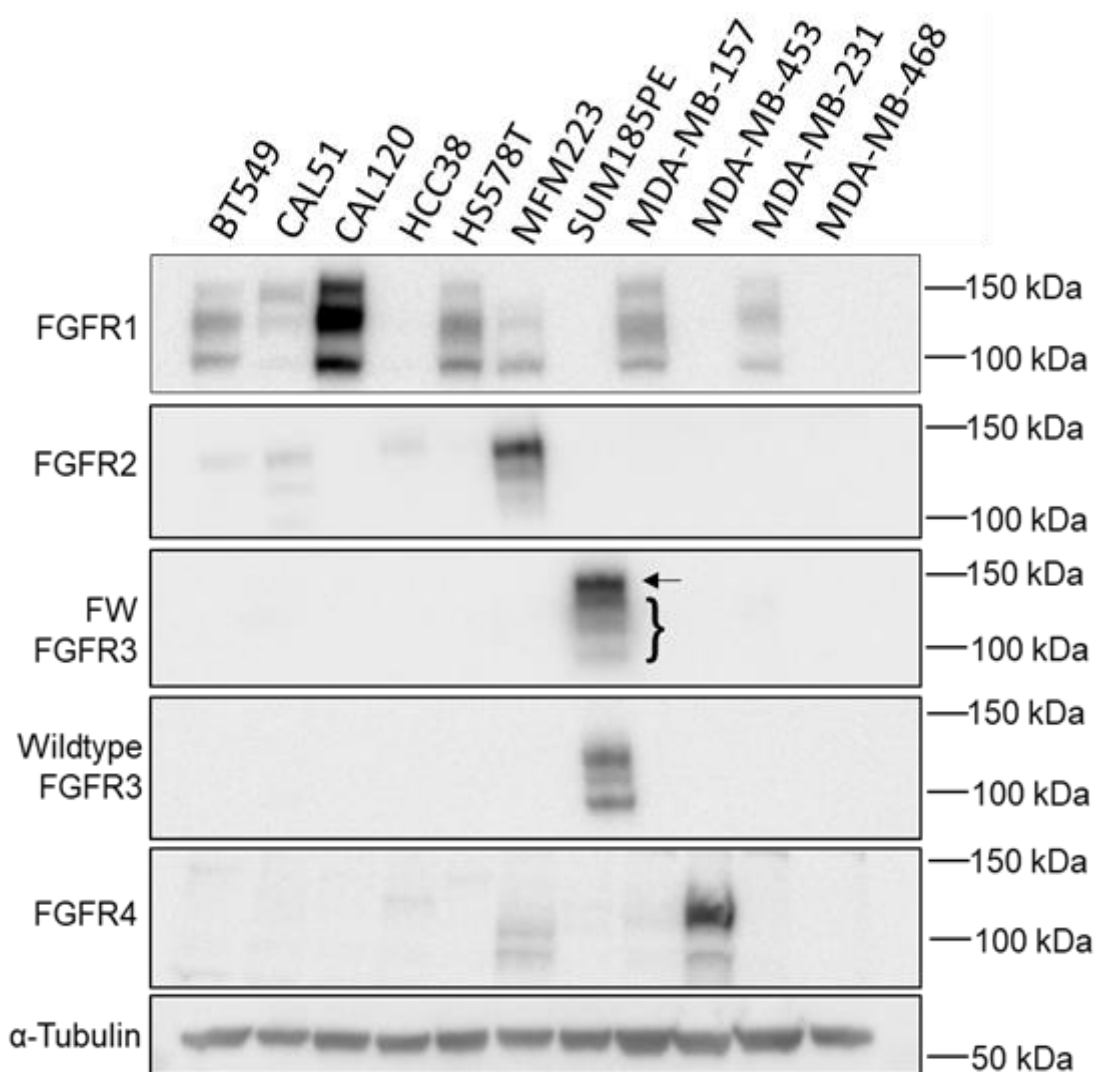


**Figure 3.2: Characterisation of FGFR1 – 4 expression in a panel of 11 TNBC cell lines.** Cell lysates were Western blotted as indicated. Arrow indicates the FGFR3-TACC3 fusion protein, bracket indicates the wildtype FGFR3.

High FGFR2 phosphorylation was detected in MFM223 cells, moderate phosphorylation in BT549 and low phosphorylation in an additional 9 cell lines (Fig. 3.1). High FGFR2 expression was detected in MFM223 cells, and low expression detected in 3 cell lines (Fig. 3.2). The results indicate that high FGFR2 phosphorylation correlates with high FGFR2 expression in MFM223 cells (Fig. 3.1-3.2).

Moderate FGFR4 phosphorylation was detected in MDA-MB-453 and MFM223 cells (Fig. 3.1), and low phosphorylation in SUM185PE cells (Fig. 3.1). High and moderate FGFR4 expression was detected in the first two cell lines, respectively (Fig. 3.2).

High FGFR3 expression and phosphorylation was detected in SUM185PE cells. In addition, moderate phosphorylation was detected in CAL51 cells and low phosphorylation in an additional 3 cell lines (Fig. 3.1-3.2). The SUM185PE cell line harbors a FGFR3-TACC3 fusion [34], and interrogation of our phosphoproteomic dataset revealed that SUM185PE cells were the only TNBC cell line to exhibit tyrosine phosphorylation of TACC3, likely reflecting autophosphorylation of the fusion protein, and the TACC3 interactor CKAP5 (Supplementary Table 3.2 and Supplementary Figure 3.1).

To distinguish between the FGFR3-TACC3 fusion and the wildtype FGFR3, two antibodies were used (Fig. 3.3). FW FGFR3 detects the region of FGFR3 between amino acid 25 – 124, thereby recognising both wildtype FGFR3 and the FGFR3-TACC3 fusion protein (detected as a slower migrating band above the wildtype FGFR3) (Fig. 3.2-3.3). The wildtype-FGFR3 antibody is selective for this form of the receptor as the epitope localises at the C-terminal region (Fig. 3.2-3.3). The results indicate that SUM185PE cells express high levels of wildtype FGFR3 as well as the FGFR3-TACC3 fusion (Fig. 3.2). The presence of both wildtype FGFR3 and an oncogenic form, FGFR3-TACC3 fusion in SUM185PE cells, apparent FGFR3 activation in other TNBC cell lines, and the lack of information regarding FGFR3 signalling and function in TNBC, led us to focus on this receptor.



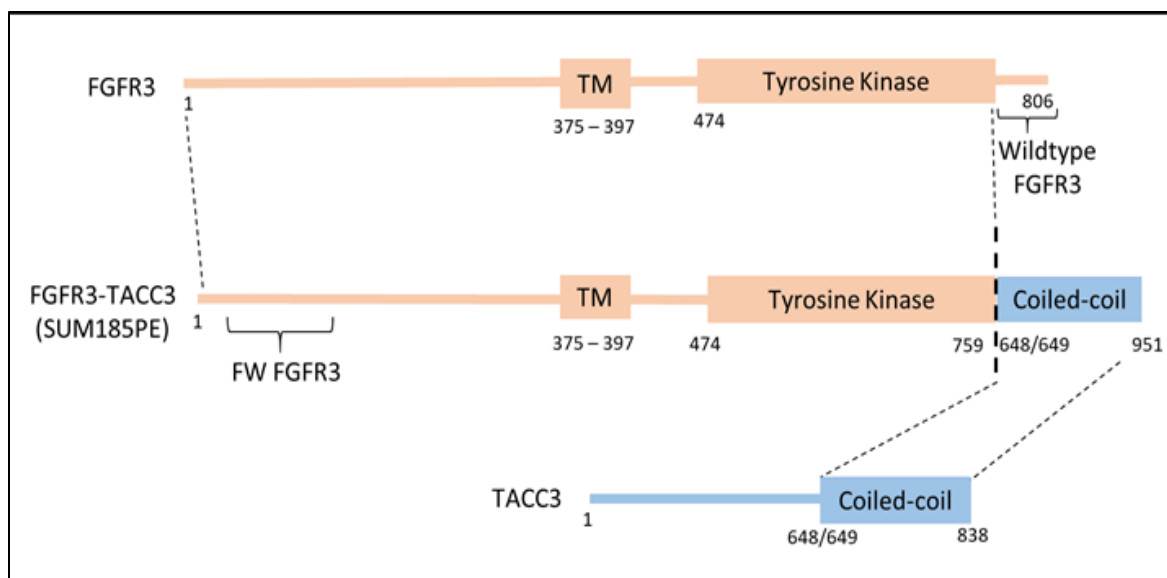


**Figure 3.3: Schematic of FGFR3-TACC3 fusion protein adapted from Shaver *et al.* (2016) [34].** The protein structure of wildtype FGFR3 is shown in pink and wildtype TACC3 is shown in blue. The grey dotted lines highlight the junction between FGFR3 and TACC3, which forms the FGFR3-TACC3 fusion protein in the SUM185PE cell line. FW FGFR3 antibody detects the region of FGFR3 between amino acids 25-124, recognising both wildtype FGFR3 and the FGFR3-TACC3 fusion protein. Wildtype FGFR3 antibody detects FGFR3 at the C-terminal region, only recognising wildtype FGFR3. TM= transmembrane.

### 3.3.2 Tyrosine phosphorylation of wildtype FGFR3 and the FGFR3-TACC3 fusion in SUM185PE cells

Since the SUM185PE cell line demonstrated high expression of both wildtype FGFR3 and the FGFR3-TACC3 fusion (Fig. 3.2), accompanied by high FGFR3 phosphorylation (Fig. 3.1), it was necessary to determine the contribution of the two receptor forms to this phosphorylation pattern. Tyrosine phosphorylated FGFR3 was enriched by immunoprecipitation using a selective antibody then blotted for FGFR3 using the two discriminatory antibodies (Fig. 3.4a). In this study, the MDA-MB-468 cell line with undetectable FGFR expression and phosphorylation (Fig. 3.1-3.2) was used as a negative control. In the SUM185PE lysate enriched for tyrosine phosphorylated FGFR3, a band of the same mobility as the FGFR3-TACC3 fusion was readily detected when immunoblotted with the FW-FGFR3 antibody (Fig.

3.4a). A faint band was detected with the wildtype FGFR3 antibody (Fig. 3.4a). However, using this approach, wildtype FGFR3 may be co-purified in the pFGFR3 fraction, but not be directly tyrosine phosphorylated.

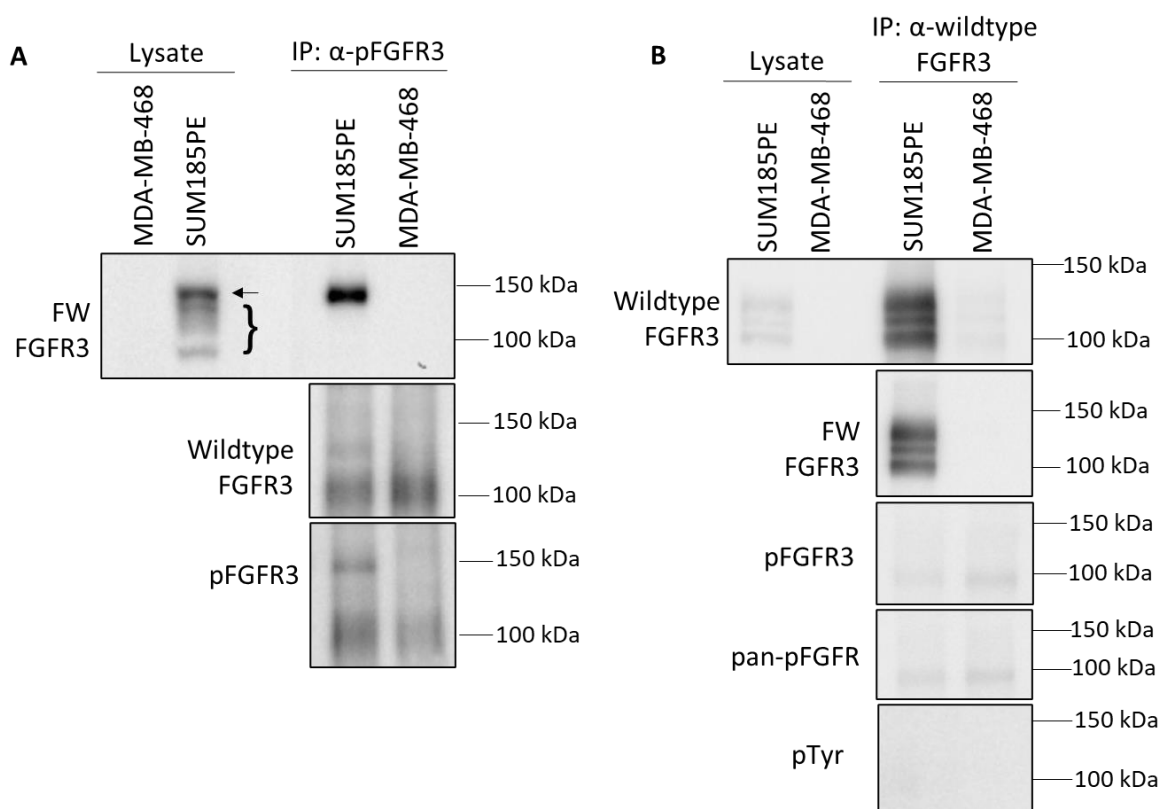


**Figure 3.4: Characterisation of FGFR3 phosphorylation in the SUM185PE cell line.**

**a** Immunoprecipitation using a pFGFR3 antibody. SUM185PE and MDA-MB-468 (negative control) cell lysates were subjected to immunoprecipitation with the pFGFR3 antibody and then Western blotted with the indicated antibodies. The arrow indicates the FGFR3-TACC3 fusion protein and the bracket indicates wildtype FGFR3. **b** Immunoprecipitation using the wildtype FGFR3 antibody. Cell lysates were subjected to immunoprecipitation with the wildtype FGFR3 antibody and blotted with the indicated antibodies.

To confirm the faint band detected in the wildtype FGFR3 blot in Figure 3.4a, wildtype FGFR3 was enriched and blotted for phosphorylation using pFGFR3, pan-pFGFR and pTyr antibodies (Fig. 3.4b). No additional bands were observed in these blots compared to the negative control, indicating phosphorylation of wildtype FGFR3 was undetectable by this approach (Fig. 3.4b).

These results indicate that the FGFR3-TACC3 fusion must contribute to the majority of phosphorylated FGFR3 in SUM185PE cells.

### **3.3.3 The FGFR3-TACC3 fusion predominantly localises to the cytoplasm and plasma membrane**

TACC3 is a microtubule-associated protein that regulates mitotic spindle organization and stabilization, with the C-terminal coiled-coil domain of TACC3 mediating localisation to the mitotic spindle [38, 42]. In glioblastoma, the FGFR3-TACC3 fusion was demonstrated to localise at the mitotic spindle poles in dividing cells, causing chromosomal segregation defects and triggering aneuploidy [35]. Furthermore, fractionation studies in MCF7 cells showed strong FGFR3-TACC3 fusion localisation to the nucleus [43]. However, a later study demonstrated that entry into the secretory pathway or plasma membrane localisation was essential for cell transformation by the FGFR3-TACC3 fusion [44]. Furthermore, in HeLa cells, the FGFR3-TACC3 fusion was found to localise outside the spindle region in membrane vesicles, causing mitotic defects by removing wildtype TACC3 from the mitotic spindle [38]. These findings indicate that the localisation and mechanism of FGFR3-TACC3 fusion may vary according to cancer type and cellular context. Consequently, it was important to address the subcellular localisation of the FGFR3-TACC3 fusion in SUM185PE TNBC cells.

Use of the wildtype FGFR3 and FW FGFR3 antibodies for indirect immunofluorescent imaging revealed immunoreactivity in the cytoplasm and plasma membrane (Fig. 3.5a-3.5b). In addition, SUM185PE cells undergoing mitosis were co-stained with tubulin antibodies and the wildtype FGFR3 or FW FGFR3 antibodies (Fig. 3.5c-3.5d, 3.6a-3.6c). SUM185PE cells stained with the wildtype FGFR3 antibody only showed localisation at the cell membrane and in the cytoplasm (Fig. 3.5c-3.5d).

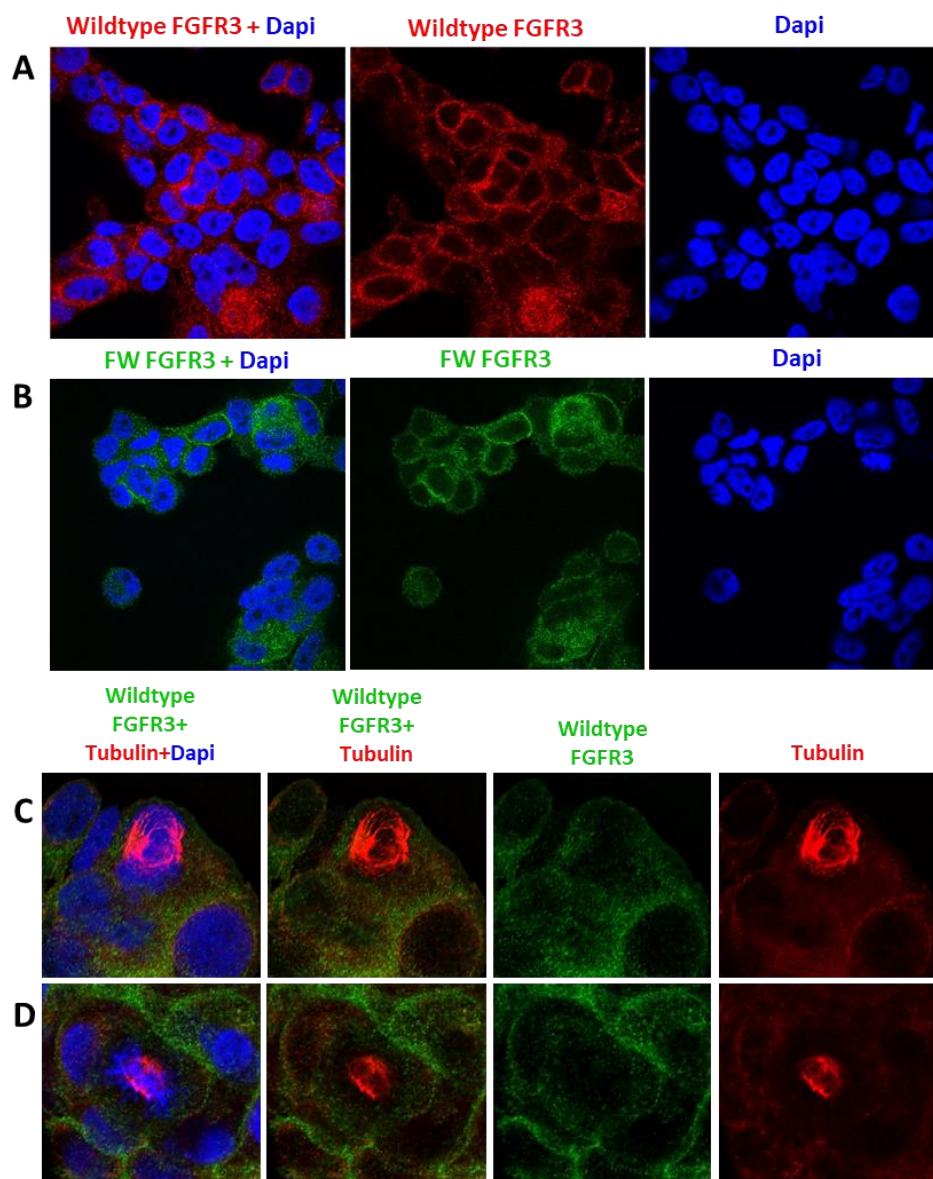


**Figure 3.5: Localisation of FGFR3-TACC3 fusion and wildtype FGFR3 by immunofluorescent staining in SUM185PE cells.** SUM185PE cells were fixed and permeabilised then immunostained with **a** wildtype FGFR3 antibody or **b** FW FGFR3 antibody detecting both FGFR3-TACC3 fusion and wildtype FGFR3. Dapi was used to stain DNA of the cells. Images were obtained by confocal microscopy and are representative of 3 biological replicates, each involving analysis of at least 10 cells. **c-d** Representative images for immunostaining with the wildtype FGFR3 antibody in mitotic SUM185PE cells. For spindle visualisation, SUM185PE cells were treated with 3 mM of thymidine to halt cell cycle progression at the G1/S phase, and then released into complete media to allow cells to undergo mitosis. Tubulin immunostaining was used to visualize the mitotic spindle.

However, upon use of the FW FGFR3 antibody, while the vast majority of dividing SUM185PE cells exhibited immunostaining at the cell membrane and in the cytoplasm (Fig. 3.6a-3.6b, 3.6d), 2 out of 28 cells examined (7%) exhibited additional localisation at the mitotic spindle (Fig. 3.6c-3.6d). Given the data obtained using the wildtype FGFR3 antibody (Fig. 3.5c-3.5d), this indicates that the additional staining must arise from the FGFR3-TACC3 fusion. Overall, these data indicate that the previously reported localisation of FGFR3-TACC3 to the mitotic spindle [35] occurs, but is not a common event in this TNBC model.

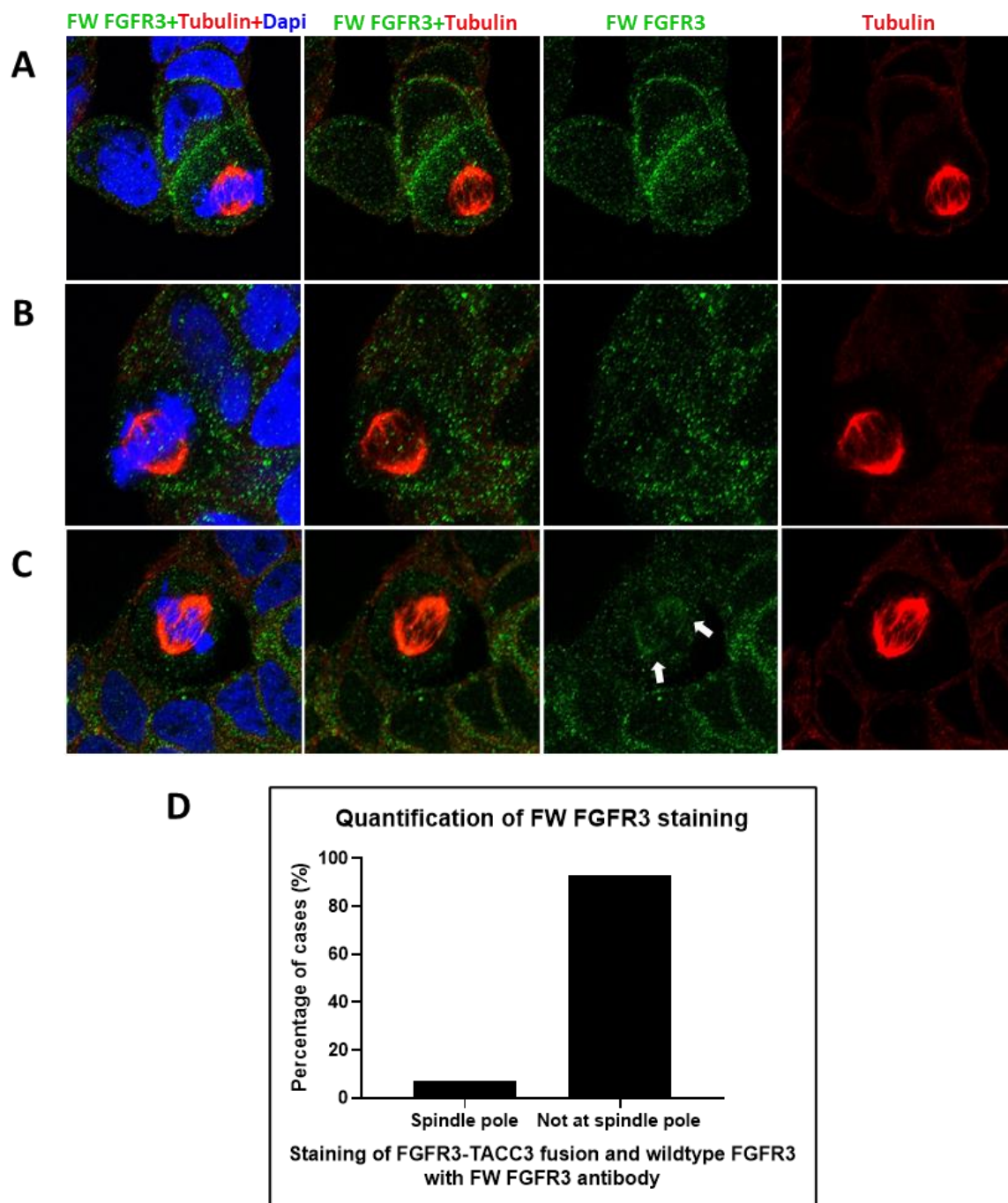


**Figure 3.6: Immunofluorescent staining of mitotic SUM185PE cells with the FW FGFR3 antibody.** **a-c** Imaging was undertaken as in Figure 3.5c-3.5d, except that the FW FGFR3 antibody was used. **d** Quantification of FW FGFR3 immunostaining localisation. Images are representative of 3 biological replicates, each involving analysis of at least 10 cells.



### **3.3.4 Wildtype FGFR3 and the FGFR3-TACC3 fusion exhibit contrasting functional roles in SUM185PE cells**

To characterise the contribution of wildtype FGFR3 and the FGFR3-TACC3 fusion, knockdowns were undertaken with siRNAs that target both the FGFR3-TACC3 fusion and wildtype FGFR3 (FW FGFR3) or only wildtype FGFR3. Knockdown of both FGFR3-TACC3 fusion and wildtype FGFR3 expression decreased phosphorylation of the downstream signalling proteins FRS2, AKT and ERK, and induced cell death in SUM185PE cells (Fig. 3.7-3.8). In contrast, knockdown of wildtype FGFR3 reduced activation of AKT, but not FRS2 and ERK, and resulted in a trend for decreased cell proliferation (Fig. 3.7-3.8).

In order to further evaluate these forms of FGFR3 as potential therapeutic targets, we also determined the effects of the small molecule inhibitor PD173074 on signalling and proliferation. This is an ATP-competitive and type-I inhibitor, which targets FGFR1-3 and to a lesser extent, VEGFR2. It has a similar binding mode to other FGFR inhibitors that are in clinical trials (e.g. Erdafitinib, BGJ398, Pemigatinib and Dovitinib). Its selectivity for FGFR1-3 is similar to that of BGJ398 and Pemigatinib, but is much greater than that of Dovitinib, which is a multikinase inhibitor that also targets VEGFRs, PDGFRs, c-kit and FLT3 and is likely to elicit differing biological effects [45, 46]. Treatment of SUM185PE cells with 5 – 75 nM PD173074 for 1 h led to a significant reduction in the phosphorylation of AKT, ERK1/2 and FRS2, with AKT phosphorylation being the most sensitive to drug treatment (Fig. 3.9).

In addition, administration of PD173074 for 24 – 72 h resulted in decreased expression of Cyclin A and pRb, and detection of cleaved PARP (Fig. 3.10a). Treatment with PD173074 also decreased SUM185PE cell proliferation in a dose-dependent manner, while no effect was observed in the negative control cell line MDA-MB-468 (Fig. 3.10b). Overall, these data indicate that the FGFR3-TACC3 fusion, and not wildtype FGFR3, is the main oncogenic driver in SUM185PE cells, and that targeting this oncoprotein leads to cell cycle arrest in the G1 phase of the cell cycle and also apoptosis.

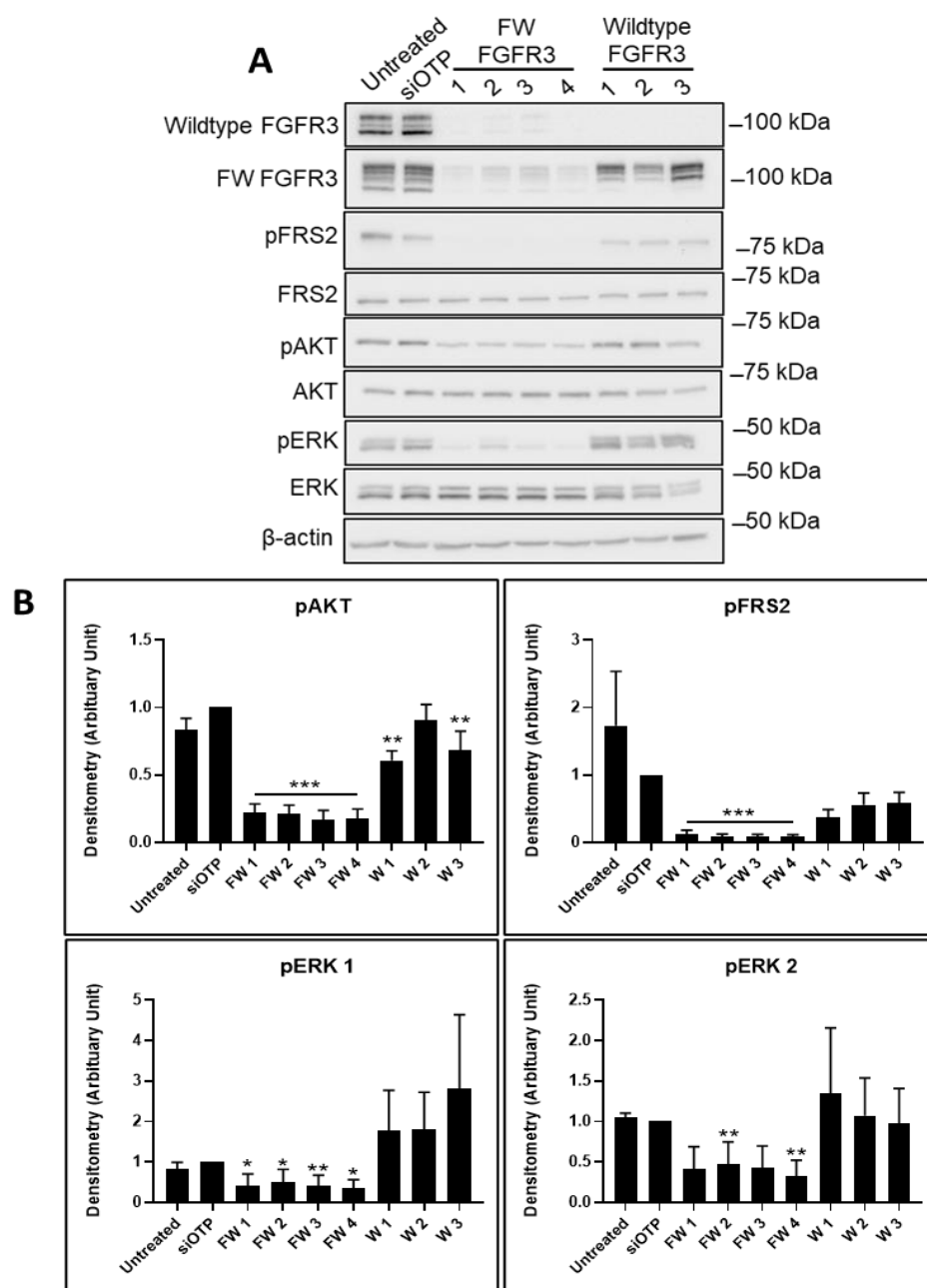


**Figure 3.7: Effect of FGFR3 knockdown on downstream signalling in SUM185PE cells.**

**a** SUM185PE cells were reverse transfected with 20 nM of individual siRNAs targeting FGFR3-TACC3 fusion and wildtype FGFR3 (FW1-FW4), or wildtype FGFR3 only (W1-W3), and the indicated downstream signalling proteins analysed by Western blot. **b** Quantification by densitometry of (a). Data were first normalized relative to the β-actin loading control, then phosphorylated proteins were normalized relative to total protein, then data were expressed relative to the siOTP control which was arbitrarily set at 1.0. Error bars: mean ± standard error, of three biological replicates. \* indicates p-value of <0.05, \*\* < 0.01, \*\*\* < 0.001.



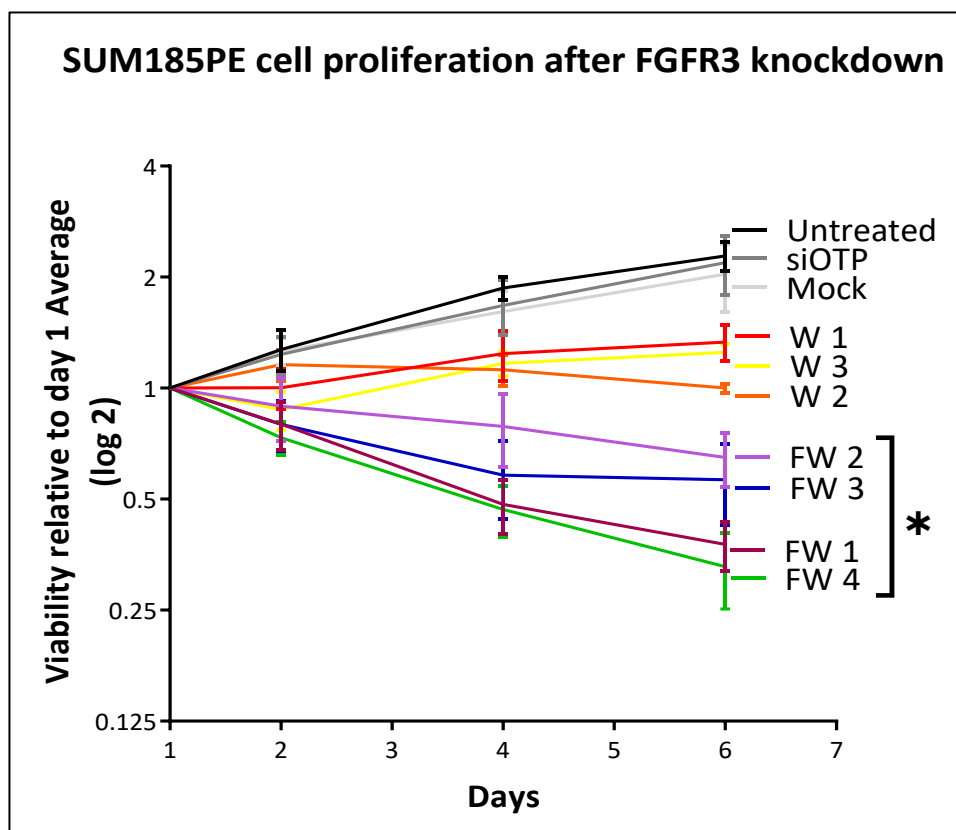


**Figure 3.8: Effect of FGFR3 knockdown on SUM185PE cell proliferation.** SUM185PE cells were reverse transfected with 20 nM of individual siRNAs targeting FGFR3-TACC3 fusion and wildtype FGFR3 (FW 1-4), or wildtype FGFR3 only (W1-3) and cell proliferation indirectly assayed via MTS absorbance. Error bars: mean  $\pm$  standard error, of three biological replicates. W1, W2 and W3 were associated with p-values of 0.17, 0.07, and 0.13, respectively. \* indicates p-value of  $<0.05$ .

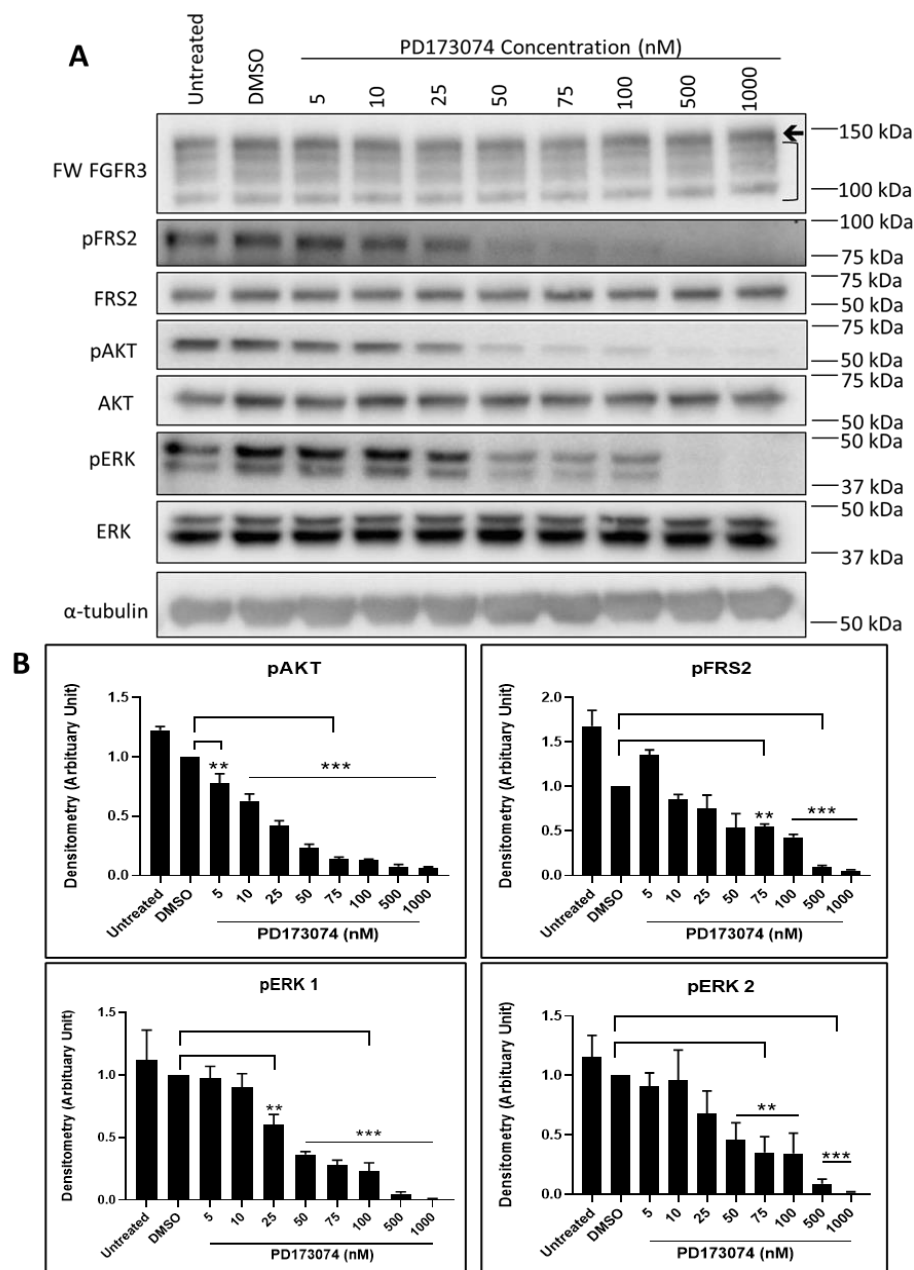


**Figure 3.9: Dose dependent effect of the FGFR inhibitor PD173074 on FGFR3 downstream signalling pathways in the SUM185PE cell line. a** Expression/activation of downstream signalling proteins 1 h post-treatment with the indicated doses of PD173074. Arrow indicates FGFR3-TACC3 fusion protein, bracket indicates wildtype FGFR3. **b** Quantification by densitometry of (a). Data were first normalized relative to the tubulin control, then phosphorylated proteins were normalized to total protein, finally data were expressed relative to the DMSO control which was arbitrarily set at 1.0. Error bars: mean  $\pm$  standard error, of three biological replicates. \*\* indicates p-value of  $<0.01$ , \*\*\*  $<0.001$ .

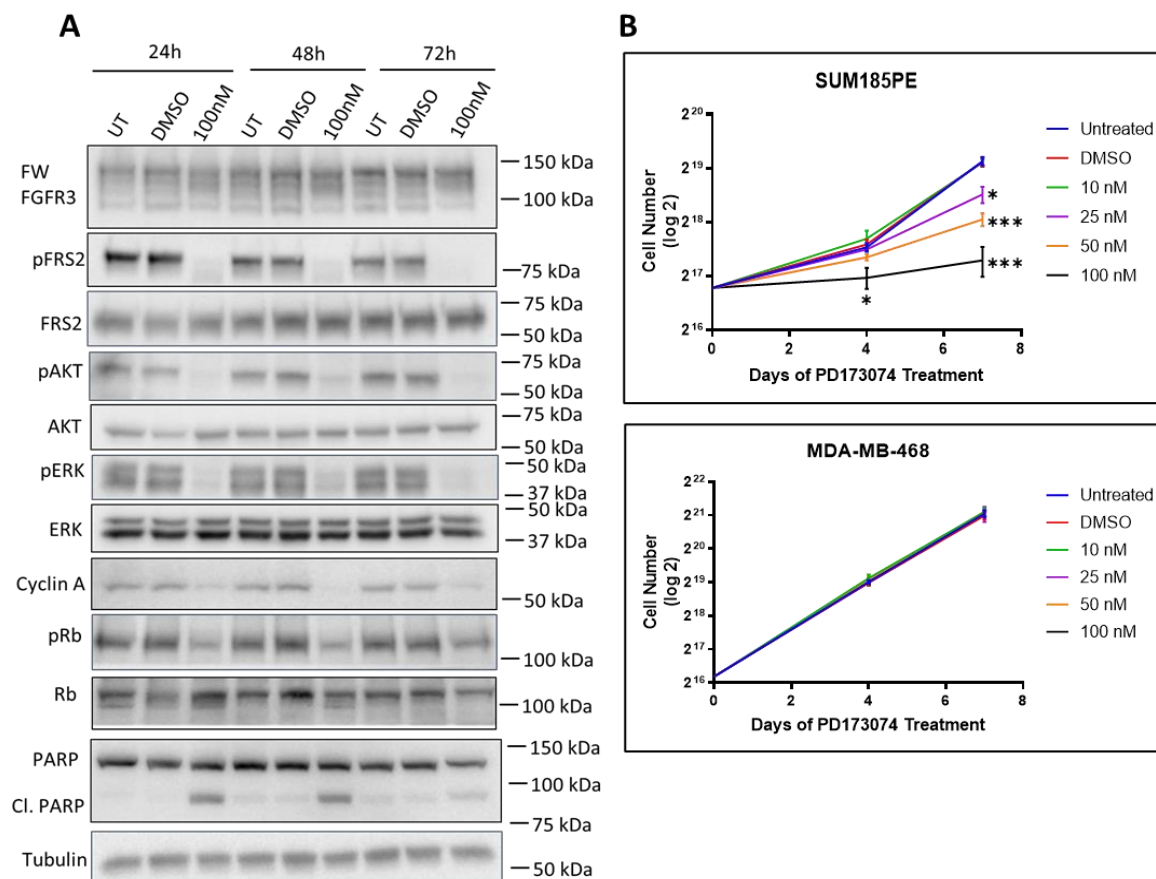


**Figure 3.10: Effect of PD173074 on proliferation and apoptosis in SUM185PE cells.**

**a** Effect on cell cycle and apoptosis markers. SUM185PE cells were treated with PD173074 for 24 h, 48 h and 72 h and the effect on the indicated proteins analysed by Western blotting. UT indicates ‘untreated group’ as a control for DMSO addition, in order to monitor any effect of DMSO on cell cycle regulators. **b** Effect of PD173074 on proliferation of SUM185PE and MDA-MB-468 cells. Cell proliferation was determined by direct cell counting. Error bars: mean  $\pm$  standard error, of three biological replicates \* indicates p-value of  $<0.05$ , \*\*\*  $< 0.001$ .

### 3.3.5 Functional role of FGFR3 in TNBC cell lines with low to moderate levels of FGFR3 phosphorylation

Three cell lines exhibited low to moderate FGFR3 phosphorylation in the phosphoproteomic dataset on sites specific to FGFR3: MDA-MB-231, MFM223 and CAL51 (Fig. 3.1). Since FGFR3 was undetectable in these cells by direct Western blot (Fig. 3.2, 3.11a), lysates were

subjected to immunoprecipitation to enrich for FGFR3 and the receptor detected by Western blot using the FW FGFR3 antibody (Fig. 3.11a). This confirmed that each of these cell lines indeed expresses FGFR3, with the identity of the receptor validated by siRNA knockdown (Fig. 3.11b). However, FGFR3 knockdown did not significantly affect cell proliferation in any of the cell lines (Fig. 3.12), indicating that the oncogenic role of FGFR3 in TNBC is likely limited to contexts where it is hyperactivated due to mutation or gene translocation events.

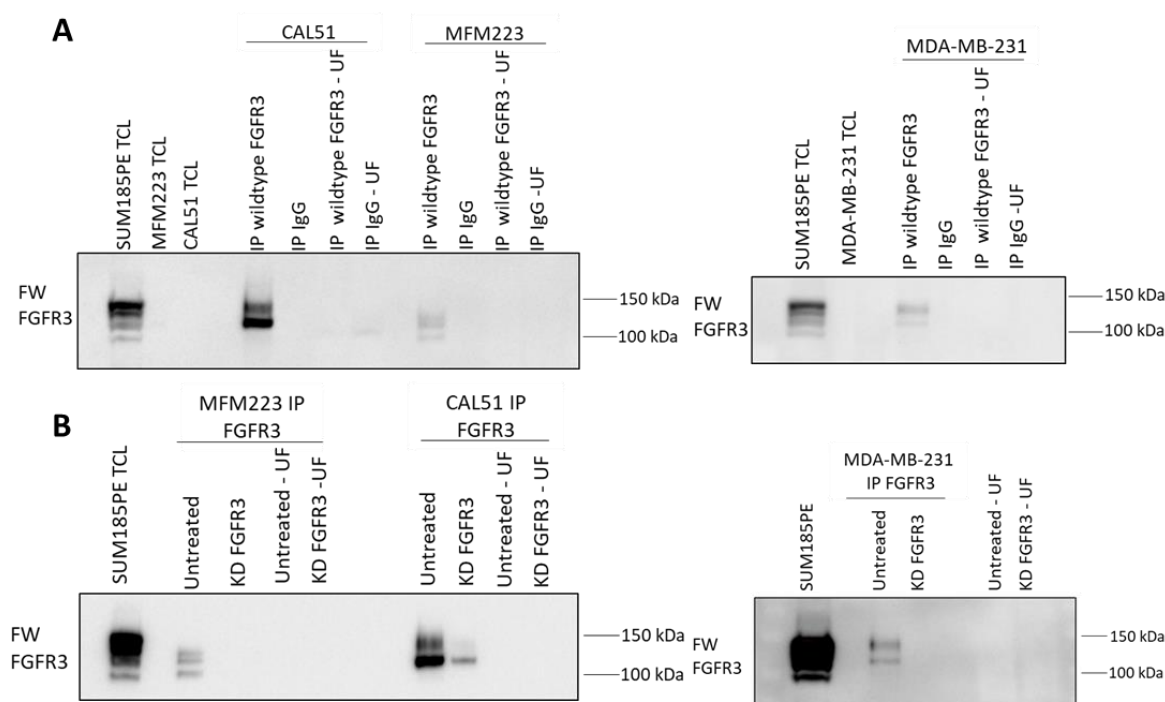


**Figure 3.11: Expression of FGFR3 in TNBC cell lines exhibiting low-moderate FGFR3 phosphorylation. a** FGFR3 expression analysed by immunoprecipitation and Western blot. Lysates from CAL51, MFM223 and MDA-MB-231 cells were subjected to immunoprecipitation of wildtype FGFR3, which was then detected by Western blotting using the FW FGFR3 antibody. IgG was used as a negative control for immunoprecipitation. TCL = total cell lysate. UF = unbound fraction. **b** Confirmation of FGFR3 expression by knockdown. Cell lines from (a) were subjected to FGFR3 knockdown prior to immunoprecipitation and Western blot analysis. KD = knockdown.

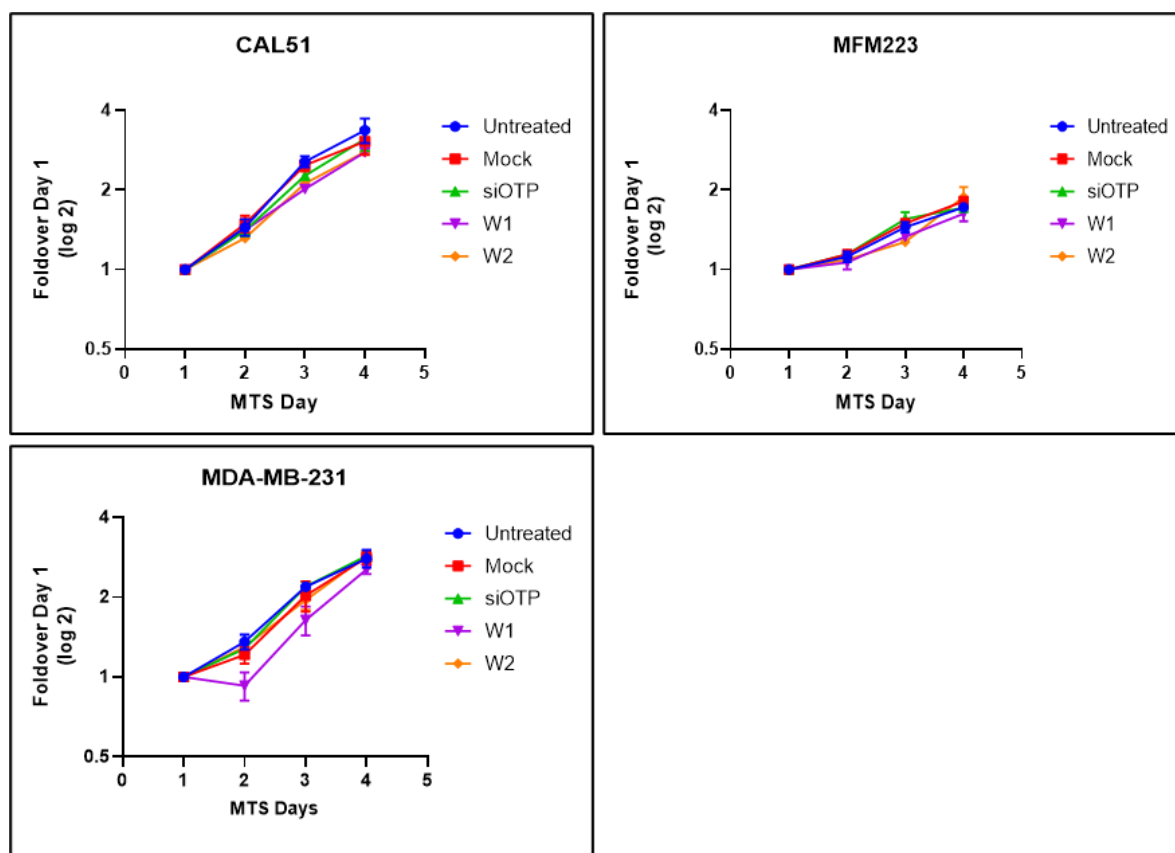


**Figure 3.12: Function of FGFR3 in TNBC cell lines exhibiting low-moderate FGFR3 phosphorylation.** Effect of FGFR3 knockdown on cell proliferation. Cells were transfected with 20 nM of individual siRNAs targeting wildtype FGFR3 (W1-2) and cell proliferation indirectly assayed via a MTS absorbance assay. Error bars: mean  $\pm$  standard error, of three biological replicates.

### 3.3.6 Evaluation of FGFR3 alterations in breast cancer patients using public datasets

The TCGA and the METABRIC datasets were analyzed using cBioportal to determine the frequency of FGFR3 alterations in terms of overexpression, mutation, amplification and deletion in different breast cancer subtypes. In the TCGA and METABRIC datasets, 43 out of 994 (4%) and 56 out of 1904 (3%) of breast cancer patients have FGFR3 alterations, respectively (Fig. 3.13a-3.13b). FGFR3 amplification, which affected 5 breast cancer patients (0.5%) and 9 cases (0.5%) in the TCGA and METABRIC datasets respectively, was observed

in the TNBC/basal, luminal A and luminal B subtypes, with FGFR3 deep deletion mostly detected in the TNBC/basal or HER2+ subtypes (Fig. 3.13a-3.13b). FGFR3 overexpression was more common in luminal subtypes than TNBC/basal. In the METABRIC dataset, breast cancer patients with amplified and/or overexpressed FGFR3 (46 out of 1903, 2%) have a significant (p-value of 0.0204) worse overall survival compared to breast cancer patients without FGFR3 alterations (Fig. 3.13c). These data confirm that potentially oncogenic FGFR3 alterations do occur in TNBC, as well as other breast cancer subtypes, albeit at low frequency.

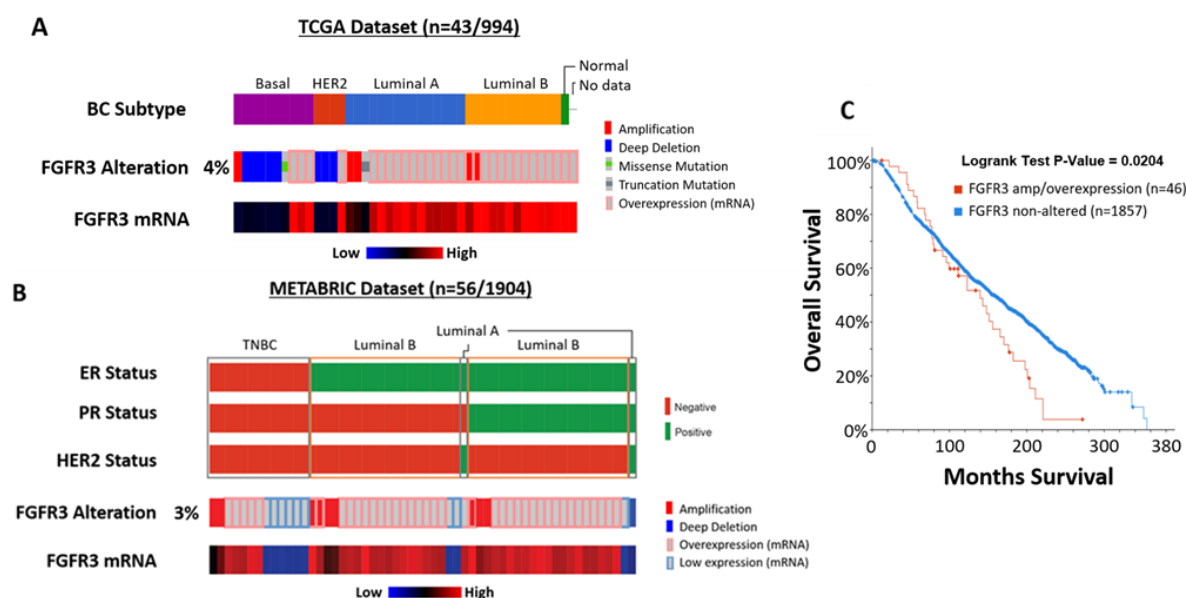


**Figure 3.13: FGFR3 alterations in human breast cancer.** Frequency of FGFR3 alterations in breast cancer patients analysed using two breast cancer patient datasets, **a** Pan-cancer Atlas dataset from TCGA and **b** METABRIC dataset, using cBioportal (note that no mutation data are available for the METABRIC dataset). Only patients with FGFR3 alterations are displayed for brevity. For both cohorts, the breast cancer subtypes based on ER/PR and HER2 receptor status are displayed. **c** A Kaplan–Meier plot showing patients with amplification and/or overexpression of FGFR3 (n=46) are significantly associated with worse overall survival compared to those without these alterations (n=1857) in the METABRIC dataset. A Logrank test was used, P-value = 0.0204 (P-value < 0.05 considered significant). Survival data for the two patient groups were extracted and downloaded from cBioportal, and survival analysis performed using in-house Matlab script.

## 3.4 Discussion

FGFR signalling has many biological roles in normal physiology, including regulation of cell proliferation, migration and survival, however in breast cancer progression, FGFR signalling is often deregulated [24, 33]. FGFR1 amplification is the most common aberration, followed by FGFR2 amplification, and the roles of these receptors have been characterised in detail [23, 28, 30]. To date, our work is the most detailed study on FGFR3, describing its activation, expression and function in TNBC.

Our characterisation of FGFR3 function in TNBC cell lines exhibiting differing levels of receptor activation demonstrated that only the aberrantly activated FGFR3-TACC3 fusion in SUM185PE cells functioned as an oncogenic driver, at least *in vitro*. This fusion is constitutively activated due to dimerization driven by the TACC3 region [35, 38].

Knockdown of wildtype FGFR3 in SUM185PE cells resulted in modest effects on AKT activation and cell proliferation, while having no effect on MFM223, CAL51 and MDA-MB-231 cell proliferation. Since expression of wildtype FGFR3 is higher in SUM185PE cells than the other cell lines, this suggests that a threshold level of expression/activation is required for detectable effects on signalling and proliferation. However, other factors that likely limit the biological role of FGFR3 in TNBC cell lines are the genetic background of the cells, and production of autocrine ligands. MFM223 cells exhibit FGFR2 amplification, which may make FGFR3 redundant. CAL51 cells express detectable FGFR1 and FGFR2 as well as autocrine FGF2 and are sensitive to PD173074 [33]. Therefore, these data and our phosphoproteomic and functional analyses, indicate that FGFR1 and FGFR2 must play a more important functional role in these cells, rather than FGFR3. However, MDA-MB-231 cells are resistant to PD173074 and express very low levels of FGF2 [33] that will limit activation of expressed FGFRs. In light of the latter finding, it remains possible that the oncogenic potential of FGFR3 may be different *in vivo*, where cancer cells are exposed to paracrine FGFs from the stroma.

This report is the first study of FGFR3-TACC3 signalling and localisation in the context of breast cancer. Consistent with previous studies on head and neck malignancies [37] and glioblastoma [35, 47], attenuation of FGFR3-TACC3 activation decreased phosphorylation of FRS2, AKT and ERK. However, while in glioblastoma, the FGFR3-TACC3 fusion reportedly localises to the mitotic spindle poles [35], we observed that the vast majority of FGFR3-TACC3 fusion and all of wildtype FGFR3 localised to the cytoplasm and plasma membrane, consistent with data from HeLa cells [38], the requirement for entry into the secretory pathway or localisation to the plasma membrane for FGFR3-TACC3 oncogenic function [44] and coupling of FGFR3-TACC3 to canonical downstream signalling pathways usually activated at the plasma membrane. That said, the occasional detection of FGFR3-TACC3 at the spindle poles indicates that this still represents a potential mechanism whereby this oncoprotein may contribute to tumour progression, for example by promoting aneuploidy in a small subpopulation of cells [35].

In the TCGA and METABRIC datasets, FGFR3 alterations are observed in a total of 99 out of 2,898 breast cancer patients (3.4%), with 16 out of 2,898 (0.6%) cases reflecting FGFR3 amplification or mutation (Fig. 10A-10B). Other studies support the presence, albeit at low frequency, of FGFR3 alterations in breast cancer. In a study of 182 ER+ breast cancer patients, FGFR3 was mutated in 3 out of 126 (2.4%) primary samples and 1 out of 57 (1.8%) metastatic samples [48]. In addition, a FGFR3-TACC3 fusion was detected in 1 out of 253 TNBC tumours (0.4%) [34]. Despite low frequencies, therapeutic targeting of FGFR3 represents a potential option for cancers exhibiting oncogenic forms of FGFR3, supported by our data regarding the efficacy of PD173074 in SUM185PE cells.

In addition to FGFR3 amplification, deep deletions of FGFR3 occur (Fig. 10A-10B). This has also been observed in inflammatory breast cancer, where 10 out of 156 (6.4%) cases had FGFR3 deletion [49]. The loss of FGFR3 is significantly associated with higher grade urothelial bladder tumours [50] and also leads to chondroma-like lesion formation by downregulating ERK signalling whilst upregulating Hedgehog signalling, suggesting tumour suppressive roles of FGFR3 [51]. Furthermore in pancreatic cancer, where FGFR3 expression is downregulated, FGFR3 functions as a tumour suppressor in cancer cells of epithelial

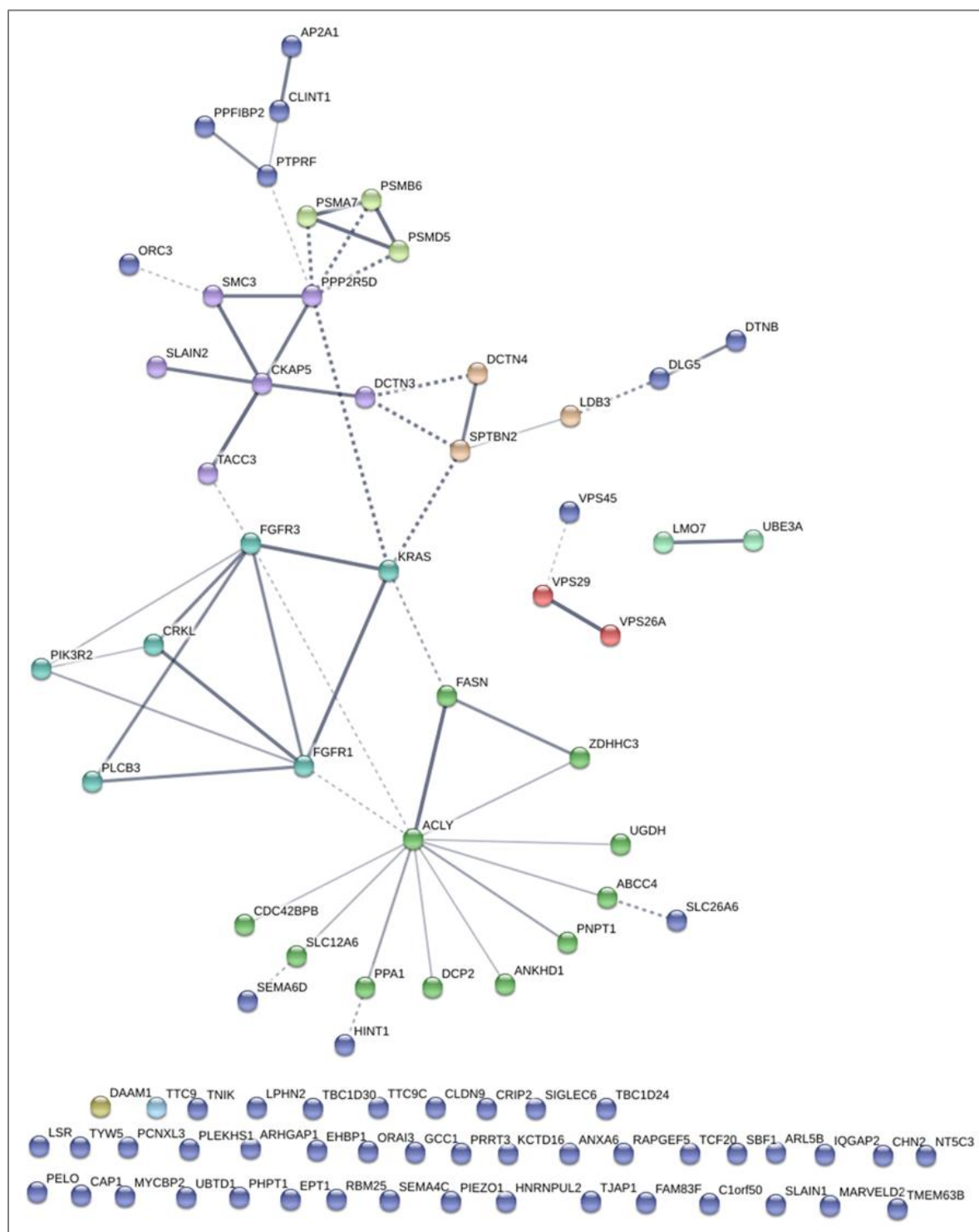


phenotype and an oncogene in cells of mesenchymal phenotype, highlighting context-dependent functional roles [52]. Despite the presence of FGFR3 deletions in a subset of breast cancer patients, amplification and/or overexpression of FGFR3 is associated with poor prognosis in the METABRIC dataset, and an immunohistochemical study in breast cancer also identified FGFR3 as a negative prognostic factor [53]. Consequently, while the presence of FGFR3 deletions raises the possibility of context-dependent tumour suppressor roles in a subset of breast cancers, strong evidence also exists for a positive role for this receptor in breast cancer progression.

### **3.5 Conclusion**

Increased expression and activation of FGFR3 occurs in TNBC but an oncogenic role could only be demonstrated for a rare example of a FGFR3-TACC3 fusion. These results indicate that targeting FGFR3 may represent a therapeutic option for TNBC, but only for a select group of patients with oncogenic FGFR3 alterations.

# 3.6 Supplementary Materials



**Supplementary Figure 3.1: Interactions of proteins exhibiting specific tyrosine phosphorylation specific to SUM185PE cell line using STRING software.**

**Supplementary Table 3.1: Quantifiable FGFR tyrosine phosphorylated peptide expression (log2) identified across 24 TNBC cell lines.**

Uniprot ID	Gene name_Yphosphosite	CAL120	CAL51	HCC1937	BT549	MDA-MB-157	MDA-MB-436	HCC38	MDA-MB-231	HS578T	MDA-MB-453	MFM223	SUM185PE	DU4475	CAL148	HCC70	HCC1500	HCC1569	CAL851	HCC1954	HCC1806	HCC1143	BT20	SUM149PT	MDA-MB-468
P11362	FGFR1_Y572				20																				
P11362	FGFR1_Y583				23					21															
P11362	FGFR1_Y585				23																				
P11362	FGFR1_Y653		20		23	18		19	19	20		19					18					17			
P11362	FGFR1_Y654				22	17		18		20		17													
P11362	FGFR1_Y605;FGFR3_Y599												27												
P11362	FGFR2_Y586											20													
P21802	FGFR2_Y608											20													
P21802	FGFR2_Y656				21			18		18	16	27	17			17	18	18							
P21802	FGFR2_Y657		18		19						16	27				17		17		16					
P21802	FGFR2_Y733											19													
P21802	FGFR2_Y616;FGFR3_Y607									16			24												
P22455	FGFR4_Y602										21														
P22455	FGFR4_Y642										23	21	17												
P22455	FGFR4_Y643										22	20	17												
P22607	FGFR3_Y305												18												
P22607	FGFR3_Y577												27												
P22607	FGFR3_Y647		19						17			16	28												
P22607	FGFR3_Y648												25												
P22607	FGFR3_Y724											22													

**Supplemental Table 3.2: Quantifiable tyrosine phosphorylated peptide expression**

**(log<sub>2</sub>) specific to SUM185PE cell line.** Tyrosine phosphorylation of TACC3 (highlighted in pink) only occurs in SUM185PE.

Uniprot ID	Gene name_Yphosphosite	SUM185PE	Uniprot ID	Gene name_Yphosphosite	SUM185PE
A2RUC4	TYW5_Y187_A2RUC4	18.49	Q86X29	LSR_Y615_Q86X29	17.97
O00459;P27986	PIK3R2_Y423;PIK3R1_Y426	20.86	Q8IU60	DCP2_Y162_Q8IU60	20.06
O14818;Q8TAA3	PSMA7_Y153;PSMA8_Y161	18.31	Q8IWZ3	ANKHD1_Y1625_Q8IWZ3	18.79
O15020	SPTBN2_Y1726_O15020	20.02	Q8N4S9	MARVELD2_Y446_Q8N4S9	20.14
O15439	ABCC4_Y1259_O15439	17.84	Q8N4S9	MARVELD2_Y531_Q8N4S9	18.50
O43699	SIGLEC6_Y446_O43699	20.44	Q8N5M4	TTC9C_Y147_Q8N5M4	19.09
O60701	UGDH_Y108_O60701	17.44	Q8ND30	PPFIBP2_Y310_Q8ND30	18.55
O60701	UGDH_Y473_O60701	18.26	Q8ND83	SLAIN1_Y289_Q8ND83	18.16
O60941	DTNB_Y245_O60941	18.44	Q8NDI1	EHBP1_Y1101_Q8NDI1	16.96
O75112	LDB3_Y661_O75112	21.55	Q8NEG4	FAM83F_Y107_Q8NEG4	16.71
O75436	VPS26A_Y40_O75436	20.9	Q8NFY4	SEMA6D_Y1011_Q8NFY4	18.92
O75592	MYCBP2_Y26_O75592	18.93	Q8NFY4	SEMA6D_Y738_Q8NFY4	20.02
O75935	DCTN3_Y67_O75935	21.87	Q8TCS8	PNPT1_Y459_Q8TCS8	17.53
O95248	SBF1_Y766_O95248	16.79	Q8TDM6	DLG5_Y188_Q8TDM6	20.01
O95484	CLDN9_Y200_O95484	20.56	Q8WWI1	LMO7_Y1672_Q8WWI1	19.06
O95490	LPHN2_Y1433_O95490	18.91	Q92508	PIEZO1_Y1638_Q92508	18.67
O95782	AP2A1_Y777_O95782	16.9	Q92565	RAPGEF5_Y70_Q92565	18.63
P01116	KRAS_Y157_P01116	18.09	Q92623	TTC9_Y180_Q92623	17.19
P08133	ANXA6_Y95_P08133	19.49	Q96CN9	GCC1_Y480_Q96CN9	19.54
P10586	PTPRF_Y1621_P10586	18.83	Q96KC2	ARL5B_Y141_Q96KC2	19.28
P11362;P22607	FGFR1_Y605;FGFR3_Y599	26.59	Q9BRQ5	ORAI3_Y35_Q9BRQ5	18.64
P22607	FGFR3_Y305_P22607	18.32	Q9BRX2	PELO_Y99_Q9BRX2	18.56
P22607	FGFR3_Y577_P22607	27.03	Q9BV19	C1orf50_Y131_Q9BV19	23.18
P22607	FGFR3_Y648_P22607	24.75	Q9BV19	C1orf50_Y163_Q9BV19	18.93
P22607	FGFR3_Y724_P22607	22.09	Q9BXS9	SLC26A6_Y29_Q9BXS9	20.91
P28072	PSMB6_Y59_P28072	17.22	Q9C0C4	SEMA4C_Y707_Q9C0C4	20.01
P46109	CRKL_Y92_P46109	18.67	Q9C0D9	EPT1_Y376_Q9C0D9	17.97
P49327	FASN_Y470_P49327	17	Q9H0P0	NT5C3A_Y146_Q9H0P0	17.84
P49756	RBM25_Y256_P49756	17.16	Q9H6A9	PCNXL3_Y763_Q9H6A9	17.48
P49773	HINT1_Y109_P49773	18.62	Q9HAC8;Q8WUN7	UBTD1_Y40;UBTD2_Y43	17.49
P52757	CHN2_Y158_P52757	18.23	Q9NRW7	VPS45_Y487_Q9NRW7	20.30
P52943	CRIP2_Y58_P52943	20.79	Q9NRX4	PHPT1_Y52_Q9NRX4	19.07
P53396	ACLY_Y1073_P53396	17.83	Q9NYG2	ZDHHC3_Y18_Q9NYG2	19.16
Q01518	CAP1_Y352_Q01518	19.65	Q9NYG2	ZDHHC3_Y295_Q9NYG2	22.89
Q01970	PLCB3_Y548_Q01970	21.72	Q9P270	SLAIN2_Y158_Q9P270	19.38
Q05086	UBE3A_Y127_Q05086	19.03	Q9P270	SLAIN2_Y336_Q9P270	20.55
Q07960	ARHGAP1_Y64_Q07960	17.59	Q9P270	SLAIN2_Y373_Q9P270	20.10
Q13576	IQGAP2_Y1197_Q13576	19.75	Q9UBD5	ORC3_Y607_Q9UBD5	22.74
Q14008	CKAP5_Y1860_Q14008	21.25	Q9UBQ0	VPS29_Y46_Q9UBQ0	19.32
Q14008	CKAP5_Y1879_Q14008	20.37	Q9UGU0	TCF20_Y1632_Q9UGU0	19.19
Q14677	CLINT1_Y114_Q14677	20.35	Q9UHW9	SLC12A6_Y156_Q9UHW9	17.41
Q14738	PPP2R5D_Y519_Q14738	19.78	Q9UJW0	DCTN4_Y150_Q9UJW0	19.09
Q14738	PPP2R5D_Y74_Q14738	18.62	Q9UKE5	TNIK_Y499_Q9UKE5	17.45
Q15181	PPA1_Y28_Q15181	18.41	Q9ULP9	TBC1D24_Y442_Q9ULP9	17.48
Q16401	PSMD5_Y478_Q16401	18.18	Q9UQE7	SMC3_Y668_Q9UQE7	19.39
Q16401	PSMD5_Y490_Q16401	18.62	Q9Y219	TBC1D30_Y621_Q9Y219	17.82
Q1KMD3	HNRNPUL2_Y741_Q1KMD3	17.34	Q9Y4D1	DAAM1_Y401_Q9Y4D1	18.24
Q5FWE3	PRRT3_Y737_Q5FWE3	20.15	Q9Y5S2	CDC42BPB_Y1118_Q9Y5S2	17.09
Q5JTD0	TJAP1_Y316_Q5JTD0	19.43	Q9Y6A5	TACC3_Y403_Q9Y6A5	19.82
Q5JTD0	TJAP1_Y326_Q5JTD0	20.25	Q9Y6A5	TACC3_Y684_Q9Y6A5	22.66
Q5SXH7	PLEKHS1_Y107_Q5SXH7	20.8	Q9Y6A5	TACC3_Y739_Q9Y6A5	22.73
Q5T3F8	TMEM63B_Y93_Q5T3F8	19.16	Q9Y6A5	TACC3_Y753_Q9Y6A5	23.94
Q68DU8	KCTD16_Y112_Q68DU8	16.89	Q9Y6A5	TACC3_Y764_Q9Y6A5	21.59

### 3.7 References

1. **Ferlay, J., I. Soerjomataram, R. Dikshit, S. Eser, C. Mathers, M. Rebelo, D.M. Parkin, D. Forman, and F. Bray,** *Cancer incidence and mortality worldwide: Sources, methods and major patterns in GLOBOCAN 2012*. International Journal of Cancer, 2015. 136(5): p. E359-E386.
2. **Reis-Filho, J.S. and A.N.J. Tutt,** *Triple negative tumours: A critical review*. Histopathology, 2008. 52(1): p. 108-118.
3. **Schneider, B.P., E.P. Winer, W.D. Foulkes, J. Garber, C.M. Perou, A. Richardson, G.W. Sledge, and L.A. Carey,** *Triple-negative breast cancer: Risk factors to potential targets*. Clinical Cancer Research, 2008. 14(24): p. 8010-8018.
4. **Liedtke, C. and A. Rody,** *New treatment strategies for patients with triple-negative breast cancer*. Current Opinion in Obstetrics and Gynecology, 2015. 27(1): p. 77-84.
5. **Mayer, I.A., V.G. Abramson, B.D. Lehmann, and J.A. Pietenpol,** *New strategies for triple-negative breast cancer-deciphering the heterogeneity*. Clinical Cancer Research, 2014. 20(4): p. 782-790.
6. **van Roozendaal, L.M., L.H.M. Smit, G.H.N.M. Duijsens, B. de Vries, S. Siesling, M.B.I. Lobbess, M. de Boer, J.H.W. de Wilt, and M.L. Smidt,** *Risk of regional recurrence in triple-negative breast cancer patients: a Dutch cohort study*. Breast Cancer Research and Treatment, 2016. 156(3): p. 465-472.
7. **Lehmann, B.D., J.A. Bauer, X. Chen, M.E. Sanders, A.B. Chakravarthy, Y. Shyr, and J.A. Pietenpol,** *Identification of human triple-negative breast cancer subtypes and preclinical models for selection of targeted therapies*. Journal of Clinical Investigation, 2011. 121(7): p. 2750-2767.
8. **Burstein, M.D., A. Tsimelzon, G.M. Poage, K.R. Covington, A. Contreras, S.A.W. Fuqua, M.I. Savage, C.K. Osborne, S.G. Hilsenbeck, J.C. Chang, G.B. Mills, C.C. Lau, and P.H. Brown,** *Comprehensive genomic analysis identifies novel subtypes and*

- targets of triple-negative breast cancer*. Clinical Cancer Research, 2015. 21(7): p. 1688-1698.
9. **Perez-Garcia, J., E. Muñoz-Couselo, J. Soberino, F. Racca, and J. Cortes**, *Targeting FGFR pathway in breast cancer*. Breast, 2018. 37: p. 126-133.
  10. **Haugsten, E.M., A. Wiedlocha, S. Olsnes, and J. Wesche**, *Roles of fibroblast growth factor receptors in carcinogenesis*. Molecular Cancer Research, 2010. 8(11): p. 1439-1452.
  11. **Turner, N. and R. Grose**, *Fibroblast growth factor signalling: From development to cancer*. Nature Reviews Cancer, 2010. 10(2): p. 116-129.
  12. **Dienstmann, R., J. Rodon, A. Prat, J. Perez-Garcia, B. Adamo, E. Felip, J. Cortes, A.J. Iafrate, P. Nuciforo, and J. Tabernero**, *Genomic aberrations in the FGFR pathway: Opportunities for targeted therapies in solid tumours*. Annals of Oncology, 2014. 25(3): p. 552-563.
  13. **Brooks, A.N., E. Kilgour, and P.D. Smith**, *Molecular pathways: Fibroblast growth factor signaling: A new therapeutic opportunity in cancer*. Clinical Cancer Research, 2012. 18(7): p. 1855-1862.
  14. **Helsten, T., S. Elkin, E. Arthur, B.N. Tomson, J. Carter, and R. Kurzrock**, *The FGFR landscape in cancer: Analysis of 4,853 tumours by next-generation sequencing*. Clinical Cancer Research, 2016. 22(1): p. 259-267.
  15. **Kim, H.R., H.N. Kang, H.S. Shim, E.Y. Kim, J. Kim, D.J. Kim, J.G. Lee, C.Y. Lee, M.H. Hong, S.M. Kim, H. Kim, K.H. Pyo, M.R. Yun, H.J. Park, J.Y. Han, H.A. Youn, M.J. Ahn, S. Paik, T.M. Kim, and B.C. Cho**, *Co-clinical trials demonstrate predictive biomarkers for dovitinib, an FGFR inhibitor, in lung squamous cell carcinoma*. Annals of Oncology, 2017. 28(6): p. 1250-1259.
  16. **Lim, S.H., J.M. Sun, Y.L. Choi, H.R. Kim, S. Ahn, J.Y. Lee, S.H. Lee, J.S. Ahn, K. Park, J.H. Kim, B.C. Cho, and M.J. Ahn**, *Efficacy and safety of dovitinib in pretreated patients with advanced squamous non-small cell lung cancer with FGFR1 amplification: A single-arm, phase 2 study*. Cancer, 2016. 122(19): p. 3027-3031.

17. **Javle, M., M. Lowery, R.T. Shroff, K.H. Weiss, C. Springfield, M.J. Borad, R.K. Ramanathan, L. Goyal, S. Sadeghi, T. Macarulla, A. El-Khoueiry, R.K. Kelley, I. Borbath, S.P. Choo, D.Y. Oh, P.A. Philip, L.T. Chen, T. Reungwetwattana, E. Van Cutsem, K.H. Yeh, K. Ciombor, R.S. Finn, A. Patel, S. Sen, D. Porter, R. Isaacs, A.X. Zhu, G.K. Abou-Alfa, and T. Bekaii-Saab, *Phase II study of BGJ398 in patients with FGFR-Altered advanced cholangiocarcinoma*. Journal of Clinical Oncology, 2018. 36(3): p. 276-282.**
18. **Reis-Filho, J.S., P.T. Simpson, N.C. Turner, M.B. Lambros, C. Jones, A. Mackay, A. Grigoriadis, D. Sarrio, K. Savage, T. Dexter, M. Iravani, K. Fenwick, B. Weber, D. Hardisson, F.C. Schmitt, J. Palacios, S.R. Lakhani, and A. Ashworth, *FGFR1 emerges as a potential therapeutic target for lobular breast carcinomas*. Clinical Cancer Research, 2006. 12(22): p. 6652-6662.**
19. **Tabernero, J., R. Bahleda, R. Dienstmann, J.R. Infante, A. Mita, A. Italiano, E. Calvo, V. Moreno, B. Adamo, A. Gazzah, B. Zhong, S.J. Platero, J.W. Smit, K. Stuyckens, M. Chatterjee-Kishore, J. Rodon, V. Peddareddigari, F.R. Luo, and J.C. Soria, *Phase I dose-escalation study of JNJ-42756493, an oral pan-fibroblast growth factor receptor inhibitor, in patients with advanced solid tumours*. Journal of Clinical Oncology, 2015. 33(30): p. 3401-3408.**
20. **Roidl, A., P. Foo, W. Wong, C. Mann, S. Bechtold, H.J. Berger, S. Streit, J.E. Ruhe, S. Hart, A. Ullrich, and H.K. Ho, *The FGFR4 Y367C mutant is a dominant oncogene in MDA-MB453 breast cancer cells*. Oncogene, 2010. 29(10): p. 1543-1552.**
21. **Penault-Llorca, F., F. Bertucci, J. Adelaide, P. Parc, F. Coulier, J. Jacquemier, D. Birnbaum, and O. DeLapeyriere, *Expression of FGF and FGF receptor genes in human breast cancer*. International Journal of Cancer, 1995. 61(2): p. 170-176.**
22. **Neve, R.M., K. Chin, J. Fridlyand, J. Yeh, F.L. Baehner, T. Fevr, L. Clark, N. Bayani, J.P. Coppe, F. Tong, T. Speed, P.T. Spellman, S. DeVries, A. Lapuk, N.J. Wang, W.L. Kuo, J.L. Stilwell, D. Pinkel, D.G. Albertson, F.M. Waldman, F. McCormick, R.B. Dickson, M.D. Johnson, M. Lippman, S. Ethier, A. Gazdar, and**

- J.W. Gray**, *A collection of breast cancer cell lines for the study of functionally distinct cancer subtypes*. Cancer Cell, 2006. 10(6): p. 515-527.
23. **Turner, N., A. Pearson, R. Sharpe, M. Lambros, F. Geyer, M.A. Lopez-Garcia, R. Natrajan, C. Marchio, E. Iorns, A. Mackay, C. Gillett, A. Grigoriadis, A. Tutt, J.S. Reis-Filho, and A. Ashworth**, *FGFR1 amplification drives endocrine therapy resistance and is a therapeutic target in breast cancer*. Cancer Research, 2010. 70(5): p. 2085-2094.
24. **André, F. and J. Cortés**, *Rationale for targeting fibroblast growth factor receptor signaling in breast cancer*. Breast Cancer Research and Treatment, 2015. 150(1): p. 1-8.
25. **Elbauomy Elsheikh, S., A.R. Green, M.B. Lambros, N.C. Turner, M.J. Grainge, D. Powe, I.O. Ellis, and J.S. Reis-Filho**, *FGFR1 amplification in breast carcinomas: a chromogenic in situ hybridisation analysis*. Breast cancer research : BCR, 2007. 9(2).
26. **Chang, J., X. Liu, S. Wang, Z. Zhang, Z. Wu, X. Zhang, and J. Li**, *Prognostic value of FGFR gene amplification in patients with different types of cancer: A systematic review and meta-analysis*. PLoS ONE, 2014. 9(8).
27. **Kim, H.R., D.J. Kim, D.R. Kang, J.G. Lee, S.M. Lim, C.Y. Lee, S.Y. Rha, M.K. Bae, Y.J. Lee, S.H. Kim, S.J. Ha, R.A. Soo, K.Y. Chung, J.H. Kim, J.H. Lee, H.S. Shim, and B.C. Cho**, *Fibroblast growth factor receptor 1 gene amplification is associated with poor survival and cigarette smoking dosage in patients with resected squamous cell lung cancer*. Journal of Clinical Oncology, 2013. 31(6): p. 731-737.
28. **Cheng, C.L., A.A. Thike, S.Y.J. Tan, P.J. Chua, B.H. Bay, and P.H. Tan**, *Expression of FGFR1 is an independent prognostic factor in triple-negative breast cancer*. Breast Cancer Research and Treatment, 2015. 151(1): p. 99-111.
29. **Wang, W., Y. Meng, B. Dong, J. Dong, M.M. Ittmann, C.J. Creighton, Y. Lu, H. Zhang, T. Shen, J. Wang, D.R. Rowley, Y. Li, F. Chen, D.D. Moore, and F. Yang**, *A Versatile Tumour Gene Deletion System Reveals a Crucial Role for FGFR1 in Breast Cancer Metastasis*. Neoplasia (United States), 2017. 19(5): p. 421-428.



30. **Turner, N., M.B. Lambros, H.M. Horlings, A. Pearson, R. Sharpe, R. Natrajan, F.C. Geyer, M. Van Kouwenhove, B. Kreike, A. MacKay, A. Ashworth, M.J. Van De Vijver, and J.S. Reis-Filho,** *Integrative molecular profiling of triple negative breast cancers identifies amplicon drivers and potential therapeutic targets.* *Oncogene*, 2010. 29(14): p. 2013-2023.
31. **Turczyk, L., K. Kitowska, M. Mieszkowska, K. Mieczkowski, D. Czaplinska, D. Piasecka, R. Kordek, A.C. Skladanowski, P. Potemski, H.M. Romanska, and R. Sadej,** *FGFR2-Driven Signaling Counteracts Tamoxifen Effect on ERα-Positive Breast Cancer Cells.* *Neoplasia (United States)*, 2017. 19(10): p. 791-804.
32. **Sun, S., Y. Jiang, G. Zhang, H. Song, X. Zhang, Y. Zhang, X. Liang, Q. Sun, and D. Pang,** *Increased expression of fibroblastic growth factor receptor 2 is correlated with poor prognosis in patients with breast cancer.* *Journal of Surgical Oncology*, 2012. 105(8): p. 773-779.
33. **Sharpe, R., A. Pearson, M.T. Herrera-Abreu, D. Johnson, A. Mackay, J.C. Welti, R. Natrajan, A.R. Reynolds, J.S. Reis-Filho, A. Ashworth, and N.C. Turner,** *FGFR signaling promotes the growth of triple-negative and basal-like breast cancer cell lines both in vitro and in vivo.* *Clinical Cancer Research*, 2011. 17(16): p. 5275-5286.
34. **Shaver, T.M., B.D. Lehmann, J.S. Beeler, C.I. Li, Z. Li, H. Jin, T.P. Stricker, Y. Shyr, and J.A. Pietenpol,** *Diverse, biologically relevant, and targetable gene rearrangements in triple-negative breast cancer and other malignancies.* *Cancer Research*, 2016. 76(16): p. 4850-4860.
35. **Singh, D., J.M. Chan, P. Zoppoli, F. Niola, R. Sullivan, A. Castano, E.M. Liu, J. Reichel, P. Porraati, S. Pellegatta, K. Qiu, Z. Gao, M. Ceccarelli, R. Riccardi, D.J. Brat, A. Guha, K. Aldape, J.G. Golfinos, D. Zagzag, T. Mikkelsen, G. Finocchiaro, A. Lasorella, R. Rabadan, and A. Iavarone,** *Transforming fusions of FGFR and TACC genes in human glioblastoma.* *Science*, 2012. 337(6099): p. 1231-1235.
36. **Williams, S.V., C.D. Hurst, and M.A. Knowles,** *Oncogenic FGFR3 gene fusions in bladder cancer.* *Human Molecular Genetics*, 2013. 22(4): p. 795-803.

37. **Yuan, L., Z.H. Liu, Z.R. Lin, L.H. Xu, Q. Zhong, and M.S. Zeng,** *Recurrent FGFR3-TACC3 fusion gene in nasopharyngeal carcinoma.* Cancer Biology and Therapy, 2014. 15(12): p. 1613-1621.
38. **Sarkar, S., E. Ryan, and S. Royle,** *FGFR3-TACC3 cancer gene fusions cause mitotic defects by removal of endogenous TACC3 from the mitotic spindle.* Open Biology, 2017. 7.
39. **Wu, Y.M., F. Su, S. Kalyana-Sundaram, N. Khazanov, B. Ateeq, X. Cao, R.J. Lonigro, P. Vats, R. Wang, S.F. Lin, A.J. Cheng, L.P. Kunju, J. Siddiqui, S.A. Tomlins, P. Wyngaard, S. Sadis, S. Roychowdhury, M.H. Hussain, F.Y. Feng, M.M. Zalupski, M. Talpaz, K.J. Pienta, D.R. Rhodes, D.R. Robinson, and A.M. Chinnaiyan,** *Identification of targetable FGFR gene fusions in diverse cancers.* Cancer Discovery, 2013. 3(6): p. 636-647.
40. **Di Stefano, A.L., A. Fucci, V. Frattini, M. Labussiere, K. Mokhtari, P. Zoppoli, Y. Marie, A. Bruno, B. Boisselier, M. Giry, J. Savatovsky, M. Touat, H. Belaid, A. Kamoun, A. Idhah, C. Houillier, F.R. Luo, J.C. Soria, J. Tabernero, M. Eoli, R. Paterra, S. Yip, K. Petrecca, J.A. Chan, G. Finocchiaro, A. Lasorella, M. Sanson, and A. Iavarone,** *Detection, characterization, and inhibition of FGFR-TACC fusions in IDH wild-type glioma.* Clinical Cancer Research, 2015. 21(14): p. 3307-3317.
41. **Hochgräfe, F., L. Zhang, S.A. O'Toole, B.C. Browne, M. Pinese, A.P. Cubas, G.M. Lehrbach, D.R. Croucher, D. Rickwood, A. Boulghourjian, R. Shearer, R. Nair, A. Swarbrick, D. Faratian, P. Mullen, D.J. Harrison, A.V. Biankin, R.L. Sutherland, M.J. Raftery, and R.J. Daly,** *Tyrosine phosphorylation profiling reveals the signaling network characteristics of basal breast cancer cells.* Cancer Research, 2010. 70(22): p. 9391-9401.
42. **Hood, F.E. and S.J. Royle,** *Pulling it together: The mitotic function of TACC3.* BioArchitecture, 2011. 1(3): p. 105-109.
43. **Nelson, K.N., A.N. Meyer, A. Siari, A.R. Campos, K. Motamedchaboki, and D.J. Donoghue,** *Oncogenic gene fusion FGFR3-TACC3 Is regulated by tyrosine phosphorylation.* Molecular Cancer Research, 2016. 14(5): p. 458-469.

44. **Nelson, K.N., A.N. Meyer, C.G. Wang, and D.J. Donoghue**, *Oncogenic driver FGFR3-TACC3 is dependent on membrane trafficking and ERK signaling*. *Oncotarget*, 2018. 9(76): p. 34306-34319.
45. **Dai, S., Z. Zhou, Z. Chen, G. Xu, and Y. Chen**, *Fibroblast Growth Factor Receptors (FGFRs): Structures and Small Molecular Inhibitors*. *Cells*, 2019. 8(6): p. 614.
46. **Ghedini, G.C., R. Ronca, M. Presta, and A. Giacomini**, *Future applications of FGF/FGFR inhibitors in cancer*. *Expert Review of Anticancer Therapy*, 2018. 18(9): p. 861-872.
47. **Daly, C., C. Castanaro, W. Zhang, Q. Zhang, Y. Wei, M. Ni, T.M. Young, L. Zhang, E. Burova, and G. Thurston**, *FGFR3-TACC3 fusion proteins act as naturally occurring drivers of tumour resistance by functionally substituting for EGFR/ERK signaling*. *Oncogene*, 2017. 36(4): p. 471-481.
48. **Fumagalli, D., T.R. Wilson, R. Salgado, X. Lu, J. Yu, C. O'Brien, K. Walter, L.Y. Huw, C. Criscitiello, I. Laios, V. Jose, D.N. Brown, F. Rothé, M. Maetens, D. Zardavas, P. Savas, D. Larsimont, M.J. Piccart-Gebhart, S. Michiels, M.R. Lackner, C. Sotiriou, and S. Loi**, *Somatic mutation, copy number and transcriptomic profiles of primary and matched metastatic estrogen receptor-positive breast cancers*. *Annals of Oncology*, 2016. 27(10): p. 1860-1866.
49. **Liang, X., S. Vacher, A. Boulai, V. Bernard, S. Baulande, M. Bohec, I. Bièche, F. Lerebours, and C. Callens**, *Targeted next-generation sequencing identifies clinically relevant somatic mutations in a large cohort of inflammatory breast cancer*. *Breast Cancer Research*, 2018. 20(1).
50. **Mhaweche-Fauceglia, P., R.T. Cheney, G. Fischer, A. Beck, and F.R. Herrmann**, *FGFR3 and p53 protein expressions in patients with pTa and pT1 urothelial bladder cancer*. *European Journal of Surgical Oncology*, 2006. 32(2): p. 231-237.
51. **Zhou, S., Y. Xie, J. Tang, J. Huang, Q. Huang, W. Xu, Z. Wang, F. Luo, Q. Wang, H. Chen, X. Du, Y. Shen, D. Chen, and L. Chen**, *FGFR3 Deficiency Causes Multiple*

- Chondroma-like Lesions by Upregulating Hedgehog Signaling*. PLoS Genetics, 2015. 11(6).
52. **Lafitte, M., I. Moranvillier, S. Garcia, E. Peuchant, J. Iovanna, B. Rousseau, P. Dubus, V. Guyonnet-Dupérat, G. Belleannée, J. Ramos, A. Bedel, H. de Verneuil, F. Moreau-Gaudry, and S. Dabernat**, *FGFR3 has tumour suppressor properties in cells with epithelial phenotype*. Molecular Cancer, 2013. 12(1).
53. **Kuroso, K., Y. Imai, M. Kobayashi, K. Yanagimoto, T. Suzuki, M. Kojima, and Y. Ueda**, *Immunohistochemical detection of fibroblast growth factor receptor 3 in human breast cancer: Correlation with clinicopathological/molecular parameters and prognosis*. Pathobiology, 2010. 77(5): p. 231-240.

**THIS PAGE HAS BEEN INTENTIONALLY LEFT BLANK**

---

## **CHAPTER 4**

# **EVALUATION OF FGFR TARGETING IN BREAST CANCER THROUGH INTERROGATION OF PATIENT-DERIVED MODELS**

---

# Chapter 4: Evaluation of FGFR targeting in breast cancer through interrogation of patient-derived models

This chapter is written around a research study to be submitted to Breast Cancer Research

4.1 Background .....	126
4.2 Results .....	128
4.2.1 Expression and phosphorylation of FGFRs in breast cancer PDXs .....	128
4.2.2 Selective inhibition of FGFR1-3 in PDX models of TNBC using AZD4547 .....	130
4.2.3 TNBC PDX KCC_P_4043 harbours a novel FGFR2-SKI fusion .....	136
4.2.4 Selective inhibition of FGFR4 in a PDX model of luminal B breast cancer using BLU9931 .....	140
4.2.5 Interrogation of FGFR2 and FGFR4 alterations in breast cancer patients using public datasets .....	142
4.2.6 Characterisation of FGFR4 expression and function in breast cancer patient-derived organoids .....	146
4.3 Discussion .....	148
4.4 Conclusion .....	150
4.5 Future direction .....	151
4.6 Acknowledgements .....	151
4.7 Supplementary Materials .....	152
4.8 References .....	159

## **4.1 Background**

As previously mentioned, TNBC is the most aggressive breast cancer subtype, associated with higher metastasis rate and tumour grade [1, 2] and lacks the expression of ER, PR and HER2, ruling out endocrine and trastuzumab therapies as treatment options [2]. While chemotherapy remains the ‘backbone’ of TNBC treatment, recent developments include the use of PARP inhibitors for BRCA mutant TNBC and targeting the PD-1 axis via immunotherapy [3]. However, given the paucity of effective targeted treatments for this disease subtype, this remains an intense and urgent area of investigation. In addition to the TNBC subtype, the luminal B subtype is characterised by increased proliferation compared to luminal A cancers, relative resistance to chemotherapy, and a relatively poor outcome with endocrine therapy considering its ER-positive status [4].

Aberrant activation of specific RTKs commonly occurs in human cancer, leading to the development of targeted approaches, including small molecule drugs, to block their activity [5]. FGFR1, FGFR2, FGFR3 and FGFR4 form a family of four highly conserved RTKs and deregulation of FGFR signalling, reflecting gene mutation, translocation, amplification and/or overexpression, occurs in a variety of human malignancies including urothelial (32% of cases) and breast cancers (18%) [6, 7]. Successful pre-clinical demonstration of the efficacy of FGFR targeting, for example using selective small molecule drugs, has led to evaluation of such approaches in human clinical trials. For example, in a translational Phase II clinical trial (2011-003718-18), 12.5 and 33% of gastric cancers exhibiting FGFR1- and FGFR2-amplification, respectively, exhibited responses to the FGFR1-3 inhibitor AZD4547 [8]. Furthermore, the pan-FGFR kinase inhibitor BGJ398 (Infigratinib) demonstrated significant activity against chemotherapy-refractory cholangiocarcinoma harbouring FGFR2 fusions in a phase II clinical study (NCT02150967) [9].

Recently, Erdafitinib (an inhibitor of FGFR1-4) was FDA-approved for patients with metastatic urothelial carcinoma exhibiting FGFR gene alterations and resistance to chemotherapy, based on phase II clinical trial results (NCT02365597) [10]. The results concluded the use of Erdafitinib was associated with 40% objective tumor response in patients



with FGFR alterations, with a median duration of 5.5 months progression free survival and 14 months overall survival. Erdafitinib, as well as other selective FGFR inhibitors including Infigratinib, Pemigatinib and Rogaratinib, are currently being evaluated in late-stage clinical trials in several solid malignancies [11]. While the initial focus of FGFR targeting was FGFR1-3, FGFR4 has recently attracted significant interest. The FGFR4 ligand FGF19 is often overexpressed in hepatocellular carcinoma (HCC) due to focal amplification of chromosome 11q13.3 [12, 13]. Selective FGFR4 inhibitors are currently in early stage clinical trials for treatment of HCC (NCT02834780) [11].

In breast cancer, FGFR1 amplification occurs in 14% of cases, and FGFR1 expression is an independent negative prognostic factor in TNBC [14, 15]. FGFR1 amplification is also associated with poor prognosis in ER-positive cancers and confers resistance to endocrine therapies [16, 17]. Similarly, FGFR2 is also positively associated with poor prognosis and endocrine resistance [18-20]. Increased FGFR3 expression is significantly associated with reduced overall survival and FGFR3-TACC3 fusions have been detected in a primary TNBC and the TNBC cell line SUM-185PE, with an oncogenic driver role defined in the latter context [21, 22]. Finally, increasing evidence supports subtype-selective roles for FGFR4 in breast cancer. An activating mutation (Y367C) in this receptor leads to an oncogenic role in the TNBC cell line MDA-MB-453 [23] and a single nucleotide polymorphism (SNP) (Gly388Arg) is also associated with reduced overall survival in breast cancer patients receiving adjuvant systemic therapy [24]. In addition, FGFR4 is implicated in metastasis and endocrine resistance in invasive lobular carcinoma [25], and a recent study indicates that FGFR4 promotes transition from a more differentiated, luminal phenotype to a highly proliferative and metastatic, HER2-enriched one [26].

Previously, the Daly Laboratory integrated global phosphoproteomic profiling of human breast cancer cell lines and genetically modified mouse models of this disease with functional analyses in order to identify subtype-selective signalling networks and candidate therapeutic targets [21, 27, 28]. In this study, I have extended this approach to breast cancer patient-derived xenografts (PDX) and organoids (PDO), powerful models that retain the genetic and phenotypic heterogeneity of the primary tumour, exhibit 3D architecture and for PDX, tumour-

stroma interactions [29-31]. My findings, which include characterisation of oncogene addiction to a novel FGFR2 fusion in a TNBC PDX and identification of an important role for FGFR4 in a subset of luminal breast cancers, support and widen opportunities for therapeutic targeting of specific FGFRs as a strategy for precision treatment of breast cancer.

## **4.2 Results**

### **4.2.1 Expression and phosphorylation of FGFRs in breast cancer PDXs**

In order to identify potential therapeutic targets, global MS-based phosphotyrosine profiling was conducted by Dr. Mimi Nguyen from the Daly Laboratory across a panel comprising 18 TNBC and 1 luminal B PDX [32]. A total of 897 tyrosine phosphorylated peptides were identified that included 115 kinase-derived peptides [32]. Evident in the heatmap was pronounced phosphorylation of specific FGFRs in particular PDX, including KCC\_P\_4043 (FGFR2), ELX14-32 and ELX11-26 (FGFR1) and HCI-009 (FGFR4) [32]. Since elevated tyrosine phosphorylation of particular FGFRs was observed for several PDX, and these RTKs are implicated in breast cancer development and progression and represent therapeutic targets, data relating to FGFR site-selective phosphorylation were extracted from the dataset for further interrogation (Fig. 4.1a). This revealed PDX with relatively high phosphorylation of both FGFR1 and FGFR2 (ELX11-26), FGFR2 alone (KCC\_P\_4043) and FGFR4 alone (HCI-009) (Fig. 4.1a).

In order to characterise FGFR expression, 17 breast cancer PDX samples were subjected to Western blot analysis using selective FGFR antibodies (Fig. 4.1b). The diversity of bands of FGFR members are generated by alternative splicing and post-translational modification, mainly through glycosylation. These modifications effect FGFRs to resolve as a doublet (FGFR2 and FGFR4) or a triplet (FGFR1 and FGFR3). In general, the results were concordant with the tyrosine phosphorylation data, indicating that increased FGFR phosphorylation was associated with elevated expression. Thus, while most PDX exhibited detectable FGFR1 expression, FGFR1 overexpression was observed in ELX12-58, ELX13-31, ELX14-32 and ELX11-26, and robust FGFR4 expression was only detected in HCI-009. However, while

strong expression of FGFR2 was detected in ELX11-26, the FGFR2 C-term antibody did not detect a band of predicted size in KCC\_P\_4043 lysate, despite this PDX exhibiting the highest relative FGFR2 phosphorylation. This issue is revisited later in the chapter.

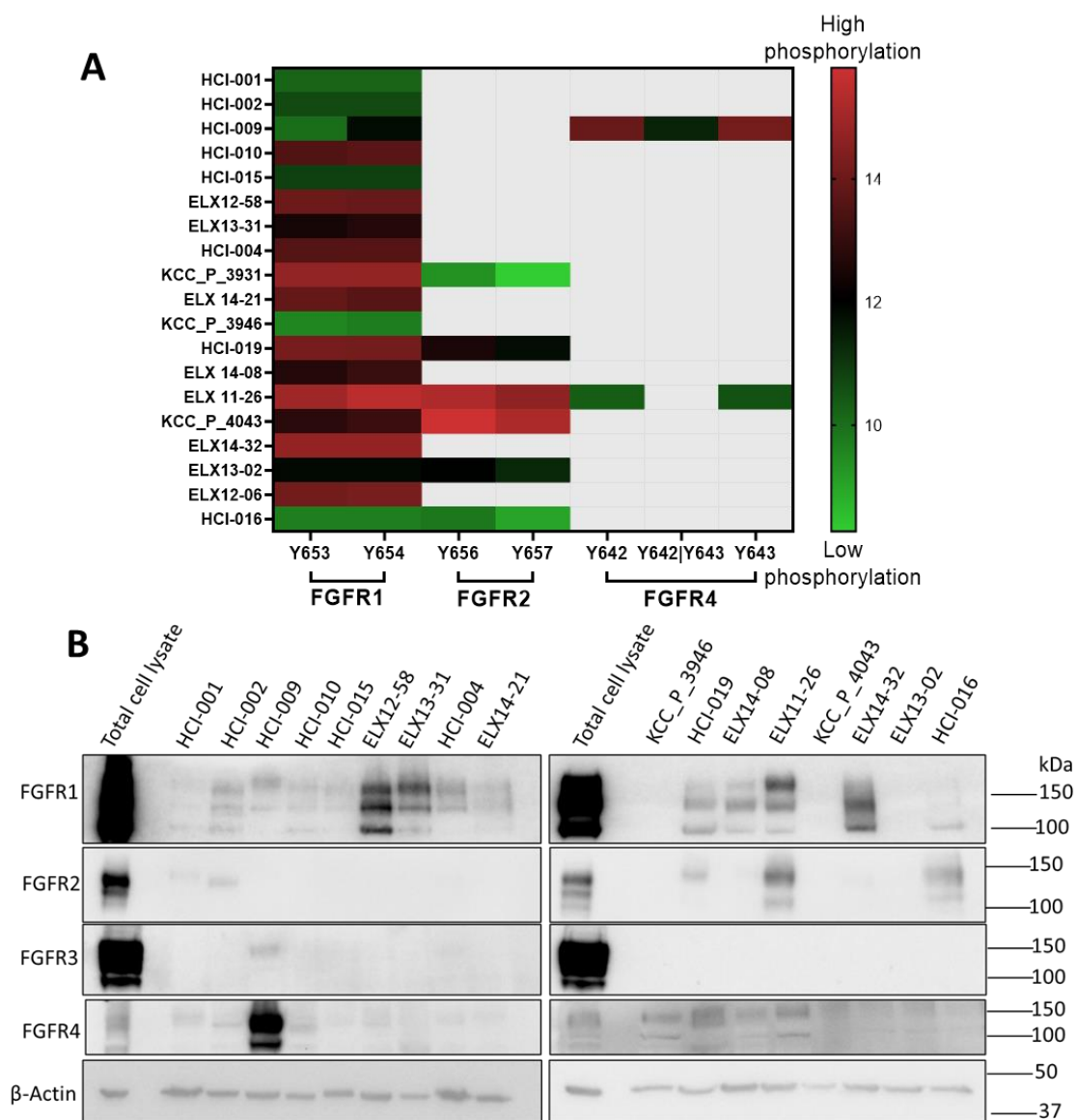


**Figure 4.1: FGFR expression and phosphorylation signatures in human breast cancer PDX as determined by MS-based tyrosine phosphorylation profiling and Western blot. a** Site-selective phosphorylation of specific FGFRs based on z-score across the 19 PDX samples. Grey shading indicates that the FGFR phosphorylation site was undetectable by MS. **b** Expression of specific FGFRs across the panel. Protein lysates from 17 PDX samples were immunoblotted with the indicated antibodies. Total cell lysate indicates lysates from specific

TNBC cell lines used as positive controls for the respective antibodies (CAL120 for FGFR1, MFM-223 for FGFR2, SUM185PE for FGFR3, and MDA-MB-453 for FGFR4).

#### **4.2.2 Selective inhibition of FGFR1-3 in PDX models of TNBC using AZD4547**

Given their high phosphorylation of FGFR1 and/or FGFR2 (Fig. 4.1a), two TNBC PDX, ELX11-26 and KCC\_P\_4043 were selected for treatment with a selective FGFR1-3 inhibitor, AZD4547 [33]. A further TNBC PDX, HCI-016, was chosen as a negative control given detectable FGFR1 and FGFR2 expression but low receptor phosphorylation (Fig. 4.1). Drug treatment of PDX was undertaken by A/Prof Alex Swarbrick's group at the Garvan Institute, while I undertook all molecular analyses.

Out of the three TNBC PDX, KCC\_P\_4043 demonstrated high sensitivity to AZD4547 (Fig. 4.2). AZD4547 treatment significantly reduced tumour volume in both the short and long-term treatment groups and also significantly reduced tumour weight at endpoint in the former group, while tumours in the long-term AZD4547 group were eliminated (Fig. 4.2a). Tumour sections stained for Ki67 revealed that short-term AZD4547 treatment significantly inhibited cell proliferation compared to the vehicle control (Fig. 4.2b). Inhibition of AKT and ERK was confirmed by Western blotting, which also revealed enhanced PARP cleavage in AZD4547-treated PDX (Fig. 4.2c). On-target FGFR2 inhibition upon AZD4547 treatment was also confirmed by MS-based phosphoproteomic analysis undertaken by Dr. Terry Lim in the Daly Laboratory (Supp. Fig. 4.1)[32]. RNAseq analysis revealed an additional effect of the drug on gene expression relating to cell metabolism, specifically glycolysis/gluconeogenesis and fructose and mannose metabolism, and also extracellular matrix organisation (Table 4.1). Overall, these data highlight on-target FGFR2 inhibition and decreased mitogenic, growth and survival signalling in KCC\_P\_4043 PDX upon AZD4547 treatment, and also novel downstream effects of this drug.

In the ELX11-26 and HCI-016 PDX models, AZD4547 had no significant effect on tumour volume and tumour weight at endpoint (Fig. 4.3 & 4.4). Aside from a possible reduction in FGFR2 expression in the AZD4547-treated ELX11-26 PDX model, there was no obvious decrease in FGFR1 or FGFR2, or activation of downstream signalling proteins upon AZD4547

treatment of ELX11-26 or the negative control HCI-016 (Fig. 4.3 & 4.4). For PDX ELX11-26, SNP arrays demonstrated the presence of an amplicon spanning the entire FGFR2 gene (Supp. Fig. 4.3), explaining the high expression of FGFR2 in this PDX (Fig. 4.1). However, despite high FGFR1 phosphorylation in this PDX, the FGFR1 gene was not amplified (Supp. Fig. 4.4). These results indicate that high FGFR phosphorylation does not always confer sensitivity to FGFR inhibition and highlights the need for additional predictive biomarkers.

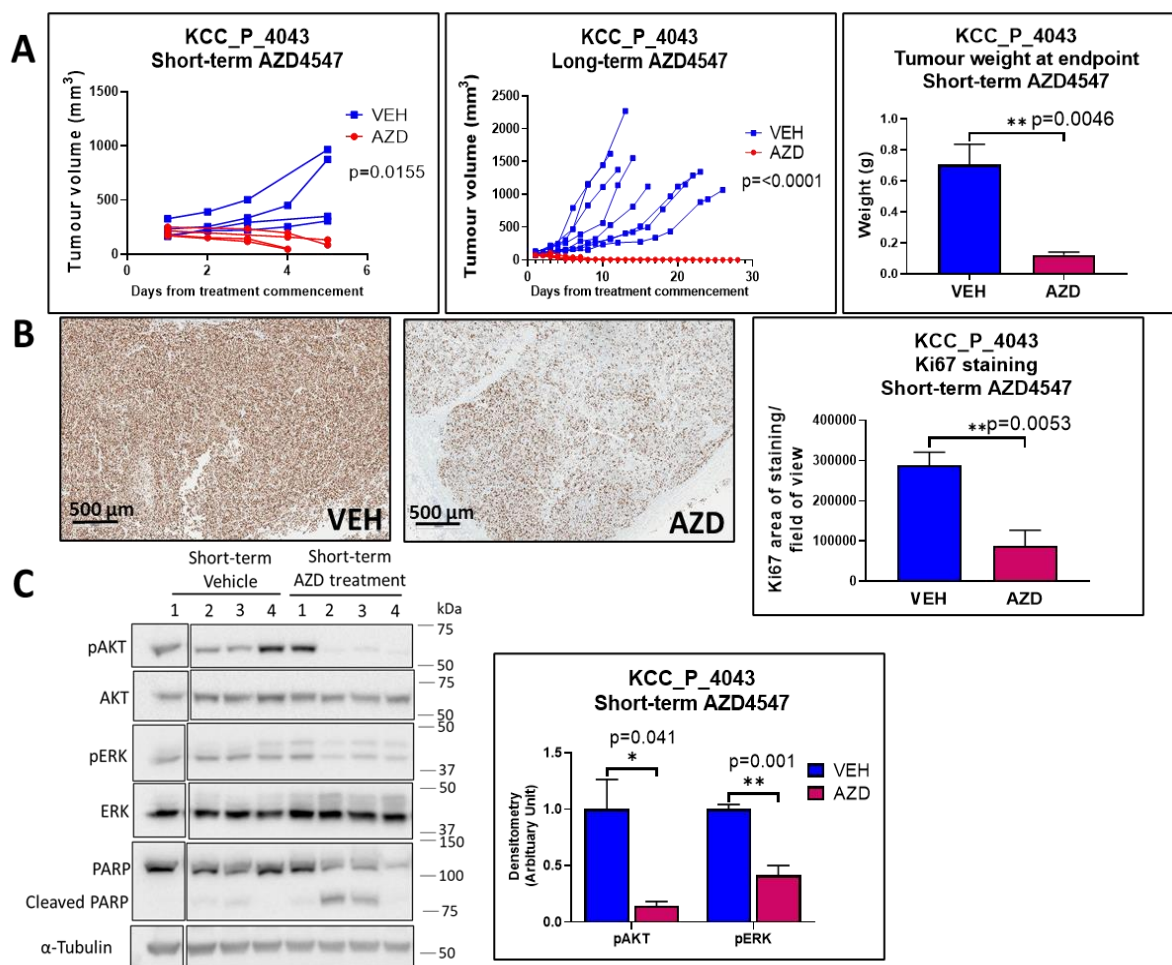


**Figure 4.2: Effect of FGFR1-3 inhibitor AZD4547 on the KCC\_P\_4043 PDX model. a** Effect on tumour growth. Mice were treated with 1% (v/v) Tween-80 with 0.5% (w/v) carboxymethylcellulose vehicle control or AZD4547 for short-term (5 d) or long-term (28 d) and the tumour volume measured daily. Tumour weight at endpoint for the short-term treatment group was also determined. **b** Effect on cell proliferation. FFPE tumour sections from the short-term treatment group were stained for Ki67 and quantified. **c** Effects on

downstream signalling determined by Western blotting. Lysates were Western blotted as indicated. Phosphorylated AKT and ERK were quantified by densitometry. Data were first normalized relative to the tubulin control, then phosphorylated proteins normalized to the total protein, and expressed relative to the average of the vehicle control which was arbitrarily set at 1.0. Mouse 1 of the AZD4547 treatment group was excluded from this analysis due to ineffective drug delivery. \* indicates p-value of  $< 0.05$ , \*\*  $< 0.01$ . Error bars: mean  $\pm$  standard error of biological replicates.

**Table 4.1: Transcriptome analysis of enriched pathways downregulated in the AZD4547 treated KCC\_P\_4043 PDX using the KEGG and Reactome database. Only the top 15 significant downregulated pathways are shown.**

## CHAPTER 4

KEGG down regulated	
Term	Genes
Glycolysis / Gluconeogenesis	ALDH3B2;LDHA;ALDOC;ALDOB;ENO2;HK2
Fructose and mannose metabolism	PFKFB4;ALDOC;ALDOB;HK2
Cushing syndrome	RB1;CACNA1I;CCND1;FZD8;LDLR;CACNA1H
Neuroactive ligand-receptor interaction	OPRD1;EDNRB;GAL;CHRNA4;MC5R;KISS1R;ADM;GPR83;S1PR2
Nitrogen metabolism	CA6;CA9
Breast cancer	RB1;SHC4;CCND1;FZD8;FOS
Gastric cancer	RB1;SHC4;CCND1;TERT;FZD8
Parathyroid hormone synthesis, secretion and action	EGR1;MMP16;PDE4C;FOS
Human T-cell leukemia virus 1 infection	RB1;FOSL1;EGR1;TERT;CCND1;FOS
Hepatocellular carcinoma	RB1;SHC4;CCND1;TERT;FZD8
Central carbon metabolism in cancer	LDHA;SLC16A3;HK2
Cortisol synthesis and secretion	CACNA1I;LDLR;CACNA1H
MAPK signaling pathway	DUSP4;CACNA1I;FOS;DUSP9;DUSP6;CACNA1H;EPHA2
AMPK signaling pathway	PFKFB4;CCND1;SCD;PPARGC1A
Prolactin signaling pathway	SHC4;CCND1;FOS
Reactome down regulated	
Term	Genes
Extracellular matrix organization	COL23A1;ICAM2;FBLN2;BCAN;ADAMTS14;COL2A1;MMP16;LOX;P4HA1;ADAMTS18;COL6A2;FMOD;ADAMTS9
Glycolysis	PFKFB4;ALDOC;ALDOB;ENO2;HK2
Collagen formation	ADAMTS14;COL2A1;LOX;P4HA1;COL6A2;COL23A1
Collagen biosynthesis and modifying enzymes	ADAMTS14;COL2A1;P4HA1;COL6A2;COL23A1
Glucose metabolism	PFKFB4;ALDOC;ALDOB;ENO2;HK2
RAF-independent MAPK1/3 activation	DUSP4;DUSP9;DUSP6
Diseases of glycosylation	BCAN;ADAMTS14;ADAMTS18;FMOD;ADAMTS9
MAPK targets/ Nuclear events mediated by MAP kinases	DUSP4;FOS;DUSP6
Gluconeogenesis	ALDOC;ALDOB;ENO2
Degradation of the extracellular matrix	BCAN;MMP16;ADAMTS18;COL23A1;ADAMTS9
O-linked glycosylation	ADAMTS14;ADAMTS18;GCNT3;CHST4;ADAMTS9
Defective B3GALTL causes Peters-plus syndrome	ADAMTS14;ADAMTS18;ADAMTS9
NCAM1 interactions	CACNA1I;COL6A2;CACNA1H
Reversible hydration of carbon dioxide	CA6;CA9
ERKs are inactivated	DUSP4;DUSP6



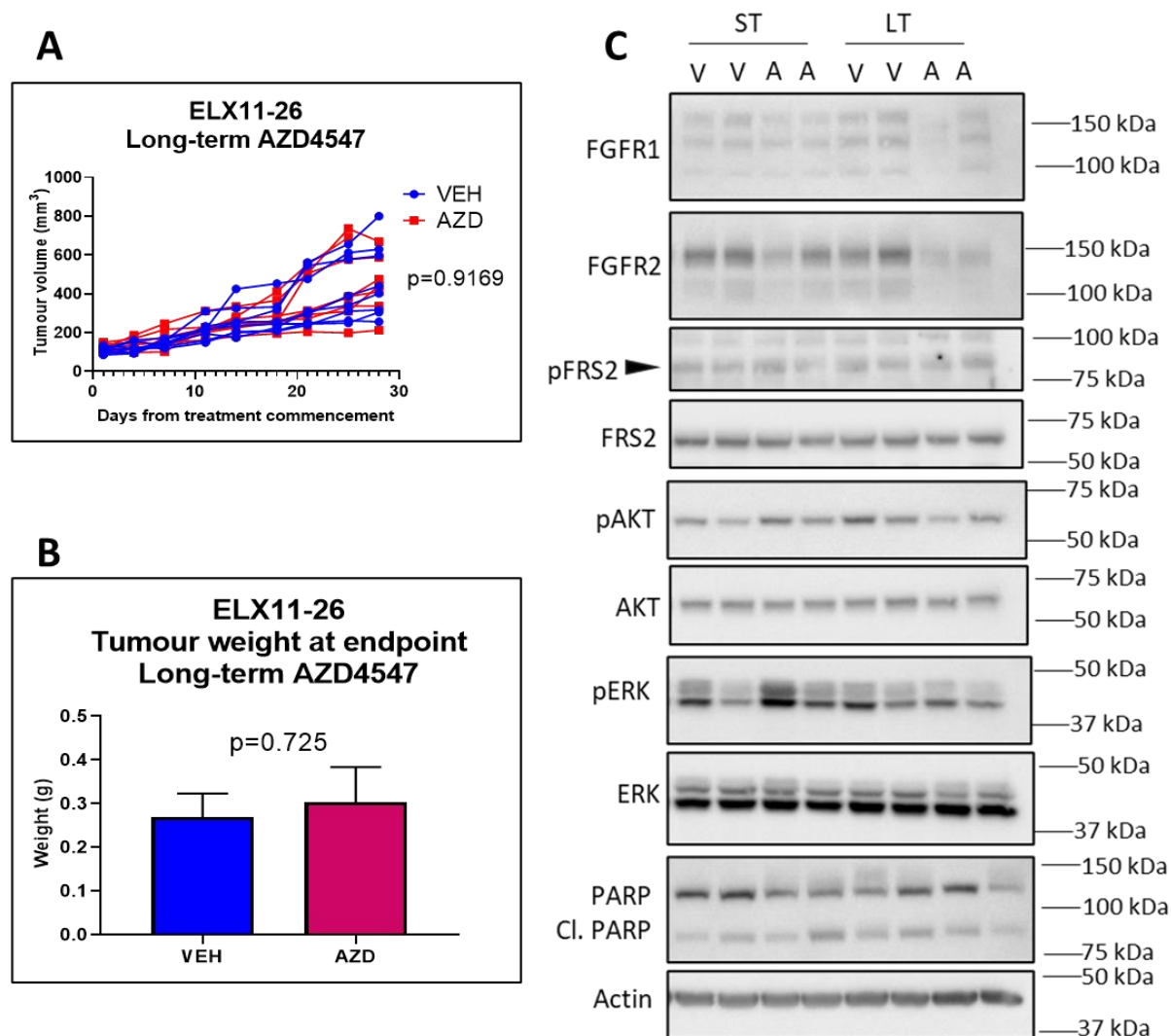


**Figure 4.3: Effect of FGFR1-3 inhibitor AZD4547 on the ELX11-26 PDX model.** **a** Effect on tumour growth. Mice were treated with vehicle control or AZD4547 for long-term (28 d) and the tumour volume measured daily. **b** Tumour weight at endpoint for the long-term treatment group was also determined. **c** Effects on downstream signalling in the short-term (ST) and long-term (LT) treatment determined by Western blotting. Lysates were Western blotted as indicated. V indicates vehicle control. A indicates AZD4547 treatment. Error bars: mean  $\pm$  standard error of biological replicates.



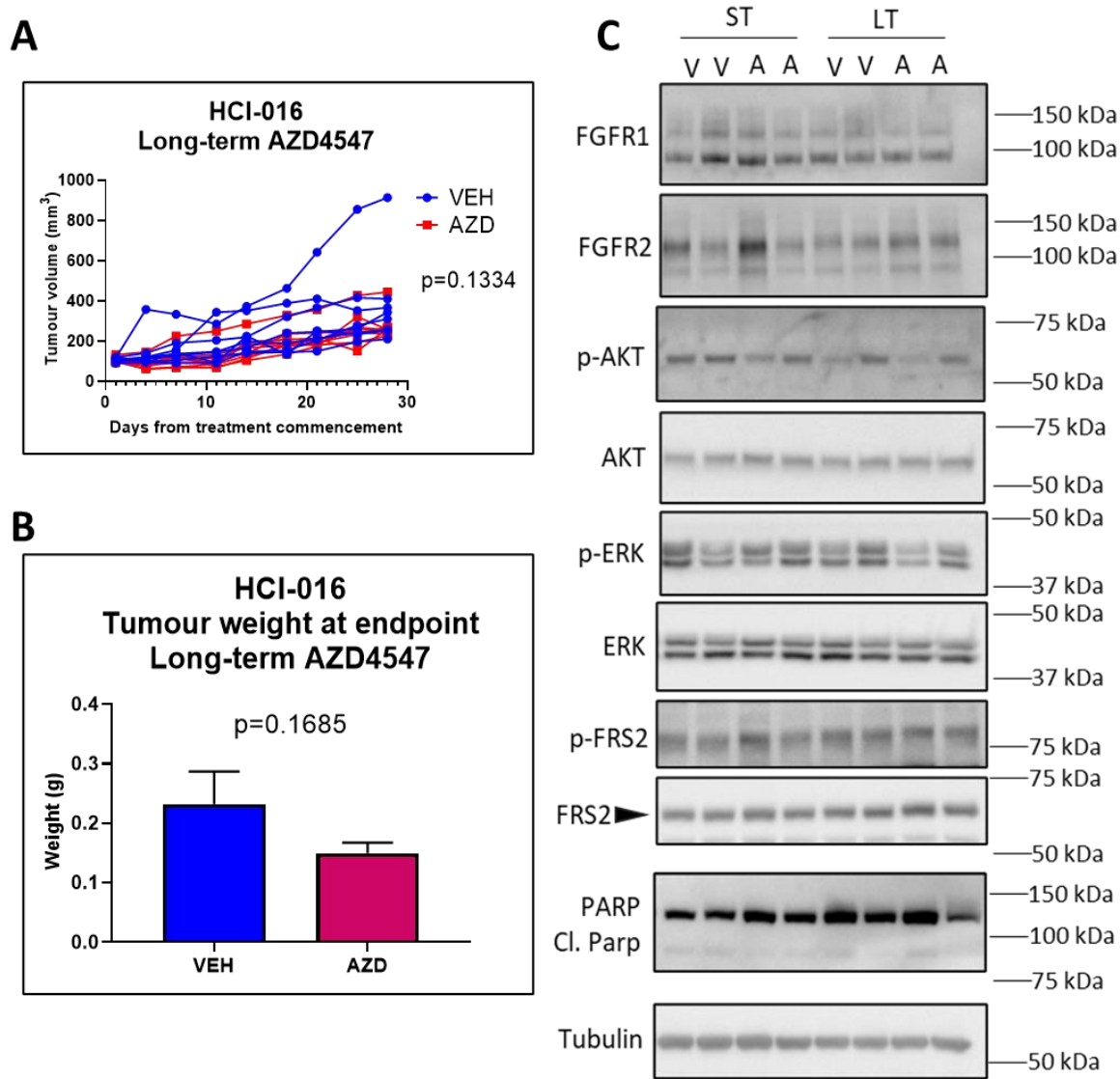


**Figure 4.4: Effect of FGFR1-3 inhibitor AZD4547 on the HCI-016 PDX model.** **a** Effect on tumour growth. Mice were treated with vehicle control or AZD4547 for long-term (28 d) and the tumour volume measured daily. **b** Tumour weight at endpoint for the long-term treatment group was also determined. **c** Effects on downstream signalling in the short-term (ST) and long-term (LT) treatment groups determined by Western blotting. Lysates were Western blotted as indicated. V indicates vehicle control. A indicates AZD4547 treatment. Error bars: mean  $\pm$  standard error of biological replicates.

### **4.2.3 TNBC PDX KCC\_P\_4043 harbours a novel FGFR2-SKI fusion**

High FGFR2 phosphorylation and AZD4547 dependency suggested a possible oncogenic form of FGFR2 in KCC\_P\_4043, which led me to conduct whole exome sequencing (WES) and RNA seq analyses. WES analysis detected 367 gene mutations, mostly non-synonymous SNVs and no mutations in the FGFR family in the KCC\_P\_4043 model [32]. A predicted splicing alteration in the tumour suppressor gene BRCA2 and a R294C mutation in centrobins (CNTROB), a centrosomal BRCA2 interacting protein were detected, which may have contributed to cancer progression in this model (Supp. Table 4.1). Other mutations associated with DNA/RNA replication (POLA1, POLR1A), the spliceosome (PRPF40A), signalling pathways (insulin, Wnt, mTOR, MAPK, ErbB, phosphatidylinositol), specific phosphatases (PPP1R3D, PLD2 and PPM1A), glycolysis/gluconeogenesis (ADPGK) and fructose and mannose metabolism (ketohexokinase) were also detected (Supp. Table 4.1).

Importantly, gene fusion analysis using the RNA sequencing data revealed a junction breakpoint involving FGFR2 and SKI on chromosome 10 and 1, respectively (Fig. 4.5a). Alignment of the junction breakpoint reads to the FGFR2 and SKI templates revealed that the breakpoint occurs at FGFR2 exon 17 and SKI exon 2 (Fig. 4.5b). These results suggest a chromosomal translocation event t(10;1)(q26.1;p36.2) in KCC\_P\_4043. This interpretation was further supported by use of SNP arrays performed by Dr. Niantao Deng from A/Prof. Alex Swarbrick's group, that identified a breakpoint in the FGFR2 gene with increased copy number towards the 5' end, that was specific to PDX and tumour, and not detected in the matching patient's blood sample (Supp. Fig. 4.2).

To confirm the presence of a FGFR2-SKI fusion in KCC\_P\_4043, 3 sets of PCR primers were designed targeting FGFR2 exons 10 to 12 (forward primers) and SKI exon 2 to 3 (reverse primers) (Fig. 4.5c) to directly detect the fusion by reverse-transcription PCR (RT-PCR) using RNA from this PDX. Amplified PCR products of the predicted sizes were identified (Fig. 4.5d), and sequencing confirmed the FGFR2-SKI fusion transcript containing the majority of the FGFR2 kinase domain (two C-terminal amino acids, glutamate and tyrosine were deleted) (Fig. 4.6).

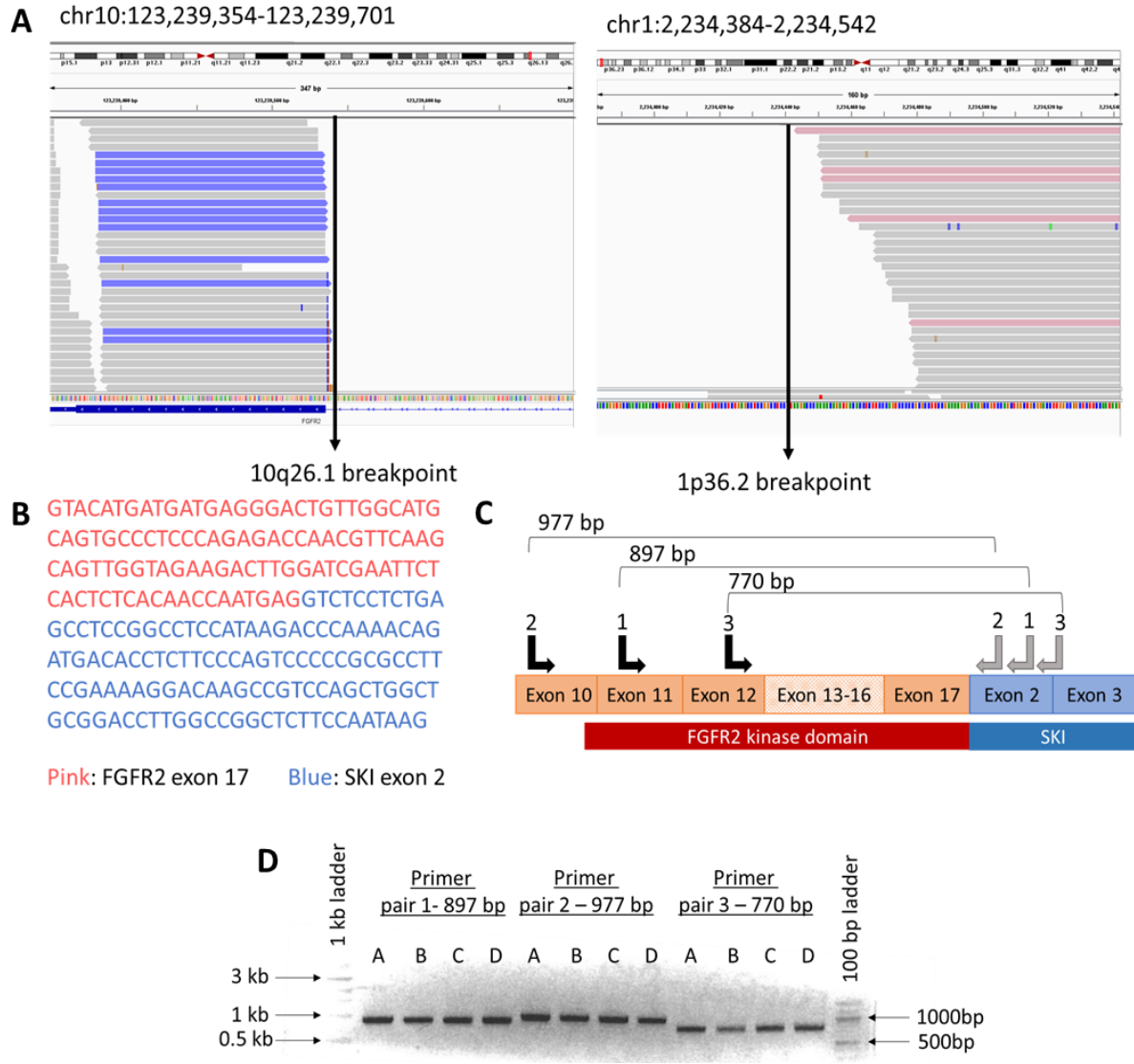
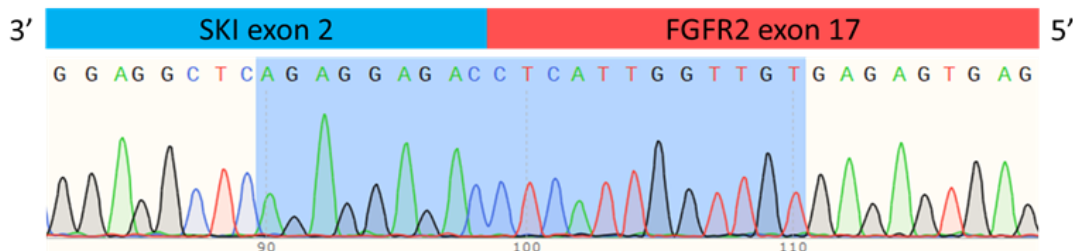
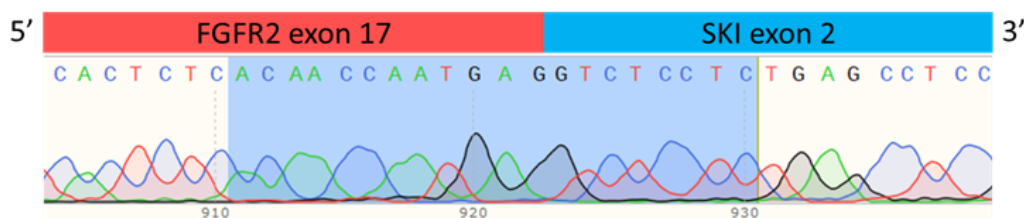


**Figure 4.5: Identification of the FGFR2-SKI fusion in the KCC\_P\_4043 model.** **a** Integrative Genomic Viewer results for breakpoint regions of chromosome 10 (containing FGFR2) and chromosome 1 (SKI). **b** Junction break point sequence of FGFR2-SKI fusion. Pink, FGFR2 exon 17; blue, SKI exon 2. **c** Schematic of the primer pairs 1 – 3 targeted to the start of the FGFR2 kinase domain at exon 10 to 12 and at SKI exon 2 to 3 for PCR. Black arrows are the forward primers, grey arrows are the reverse primers. The predicted PCR product sizes are indicated. **d** FGFR2-SKI RT-PCR. The PCR products using primer pairs 1 – 3 from (c) were resolved by DNA gel electrophoresis and the bands were imaged using a fluorescent illuminator.

**A** Reverse primer



Forward primer



**B**

MVSWGRFICLVVVTMATLSLARPSFSLVEDTTLEPEDAISSGDEDDTDGAEDFVSENSNNKRAP  
 YWTNTEKMEKRLHAVPAANTVKFRCPAGGNPMPTMRWLKNGKEFKQEHRIGGYKVRNQHWS  
 LIMEVVPSPDKGNYTCVVENEYGSINHTYHLDVVERSHPRPILQAGLPANASTVVGDFEVCKV  
 YSDAQPHIQWIKHVEKNGSKYGPDGLPYLKVLAAGVNTTDKEIEVLYIRNVTTFEDAGEYTCLAG  
 NSIGISFHSAWLTVLPAPGREKEITASPDYLEIAIYCIGVFLIACMVVTVILCRMKNNTTKPDFSSQPA  
 VHKLTKRIPLRRQVTVSAESSSSMNSNTPLVRITRLSSTADTPMLAGVSEYELPEDPKWEFP**RDKL**  
**TLGKPLGEGCFGQVVM**AEAVGIDKDKPKEAVTVAVKMLKDDATEKDLSDLVSEMEMMMKMIGK  
 HKNIINLLGACTQDGPLYVIVEYASKGNLREYLRRARRPPGMEYSYDINRVPEEQMTFKDLVSCTYQ  
 LARGMEYLASQKCIHRDLAARNVLVTENNVMKIADFLARDINNIDYKKTNGRLPVKWMAP**E**  
**ALFDRVYTHQSDVVSFGVLMWEIFTLGGSPYPGIPVEELFKLLKEGHRMDKPANCTNELYMMM**  
**RDCWHAVPSQRPTFKQLVEDLDRILTLTNE****(EY)**VSSEPPASIRPKTDDTSSQSPAPSEKDKPSSWL  
 RTLAGSSNKS LGCVHPRQLSAFRPWSPAVSASEKELSPHLPALIRDSFYYSKFETAVAPNVALAPP  
 AQQKVVSPPCAA AVSRAPELATCTQPRKRRLTVDTPGAPETLAPVAAP EEDKDSEAEVEVESRE  
 EFTSSLSLSSPSFTSSSSAKDLGSPGARALPSAVPDAAAPADAPSGLEAELEHLRQALEGGLDTKE  
 AKEKFLHEVVKM RVKQEEKLSAALQAKRSLHQELEFLRVAKKEKLREATEAKRNLKEIERLRAENE  
 KKMKEANESRLRLKRELEQARQARVCDKGCEAGRLRAKYS AQIEDLQVKLQHAEADREQLRADL  
 LREREAREHLEKVVKELQEQLWPRARPEAAGSEGA AELEP

**Figure 4.6: Sanger sequencing of the KCC\_P\_4043 PDX model PCR product.** **a** Sequence of the FGFR2-SKI fusion junction in KCC\_P\_4043 derived from RT-PCR products. **b** Amino acid sequence of the FGFR2-SKI fusion showing that the majority of the FGFR2 kinase domain (highlighted in yellow) is present in the FGFR2-SKI fusion. Only 2 amino acids, glutamate and tyrosine are missing (highlighted in green) from the FGFR2 kinase domain of the FGFR2-SKI fusion. Red, FGFR2; blue, SKI.

Previously, FGFR2 expression could not be detected in KCC\_P\_4043 lysate using the FGFR2 C-term antibody (Fig. 4.1b). This is explained by the gene fusion event, that removes the C-terminal region of FGFR2 (Fig. 4.7a). Indeed, Western blotting with an antibody raised against the N-terminal region of FGFR2 detected a band at approximately 200 kDa, a lower mobility than endogenous FGFR2 in FGFR2-amplified MFM-223 breast cancer cells and the PDX HCl-016 (140-150 kDa) (Fig. 4.7b). Allowing for the known glycosylation of FGFRs, and the phosphorylation-induced gel retardation of SKI through phosphorylation at S515 [34], this gel mobility is consistent with that expected for the FGFR2-SKI fusion.

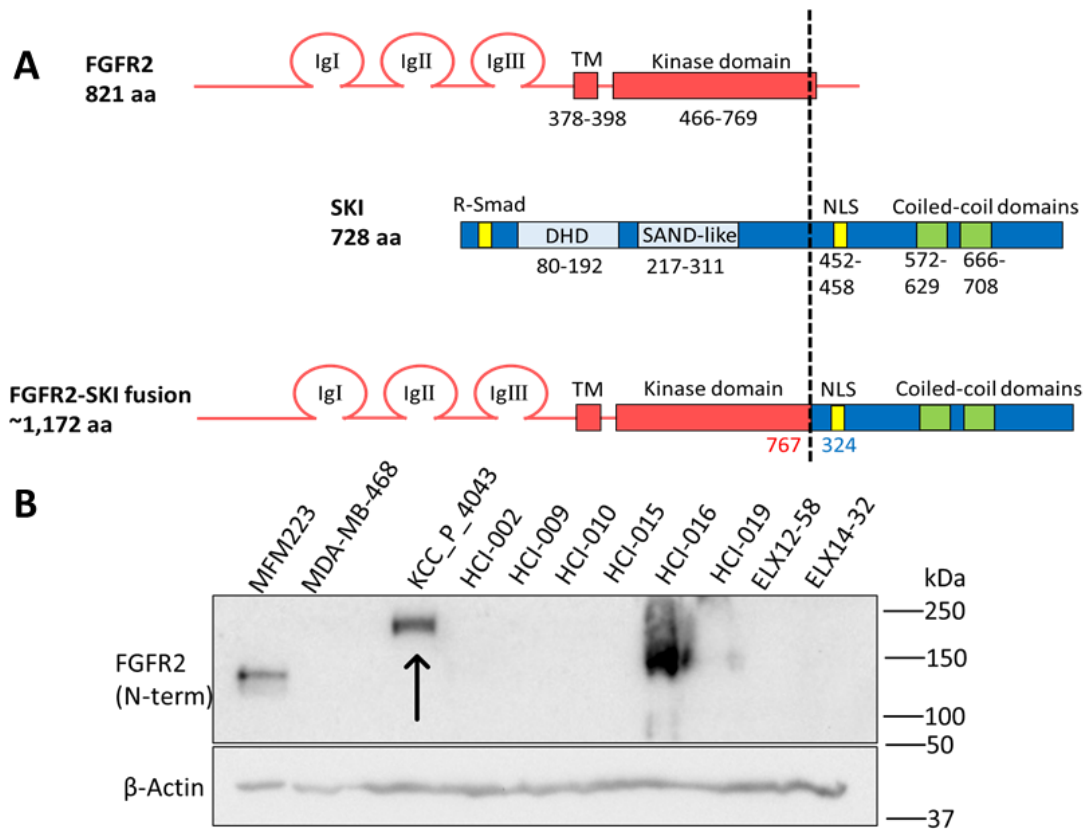


**Figure 4.7: Characterisation of the FGFR2-SKI fusion in the KCC\_P\_4043 PDX model.**

**a** Schematic of the FGFR2-SKI fusion in KCC\_P\_4043. Domain structure and amino acid residues of FGFR2 and SKI are indicated. In FGFR2, IgI-IgIII: immunoglobulin 1–3. TM: transmembrane domain. In SKI, R-smad: corresponding binding domain. DHD: Dachshung homology domain. SAND: Sp100, AIRE1, NucP41/75 and DEAF1. NLS: nuclear localization sequence. The dotted line highlights the junction between FGFR2 and SKI. **b** Confirmation of FGFR2-SKI expression by Western blotting. Protein lysates from 9 PDX samples were

immunoblotted with a FGFR2 N-term antibody. MFM-223 and MDA-MB-468 lysates were used as positive and negative controls, respectively.

#### **4.2.4 Selective inhibition of FGFR4 in a PDX model of luminal B breast cancer using BLU9931**

The HCI-009 PDX model exhibiting high FGFR4 expression and phosphorylation was subjected to treatment with a FGFR4 inhibitor, BLU9931 [12] to characterise effects on tumour growth *in vivo*, cell proliferation and FGFR4 downstream signalling [32] (Fig. 4.8). As previous, drug treatment of PDX was undertaken by A/Prof. Alex Swarbrick's group while I performed molecular analyses. Long-term BLU9931 treatment significantly decreased tumour volume, tumour weight at endpoint and decreased cell proliferation within tumours as assessed by Ki67 staining (Fig. 4.8a & 4.8b). Western blot analysis was also performed to identify on-target effects of BLU9931 on FGFR4 downstream signalling proteins, however no obvious decrease was observed (Fig. 4.8c). Therefore, MS-based phosphoproteomic analysis was undertaken to determine the effect on downstream signalling and confirmed on-target FGFR4 inhibition by BLU9931. FGFR4 phosphorylation at Y639 displayed the largest decrease in the phosphorylated tyrosine enrichment dataset, confirming efficient FGFR4 targeting by BLU9931 (Supp. Fig. 4.5). Downstream targets of FGFR4 signalling, including PLCG1, GAB1 and AKT1 also exhibited reduced phosphorylation (Supp. Fig. 4.5). In particular, reduction in AKT1 at phosphorylation sites S473 and S477 were detected by MS but not by Western blotting that utilised a phosphorylated AKT S473 antibody. This is likely that the pAKT antibody detects all AKT isoforms (AKT1-3), which could not be distinguished by Western blotting.

The MS-based phosphoproteomic experiments and analysis were performed by Dr. Terry Lim from the Daly Laboratory. Interestingly, despite the marked overexpression of FGFR4 in HCI-009, the FGFR4 gene was not amplified in this PDX, as determined by SNP arrays (Supp. Fig. 4.6).



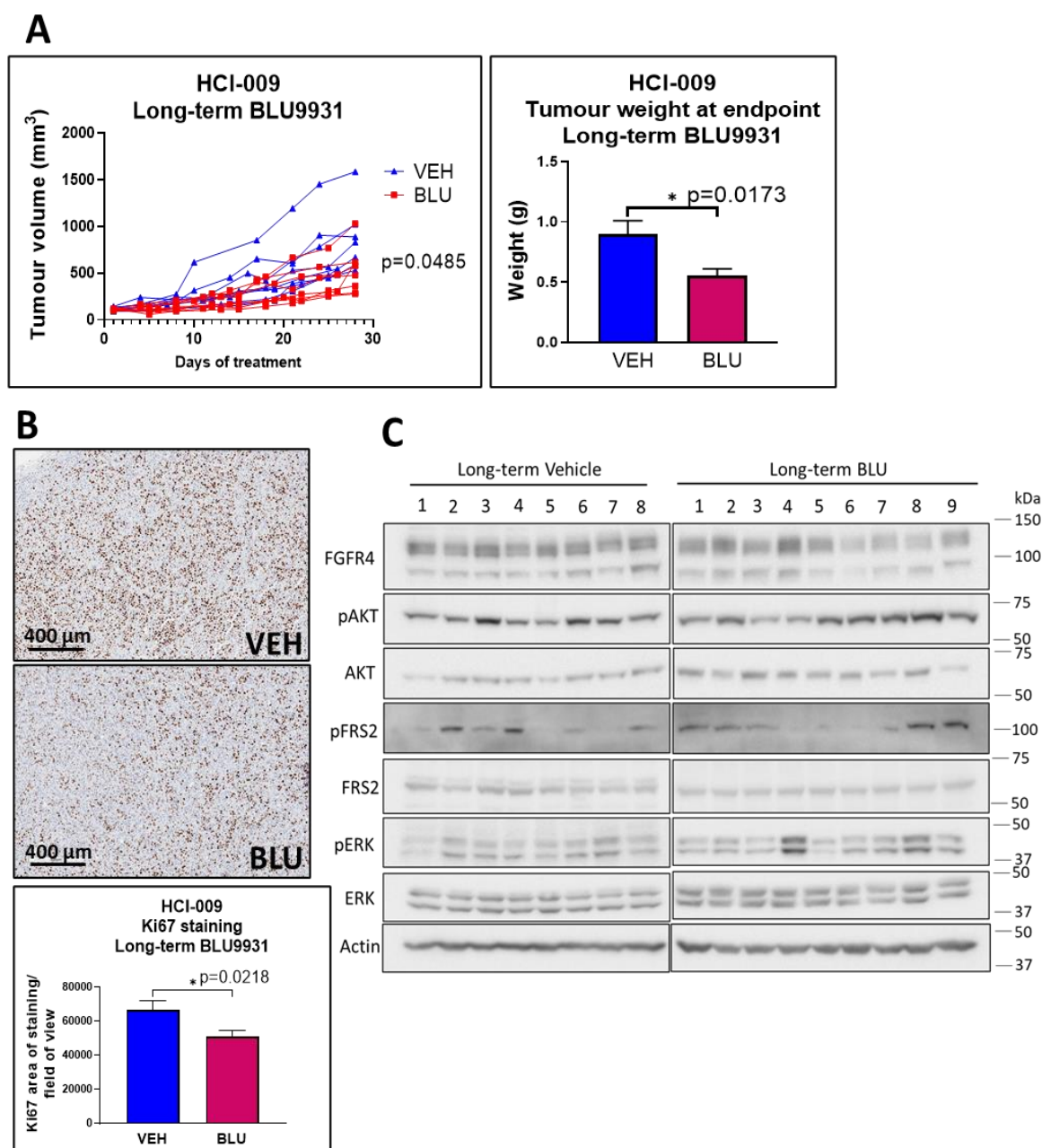


**Figure 4.8: Effect of FGFR4 inhibitor BLU9931 on the HCI-009 PDX model.** **a** Effect on tumour growth. Mice were treated with vehicle control or BLU9931 for long-term (28 d) and the tumour volume measured daily. Tumour weight at endpoint for the long-term treatment group was also measured. **b** Effect on tumour cell proliferation. FFPE tumour sections from the long-term treatment group were stained for Ki67 and the data quantified. **c** Effects on downstream signalling in the long-term treatment determined by Western blotting. Lysates were Western blotted as indicated.

### **4.2.5 Interrogation of FGFR2 and FGFR4 alterations in breast cancer patients using public datasets**

Our data highlighting effective targeting of oncogenic FGFR2 and FGFR4 alterations in specific PDX led to analyse the METABRIC and TCGA datasets using cBioportal to determine the frequency of FGFR2 and FGFR4 genomic and expression changes in different breast cancer subtypes (Fig. 4.9a). In the METABRIC dataset, 247 out of 1904 (13%) breast cancer patients have FGFR2 (6%) and/or FGFR4 (7%) alterations (Fig. 5a). In the TCGA dataset, 126 out of 994 (13%) breast cancer patients have FGFR2 (7%) and/or FGFR4 (6%) alterations (Fig. 4.9b).

FGFR2 amplification, which occurred in 26 (1.4%) and 15 (1.5%) breast cancer patients in the METABRIC and TCGA datasets respectively, was observed in all subtypes except the claudin-low subtype (Fig. 4.9). FGFR2 overexpression occurred in both the TNBC/basal and luminal subtypes and was rarely observed in HER2 cancers (Fig. 4.9), while 19 breast cancer patients (1.9%) exhibited mutation or fusion of FGFR2 in the TCGA dataset (Fig. 4.9b).

FGFR4 amplification occurred in 30 (1.6%) and 13 (1.3%) breast cancer patients in the METABRIC and TCGA datasets respectively, and was observed in all subtypes, except normal (Fig. 4.9). FGFR4 overexpression was mostly detected in the HER2 subtype, followed by the luminal subtypes (Fig. 4.9). Only 5 patients exhibited FGFR4 mutation in the TCGA dataset, with no fusions reported (Fig. 4.9b).

To complement these analyses, formalin-fixed paraffin embedded (FFPE) tissue sections from luminal and TNBCs were subjected to IHC staining for FGFR4, with conditions optimised using HCI-009 and ELX11-26 PDX as positive and negative controls, respectively (Fig. 4.10). Approximately one third (4 out of 13) of the TNBC specimens exhibited FGFR4 positivity, while the majority (9 out of 12) of luminal samples scored positive (Fig. 4.10). Furthermore, FGFR4 association with overall survival in breast cancer patients was also interrogated. In the METABRIC dataset, breast cancer patients (no subtyping) with high FGFR4 expression or amplified FGFR4 exhibited a significantly worse overall survival compared to breast cancer



patients with low FGFR4 expression and unaltered FGFR4 (neutral), respectively (Fig. 4.11a). Among breast cancer subtypes, TNBC/basal breast cancer patients with high FGFR4 expression and luminal A patients with amplified FGFR4 displayed a significantly worse overall survival (Fig. 4.11b).

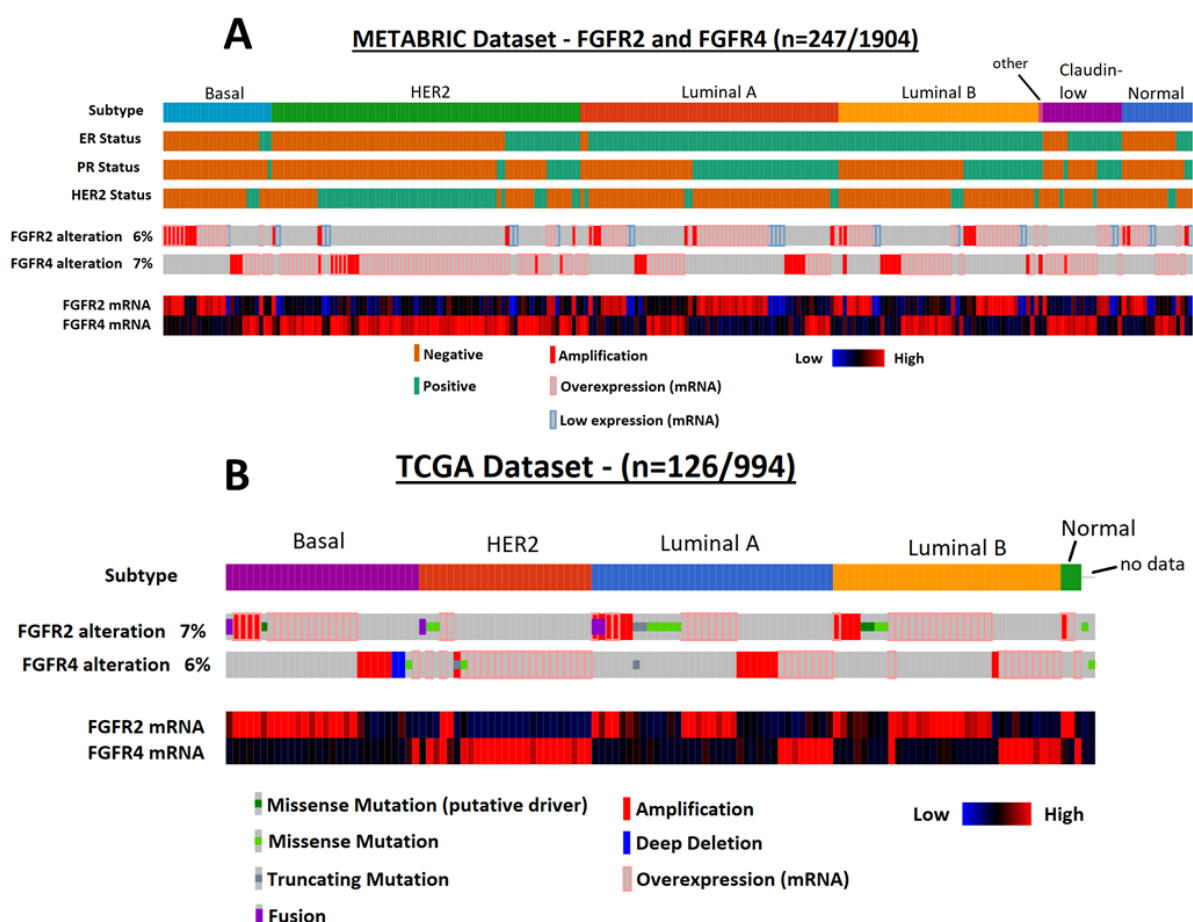


**Figure 4.9: FGFR2 and FGFR4 alterations in breast cancer patients.** Frequency of FGFR2 and FGFR4 alterations in different breast cancer subtypes. Data were extracted from the **a** METABRIC and **b** TCGA datasets in cBioportal. Only patients with FGFR alterations are displayed for brevity.

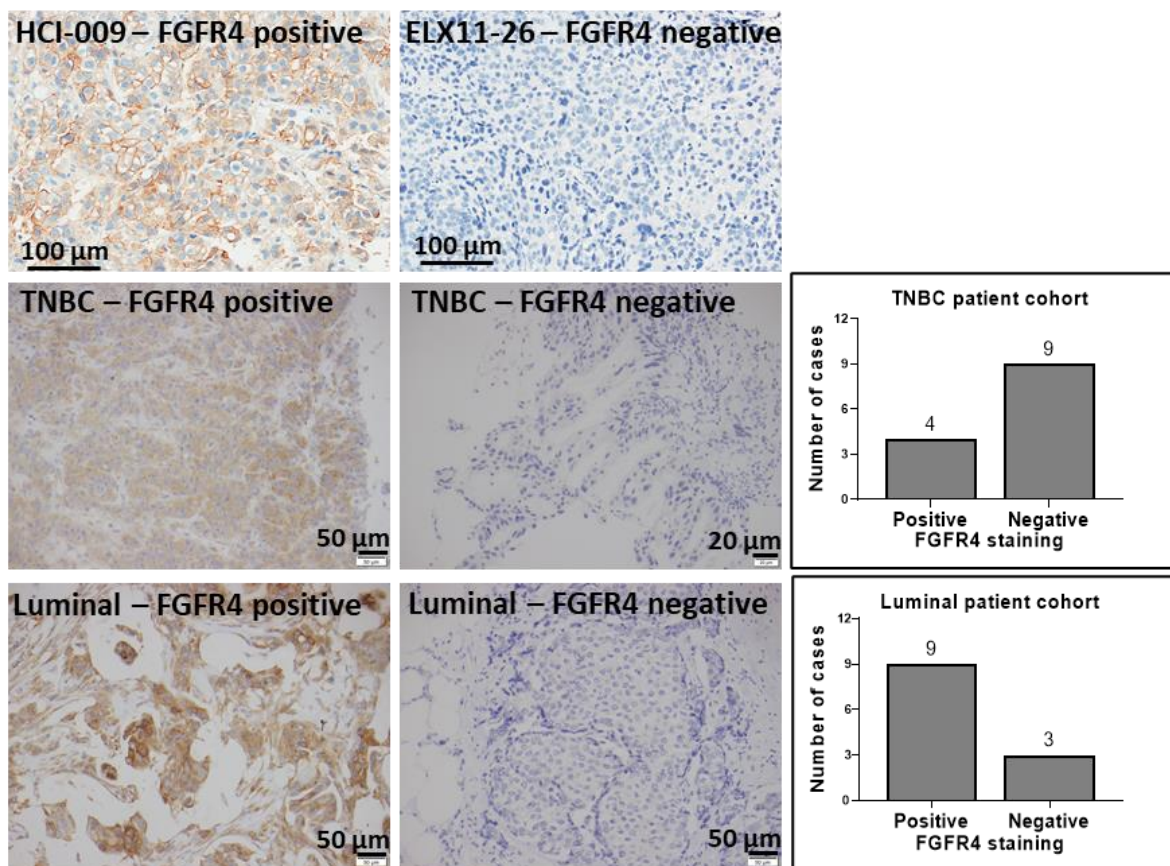


**Figure 4.10: Immunohistochemical staining for FGFR4 on breast cancer specimens.** PDX HCI-009 and ELX11-26 were used as positive and negative controls, respectively. A cohort of 12 luminal breast cancer and 13 TNBC samples were stained for FGFR4 expression. The frequency of positive and negative staining in these cohorts is represented in the bar graphs.

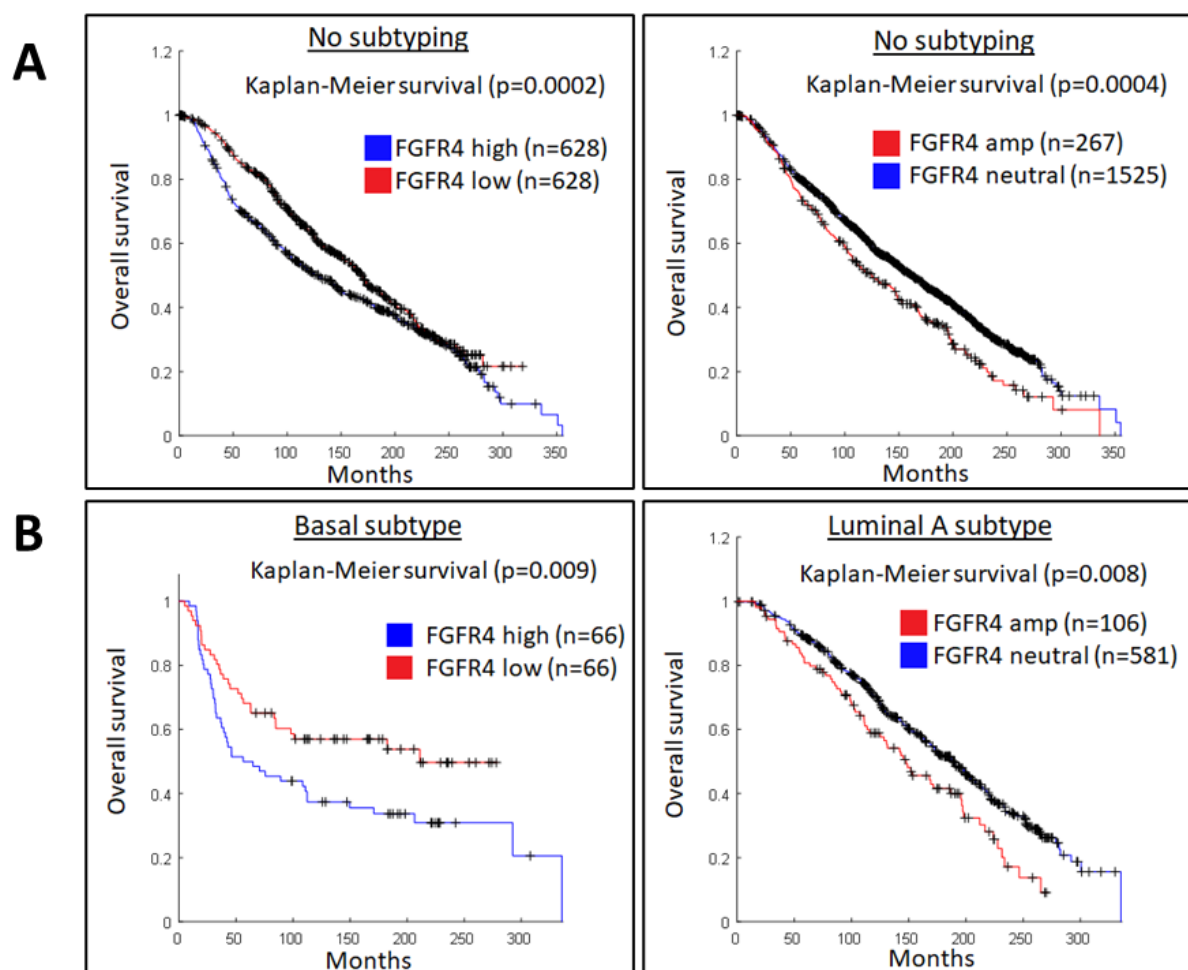


**Figure 4.11: The association of FGFR4 alterations with overall survival in breast cancer patients.** Association of FGFR4 alterations with breast cancer patient prognosis were analysed as a whole group, **a** no subtyping or **b** into basal or luminal A subtypes. Kaplan-Meier plots using data from the METABRIC dataset indicated that patients with FGFR4 overexpression (FGFR4 high) or amplification (FGFR4 amp) exhibit worse overall survival compared to those with low FGFR4 expression or neutral FGFR4. A Logrank test was used where a p-value of  $< 0.05$  was considered significant. Survival data for the different patient groups were extracted and downloaded from cBioportal and survival analysis performed using an in-house Matlab script.

### **4.2.6 Characterisation of FGFR4 expression and function in breast cancer patient-derived organoids**

The occurrence of FGFR4 genomic and/or expression changes in particular breast cancer subtypes and the association of these changes with poor prognosis led to further interrogate FGFR4 function using a panel of breast cancer patient-derived organoids (PDOs) spanning the luminal A, HER2 and TNBC subtypes. These were initially screened for FGFR4 expression by IHC (Fig. 4.12). Only the luminal A HBC22 organoid line exhibited strong positive FGFR4 staining, while low or undetectable FGFR4 staining was observed in the remaining lines (Fig. 4.12). HBC22 was selected as a candidate line to investigate the effect of FGFR4 inhibitor BLU9931 on organoid proliferation, with HBC30 used as a negative control (Fig. 4.13). BLU9931 significantly decreased organoid proliferation in the HBC22 line, compared to the HBC30 negative control (Fig. 4.13). These findings build upon our effective inhibition of aberrant FGFR4 signalling in the HCI-009 luminal B PDX (Fig. 4.8), highlighting FGFR4 expression as a potential therapeutic target in the luminal, and potentially other, breast cancer subtypes.

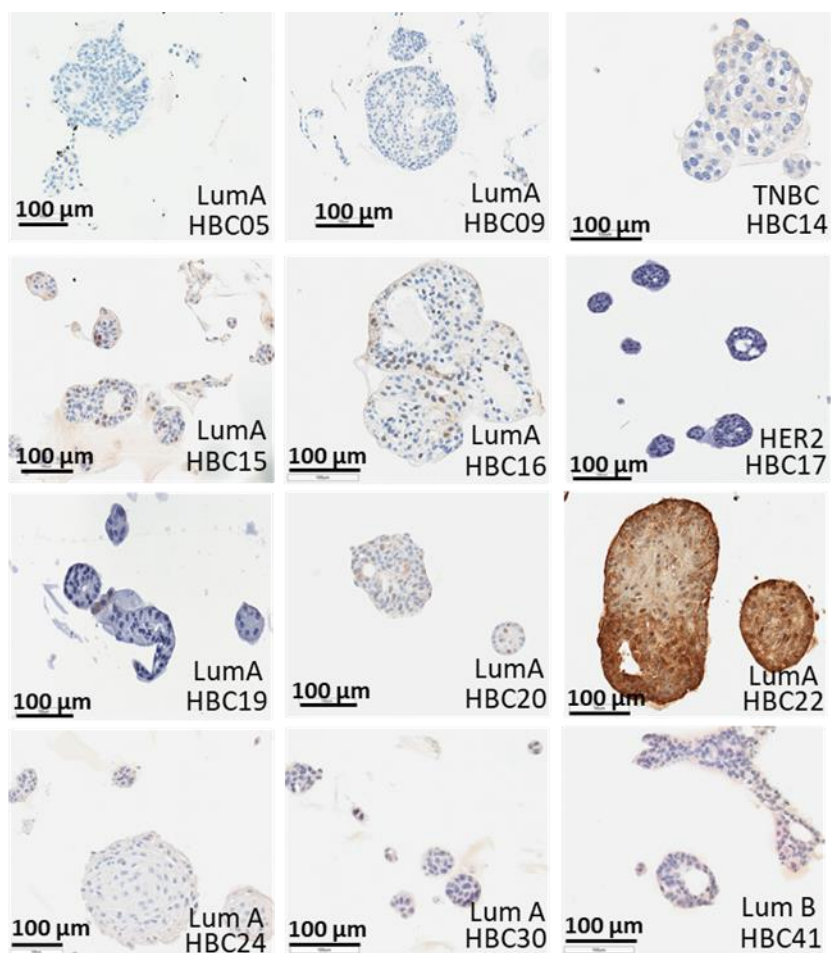


**Figure 4.12: Characterization of FGFR4 expression in human breast cancer organoids.** Immunohistochemical staining for FGFR4 across a panel of 9 human breast cancer organoid lines.

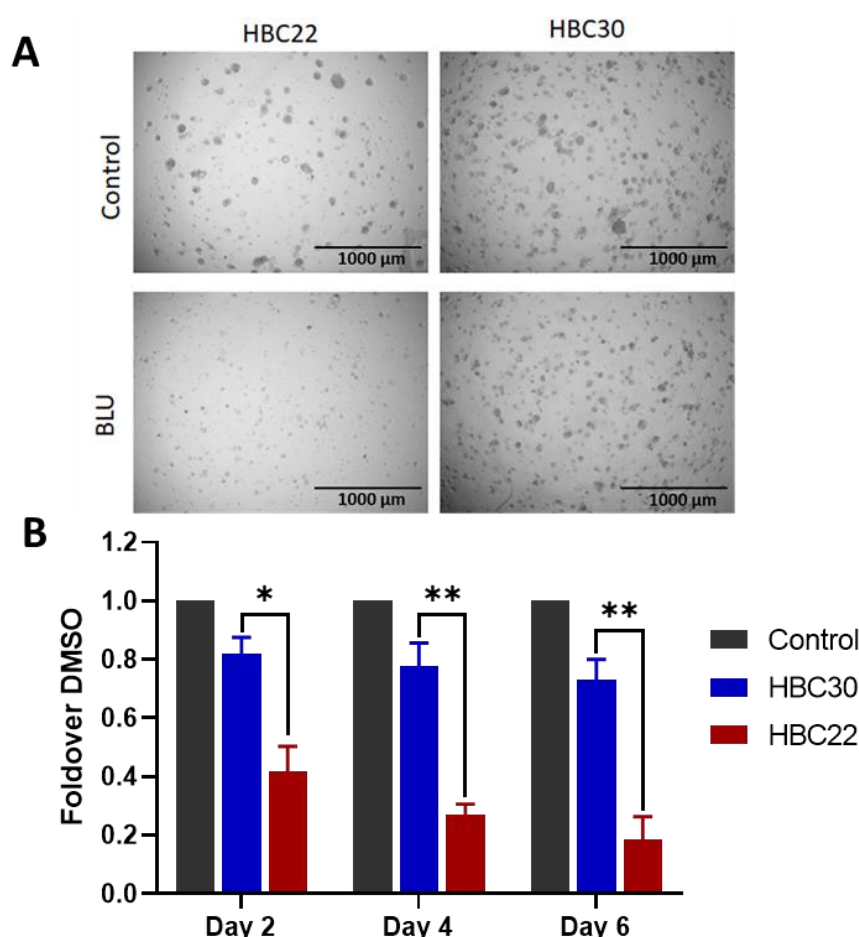


**Figure 4.13: Effect of the FGFR4 inhibitor BLU9931 on organoid growth.** **a** Images of DMSO control or BLU9931-treated FGFR4-high HBC22 and FGFR4-low HBC30 organoids at endpoint. **b** Quantification of (a) comparing the FGFR4-high HBC22 organoid line (red) with the FGFR4-low HBC30 line (blue) normalized to the DMSO control. \* indicates p-value of  $< 0.05$ , \*\*  $< 0.01$ . Error bars: mean  $\pm$  standard error of three biological replicates.

## 4.3 Discussion

This chapter combined integrated, multi-omics analyses with use of powerful patient-derived models to identify aberrant FGFR signalling as a potential therapeutic target in specific breast cancer subtypes. Importantly, this approach detected a novel FGFR2 fusion and marked FGFR4 overexpression and activation that would not have been identified by WES and determined that the corresponding PDX are sensitive to corresponding selective FGFR



inhibitors. This provides further evidence that targetable FGFR fusions do occur in breast cancer, albeit at low frequency, and adds further weight to emerging evidence highlighting FGFR4 as a potential therapeutic target in this malignancy [25, 26].

An interesting finding was the identification of a novel FGFR2-SKI fusion in a TNBC PDX with marked sensitivity to AZD4547, indicating an oncogenic addiction to the fusion. Fusion partners of FGFR2 reported specifically in breast cancer are AFF3, CASP7 and CCDC6 [35, 36], while partners identified in other cancers include TACC and KIAA family members, PPHLN1, NTRK1, BICC1, AHCYL1, OFD1 and SLC45A3 [35, 37-39]. These are often fused to the C-terminal region of FGFR2, and by providing additional domains that mediate oligomerization, drive activation of the fusion receptor and ligand-independent signalling [35]. SKI is a proto-oncogene that was first discovered as the cellular counterpart of the transforming protein of the Sloan-Kettering avian retrovirus [40]. It can reside in the nucleus or cytoplasm and exhibits aberrant expression in a variety of cancers, but fusions involving SKI have not been reported. Its best-characterised function is as a negative regulator of the TGF- $\beta$  signalling pathway, where it forms an inhibitory complex with SMAD proteins on TGF- $\beta$  target gene promoters, and this complex recruits histone deacetylases and other repressors to inhibit gene transcription [40]. In the FGFR2-SKI fusion, the C-terminal region of SKI containing the coiled-coil domains is joined to the extreme end of the FGFR2 kinase domain, and the coiled-coil domains originating from SKI are likely to promote homodimerization [41]. The structure of this fusion, which contains the majority of the RTK FGFR2 and also the nuclear localization signals of SKI, raises the possibility that it may signal in the plasma membrane and/or nuclear compartment.

While the TNBC PDX model ELX11-26 exhibited high FGFR1 phosphorylation (but not gene amplification), FGFR2 gene amplification and also FGFR2 phosphorylation only slightly lower than KCC\_P\_4043, it did not respond to AZD4547. Since a previous clinical trial and studies using pre-clinical models have reported an association between high level amplification of FGFR2 and response to selective FGFR1-3 inhibitors, with marked elevation of FGFR2 resulting in an oncogene addiction phenotype via transactivation of other RTKs, it is possible that the modest overexpression of FGFR1/2 in ELX11-26 does not traverse the threshold

required to impart AZD4547 sensitivity [6, 8]. A further contributing factor to the resistance of this PDX to drug treatment may be the high activation of other kinases indicated in the original MS profiling data [32], that identified increased activation of RTKs EPHB1/3/4 and PDGFRA, and the cytoplasmic tyrosine kinases ABL2 and PTK2, which may make signalling by FGFR1/2 redundant.

Importantly, this chapter supports a role for FGFR4 as a therapeutic target in specific breast cancer subtypes. Currently, the mechanisms underpinning FGFR4 overexpression in breast cancer are unclear. The luminal B PDX HCI-009 exhibited extremely high FGFR4 expression in the absence of gene amplification [32], suggesting a transcriptional or post-transcriptional mechanism, and limited correlation between FGFR4 DNA and mRNA has been noted in other studies [42]. However, both HCI-009 and the FGFR4-overexpressing luminal A PDO HBC22 exhibited significant sensitivity to the selective FGFR4 inhibitor BLU9931. In this regard, several previous studies have reported an association between FGFR4 and progression of luminal breast cancers. Specifically, enhanced expression of FGFR4 is associated with development of endocrine resistance *in vitro* [42] and poor outcome in tamoxifen-treated patients [43]. In addition, FGFR4 is overexpressed in metastases derived from luminal A breast cancers compared to the primary tumour [44] and high FGFR4 expression and hotspot mutations occur in endocrine therapy-treated distant breast cancer metastases, particularly derived from invasive lobular carcinoma [25]. Moreover, a recent study has determined that FGFR4 drives phenotypic switching of luminal A breast cancers to a HER2-enriched gene expression phenotype, and that a FGFR4-induced expression signature is positively associated with poor outcome and site-selective metastasis [26]. In the latter study, treatment of an ER-positive, HER2-enriched and FGFR4-positive PDX with BLU9931 resulted in marked inhibition of tumour growth [26]. Collectively, this work indicates that FGFR4 inhibitors may have significant impact in management of advanced, endocrine resistant luminal breast cancer.

## **4.4 Conclusion**

This work demonstrates the power of applying an integrated, multi-omics approach to patient-derived models in order to identify potential therapeutic targets, provides further evidence that



FGFR fusions, while occurring at a relatively low frequency in breast cancer, can confer oncogenic addiction and result in marked therapeutic responses to corresponding targeted therapy, and highlights FGFR4 as an attractive target in a subset of advanced luminal breast cancer.

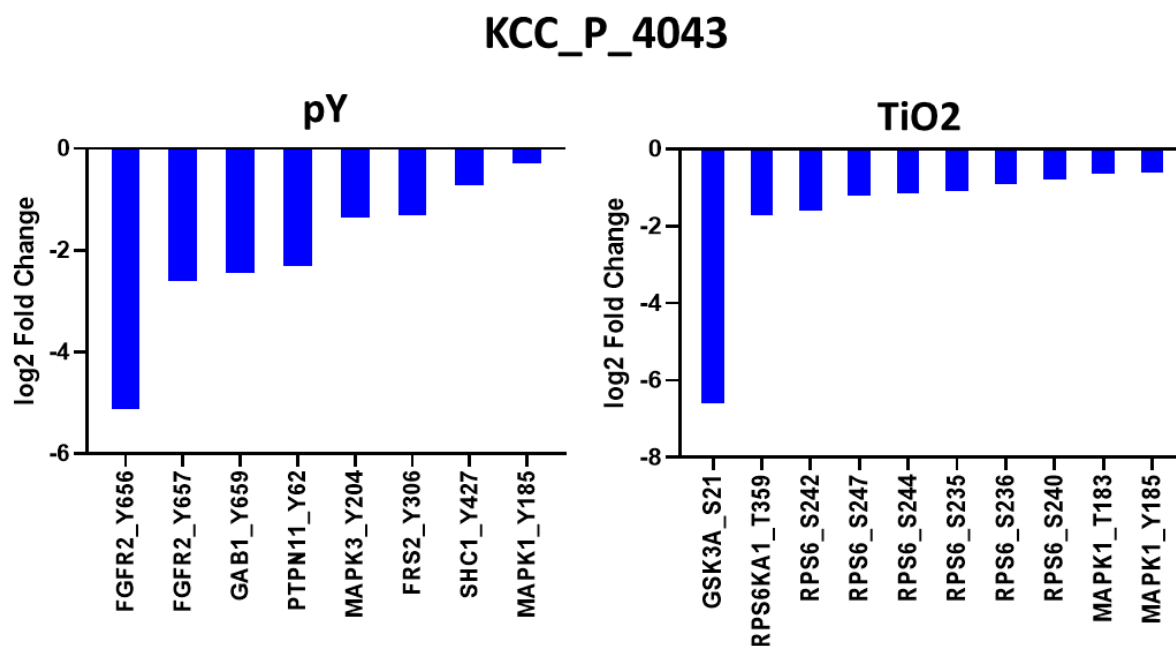
## **4.5 Future direction**

These results have identified a novel FGFR2-SKI fusion in the KCC\_P\_4043 TNBC PDX model. Given the additional localisation signals from SKI, the localisation of the FGFR2-SKI fusion could be characterised to determine whether it undertakes signalling in the plasma membrane and/or nuclear compartment. The other TNBC PDX, ELX11-26, also had high FGFR1 and FGFR2 expression but did not respond to AZD4547. This may be due to high activation of other tyrosine kinases, so corresponding tyrosine kinase inhibitors could be tested in combination with FGFR inhibitors as novel therapeutic approaches. With regard to FGFR4 in breast cancer, the effect of FGFR4 inhibitor BLU9931 on organoid morphology, sensitivity to other therapies (e.g., Tamoxifen, Fulvestrant) and downstream signalling could be determined in organoid lines with differential FGFR4 expression (low, moderate, and high). In addition, it will be important to characterise regulatory mechanisms underpinning marked FGFR4 overexpression in the absence of gene amplification.

## **4.6 Acknowledgements**

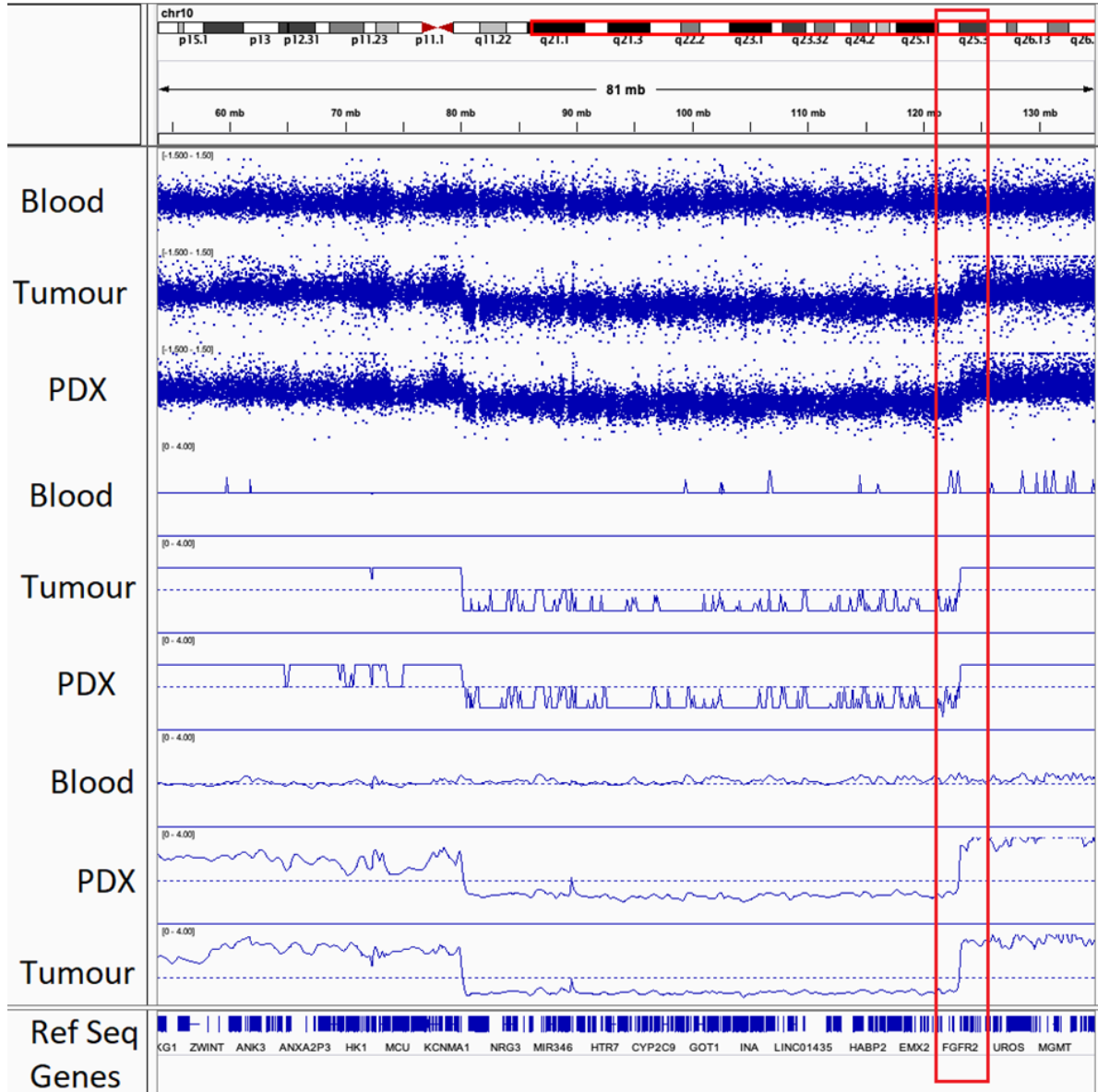
This chapter is part of a research article that will be submitted to Breast Cancer Research. I acknowledge the assistance from Alex Swarbrick's group (Garvan Institute of Medical Research) for undertaking inhibitor treatments of the mouse models.

## 4.7 Supplementary Materials



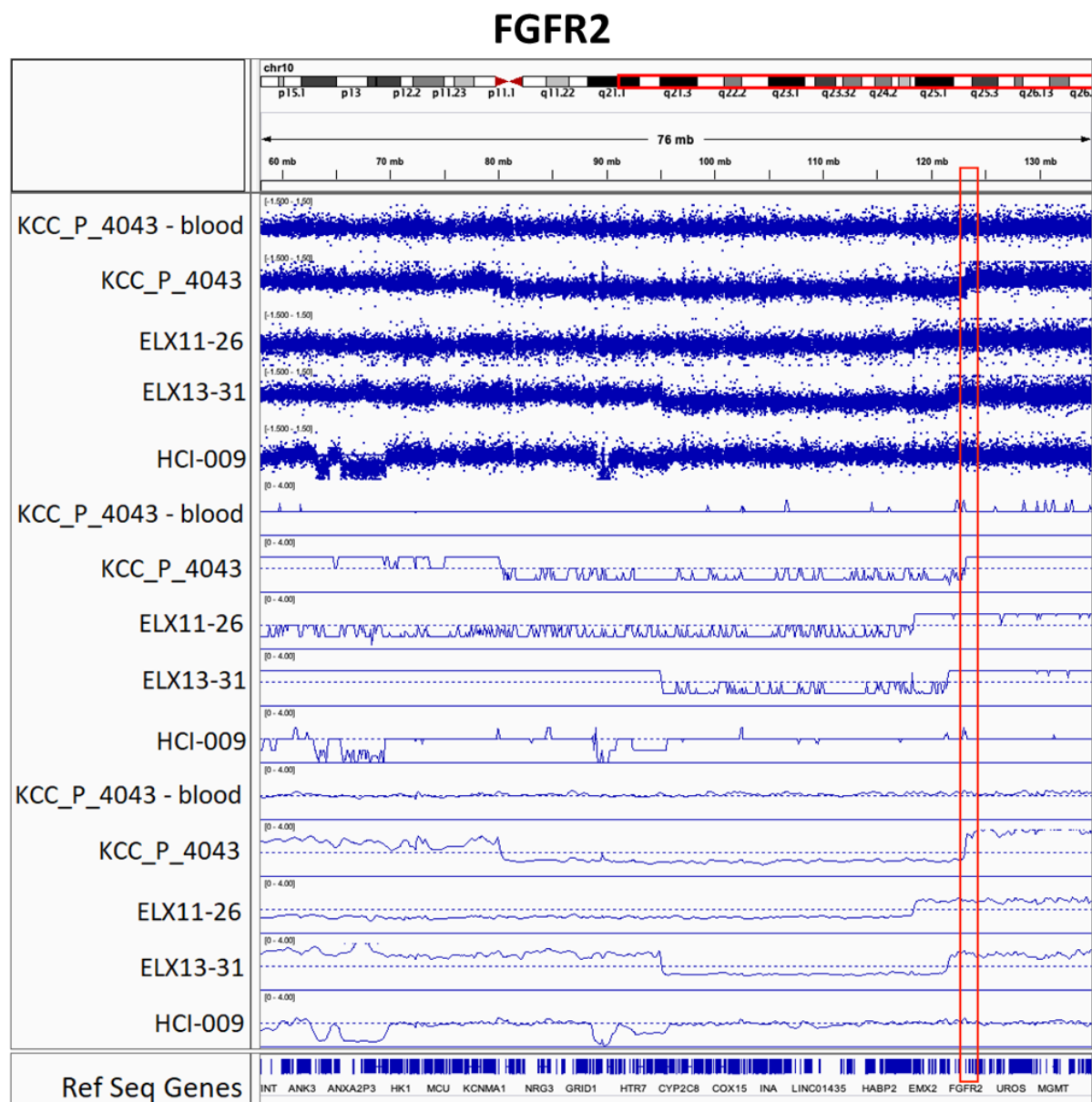
**Supplementary Figure 4.1: Effects on site-selective protein phosphorylation as determined by MS-based phosphoproteomics.** Data from phosphotyrosine- and TiO<sub>2</sub>-enrichment workflows are presented, highlighting phosphosites downregulated in response to AZD4547. Analysis performed by Dr. Terry Lim.

## KCC\_P\_4043



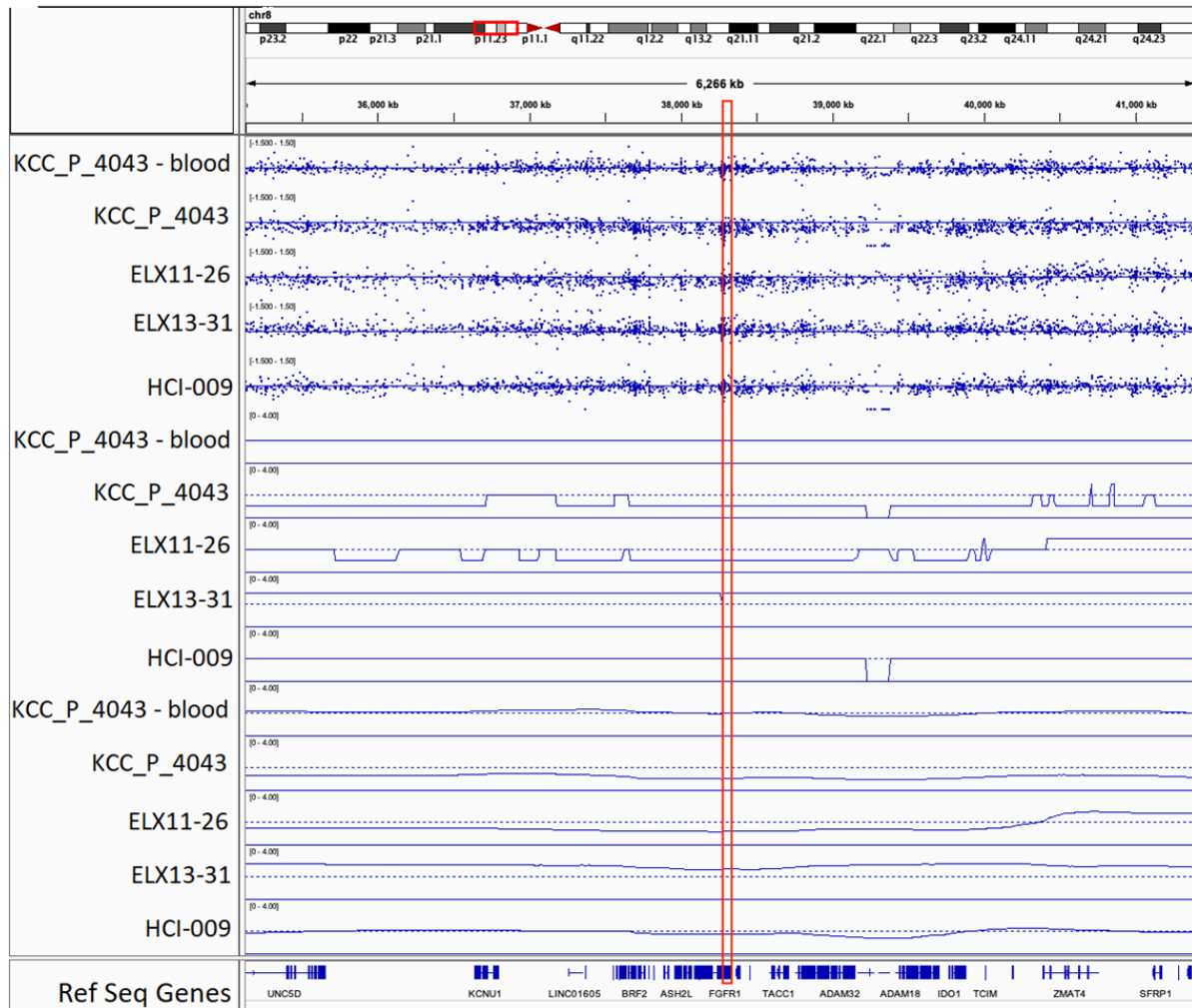
**Supplementary Figure 4.2: Analysis of FGFR2 in the KCC\_P\_4043 using SNP arrays.**

Top three tracks are copy number raw logRatio data from the array; middle three tracks are copy number segmentation from the raw logRatio; bottom three tracks are smoothed copy number signal. The red box highlights FGFR2 on chromosome 10. Analysis performed by Dr. Niantao Deng.



**Supplementary Figure 4.3: SNP arrays showing FGFR2 alterations in specific PDX.** Track order as for supplementary figure 4.2. ELX13-31 is a PDX with FGFR2 copy number gain included as a positive control. The red box highlights FGFR2. Analysis performed by Dr. Niantao Deng.

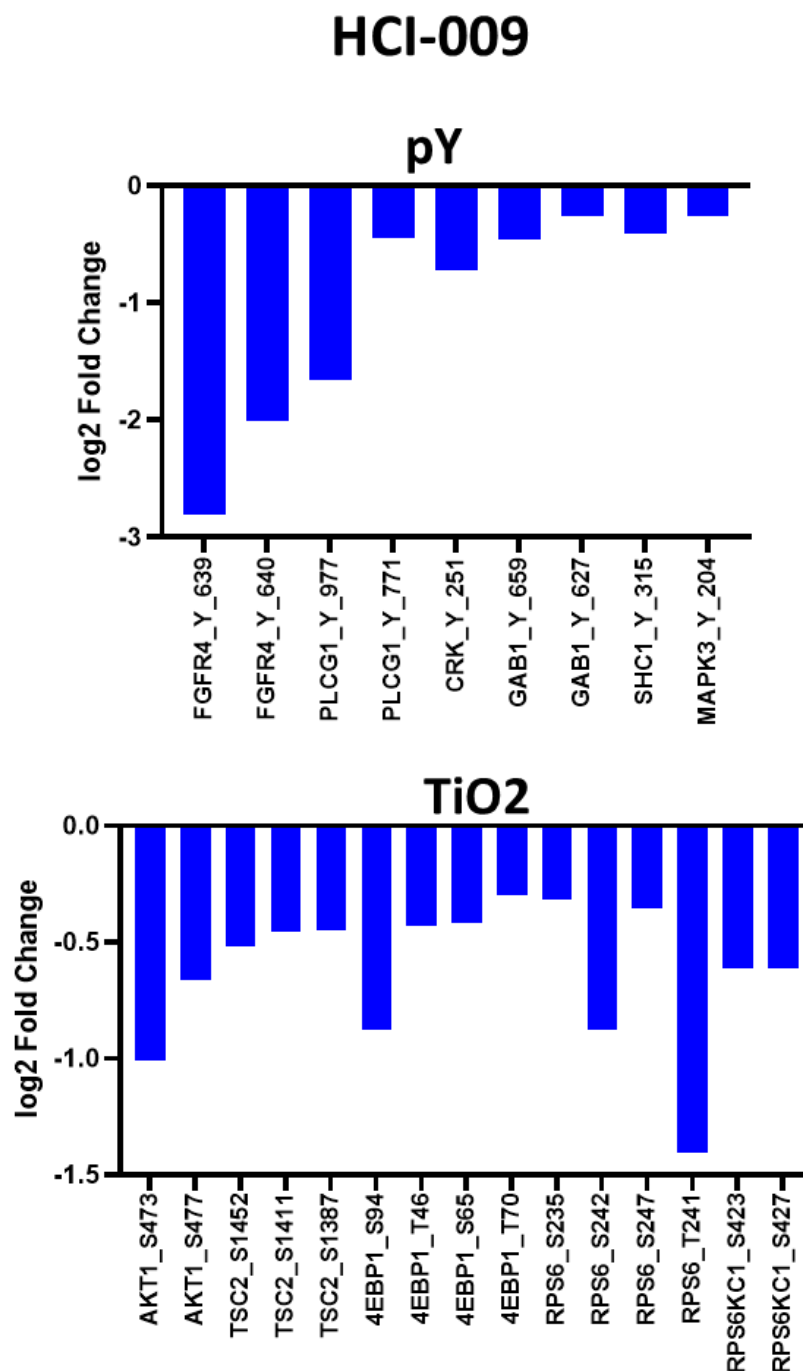
# FGFR1



**Supplementary Figure 4.4: SNP arrays showing FGFR1 alterations in specific PDX.** The red box highlights FGFR1. Analysis performed by Dr. Niantao Deng.

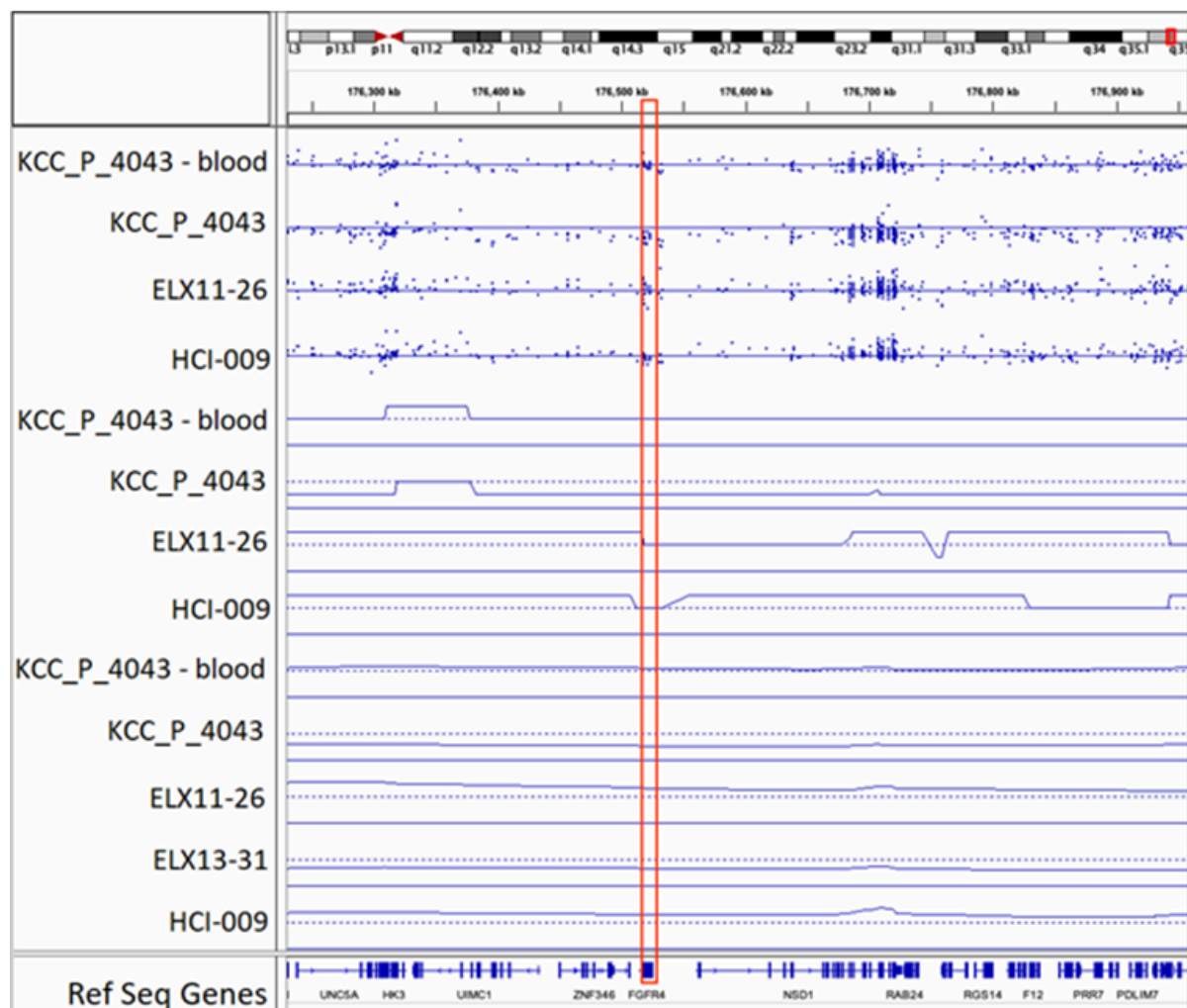
Supplementary Table 4.1: SNVs in KCC\_P\_4043 tumour.

Gene in KEGG pathway database			Other Genes					
PLOD1	NOTCH1	TIAM1	NEK1	NEURL4	CCDC27	BICC1	MAPK15	
PTCH2	MINPP1	PFKL	MRPS30	CNTROB	KAZN	LCOR	TTC39B	
DHCR24	NUP98	SLC19A1	SREK1	SLC5A10	TCEA3	FAM53B	SAXO1	
DNASE2B	PDE3B	GSTT1	NSA2	AKAP10	HPCA	ZNF511	SAXO1	
TTF2	MRPL11	CACNA1I	PGGT1B	KRT13	SZT2	SIGIRR	CAAP1	
NOTCH2	SHANK2	PPP2R3B	APBB3	RUNDC1	HECTD3	BRSK2	RUSC2	
APH1A	ARHGEF12	POLA1	PCDHB8	MEOX1	MROH7	RASSF10	ESX1	
THBS3	ST3GAL4	PPP1R3F	PCDHGA2	MPP3	ROR1	NAV2	TUT7	
KHK	SCNN1A	OGT	ZNF300	CDC42EP4	LRRC40	ACCSL	FBXO7	
EHD3	SCNN1A	MCM7	FAT2	ELP2	LRRC40	PRDM11	ZNF618	
DYNC2LI1	HDAC7	PTPRZ1	SIMC1	PLIN4	GBP5	AHNAK	TTC16	
EPAS1	KMT2D	WASL	N4BP3	FEM1A	TAFA3	CDC42BPG	CIZ1	
REL	NPFF	SND1	DEK	ZNF358	ZNF697	RIN1	GLE1	
POLR1A	WIF1	NAPRT	ABCF1	SMARCA4	RPTN	C11orf24	GLRA4	
SEMA4C	LGR5	NPR2	BRD2	MAST1	FLG2	PPP6R3	SNAPC4	
PRPF40A	DYNLL1	TJP2	BRPF3	SMIM7	MUC1	CEP295	SEC16A	
DPP4	BRCA2	NUP214	LRFN2	NIBAN3	SLC9C2	KDM4D	KLF6	
TTN	COL4A1	VAV2	FAM135A	ANKRD27	NUAK2	ATN1	SFMBT2	
NUP35	RASA3	NOD1	FILIP1	SAMD4B	ACBD3	SLC2A14	MCM10	
COL3A1	MYH7	GHRHR	ANKRD6	ZNF404	CDC42BPA	PZP	MPP7	
CASP8	AP1G2	ADCY1	ASCC3	IZUMO2	OBSCN	C12orf40	ZNF33A	
ALPI	PPM1A	PSPH	MCM9	ZNF611	LYST	GDF11	IQCA1	
DNAH1	ADPGK	HSPB1	TTYH3	ZNF761;ZNF765-ZNF761	ZBTB18	PTPRQ	CROCC2	
MITF	ULK3	SEMA3C	RNF216	ECE2;EEF1AKMT4-ECE2	PUS10	FGD6	LMCD1	
GBE1	SIN3A	PEX1	CRPPA	PEG3	PLEK	BTBD11	TOP2B	
HTR3D	SV2B	ARPC1B	SNX13	ZNF544	DUSP11	ACAD10	SCN11A	
KNG1	PIGQ	CYP4F22	HOXA7	RALGAPA2	CCDC142	BICDL1	FBXW12	
ACAP2	TAOK2	JAK3	HOXA13	REMI	DQX1	CCDC92	NISCH	
MYL5	ITGAD	PPP1R15A	KRIT1	EFCAB8	ATOH8	SLC15A4	NISCH	
WFS1	TAT	NAPSA	ARR3	SPECC1L	PTCD3	SACS	LRIG1	
MAPK10	AP1G1	GP6	PDK4	SPECC1L	ANKRD36C	TRPC4	CADM2	
NFKB1	OR1E1	NFATC2	NYAP1	LRRC75B	TBC1D8	STK24	CD200R1L	
SNCAIP	PLD2	PPP1R3D	ZAN	ASCC2	NPHP1	TUBGCP3	RYK	
NRG2	POLR2A	PPP1R3D	CUX1	HORMAD2	NEB	MCF2L	KY	
LARS	ATP1B2	MOCS1	LMOD2	HORMAD2	METAP1D	POTEM	PRR23B	
PDE6A	MAPK7	NFKBIE	CLIC2	DEPDC5	CWC22	OR4Q2	LRRC34	
VARS2	CCL3L1;CCL3L3	TAAR2	RPIL1	HEPACAM2	ANKAR	DHRS2	TMEM41A	
ATF6B	STAT5B	SYNJ2	XKR4	KIAA0930	GPR1	IPO4	MUC4	
HLA-DMB	ENGASE	THBS2	VPS13B	AKAP17A	ZNF142	SDR39U1	MUC4	
ATG4D	TYMS	GALNT1	ZNF572	SLC9A7	CFAP65	RTN1	CORIN	
PKN1	CDH2		KCTD19	TSPYL2	ATXN2L	HEATR4	PTPN13	
			TANGO6	STAR08	FBR5	OIP5	ISOC2	
			HAS3	SPATA31A3	TGFB1I1	CTRB1	MGA	
			HYDIN	MAGEE2	CDH8	IL17C	THAP10	
			HYDIN	MAGEE1	ACTR5	MYO1C	RCN2	
			WDR87	TMEM209	NCOA3	SLC13A5	NR2F2	
			EIF3K	ADAMTS13	TPTE	XAF1	MRTFB	
			SDK2	AMMECR1	PCBP3	RNF128	ZNF70	
			SDK2	PALM2-AKAP2	DIP2A	CBX4	CD93	



**Supplementary Figure 4.5: Effects on site-selective protein phosphorylation as determined by MS-based phosphoproteomics.** Data from phosphotyrosine- and TiO<sub>2</sub>-enrichment workflows are presented, highlighting phosphosites downregulated in response to BLU9931. Analysis performed by Dr. Terry Lim.

# FGFR4



**Supplementary Figure 4.6: SNP arrays showing FGFR4 alterations in specific PDX.** The red box highlights FGFR4. Analysis performed by Dr. Niantao Deng.



## 4.8 References

1. **Lehmann, B.D., J.A. Bauer, X. Chen, M.E. Sanders, A.B. Chakravarthy, Y. Shyr, and J.A. Pietenpol**, *Identification of human triple-negative breast cancer subtypes and preclinical models for selection of targeted therapies*. *Journal of Clinical Investigation*, 2011. 121(7): p. 2750-2767.
2. **Burstein, M.D., A. Tsimelzon, G.M. Poage, K.R. Covington, A. Contreras, S.A.W. Fuqua, M.I. Savage, C.K. Osborne, S.G. Hilsenbeck, J.C. Chang, G.B. Mills, C.C. Lau, and P.H. Brown**, *Comprehensive genomic analysis identifies novel subtypes and targets of triple-negative breast cancer*. *Clinical Cancer Research*, 2015. 21(7): p. 1688-1698.
3. **Azim, H.A., M. Ghosn, K. Oualla, and L. Kassem**, *Personalized treatment in metastatic triple-negative breast cancer: The outlook in 2020*. *Breast Journal*, 2020. 26(1): p. 69-80.
4. **Tran, B. and P.L. Bedard**, *Luminal-B breast cancer and novel therapeutic targets*. *Breast Cancer Research*, 2011. 13(6): p. 221.
5. **Fleuren, E.D.G., L. Zhang, J. Wu, and R.J. Daly**, *The kinome 'at large' in cancer*. *Nature Reviews Cancer*, 2016. 16(2): p. 83-98.
6. **Babina, I.S. and N.C. Turner**, *Advances and challenges in targeting FGFR signalling in cancer*. *Nature Reviews Cancer*, 2017. 17(5): p. 318-332.
7. **Perez-Garcia, J., E. Muñoz-Couselo, J. Soberino, F. Racca, and J. Cortes**, *Targeting FGFR pathway in breast cancer*. *Breast*, 2018. 37: p. 126-133.
8. **Pearson, A., E. Smyth, I.S. Babina, M.T. Herrera-Abreu, N. Tarazona, C. Peckitt, E. Kilgour, N.R. Smith, C. Geh, C. Rooney, R. Cutts, J. Campbell, J. Ning, K. Fenwick, A. Swain, G. Brown, S. Chua, A. Thomas, S.R.D. Johnston, M. Ajaz, K. Sumpter, A. Gillbanks, D. Watkins, I. Chau, S. Popat, D. Cunningham, and N.C. Turner**, *High-level clonal FGFR amplification and response to FGFR inhibition in a translational clinical trial*. *Cancer Discovery*, 2016. 6(8): p. 838-851.

9. **Javle, M., M. Lowery, R.T. Shroff, K.H. Weiss, C. Springfield, M.J. Borad, R.K. Ramanathan, L. Goyal, S. Sadeghi, T. Macarulla, A. El-Khoueiry, R.K. Kelley, I. Borbath, S.P. Choo, D.Y. Oh, P.A. Philip, L.T. Chen, T. Reungwetwattana, E. Van Cutsem, K.H. Yeh, K. Ciombor, R.S. Finn, A. Patel, S. Sen, D. Porter, R. Isaacs, A.X. Zhu, G.K. Abou-Alfa, and T. Bekaii-Saab, *Phase II study of BGJ398 in patients with FGFR-Altered advanced cholangiocarcinoma*. Journal of Clinical Oncology, 2018. 36(3): p. 276-282.**
  
10. **Loriot, Y., A. Necchi, S.H. Park, J. Garcia-Donas, R. Huddart, E. Burgess, M. Fleming, A. Rezazadeh, B. Mellado, S. Varlamov, M. Joshi, I. Duran, S.T. Tagawa, Y. Zakharia, B. Zhong, K. Stuyckens, A. Santiago-Walker, P. De Porre, A. O'Hagan, A. Avadhani, and A.O. Siefker-Radtke, *Erdafitinib in Locally Advanced or Metastatic Urothelial Carcinoma*. New England Journal of Medicine, 2019. 381(4): p. 338-348.**
  
11. **Facchinetti, F., A. Hollebecque, R. Bahleda, Y. Loriot, K.A. Olaussen, C. Massard, and L. Friboulet, *Facts and new hopes on selective FGFR inhibitors in solid tumours*. Clinical Cancer Research, 2020. 26(4): p. 764-774.**
  
12. **Hagel, M., C. Miduturu, M. Sheets, N. Rubin, W. Weng, N. Stransky, N. Bifulco, J.L. Kim, B. Hodous, N. Brooijmans, A. Shutes, C. Winter, C. Lengauer, N.E. Kohl, and T. Guzi, *First selective small molecule inhibitor of FGFR4 for the treatment of hepatocellular carcinomas with an activated FGFR4 signaling pathway*. Cancer Discovery, 2015. 5(4): p. 424-437.**
  
13. **Joshi, J.J., H. Coffey, E. Corcoran, J. Tsai, C.L. Huang, K. Ichikawa, S. Prajapati, M.H. Hao, S. Bailey, J. Wu, V. Rimkunas, C. Karr, V. Subramanian, P. Kumar, C. MacKenzie, R. Hurley, T. Satoh, K. Yu, E. Park, N. Rioux, A. Kim, W.G. Lai, L. Yu, P. Zhu, S. Buonamici, N. Larsen, P. Fekkes, J. Wang, M. Warmuth, D.J. Reynolds, P.G. Smith, and A. Selvaraj, *H3B-6527 Is a potent and selective inhibitor of FGFR4 in FGF19-Driven hepatocellular carcinoma*. Cancer Research, 2017. 77(24): p. 6999-7013.**

14. **Chang, J., X. Liu, S. Wang, Z. Zhang, Z. Wu, X. Zhang, and J. Li**, *Prognostic value of FGFR gene amplification in patients with different types of cancer: A systematic review and meta-analysis*. PLoS ONE, 2014. 9(8).
15. **Cheng, C.L., A.A. Thike, S.Y.J. Tan, P.J. Chua, B.H. Bay, and P.H. Tan**, *Expression of FGFR1 is an independent prognostic factor in triple-negative breast cancer*. Breast Cancer Research and Treatment, 2015. 151(1): p. 99-111.
16. **Turner, N., A. Pearson, R. Sharpe, M. Lambros, F. Geyer, M.A. Lopez-Garcia, R. Natrajan, C. Marchio, E. Iorns, A. Mackay, C. Gillett, A. Grigoriadis, A. Tutt, J.S. Reis-Filho, and A. Ashworth**, *FGFR1 amplification drives endocrine therapy resistance and is a therapeutic target in breast cancer*. Cancer Research, 2010. 70(5): p. 2085-2094.
17. **Elbauomy Elsheikh, S., A.R. Green, M.B. Lambros, N.C. Turner, M.J. Grainge, D. Powe, I.O. Ellis, and J.S. Reis-Filho**, *FGFR1 amplification in breast carcinomas: a chromogenic in situ hybridisation analysis*. Breast cancer research : BCR, 2007. 9(2).
18. **Turner, N., M.B. Lambros, H.M. Horlings, A. Pearson, R. Sharpe, R. Natrajan, F.C. Geyer, M. Van Kouwenhove, B. Kreike, A. MacKay, A. Ashworth, M.J. Van De Vijver, and J.S. Reis-Filho**, *Integrative molecular profiling of triple negative breast cancers identifies amplicon drivers and potential therapeutic targets*. Oncogene, 2010. 29(14): p. 2013-2023.
19. **Turczyk, L., K. Kitowska, M. Mieszkowska, K. Mieczkowski, D. Czaplinska, D. Piasecka, R. Kordek, A.C. Skladanowski, P. Potemski, H.M. Romanska, and R. Sadej**, *FGFR2-Driven Signaling Counteracts Tamoxifen Effect on ERα-Positive Breast Cancer Cells*. Neoplasia (United States), 2017. 19(10): p. 791-804.
20. **Sun, S., Y. Jiang, G. Zhang, H. Song, X. Zhang, Y. Zhang, X. Liang, Q. Sun, and D. Pang**, *Increased expression of fibroblastic growth factor receptor 2 is correlated with poor prognosis in patients with breast cancer*. Journal of Surgical Oncology, 2012. 105(8): p. 773-779.

21. **Chew, N.J., E.V. Nguyen, S.-P. Su, K. Novy, H.C. Chan, L.K. Nguyen, J. Luu, K.J. Simpson, R.S. Lee, and R.J. Daly**, *FGFR3 signaling and function in triple negative breast cancer*. Cell Communication and Signaling, 2020. 18(1): p. 13.
22. **Shaver, T.M., B.D. Lehmann, J.S. Beeler, C.I. Li, Z. Li, H. Jin, T.P. Stricker, Y. Shyr, and J.A. Pietenpol**, *Diverse, biologically relevant, and targetable gene rearrangements in triple-negative breast cancer and other malignancies*. Cancer Research, 2016. 76(16): p. 4850-4860.
23. **Roidl, A., P. Foo, W. Wong, C. Mann, S. Bechtold, H.J. Berger, S. Streit, J.E. Ruhe, S. Hart, A. Ullrich, and H.K. Ho**, *The FGFR4 Y367C mutant is a dominant oncogene in MDA-MB453 breast cancer cells*. Oncogene, 2010. 29(10): p. 1543-1552.
24. **Thussbas, C., J. Nahrig, S. Streit, J. Bange, M. Kriner, R. Kates, K. Ulm, M. Kiechle, H. Hoefler, A. Ullrich, and N. Harbeck**, *FGFR4 Arg388 allele is associated with resistance to adjuvant therapy in primary breast cancer*. Journal of Clinical Oncology, 2006. 24(23): p. 3747-3755.
25. **Levine, K.M., N. Priedigkeit, A. Basudan, N. Tasdemir, M.J. Sikora, E.S. Sokol, R.J. Hartmaier, K. Ding, N.Z. Ahmad, and R.J. Watters**, *FGFR4 overexpression and hotspot mutations in metastatic ER+ breast cancer are enriched in the lobular subtype*. NPJ breast cancer, 2019. 5(1): p. 1-5.
26. **Garcia-Recio, S., A. Thennavan, M.P. East, J.S. Parker, J.M. Cejalvo, J.P. Garay, D.P. Hollern, X. He, K.R. Mott, and P. Galván**, *FGFR4 regulates tumour subtype differentiation in luminal breast cancer and metastatic disease*. The Journal of clinical investigation, 2020. 130(9).
27. **Hochgräfe, F., L. Zhang, S.A. O'Toole, B.C. Browne, M. Pinese, A.P. Cubas, G.M. Lehrbach, D.R. Croucher, D. Rickwood, A. Boulghourjian, R. Shearer, R. Nair, A. Swarbrick, D. Faratian, P. Mullen, D.J. Harrison, A.V. Biankin, R.L. Sutherland, M.J. Raftery, and R.J. Daly**, *Tyrosine phosphorylation profiling reveals the signaling network characteristics of basal breast cancer cells*. Cancer Research, 2010. 70(22): p. 9391-9401.

28. **Ali, N.A., J. Wu, F. Hochgräfe, H. Chan, R. Nair, S. Ye, L. Zhang, R.J. Lyons, M. Pinese, H.C. Lee, N. Armstrong, C.J. Ormandy, S.J. Clark, A. Swarbrick, and R.J. Daly**, *Profiling the tyrosine phosphoproteome of different mouse mammary tumour models reveals distinct, model-specific signalling networks and conserved oncogenic pathways*. Breast Cancer Research, 2014. 16(5).
29. **Whittle, J.R., M.T. Lewis, G.J. Lindeman, and J.E. Visvader**, *Patient-derived xenograft models of breast cancer and their predictive power*. Breast Cancer Research, 2015. 17(1): p. 17.
30. **DeRose, Y.S., G. Wang, Y.-C. Lin, P.S. Bernard, S.S. Buys, M.T. Ebbert, R. Factor, C. Matsen, B.A. Milash, and E. Nelson**, *Tumour grafts derived from women with breast cancer authentically reflect tumour pathology, growth, metastasis and disease outcomes*. Nature medicine, 2011. 17(11): p. 1514-1520.
31. **Sachs, N., J. de Ligt, O. Kopper, E. Gogola, G. Bounova, F. Weeber, A.V. Balgobind, K. Wind, A. Gracanin, and H. Begthel**, *A living biobank of breast cancer organoids captures disease heterogeneity*. Cell, 2018. 172(1-2): p. 373-386. e10.
32. **Chew, N.J., T.C.C. Lim Kam Sian, E.V. Nguyen, S.-Y. Shin, J. Yang, M.N. Hui, N. Deng, C.A. McLean, A.L. Welm, E. Lim, P. Gregory, T. Nottle, T. Lang, M. Vereker, G. Richardson, G. Kerr, D. Micati, T. Jarde, H.E. Abud, R.S. Lee, A. Swarbrick, and R.J. Daly**, *Evaluation of FGFR targeting in breast cancer through interrogation of patient-derived models*. 2020.
33. **Gavine, P.R., L. Mooney, E. Kilgour, A.P. Thomas, K. Al-Kadhimi, S. Beck, C. Rooney, T. Coleman, D. Baker, M.J. Mellor, A.N. Brooks, and T. Klinowska**, *AZD4547: An orally bioavailable, potent, and selective inhibitor of the fibroblast growth factor receptor tyrosine kinase family*. Cancer Research, 2012. 72(8): p. 2045-2056.
34. **Nagata, M., S. Nagata, K. Yuki, K. Isogaya, M. Saitoh, K. Miyazono, and K. Miyazawa**, *Identification of a phosphorylation site in c-Ski as serine 515*. The journal of biochemistry, 2010. 148(4): p. 423-427.

35. **Wu, Y.M., F. Su, S. Kalyana-Sundaram, N. Khazanov, B. Ateeq, X. Cao, R.J. Lonigro, P. Vats, R. Wang, S.F. Lin, A.J. Cheng, L.P. Kunju, J. Siddiqui, S.A. Tomlins, P. Wyngaard, S. Sadis, S. Roychowdhury, M.H. Hussain, F.Y. Feng, M.M. Zalupski, M. Talpaz, K.J. Pienta, D.R. Rhodes, D.R. Robinson, and A.M. Chinnaiyan**, *Identification of targetable FGFR gene fusions in diverse cancers*. Cancer Discovery, 2013. 3(6): p. 636-647.
36. **De Luca, A., D. Frezzetti, M. Gallo, and N. Normanno**, *FGFR-targeted therapeutics for the treatment of breast cancer*. Expert Opinion on Investigational Drugs, 2017. 26(3): p. 303-311.
37. **Arai, Y., Y. Totoki, F. Hosoda, T. Shiota, N. Hama, H. Nakamura, H. Ojima, K. Furuta, K. Shimada, and T. Okusaka**, *Fibroblast growth factor receptor 2 tyrosine kinase fusions define a unique molecular subtype of cholangiocarcinoma*. Hepatology, 2014. 59(4): p. 1427-1434.
38. **Ross, J.S., K. Wang, L. Gay, R. Al-Rohil, J.V. Rand, D.M. Jones, H.J. Lee, C.E. Sheehan, G.A. Otto, G. Palmer, R. Yelensky, D. Lipson, D. Morosini, M. Hawryluk, D.V.T. Catenacci, V.A. Miller, C. Churi, S. Ali, and P.J. Stephens**, *New routes to targeted therapy of intrahepatic cholangiocarcinomas revealed by next-generation sequencing*. The oncologist, 2014. 19(3): p. 235-242.
39. **Sia, D., B. Losic, A. Moeini, L. Cabellos, K. Hao, K. Revill, D. Bonal, O. Miltiadous, Z. Zhang, Y. Hoshida, H. Cornella, M. Castillo-Martin, R. Pinyol, Y. Kasai, S. Roayaie, S.N. Thung, J. Fuster, M.E. Schwartz, S. Waxman, C. Cordon-Cardo, E. Schadt, V. Mazzaferro, and J.M. Llovet**, *Massive parallel sequencing uncovers actionable FGFR2-PPHLN1 fusion and ARAF mutations in intrahepatic cholangiocarcinoma*. Nature Communications, 2015. 6(1): p. 6087.
40. **Tecalco-Cruz, A.C., D.G. Ríos-López, G. Vázquez-Victorio, R.E. Rosales-Alvarez, and M. Macías-Silva**, *Transcriptional cofactors Ski and SnoN are major regulators of the TGF- $\beta$ /Smad signaling pathway in health and disease*. Signal Transduction and Targeted Therapy, 2018. 3(1): p. 1-15.

41. **Burkhard, P., J. Stetefeld, and S.V. Strelkov**, *Coiled coils: a highly versatile protein folding motif*. Trends in cell biology, 2001. 11(2): p. 82-88.
42. **Levine, K.M., K. Ding, L. Chen, and S. Oesterreich**, *FGFR4: A promising therapeutic target for breast cancer and other solid tumours*. Pharmacology & Therapeutics, 2020: p. 107590.
43. **Meijer, D., A.M. Sieuwerts, M.P. Look, T. Van Agthoven, J.A. Foekens, and L.C.J. Dorssers**, *Fibroblast growth factor receptor 4 predicts failure on tamoxifen therapy in patients with recurrent breast cancer*. Endocrine-Related Cancer, 2008. 15(1): p. 101-111.
44. **Cejalvo, J.M., E.M. de Dueñas, P. Galván, S. García-Recio, O.B. Gasión, L. Paré, S. Antolin, R. Martinello, I. Blancas, and B. Adamo**, *Intrinsic subtypes and gene expression profiles in primary and metastatic breast cancer*. Cancer research, 2017. 77(9): p. 2213-2221.

**THIS PAGE HAS BEEN INTENTIONALLY LEFT BLANK**



---

## **CHAPTER 5**

### **THE FGFR4 SIGNALLING NETWORK AND MECHANISMS OF RESISTANCE TO ANTI- FGFR4 THERAPY**

---

# Chapter 5: The FGFR4 signalling network and mechanisms of resistance to anti-FGFR4 therapy

5.1 Background .....	168
5.2 Results .....	170
5.2.1 The selective FGFR4 inhibitor BLU9931 inhibits FGFR4 downstream signalling and proliferation of MDA-MB-453 cells.....	170
5.2.2 Upregulated RTKs in BLU9931-resistant MDA-MB-453 cells.....	180
5.2.3 A selective FGFR4 inhibitor H3B-6527 inhibits FGFR4 downstream signalling and proliferation of Hep3B cells .....	189
5.2.4 Upregulated RTKs in H3B-6527-resistant Hep3B cells.....	193
5.3 Discussion .....	198
5.4 Conclusion.....	199
5.5 Future direction .....	200
5.6 References .....	201

## 5.1 Background

Based on a pan-cancer TCGA analysis, breast cancer is among the top cancers affected by FGFR4 overexpression [1] and the overexpression of FGFR4 represents a potential therapeutic target in many cancer types including breast cancer [2-4]. The overexpression at the RNA level, overexpression of FGF19 (a ligand specific to FGFR4) and a FGFR4 single nucleotide polymorphism (SNP) G388R are frequently detected in many tumours. Like other FGFR members, aberrant FGFR4 activation is associated with cancer progression and its knockdown or inhibition decreases tumour growth and metastasis in *in vitro* and *in vivo* models [5-7]. FGFR4 amplification is rarely reported as its oncogenic activation is often linked to mutation or ligand amplification [8]. Our group previously reported high FGFR4 expression and phosphorylation in a TNBC cell line, MDA-MB-453 [9]. These cells harbour an activating mutation Y367C in FGFR4 that causes constitutive activation of downstream signalling to ERK and increased proliferation [2]. The inhibition of FGFR4 Y367C by siRNA silencing in MDA-MB-453 cells resulted in a 50% reduction of FGFR4 protein and MAPK signalling, however these cells developed resistance to a FGFR4 antagonistic monoclonal antibody, 10F10 [2]. Hence, there is growing evidence from breast cancer studies implicating the role of FGFR4 in oncogenesis and tumour progression [7, 10].

Among the FGFR family, FGFR4 share the least homology with the other FGFR members [11]. FGFR4 has a unique cysteine residue (Cys552) within the ATP binding pocket [12], which enabled the development of specific FGFR4 inhibitors. Most FGFR1-3 small molecule inhibitors have lower affinity to FGFR4 [8], which makes specific targeting of FGFR4 in FGFR4-driven cancers a challenge. Additionally, the application of pan-FGFR inhibitors to target FGFR4 are restricted by the on-target FGFR1-3 dose-limiting toxicities and off-target VEGFR blockage [13, 14]. Currently, the therapeutic evaluation of FGFR4 inhibitors such as BLU9931 and H3B-6527 in cancer models and patients are underway. BLU9931 is a potent and irreversible small molecule inhibitor of FGFR4 that showed significant anti-tumour activity in breast cancer and hepatocellular carcinoma (HCC) overexpressing FGF19 [5, 7]. H3B-6527 is a highly selective and covalent FGFR4 inhibitor generated for FGF19-driven HCC to overcome potential dose limiting toxicity of pan-FGFR inhibitors [15]. H3B-6527 is

currently under evaluation in a phase 1 clinical trial for HCC patients with high FGF19 (NCT02834780). However, the kinetic evaluation of H3B-6527 in a HCC cell line Hep3B, has demonstrated recovery of FGFR4 downstream protein ERK [15]. This perturbation of ERK signalling implies rewiring of the FGFR4 signalling network, which can limit the efficacy of the targeted therapy. Consequently, this initiated the approach of utilising combination therapy against cancers that would likely develop resistance to anti-FGFR4 therapy. In invasive lobular breast carcinoma cells, co-targeting FGFR4 and ER resulted in synergistic decrease in cell growth [16]. These results suggest that combination therapy approaches may be a more effective therapeutic strategy in inhibiting cancer progression and overcoming the resistance to anti-FGFR4 therapy.

The occurrence of gatekeeper mutations poses another challenge for FGFR4 inhibition efficacy. Gatekeeper mutations are non-synonymous mutations that modulate the accessibility of the inhibitor to the ATP-binding domain of a kinase [8]. Gatekeeper mutations V561M in FGFR1, N550K/H in FGFR2 and V555M in FGFR3 induce resistance to anti-FGFR inhibitors *in vitro* [17-19]. Particularly in FGFR4, the gatekeeper mutation V550M/L mediated resistance to a FGFR4 inhibitor Fisogatinib both *in vitro* and *in vivo* in HCC [10]. The significance of FGFR gatekeeper mutations is that studies have implicated its occurrence as the primary form of resistance to anti-FGFR therapy [17, 18, 20], hence it is important to identify potential gatekeeper mutations that may reduce the efficacy of FGFR inhibitors in cancer.

FGFR4 is activated by FGF19, and the aberration of the FGF19-FGFR4 signalling pathway was reported in cancers, including breast cancer, HCC and prostate cancer [7, 15, 21]. HCC has the fourth highest mortality rate and globally is the sixth most common cancer type [22]. It is also the most common form of primary liver cancer in adults [23]. A multi-kinase inhibitor, Sorafenib is currently used as the standard therapy for advanced HCC patients [24]. Despite improvements in therapeutic strategies, the overall patient survival rate and response rate are still low [15]. Complete remission has yet to be achieved and the molecular mechanism underlying resistance to Sorafenib remains unknown [24]. HCC genomic studies have described focal amplification of chromosome 11q13.3 that contains the gene encoding for FGF19 [15]. Furthermore, high FGF19 gene amplification is positively associated with poor

prognosis and progression of HCC [25]. Constitutive FGFR4 signalling can lead to neoplastic progression and uncontrolled proliferation in HCC tumours that overexpress FGF19 [26].

These findings indicate that aberrant FGF19-FGFR4 signalling is responsible in driving cancer cell proliferation, metastasis and resistance to apoptosis, consequently highlighting this pathway as an attractive therapeutic target in HCC [25, 27].

In this chapter, cancer cell lines MDA-MB-453 (TNBC) and Hep3B (HCC), and FGFR4 inhibitors BLU9931 and H3B-6527 were utilised to assess how network rewiring impacts sensitivity to the drugs. FGFR4 inhibitor-resistant cells were generated by culturing cells at low density in the presence of drug until resistant colonies formed. The resistant cancer cells were characterised using RTK assays and the activity of upregulated RTKs suppressed to discover novel therapeutic combinations. These investigations aim to identify novel drug combinations as improved strategies for targeted therapy.

## **5.2 Results**

### **5.2.1 The selective FGFR4 inhibitor BLU9931 inhibits FGFR4 downstream signalling and proliferation of MDA-MB-453 cells**

To determine the effects of the selective and irreversible FGFR4 inhibitor BLU9931 on FGFR4 downstream signalling and proliferation in TNBC, the MDA-MB-453 cell line that exhibits high FGFR4 expression and phosphorylation was used in this analysis. The MDA-MB-468 cell line with no detected FGFRs was used as a negative control. The kinetics of BLU9931 treatment was evaluated to also identify the short-term mechanisms of resistance to anti-FGFR4 therapy. MDA-MB-453 TNBC cells were treated with the FGFR4 inhibitor BLU9931 and demonstrated a significant decrease in downstream signalling proteins pFRS2, pERK and pAKT after 1 h at concentrations of 3 nM and higher (Fig. 5.1). Total FGFR4 expression was not affected by BLU9931, but the treatment decreased pFGFR at concentrations of 3 nM onwards (Fig. 5.1). BLU9931 also significantly decreased cell proliferation of MDA-MB-453 cells at 10 nM from day 3 onwards compared to DMSO control and did not affect the negative FGFR control TNBC cell line MDA-MB-468 (Fig. 5.2).

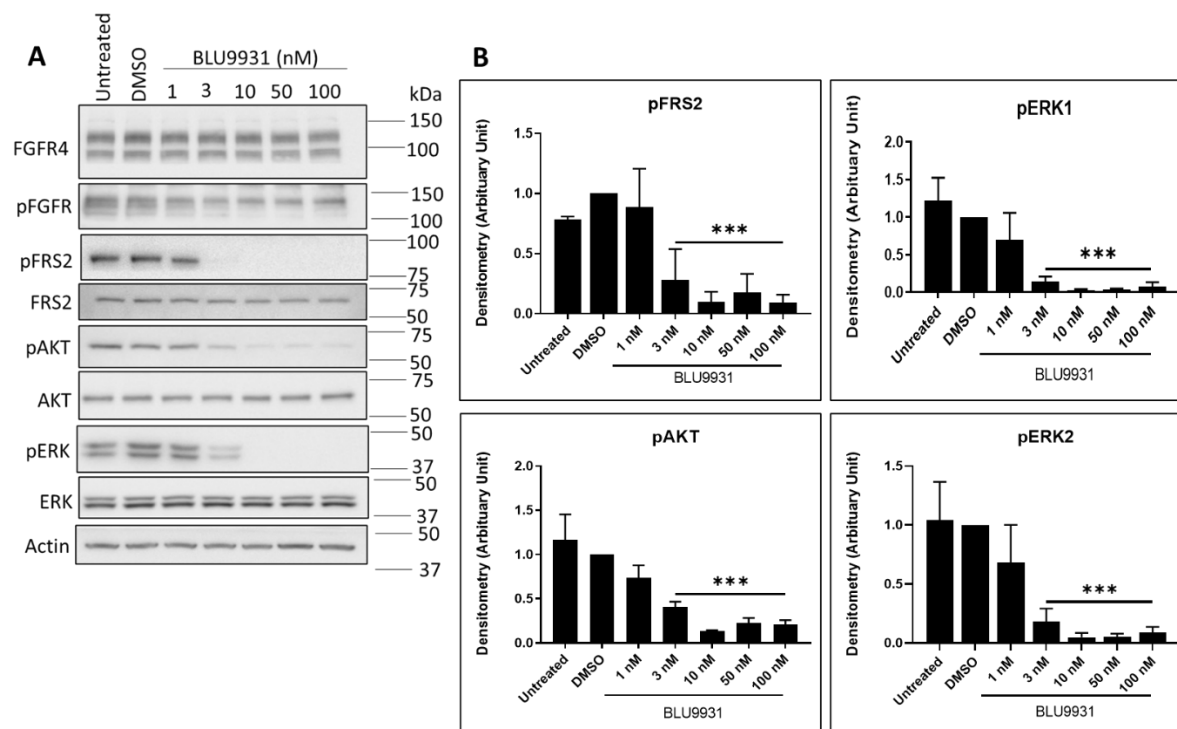


**Figure 5.1: Dose dependent effect of the FGFR4 inhibitor BLU9931 on FGFR4 downstream signalling pathways in the MDA-MB-453 cell line.** **a**, Expression and activation of downstream signalling proteins 1 h post-treatment with the indicated doses of BLU9931. **b**, Quantification by densitometry of (a). Data were first normalised relative to the tubulin control, then phosphorylated proteins were normalised to total protein, finally data were expressed relative to DMSO control which was arbitrarily set at 1.0. Error bars: mean  $\pm$  standard error of three biological replicates. \*\*\* indicates p-value of  $< 0.001$ , comparing individual BLU9931 concentrations to the DMSO vehicle control.

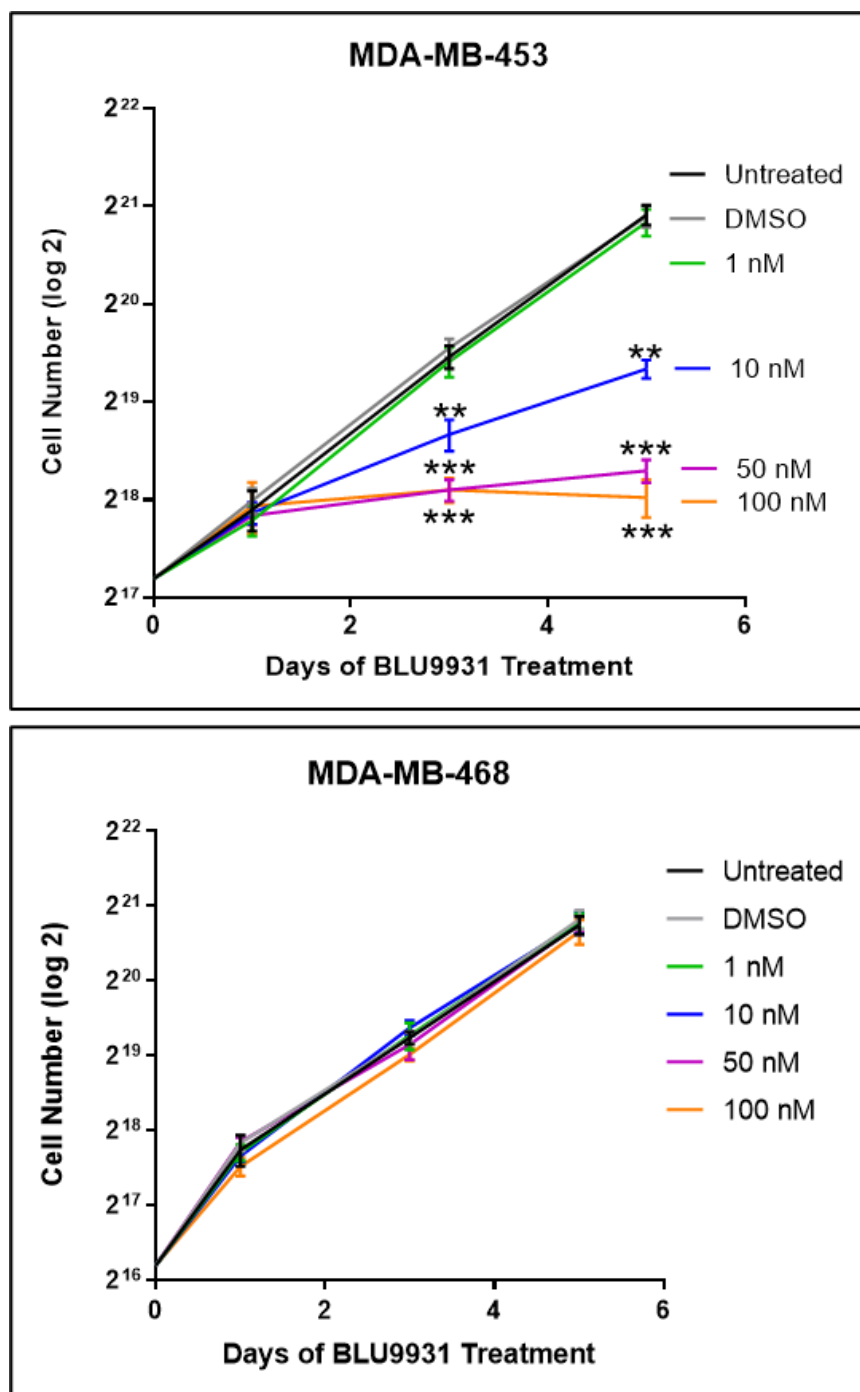


**Figure 5.2: Effect of BLU9931 on proliferation in MDA-MB-453 and MDA-MB-468 cell lines.** Cell proliferation was determined by direct cell counting. Error bars: mean  $\pm$  standard error of three biological replicates. \*\* indicates p-value of  $< 0.01$  and \*\*\*  $< 0.001$  compared to the DMSO vehicle control.

The kinetics of FGFR4 inhibition was evaluated by subjecting MDA-MB-453 cells to 10 nM of BLU9931 for 1, 4, 8 and 24 h (Fig. 5.3). The activity of pFRS2 and pERK was initially decreased, followed by some signal recovery at 24 h, possibly due to pathway rewiring (Fig. 5.3). Moreover, pAKT levels decreased after 1 h of 10 nM BLU9931 treatment but the signal recovered at 4 h and then increased at 8 h and 24 h relative to the DMSO vehicle control (Fig. 5.3). This suggests that the FGFR4 signalling network is being rewired following the inhibitor treatment, likely due to loss of negative feedback mechanisms. To identify if the ‘bounce-back’ of pAKT is independent of the inhibitor used, MDA-MB-453 cells were treated with another FGFR4 inhibitor, H3B-6527 and this resulted in the same pAKT ‘bounce-back’ effect at the same time points (Fig. 5.4). This suggests a general phenomenon following FGFR4 inhibition in MDA-MB-453 cells.



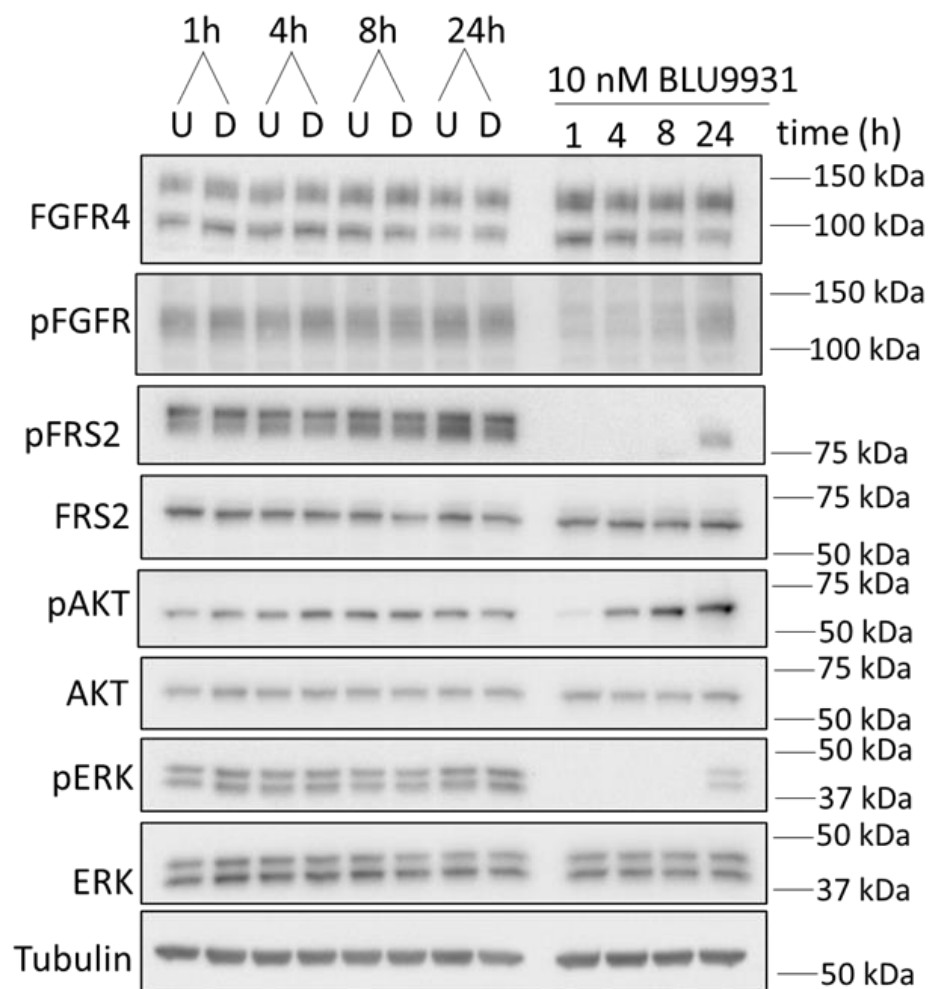


**Figure 5.3: Time course analysis of 10 nM FGFR4 inhibitor BLU9931 on FGFR4 downstream signalling pathways in the MDA-MB-453 cell line.** Expression and activation of downstream signalling proteins 1, 4, 8 and 24 h post-treatment with 10 nM of BLU9931. U indicates untreated control, D indicates DMSO vehicle control. Representative of three biological replicates.

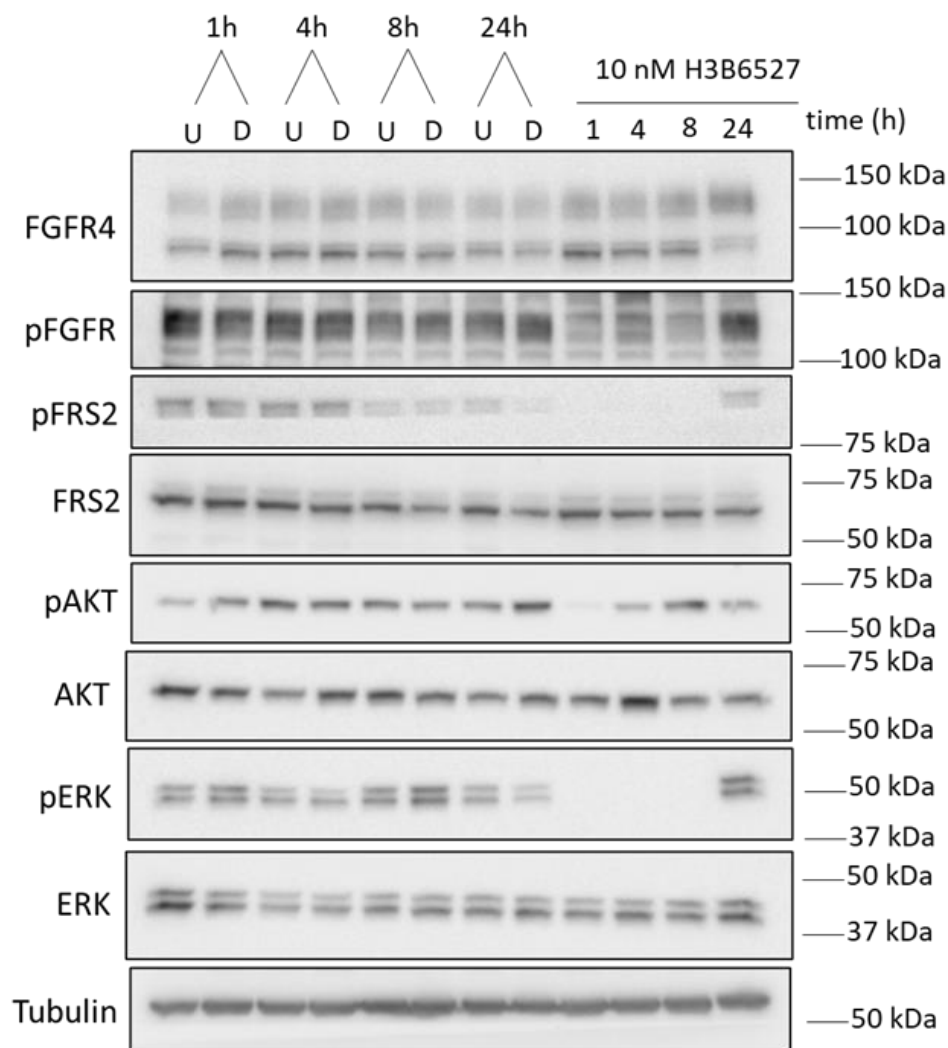


**Figure 5.4: Time course analysis of 10 nM FGFR4 inhibitor H3B-6527 on FGFR4 downstream signalling pathways in the MDA-MB-453 cell line.** a, Expression and activation of downstream signalling proteins 1, 4, 8 and 24 h post-treatment with 10 nM of H3B-6527. U indicates untreated control, D indicates DMSO vehicle control. Representative of three biological replicates.

The marked recovery of pAKT in MDA-MB-453 cells after BLU9931 (and similarly H3B-6527) treatment suggest pathway rewiring to compensate the FGFR4 inhibition. To determine if these cells by-pass the inhibition by using the PI3K/AKT signalling pathway through other means (e.g., upregulation of other RTKs) or solely via increased AKT activation, PI3K inhibitors and an AKT inhibitor were used.

To suppress the activity of AKT in MDA-MB-453 cells, cells were treated with PI3K- $\alpha$  inhibitor BYL719, pan-PI3K inhibitor BKM120 or AKT inhibitor MK2206 for 1 h with the indicated concentrations (Fig. 5.5). These results allow selection of specific concentrations of each inhibitor to use in combination with BLU9931 (Fig. 5.6-5.7). MDA-MB-453 cells were treated with single treatment of the BLU9931 and PI3K inhibitors (BYL719 or BKM120) or in combination with increasing concentrations for 1 and 24 h (Fig. 5.6). Compared to the 1 h DMSO vehicle control, BLU9931, BYL719 and 500 nM BKM120 single treatments for 1 h decreased pAKT, while all the combination treatments completely suppressed pAKT levels after 1 h (Fig. 5.6). However, the pAKT signal recovered after 24 h in all the treatment conditions except in the single BLU9931 treatment that showed increased pAKT levels compared to the 1 h DMSO control (Fig. 5.6). The pAKT signal recovery in the combination treatments is less than in the BLU9931 single treatment, but similar to the PI3K inhibitors single treatment (Fig. 5.6).

On the other hand, MDA-MB-453 cells that were treated with the BLU9931 with AKT inhibitor MK2206 combination successfully suppressed pAKT at 24 h compared to the DMSO control (Fig. 5.7). The single treatment of MK2206 also suppressed pAKT compared to the BLU9931 single treatment at 4 h (Fig. 5.7). The suppression of pAKT is expected using MK2206 because AKT is inhibited directly, unlike the PI3K inhibitors, which inhibits PI3K upstream of AKT. In terms of proliferation, single treatment of the PI3K inhibitors BYL719 and BKM120, and AKT inhibitor MK2206 significantly decreased proliferation of MDA-MB-453 cells compared to the DMSO control (Fig. 5.8). However, only the BLU9931 with MK2206 combination treatment had a more robust effect on cell proliferation than either agent alone (Fig. 5.8). This was not observed in the BLU9931 with PI3K combination treatments, and their combination exhibited a similar effect to single inhibitor treatment (Fig. 5.8). These results suggest that the efficacy of BLU9931 is limited by the ‘bounce-back’ of AKT and could not be blocked with either PI3K inhibitors. However, the AKT inhibitor is able to completely abolish the AKT activation including the ‘bounce-back’. The combination of BLU9931 with MK2206 gives an additive effect because the former inhibits other signalling pathways, (e.g. the ERK signalling pathway), while the latter inhibits AKT. Therefore, both inhibitors contribute to a significant decrease in MDA-MB-453 cell proliferation.

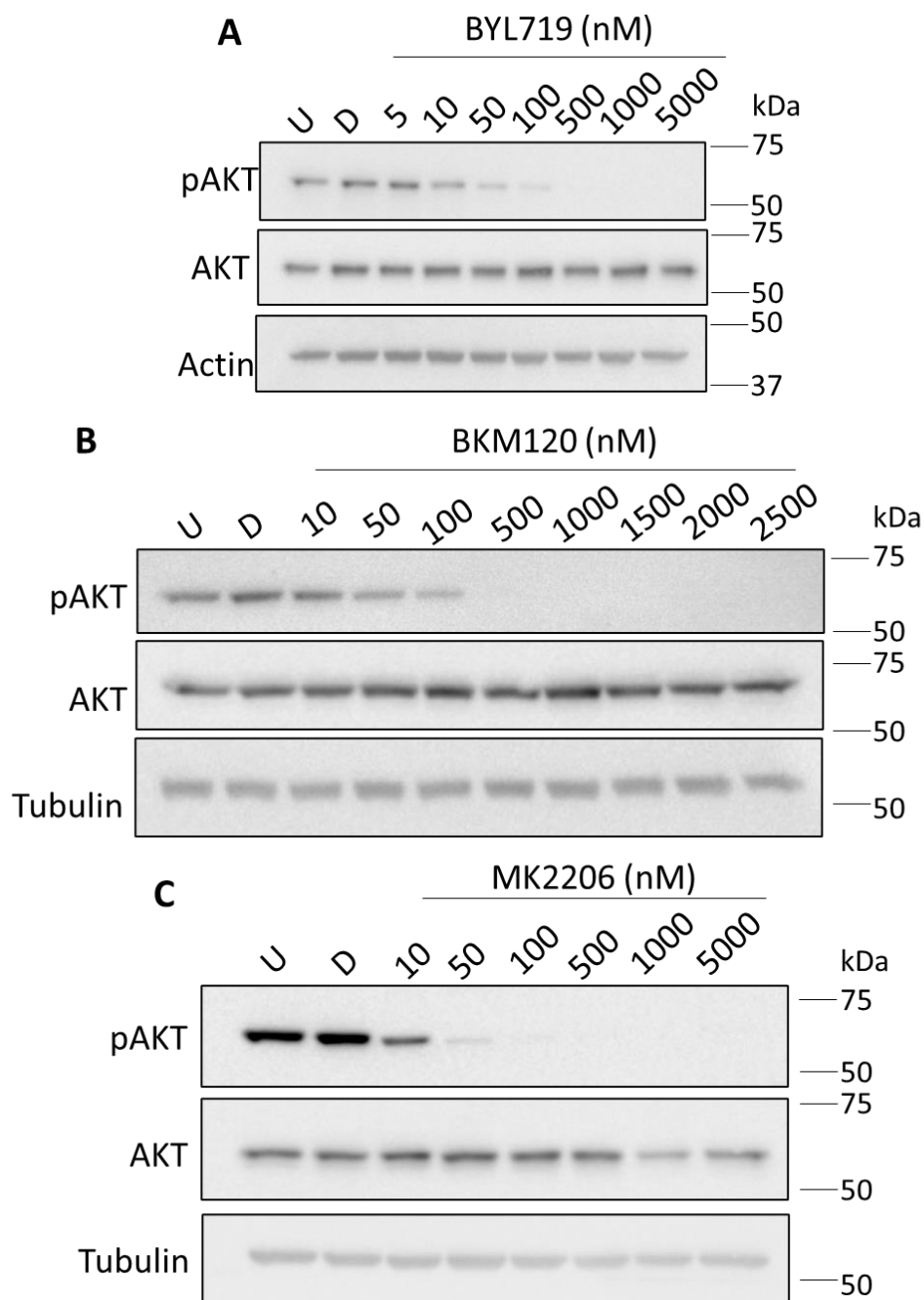


**Figure 5.5: Dose dependent effect of PI3K- $\alpha$  inhibitor BYL719, pan-PI3K inhibitor BKM120 and AKT inhibitor MK2206 on AKT phosphorylation in the MDA-MB-453 cell line.** Expression and activation of AKT after 1 h treatment with the indicated inhibitors. U indicates untreated control, D indicates DMSO vehicle control. Representative of three biological replicates.

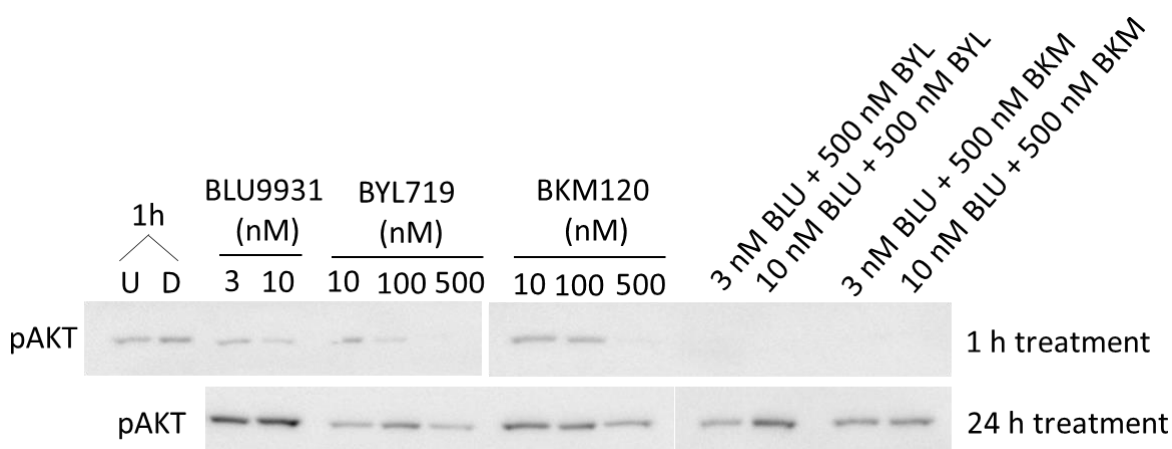


**Figure 5.6: Dose dependent effect of the FGFR4 inhibitor BLU9931 in combination with PI3K- $\alpha$  inhibitor BYL719 or pan-PI3K inhibitor BKM120 on AKT phosphorylation in the MDA-MB-453 cell line.** Activation of AKT 1 h and 24 h post-treatment with the indicated doses of single or combination treatment using BLU9931, BYL719 and BKM120. U indicates untreated control, D indicates DMSO vehicle control. Representative of two biological replicates.

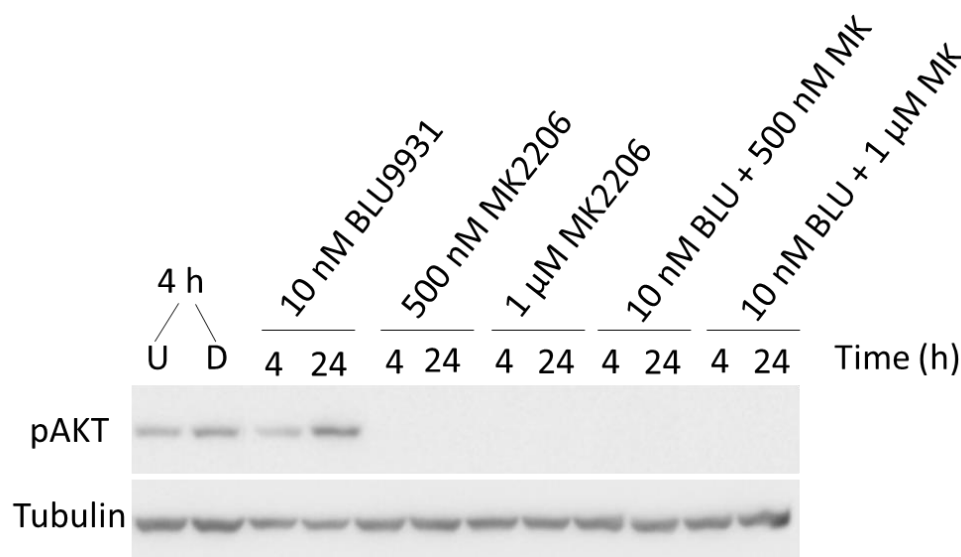


**Figure 5.7: Dose dependent effect of the FGFR4 inhibitor BLU9931 and AKT inhibitor MK2206 on AKT phosphorylation in the MDA-MB-453 cell line.** Activation of AKT 4 and 24 h post-treatment with the indicated doses of single or combination treatment using BLU9931 and MK2206. U indicates untreated control, D indicates DMSO vehicle control. Representative of two biological replicates.

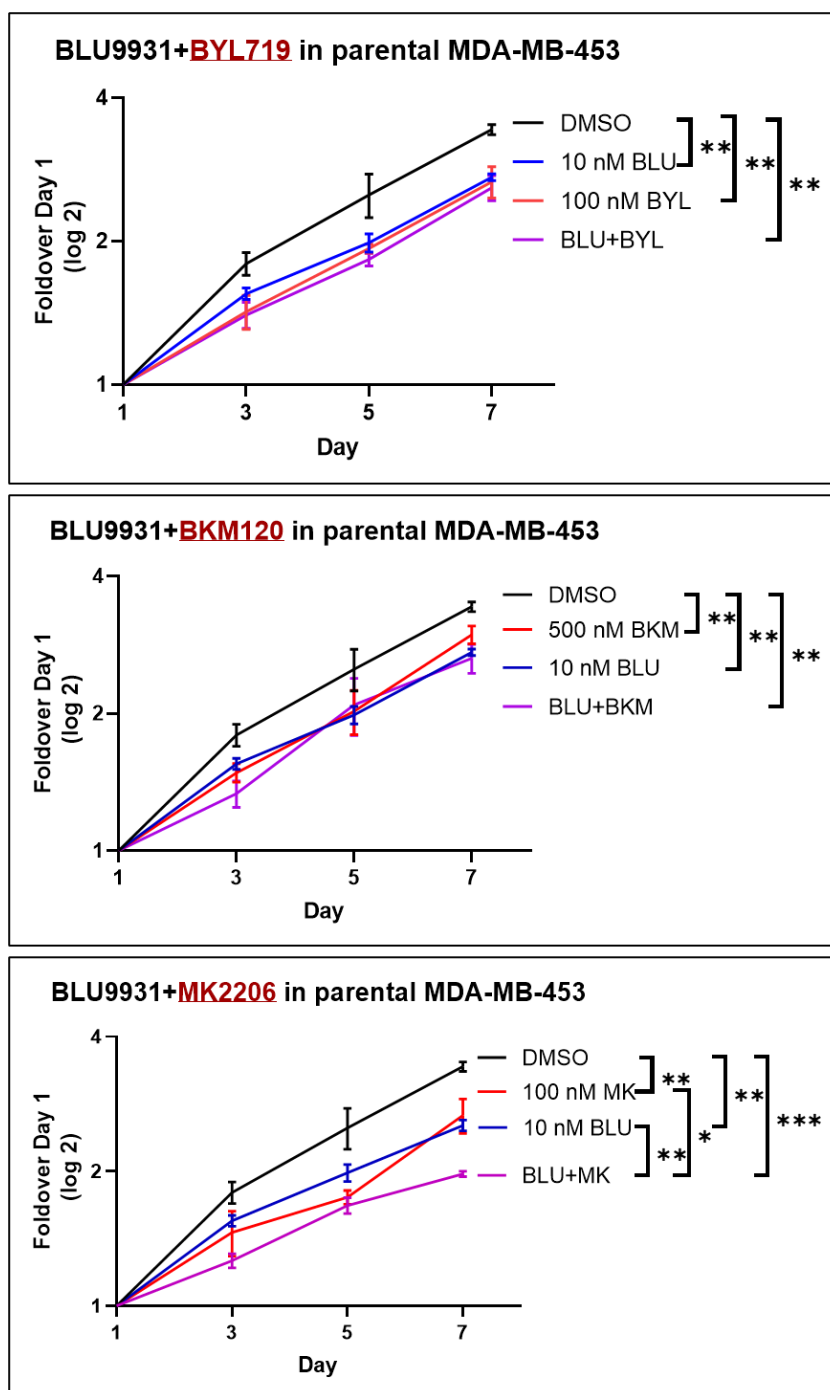


**Figure 5.8: Effect of FGFR4 inhibitor BLU9931, in combination with PI3K- $\alpha$  inhibitor BYL719, pan-PI3K inhibitor BKM120 or AKT inhibitor MK2206 in parental MDA-MB-453 cells.** Parental MDA-MB-453 cells were subjected to single inhibitor treatment or in combination as indicated. Cell proliferation was determined by MTS assay. Error bars: mean  $\pm$  standard error of four biological replicates. \* indicates p-value of  $< 0.05$ , \*\*  $< 0.01$ , \*\*\*  $< 0.001$ .

### **5.2.2 Upregulated RTKs in BLU9931-resistant MDA-MB-453 cells**

The previous section investigated the short-term remodelling of the FGFR4 network after anti-FGFR4 treatment. In this section, MDA-MB-453 cells were exposed long-term to BLU9931 treatment and resistant cells were isolated, to identify novel upregulations in long-term signalling network remodelling. This approach aimed to also evaluate potential targets for novel therapeutic combinations.

In short, parental MDA-MB-453 cells were cultured at low density and treated with DMSO (vehicle control), 10 nM or 100 nM of BLU9931 for at least 5 months, until visible resistant colonies formed. The resistant colonies were then isolated and cultured in the presence of their respective treatments. Then, the upregulated RTKs in the long-term DMSO or BLU9931 cells were characterised using a proteome profiler human phospho-RTK assay kit, a membrane-based antibody array for the parallel determination of the relative phosphorylation of human RTKs (Fig. 5.10). The two purposes of including the long-term DMSO control group are, to confirm that the long-term exposure of DMSO does not affect the cells compared to parental cells, and to confirm that the upregulated RTKs detected in the long-term BLU9931 treatment groups solely result from FGFR4 inhibition and not ‘drift’ of cell phenotype.

To examine if the long-term BLU9931 cells were resistant to BLU9931, drug treatment analysis on cell proliferation was performed by comparing DMSO- and BLU9931-treated parental cells with the long-term DMSO or BLU9931 cells (Fig. 5.9). There is a significant difference between the DMSO- and 10 nM BLU9931-treated parental cells, but not between the long-term DMSO and BLU9931 cells. The proliferation of the long-term 10 nM BLU9931 cells were also significantly greater than the parental cells treated with 10 nM BLU9931, which indicates that the long-term 10 nM BLU9931 is resistant to BLU9931. In the 100 nM BLU9931 treatment group, a significant difference was observed between the DMSO- and 100 nM BLU9931-treated parental cells, and between the long-term DMSO and 100 nM BLU9931 cells. However, the proliferation of the long-term 100 nM BLU9931 cells was significantly greater than the parental cells treated with 100 nM BLU9931. Altogether these results indicate

that the long-term 100 nM BLU9931 is relatively resistant to BLU9931 compared to the parental cells, but not completely resistant like the long-term 10 nM BLU9931 cells.

Next, the upregulated RTKs in the long-term cells were identified using a proteome profiler phospho-RTK kit. Parental cells treated with DMSO or BLU9931 for 24 h were also interrogated in the analysis for comparison to determine if the upregulation detected in the long-term group also occurs in the short-term setting. The proteome profiler phospho-RTK kit identified upregulation of phosphorylated ALK, ErbB2, ErbB3, IR and IGF-1R in the parental cell after 24 h BLU9931 treatment and in the long-term BLU9931 cells (Fig. 5.10-5.11). FGFR4 phosphorylation was also decreased in the long-term BLU9931 cells and in the parental cells treated with 100 nM BLU9931, but was slightly higher in the latter following 10 nM BLU9931 treatment (Fig. 5.10-5.11).



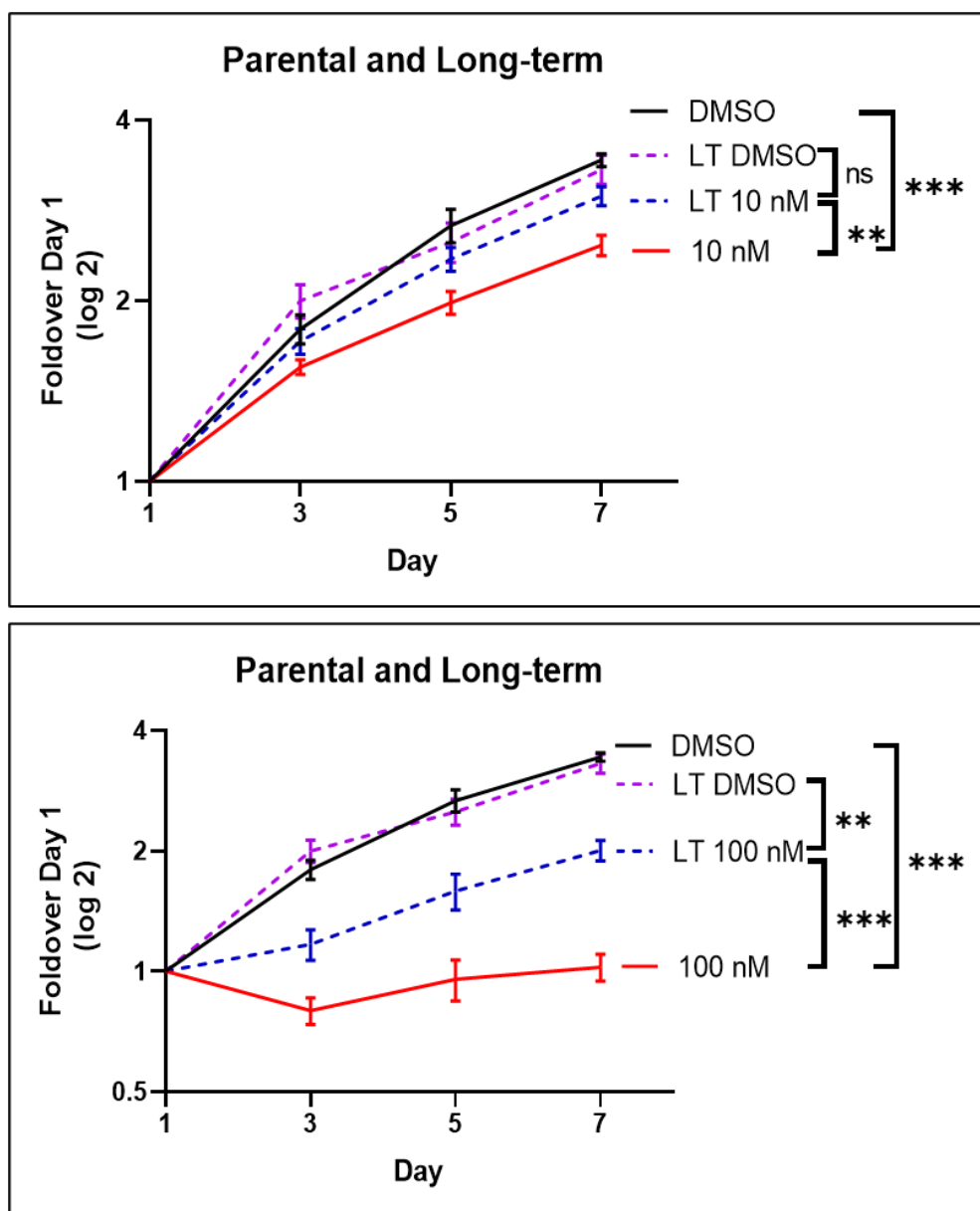


**Figure 5.9: Effect of BLU9931 on parental MDA-MB-453 and long-term BLU9931-treated MDA-MB-453 cells.** The proliferation of parental MDA-MB-453 cells treated with DMSO vehicle control, 10 nM or 100 nM BLU9931 were compared to long-term 10 nM or 100 nM BLU9931 MDA-MB-453 cells. Cell proliferation was determined by MTS assay. Solid lines indicate parental cells treated with DMSO or BLU9931. Dotted lines indicate the long-term DMSO or long-term BLU9931 cells. Error bars: mean  $\pm$  standard error of six biological replicates. \*\* indicates p-value of  $< 0.01$ , \*\*\*  $< 0.001$ . NS indicates not significant.

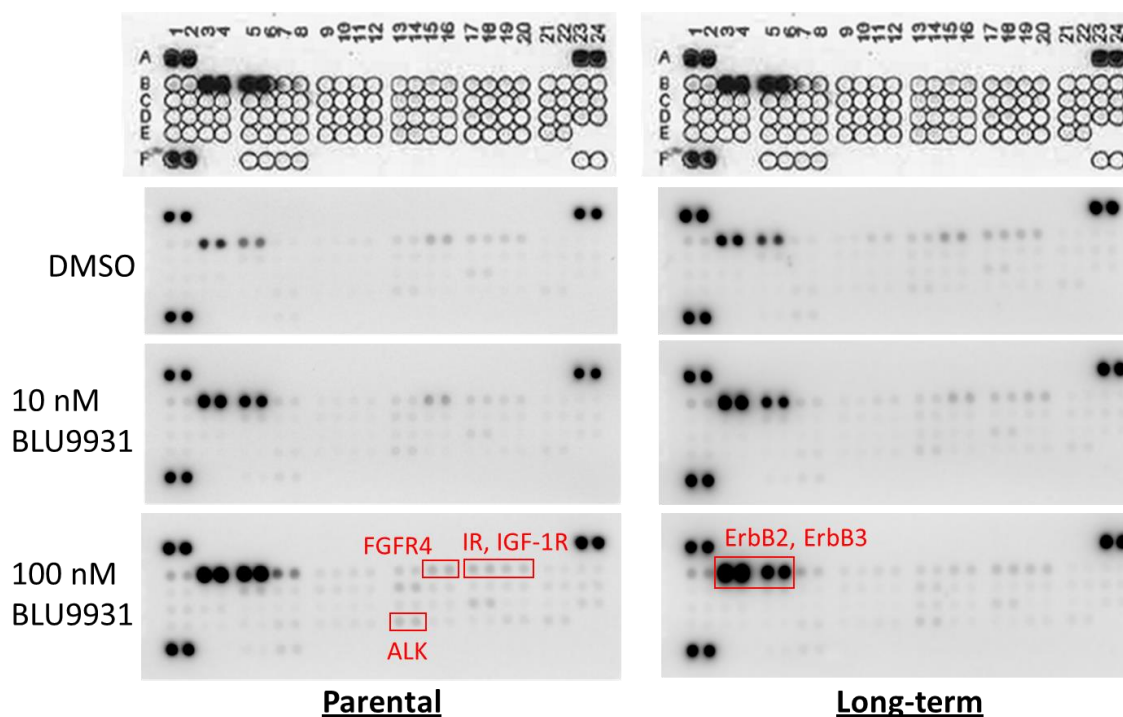


**Figure 5.10: Identification of upregulated RTKs in parental MDA-MB-453 after 24 h BLU9931 treatment and in long-term BLU9931 MDA-MB-453 cells.** Upregulated RTKs were analysed using RTK array blotting kits. Membranes from the RTK array kits were pre-spotted with specific antibodies. The top blots are reference for the locations on the membrane as follows: reference spots (A1, A2), (A23, A24), (F1, F2); EGFR (B1, B2); ErbB2 (B3, B4); ErbB3 (B5, B6); ErbB4 (B7, B8); FGFR1 (B9, B10); FGFR2 $\alpha$  (B11, B12); FGFR3 (B13, B14); FGFR4 (B15, B16); Insulin-R (B17, B18); IGF-1R (B19, B20); Ax1 (B21, B22); Dtk (B23, B24); Mer (C1, C2); HGFR (C3, C4); MSPR (C5, C6); PDGFR $\alpha$  (C7, C8); PDGFR $\beta$  (C9, C10); SCFR (C11, C12); Flt-3 (C13, C14); M-CSFR (C15, C16); c-Ret (C17, C18); ROR1 (C19, C20); ROR2 (C21, C22); Tie-1 (C23, C24); Tie-2 (D1, D2); TrkA (D3, D4); TrkB (D5, D6); TrkC (D7, D8); VEGFR1 (D9, D10); VEGFR2 (D11, D12); VEGFR3 (D13, D14); MuSK (D15, D16); EphA1 (D17, D18); EphA2 (D19, D20); EphA3 (D21,22) EphA4 (D23, D24); EphA6 (E1, EE2); EphA7 (E3, E4); EphB1 (E5, E6); EphB2 (E7, E8); EphB4 (E9, E10); EphB6 (E11, E12); ALK (E13, E14); DDR1 (E15, E16); DDR2 (E17, E18); EphA5 (E19, E20); EphA10 (E21, E22); EphB3 (F5, F6); RYK (F7, F8); negative control (F23, F24). Parental MDA-MB-453 cells (left panels) were treated with the indicated treatment for 24 h, while the long-term MDA-MB-453 cells (right panels) were seeded in their respective conditions for 24 h before harvesting.

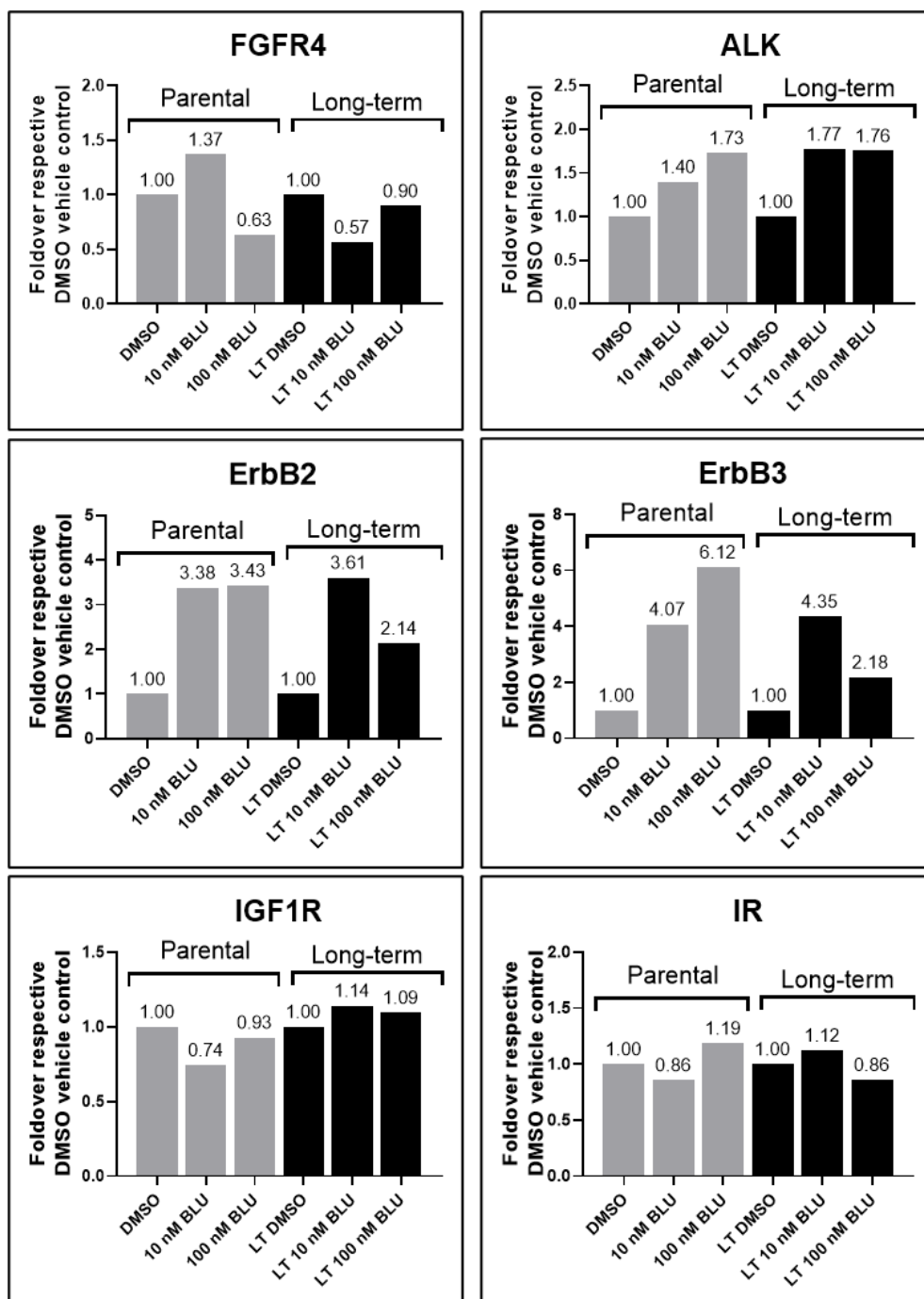


**Figure 5.11: Identification of upregulated RTKs in parental MDA-MB-453 cells after 24 h BLU9931 treatment and in long-term BLU9931 MDA-MB-453 cells.** Quantification by densitometry of Figure 10. Data were first normalised relative to the reference points, then data were expressed relative to the respective DMSO vehicle control which was arbitrarily set at 1.0.

To confirm the expression and phosphorylation of the detected upregulated candidates in the parental and long-term BLU9931 groups, these cells were subjected to immunoblotting with phosphospecific and total antibodies for specific receptors and downstream signalling proteins (Fig. 5.12), which gave additional site-selective information and insights into total expression levels. Parental cells were treated with DMSO control, 10 nM and 100 nM BLU9931 for 1 and 24 h, compared to the long-term DMSO and BLU9931 cells (Fig. 5.12). The results demonstrated similar upregulation of phosphorylated ALK, ErbB2, ErbB3, GSK3 $\alpha$ - $\beta$ , AKT, IGF-1R and IRS-1 in both parental cells after 24 h BLU9931 treatment and in the long-term BLU9931 cells compared to their respective controls (Fig. 5.12). There was also a decreased in pFRS2, pAKT and pERK after 1 h of BLU9931 treatment in the parental cells, but the pFRS2 and pERK signal recovered for the 10 nM BLU9931 treatment at 24 h while pAKT increased after 24 h for the 10 nM and 100 nM BLU9931 treatments. This pattern was also observed in the long-term BLU9931 cells. Uniquely in the long-term BLU9931 cells, phosphorylated GSK3 $\alpha$ - $\beta$  and Y1248 ErbB2 were higher and the expression of IGF-1R and IRS-1 were lower than in the parental cells after 24 h BLU9931 treatment and the long-term DMSO control (Fig. 5.12).

These results indicate that signalling pathway rewiring occurs within 24 h of BLU9931 treatment and is maintained in the long-term cells. There may also be additional mechanisms that the long-term BLU9931 cells adopted as observed in the increase of pGSK3 $\alpha$ - $\beta$  and pY1248 ErbB2. GSK3 regulates many intracellular signalling pathways and has dual roles in regulating cell death and mediating cell survival. The upregulation of pGSK3 $\alpha$ - $\beta$  in the long-term BLU9931 cells may provide a pro-survival advantage over the parental cells treated with BLU9931. Altogether, these results suggest that although the majority of the RTKs with enhanced activation in the long-term BLU9931 cells are also upregulated in the parental cells after 24 h of BLU9931 treatment, there are additional effects on receptor activation and downstream signalling that likely underpin long-term, marked resistance to BLU9931.

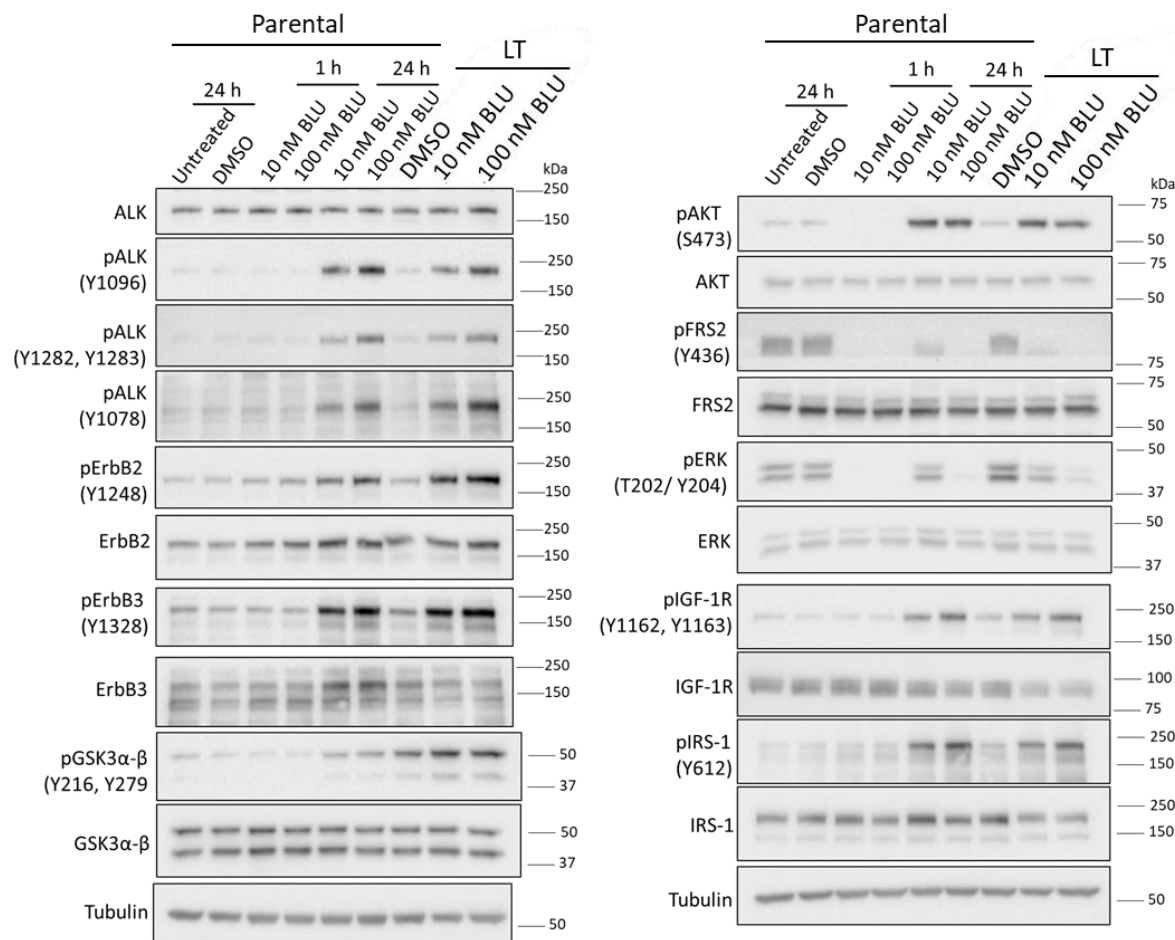


**Figure 5.12: Comparison of upregulated RTKs and downstream signalling in BLU9931-treated MDA-MB-453 parental cells and long-term BLU9931 cells.** Expression and activation of upregulated RTKs and FGFR4 downstream signalling proteins at 1 and 24 h post-treatment with the indicated BLU9931 concentrations in parental MDA-MB-453 cells. Long-term (LT) BLU9931 MDA-MB-453 cells were harvested 24 h post-seeding.

The upregulation of specific RTKs in the long-term BLU9931 cells provided potential insights into the mechanism of resistance to anti-FGFR4 therapy, and the upregulated RTKs represented potential targets for combination treatment. Since ErbB2 and ErbB3 showed the highest increase compared to their respective DMSO controls (Fig. 5.11), and ErbB2 pY1248 was aberrantly activated in the long-term cells (Fig. 5.12), these receptors represented potential therapeutic targets for combination treatment with BLU9931. Therefore, the ErbB2 inhibitor

Lapatinib was used in combination with BLU9931 to investigate the effect on cell proliferation in the long-term BLU9931 cells.

To suppress the activity of ErbB2, the long-term 10 nM and 100 nM BLU9931 MDA-MB-453 cells were treated with Lapatinib for 1 h with the indicated concentrations (Fig. 5.13). Lapatinib at 100 nM modestly inhibited pErbB2 in the long-term 10 nM BLU9931 cells but demonstrated significant inhibition of pErbB2 in the long-term 100 nM BLU9931 cells (Fig. 5.13). Considering the minimum effective dose and potential off-target effects at higher concentrations, 100 nM Lapatinib was selected to investigate the combination treatment effect on cell proliferation (Fig. 5.13). Lapatinib treatment alone had no effect on either parental or resistant cells. At 10 nM BLU9931, combination treatment with Lapatinib restored growth inhibition in the resistant cells that was not observed with BLU9931 alone, suggesting a by-pass mechanism. At 100 nM BLU9931, the combination treatment caused cell death in both parental and resistant cells and was sufficient to block the continued proliferation of the resistant cells in the presence of BLU9931 alone. These results suggest that though the parental cells exhibit similar RTKs upregulated 24 h post-BLU9931 treatment, the long-term BLU9931 cells may be more dependent on ErbB2 due to an established by-pass mechanism, as indicated by enhanced phosphorylation at Y1248.

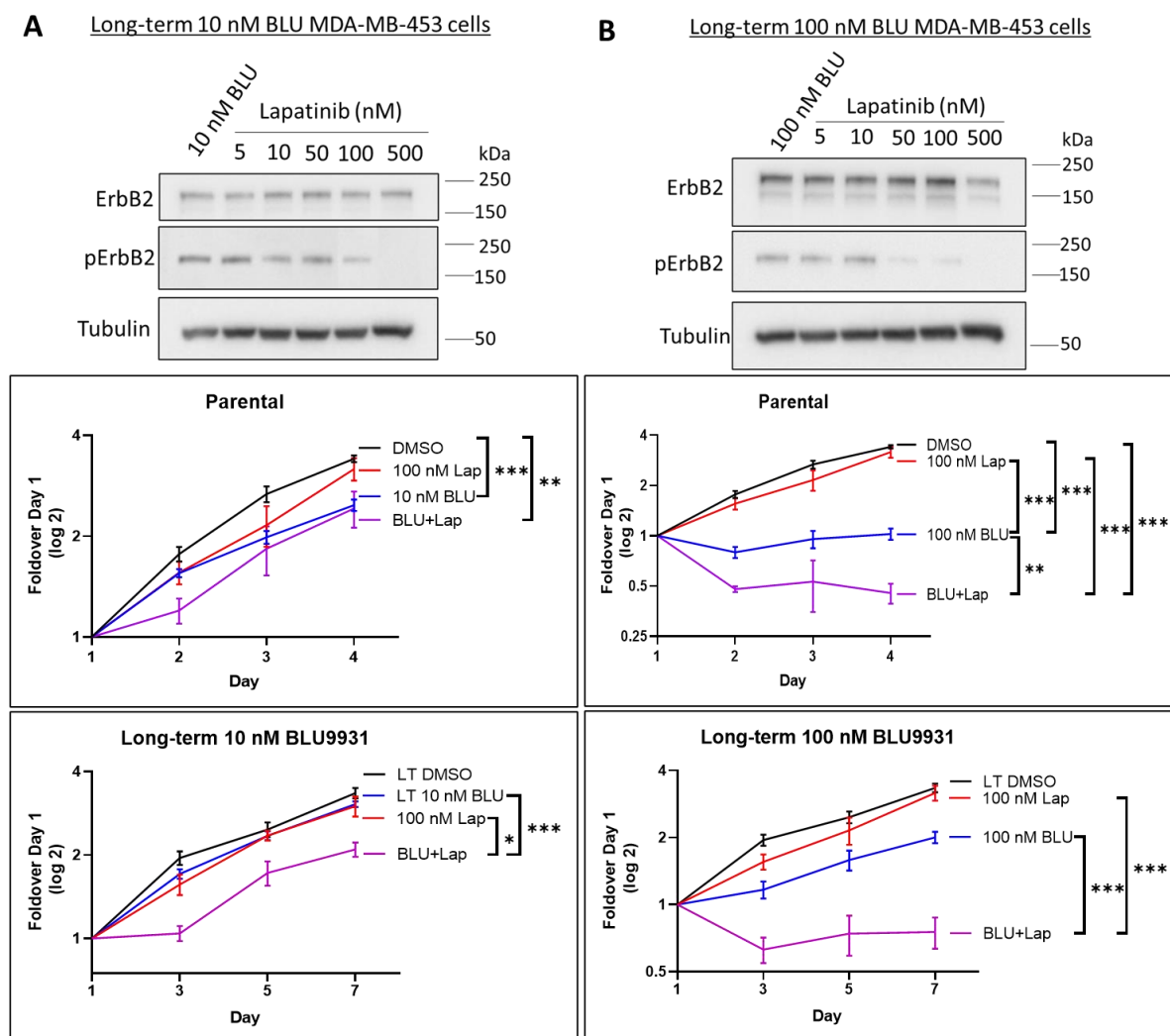


**Figure 5.13: Effect of co-targeting ErbB2 and FGFR4 on proliferation in long-term BLU9931 MDA-MB-453 cells using Lapatinib and BLU9931.** Dose dependent effect of Lapatinib on expression and activation of ErbB2 in **a**, long-term 10 nM or **b**, 100 nM BLU9931 cells. Long-term 10 nM or 100 nM BLU9931 cells were subjected to the single inhibitor treatment or combination treatment with 100 nM Lapatinib. Cell proliferation was determined by MTS assay. Error bars: mean  $\pm$  standard error of three biological replicates. \* indicates p-value of  $<0.05$ , \*\* $<0.01$ , \*\*\* $<0.001$ . Only significant differences are plotted.

### **5.2.3 A selective FGFR4 inhibitor H3B-6527 inhibits FGFR4 downstream signalling and proliferation of Hep3B cells**

The FGFR4 ligand, FGF19 is often amplified in HCC and high FGF19 gene amplification is positively associated with poor prognosis and progression of HCC [15]. H3B-6527 is a selective and covalent FGFR4 inhibitor that was recently developed to overcome dose limiting toxicities of pan-FGFR inhibitors for FGF19-driven HCC. The kinetic evaluation of H3B-6527 showed recovery of pERK levels after 8 h likely due to network rewiring [15]. To further investigate the mechanisms underlying anti-FGFR4 treatment rewiring, H3B-6527 and HCC cell line Hep3B were used to assess network rewiring and identify potential upregulated RTKs.

Hep3B cells were treated with the H3B-6527 and demonstrated a decrease in downstream signalling proteins pFRS2 and pERK after 1 h at concentrations of 5 nM and higher (Fig. 5.14a). Interestingly, AKT phosphorylation was not affected by H3B-6527 treatment in these cells. H3B-6527 also significantly decreased Hep3B cell proliferation at 5 nM at day 4 compared to DMSO control (Fig. 5.14b). The kinetic evaluation of H3B-6527 treatment on Hep3B cells showed partial recovery of pERK levels after 24 h (Fig. 5.15). This suggests that the FGFR4 signalling network in HCC is also rewired following inhibitor treatment, though the effect is less pronounced than in the TNBC cell line.



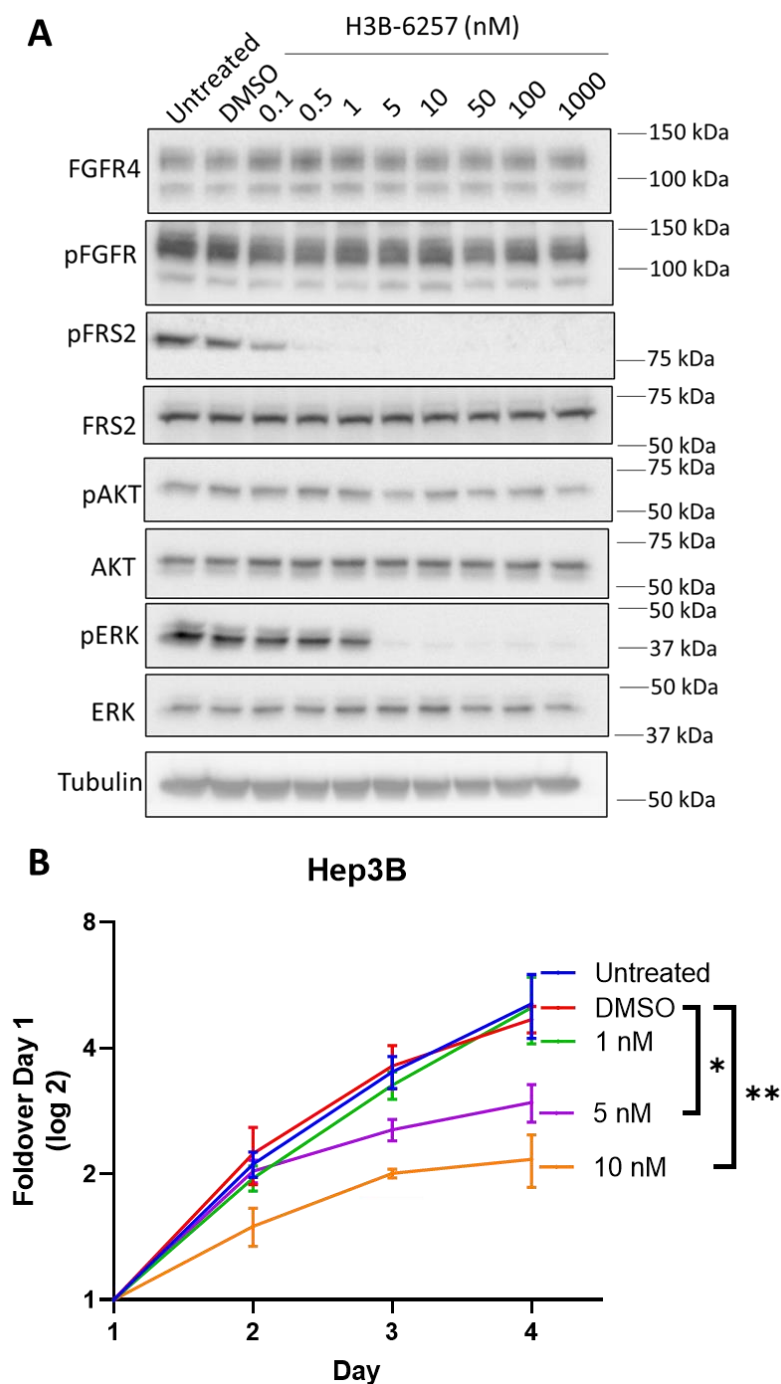


**Figure 5.14: Effect of the FGFR4 inhibitor H3B-6527 on FGFR4 downstream signalling and proliferation in the Hep3B cell line.** **a**, Expression and activation of downstream signalling proteins 1 h post-treatment with the indicated doses of H3B-6527. **b**, Effect of H3B-6527 on proliferation of Hep3B cells. Cell proliferation was indirectly assayed via a MTS absorbance assay. Error bars: mean  $\pm$  standard error of three biological replicates. \* indicates p-value of  $< 0.05$ , \*\*  $< 0.01$ .

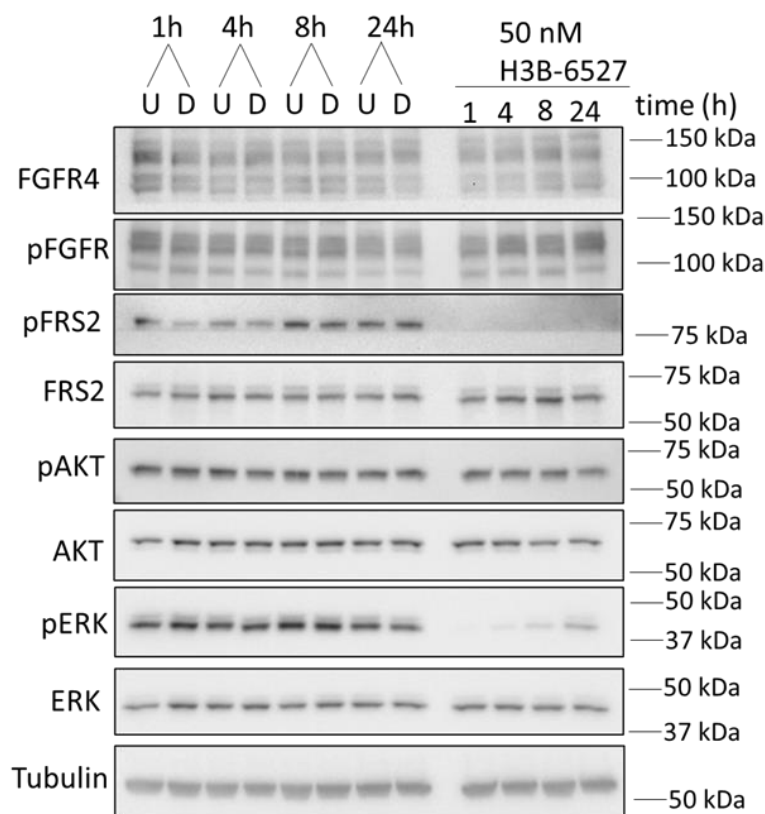


**Figure 5.15: Time course analysis of 50 nM FGFR4 inhibitor H3B-6527 on FGFR4 downstream signalling pathways in the Hep3B cell line.** Expression and activation of downstream signalling proteins 1, 4, 8 and 24 h post-treatment with 50 nM of H3B-6527. U indicates untreated control, D indicates DMSO vehicle control.

The partial signal recovery of pERK in Hep3B cells after H3B-6527 treatment suggest pathway rewiring. To determine if these cells by-pass FGFR4 inhibition by using the ERK signalling pathway, Trametinib, a MEK inhibitor that targets the MAPK signalling pathway upstream of ERK, was used to suppress the activity of ERK in Hep3B cells. Cells were treated with Trametinib for 1 h with the indicated concentrations (Fig. 5.16a). Trametinib decreased pERK at 5 nM upwards in Hep3B cells (Fig. 5.16a). Next, Hep3B cells were subjected to single or combination treatment using H3B-6527 and Trametinib (Fig. 5.16b). H3B-6527 and Trametinib single treatments significantly decreased Hep3B cell proliferation compared to DMSO control, while the combination had a significantly greater effect (Fig. 5.16b). This suggests that the efficacy of H3B-6527 is improved by blocking the ERK ‘bounce-back’ and highlights this combination treatment as a promising therapeutic treatment for HCC.

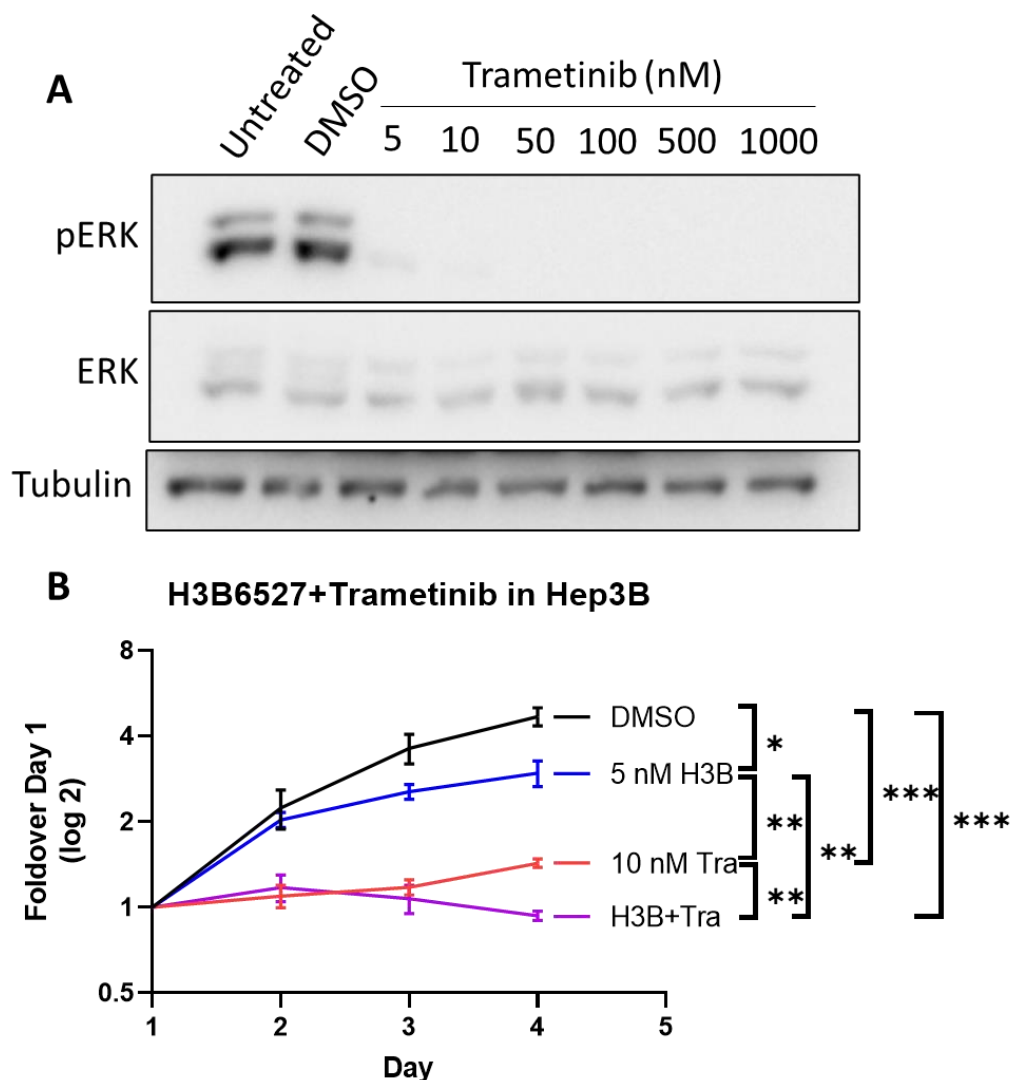


**Figure 5.16: Effect of FGFR4 inhibitor H3B-6527, in combination with MEK inhibitor Trametinib in parental Hep3B cells. a,** Dose dependent effect of MEK inhibitor Trametinib on ERK phosphorylation in the Hep3B cell line. Expression and activation of ERK after 1 h treatment with the indicated concentrations. **b,** Parental Hep3B cells were subjected to single inhibitor treatments or in combination as indicated. Cell proliferation was determined by MTS assay. Error bars: mean  $\pm$  standard error of four biological replicates. \* indicates p-value of  $< 0.05$ , \*\* $< 0.01$ , \*\*\*  $< 0.001$ .

### **5.2.4 Upregulated RTKs in H3B-6527-resistant Hep3B cells**

The partial signal recovery of ERK in the Hep3B was a result of short-term remodelling of the FGFR4 network after anti-FGFR4 treatment. As described in the previous section on TNBC, Hep3B cells were exposed long-term to H3B-6527 to identify novel upregulations in long-term signalling network remodelling.

H3B-6527-resistant Hep3B cells were generated using the same methodology as with the TNBC MDA-MB-453 cell line. Briefly, parental cells at low density were cultured in DMSO (vehicle control), 10 nM or 50 nM H3B-6527 for at least 5 months, until resistant colonies formed. Drug treatment analysis on cell proliferation demonstrate that these cells were relatively resistant to H3B-6527 compared to parental cells (Fig. 5.17). However, characterisation of the long-term H3B-6527 Hep3B cells using the RTK array blots showed small differences compared to the long-term DMSO vehicle control (Fig. 5.18). Only IGF-1R and IR phosphorylation were markedly increased in the parental Hep3B cells after H3B-6527 treatment (Fig. 5.19). However, the long-term H3B-6527 cells only exhibited modest (1.3-1.5 fold) increases in these receptors (Fig. 5.19). This suggests that the upregulation of IR and IGF-1R due to network rewiring occurs within 24 h of BLU9931 treatment but is not maintained in the long-term H3B-6527 cells. This suggests that the long-term H3B-6527 cells may be utilising additional mechanisms of resistance to FGFR4 inhibition, such as receptor mutation, loss of negative feedback loops, decrease of phosphatases or by-pass mechanisms of downstream signalling.

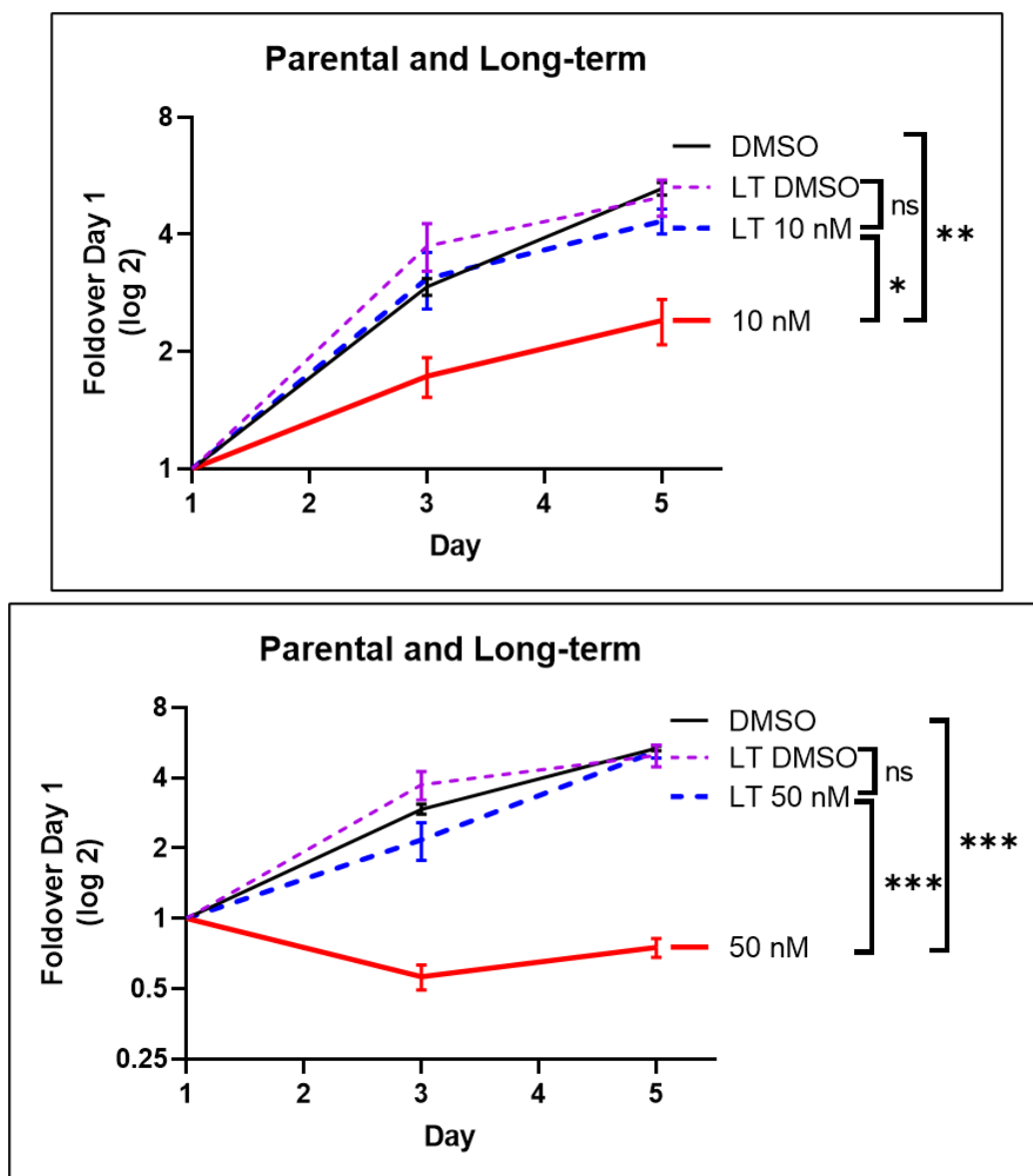


**Figure 5.17: Effect of H3B-6527 on parental Hep3B and long-term H3B-6527 Hep3B cells.** The proliferation of parental Hep3B cells treated with DMSO vehicle control, 10 nM or 50 nM H3B-6527 was compared to long-term 10 nM or 50 nM H3B-6527 Hep3B cells. Solid lines indicate parental cells treated with DMSO or BLU9931. Dotted lines indicate the long-term DMSO or long-term H3B-6527 cells. Cell proliferation was determined by MTS assay. Error bars: mean  $\pm$  standard error of six biological replicates. \* indicates p-value of  $< 0.05$ , \*\*  $< 0.01$ , \*\*\*  $< 0.001$ . NS indicates not significant.

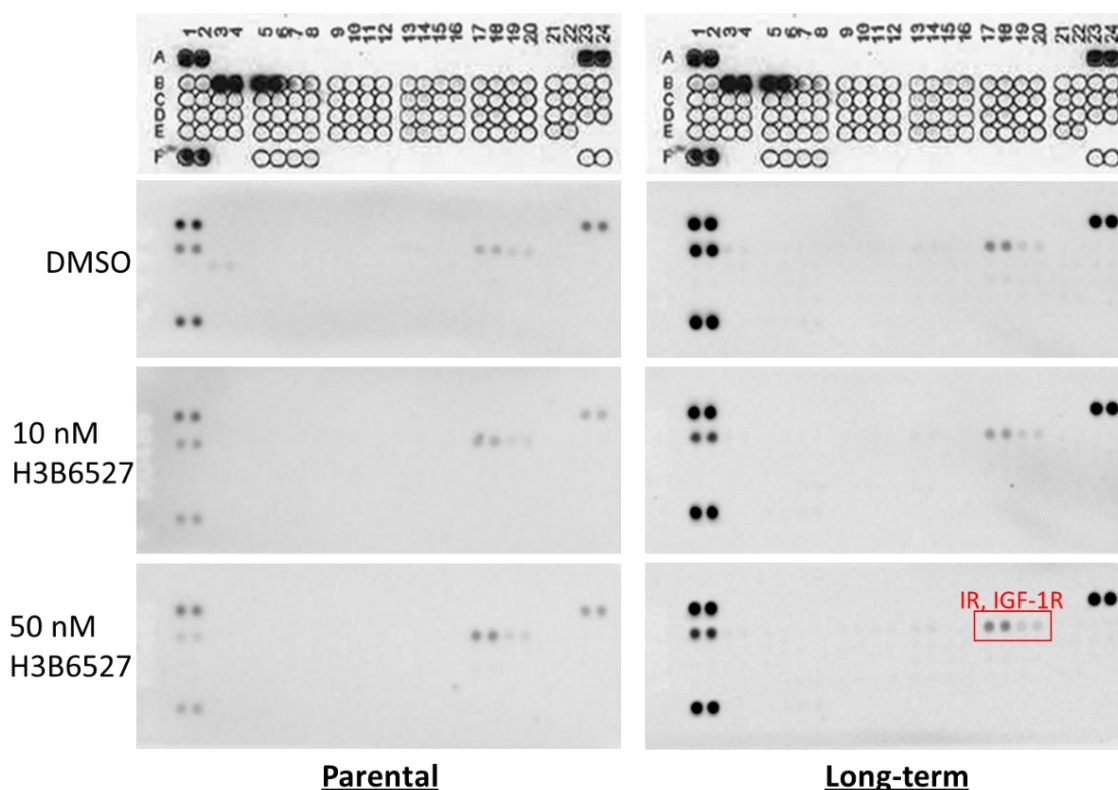


**Figure 5.18: Identification of upregulated RTKs in parental Hep3B after 24 h H3B-6527 treatment and in long-term H3B-6527 Hep3B cells.** Upregulated RTKs were analysed using RTK array blotting kits. Membranes from the RTK array kits were pre-spotted with specific antibodies. The top blots are reference for the locations on the membrane as follows: reference spots (A1, A2), (A23, A24), (F1, F2); EGFR (B1, B2); ErbB2 (B3, B4); ErbB3 (B5, B6); ErbB4 (B7, B8); FGFR1 (B9, B10); FGFR2 $\alpha$  (B11, B12); FGFR3 (B13, B14); FGFR4 (B15, B16); Insulin-R (B17, B18); IGF-1R (B19, B20); Axl (B21, B22); Dtk (B23, B24); Mer (C1, C2); HGFR (C3, C4); MSPR (C5, C6); PDGFR $\alpha$  (C7, C8); PDGFR $\beta$  (C9, C10); SCFR (C11, C12); Flt-3 (C13, C14); M-CSFR (C15, C16); c-Ret (C17, C18); ROR1 (C19, C20); ROR2 (C21, C22); Tie-1 (C23, C24); Tie-2 (D1, D2); TrkA (D3, D4); TrkB (D5, D6); TrkC (D7, D8); VEGFR1 (D9, D10); VEGFR2 (D11, D12); VEGFR3 (D13, D14); MuSK (D15, D16); EphA1 (D17, D18); EphA2 (D19, D20); EphA3 (D21,22) EphA4 (D23, D24); EphA6 (E1, E2); EphA7 (E3, E4); EphB1 (E5, E6); EphB2 (E7, E8); EphB4 (E9, E10); EphB6 (E11, E12); ALK (E13, E14); DDR1 (E15, E16); DDR2 (E17, E18); EphA5 (E19, E20); EphA10 (E21, E22); EphB3 (F5, F6); RYK (F7, F8); negative control (F23, F24). Parental Hep3B cells (left panels) were treated with the indicated treatment for 24 h, while the long-term Hep3B cells (right panels) were grown in their respective conditions for 24 h before harvesting.

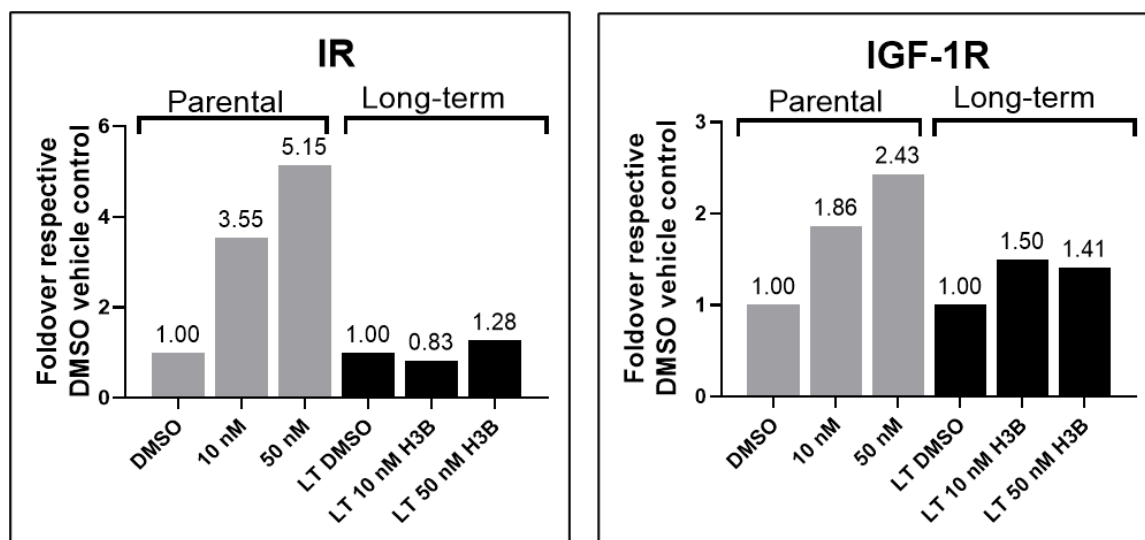
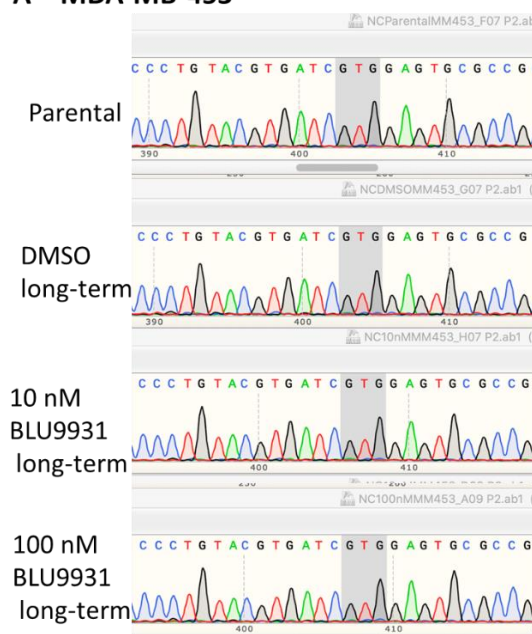


**Figure 5.19: Identification of upregulated RTKs in parental Hep3B treated with H3B-6527 for 24 h and H3B-6527-resistant Hep3B cells.** Quantification by densitometry of Figure 18. Data were first normalised relative to the reference points, then data were expressed relative to DMSO 24 h control which was arbitrarily set at 1.0.

One important anti-FGFR4 resistance mechanism is the presence of FGFR4 gatekeeper mutations in the kinase domain that prevents the binding of the FGFR4 inhibitor. To identify potential mutations in the FGFR4 kinase domain in the MDA-MB-453 and Hep3B cell line, RNA was extracted from the parental and long-term BLU9931/H3B-6527 cell groups and following RT-PCR, the FGFR4 kinase domain sequenced. Gatekeeper mutations changes the original GTG that codes for valine in the ATCGTGGAGTGCGCC sequence to other amino acids that obstructs the binding site of FGFR4 inhibitors. However, the results show no evidence of FGFR4 gatekeeper mutations, with normal ATCGTGGAGTGCGCC sequences in the kinase domain of the parental and long-term BLU9931/H3B-6527 groups of MDA-MB-453 and Hep3B cell lines (Fig. 5.20). This eliminates the possibility of FGFR4 gatekeeper mutations contributing to the mechanism of resistance to anti-FGFR4 therapy.

**A – MDA-MB-453**



**B – Hep3B**

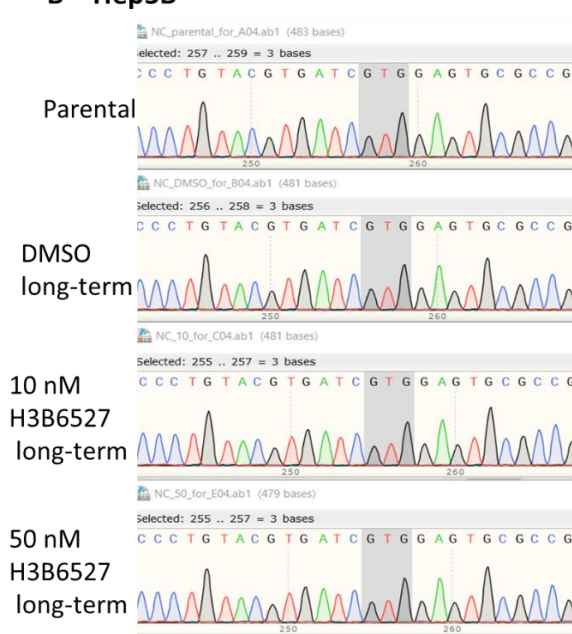


**Figure 5.20: FGFR4 kinase domain analysis for gatekeeper mutations.** RNA was extracted from parental and long-term FGFR4 inhibitor treated MDA-MB-453 and Hep3B cell lines, followed by RT-PCR and Sanger sequencing analysis. If a FGFR4 gatekeeper mutation is present, the original GTG coding for valine in the DNA sequence ATCGTGGAGTGC GCC would have a base pair change, changing the amino acid. Example FGFR4 gatekeeper mutations are V550M/V550L.



## 5.3 Discussion

The FGF19-FGFR4 signalling pathway is implicated in driving tumourigenesis in many cancers including TNBC and HCC [15]. FGFR4 overexpression enhances basal-like breast cancer cell survival and its inhibition reduces *in vivo* tumour growth and metastasis [6, 7]. In HCC, genomic and functional analyses identified FGF19 as an oncogenic driver [24, 26, 28]. Inhibiting the FGFR4 signalling pathway is a promising treatment strategy, especially for cancers that have few effective targeted treatments. Despite great successes in targeted treatment in cancers, resistance to targeted therapy usually emerges over time and is attenuates efficacy of inhibitors [8]. Combination treatment may be a valid approach [29], highlighting an urgent area of investigation to identify and characterise the mechanisms of resistance to targeted therapy, in this context anti-FGFR4 therapy, enabling rational design of such treatments.

Most combination treatments utilising FGFR inhibitors target FGFR1-3, and while FGFR4 has been used in combination treatments, these are mostly with radio/chemotherapeutics [30, 31]. The findings in this chapter may be one of the first to identify novel targeted combinations involving FGFR4 and other signalling proteins or RTKs. In this chapter, the TNBC cell line MDA-MB-453 and the HCC cell line Hep3B demonstrated respective ‘bounce-back’ and/or upregulation of signalling proteins AKT and ERK in response to anti-FGFR4 treatment in the short-term setting. These results highlight that the FGFR4 network is rewired through signalling by-pass mechanisms to overcome the FGFR4 inhibition. AKT signalling is critical for FGF19-FGFR4 mediated growth in breast cancer cells [7]. In this Chapter, studies on MDA-MB-453 cells harbouring the activating FGFR4 mutation highlighted the AKT signalling pathway as important in limiting the efficacy of BLU9931. In different cancer types expressing other FGFR members, the use of the selective FGFR1-3 inhibitor AZD4547 and AKT inhibitor AZD5363 had marked additive effects *in vitro* and *in vivo* in FGFR1-expressing prostate cancer [32]. Since mTOR is regulated by the AKT signalling pathway and small molecule drugs are available, the use of mTOR inhibitors may also be promising in combination therapy. The mTOR inhibitor AZD2014 in combination with AZD4547 demonstrated tumour growth attenuation in tumour xenografts generated from FGFR1-

dependent lung cancer cells [33]. With regards to the Hep3B cells, the partial signal recovery of ERK and co-targeting of FGFR4 and MEK (upstream of ERK) resulted in greater decreased in cell proliferation, indicating that the ERK signalling pathway may be critical in these cells for limiting FGFR4 inhibitor efficacy. Similarly, in a previous study, the combination of targeting MEK and FGFR1 using the MEK inhibitor Trametinib and a multi-kinase pan-FGFR inhibitor Ponatinib enhanced tumour cell death *in vitro* and *in vivo* in lung adenocarcinoma [34]. Altogether these results demonstrate co-targeting FGFR4 and AKT/ERK as novel treatment strategies to improve the efficacy of FGFR4 inhibitors and reduce tumour progression *in vivo*.

The interrogation of long-term FGFR4 inhibition in the TNBC and HCC cell lines provided insights into how the FGFR4 pathway is rewired to overcome the inhibition. In the TNBC cell line, MDA-MB-453, the analysis identified alternative upregulated RTKs that contribute to cancer cell survival through by-pass signalling pathways. ErbB2 exhibited a marked increase in these cells and co-targeting of FGFR4 and ErbB2 significantly decreased cell proliferation. This is consistent with the activation of alternative RTKs as an escape mechanism in FGFR-resistance models [35, 36]. For example, FGFR3-dependent bladder cancer cell lines developed resistance to the pan-FGFR inhibitor BGJ398 by switching receptor signalling to ErbB2 or ErbB3, and the dual inhibition of FGFR3 and ErbB activity resulted in increased cell death [35]. Unbiased screening using pTyr RTK arrays also identified high levels of pEGFR and pErbB2 in two FGFR-dependent basal-like breast cancer tumour xenografts after FGFR inhibition [37]. Subsequently, the combination of pan-ErbB inhibitor AEE788 and multi-kinase pan-FGFR inhibitor Dovitinib resulted in inhibition of the downstream FRS2-ERK and AKT pathways, tumour growth and metastasis [37].

## **5.4 Conclusion**

Based on the findings described in this Chapter and previous studies, the identification and characterisation of upregulated RTKs post-FGFR inhibition is important to reveal mechanisms of resistance to targeted therapy including the switch in receptor dependency, and highlight promising treatment strategies for clinical trials.

## 5.5 Future direction

These results have identified mechanisms of FGFR4 pathway rewiring and identified potential combination targeted therapies with increased efficacy. These findings regarding co-targeting can be further investigated *in vivo* using mice models to identify the best treatment combinations for specific cancers. For example, since both ErbB2 and ErbB3 were upregulated in the MDA-MB-453 line, a pan-ErbB inhibitor can be considered for future *in vivo* experimental interrogations and likely demonstrate greater inhibition of proliferation. Similarly, this combination can be compared with the FGFR4 and AKT co-inhibition to identify the greater significant outcome, which can progress into clinical trials to provide additional strategies for patient treatment. The characterisation of drug-induced perturbations in the FGFR4 signalling network will be useful in building computational models to predict the outcome of specific targeted therapies, new combination treatments and patient response. Furthermore, the identified mechanisms of resistance to anti-FGFR4 therapy may also be found in other cancers. Given that co-targeting FGFR4 and ErbB2 significantly reduced cell proliferation, there is potential in expanding this targeted treatment strategy to other breast cancer subtypes of poor prognosis, including luminal B and HER2 breast cancers.

## 5.6 References

1.     **Weinstein, J.N., E.A. Collisson, G.B. Mills, K.R.M. Shaw, B.A. Ozenberger, K. Ellrott, I. Shmulevich, C. Sander, J.M. Stuart, and C.G.A.R. Network,** *The cancer genome atlas pan-cancer analysis project*. Nature genetics, 2013. 45(10): p. 1113.
2.     **Roidl, A., P. Foo, W. Wong, C. Mann, S. Bechtold, H.J. Berger, S. Streit, J.E. Ruhe, S. Hart, A. Ullrich, and H.K. Ho,** *The FGFR4 Y367C mutant is a dominant oncogene in MDA-MB453 breast cancer cells*. Oncogene, 2010. 29(10): p. 1543-1552.
3.     **Ho, H.K., S. Pok, S. Streit, J.E. Ruhe, S. Hart, K.S. Lim, H.L. Loo, M.O. Aung, S.G. Lim, and A. Ullrich,** *Fibroblast growth factor receptor 4 regulates proliferation, anti-apoptosis and alpha-fetoprotein secretion during hepatocellular carcinoma progression and represents a potential target for therapeutic intervention*. Journal of hepatology, 2009. 50(1): p. 118-127.
4.     **Zaid, T.M., T.-L. Yeung, M.S. Thompson, C.S. Leung, T. Harding, R.S. Schmandt, S.-Y. Kwan, C. Rodriguez-Aguay, G. Lopez-Berestein, and A.K. Sood,** *Identification of FGFR4 as a potential therapeutic target for advanced-stage, high-grade serous ovarian cancer*. Clinical Cancer Research, 2013. 19(4): p. 809-820.
5.     **Hagel, M., C. Miduturu, M. Sheets, N. Rubin, W. Weng, N. Stransky, N. Bifulco, J.L. Kim, B. Hodous, N. Brooijmans, A. Shutes, C. Winter, C. Lengauer, N.E. Kohl, and T. Guzi,** *First selective small molecule inhibitor of FGFR4 for the treatment of hepatocellular carcinomas with an activated FGFR4 signaling pathway*. Cancer Discovery, 2015. 5(4): p. 424-437.
6.     **Tiong, K., B. Tan, H. Choo, F. Chung, L. Hii, S. Tan, N. Khor, S. Wong, S. See, Y. Tan, R. Rosli, S. Cheong, and C. Leong,** *Fibroblast growth factor receptor 4 (FGFR4) and fibroblast growth factor 19 (FGF19) autocrine enhance breast cancer cells survival*. Oncotarget, 2016.

7. **Zhao, X., F. Xu, N.P. Dominguez, Y. Xiong, Z. Xiong, H. Peng, C. Shay, and Y. Teng**, *FGFR4 provides the conduit to facilitate FGF19 signaling in breast cancer progression*. *Molecular Carcinogenesis*, 2018. 57(11): p. 1616-1625.
8. **Babina, I.S. and N.C. Turner**, *Advances and challenges in targeting FGFR signalling in cancer*. *Nature Reviews Cancer*, 2017. 17(5): p. 318-332.
9. **Chew, N.J., E.V. Nguyen, S.-P. Su, K. Novy, H.C. Chan, L.K. Nguyen, J. Luu, K.J. Simpson, R.S. Lee, and R.J. Daly**, *FGFR3 signaling and function in triple negative breast cancer*. *Cell Communication and Signaling*, 2020. 18(1): p. 13.
10. **Hatlen, M.A., O. Schmidt-Kittler, C.A. Sherwin, E. Rozsahegyi, N. Rubin, M.P. Sheets, J.L. Kim, C. Miduturu, N. Bifulco, N. Brooijmans, H. Shi, T. Guzi, A. Boral, C. Lengauer, M. Dorsch, R.D. Kim, Y.K. Kang, B.B. Wolf, and K.P. Hoefflich**, *Acquired on-target clinical resistance validates fgfr4 as a driver of hepatocellular carcinoma*. *Cancer Discovery*, 2019. 9(12): p. 1686-1695.
11. **Kostrzewa, M. and U. Müller**, *Genomic structure and complete sequence of the human FGFR4 gene*. *Mammalian genome*, 1998. 9(2): p. 131-135.
12. **Fairhurst, R.A., T. Knoepfel, C. Leblanc, N. Buschmann, C. Gaul, J. Blank, I. Galuba, J. Trappe, C. Zou, and J. Voshol**, *Approaches to selective fibroblast growth factor receptor 4 inhibition through targeting the ATP-pocket middle-hinge region*. *MedChemComm*, 2017. 8(8): p. 1604-1613.
13. **Touat, M., E. Ileana, S. Postel-Vinay, F. André, and J.C. Soria**, *Targeting FGFR signaling in cancer*. *Clinical Cancer Research*, 2015. 21(12): p. 2684-2694.
14. **Packer, L.M. and P.M. Pollock**, *Paralog-specific kinase inhibition of FGFR4: Adding to the arsenal of anti-FGFR agents*. *Cancer Discovery*, 2015. 5(4): p. 355-357.
15. **Joshi, J.J., H. Coffey, E. Corcoran, J. Tsai, C.L. Huang, K. Ichikawa, S. Prajapati, M.H. Hao, S. Bailey, J. Wu, V. Rimkunas, C. Karr, V. Subramanian, P. Kumar, C. MacKenzie, R. Hurley, T. Satoh, K. Yu, E. Park, N. Rioux, A. Kim, W.G. Lai, L. Yu, P. Zhu, S. Buonamici, N. Larsen, P. Fekkes, J. Wang, M. Warmuth, D.J. Reynolds, P.G. Smith, and A. Selvaraj**, *H3B-6527 Is a potent and selective inhibitor*

- of FGFR4 in FGF19-Driven hepatocellular carcinoma.* Cancer Research, 2017. 77(24): p. 6999-7013.
16. **Levine KM, C.J., Sikora MJ, Tasdemir N, Priedigkeit N, Tseng GC, Puhalla SL, Jankowitz RC, Dabbs DJ, McAuliffe PF, Lee AV, Oesterreich S,** *Combination FGFR4 and ER-targeted therapy for invasive lobular carcinoma.* Cancer Research, 2017.
  17. **Byron, S.A., H. Chen, A. Wortmann, D. Loch, M.G. Gartside, F. Dehkhoda, S.P. Blais, T.A. Neubert, M. Mohammadi, and P.M. Pollock,** *The N550K/H mutations in FGFR2 confer differential resistance to PD173074, dovitinib, and ponatinib ATP-competitive inhibitors.* Neoplasia, 2013. 15(8): p. 975-IN30.
  18. **Chell, V., K. Balmanno, A.S. Little, M. Wilson, S. Andrews, L. Blockley, M. Hampson, P.R. Gavine, and S.J. Cook,** *Tumour cell responses to new fibroblast growth factor receptor tyrosine kinase inhibitors and identification of a gatekeeper mutation in FGFR3 as a mechanism of acquired resistance.* Oncogene, 2013. 32(25): p. 3059-3070.
  19. **Ryan, M.R., C.D. Sohl, B. Luo, and K.S. Anderson,** *The FGFR1 V561M gatekeeper mutation drives AZD4547 resistance through STAT3 activation and EMT.* Molecular Cancer Research, 2019. 17(2): p. 532-543.
  20. **Goyal, L., L. Shi, L.Y. Liu, F.F. de la Cruz, J.K. Lennerz, S. Raghavan, I. Leschiner, L. Elagina, G. Siravegna, and R.W. Ng,** *TAS-120 overcomes resistance to ATP-competitive FGFR inhibitors in patients with FGFR2 Fusion–Positive intrahepatic cholangiocarcinoma.* Cancer discovery, 2019. 9(8): p. 1064-1079.
  21. **Feng, S., O. Dakhova, C.J. Creighton, and M. Ittmann,** *Endocrine fibroblast growth factor FGF19 promotes prostate cancer progression.* Cancer research, 2013. 73(8): p. 2551-2562.
  22. **Bray, F., J. Ferlay, I. Soerjomataram, R.L. Siegel, L.A. Torre, and A. Jemal,** *Global cancer statistics 2018: GLOBOCAN estimates of incidence and mortality*

- worldwide for 36 cancers in 185 countries*. CA Cancer Journal for Clinicians, 2018. 68(6): p. 394-424.
23. **Chen, B., L. Garmire, D.F. Calvisi, M.-S. Chua, R.K. Kelley, and X. Chen**, *Harnessing big 'omics' data and AI for drug discovery in hepatocellular carcinoma*. Nature Reviews Gastroenterology & Hepatology, 2020. 17(4): p. 238-251.
24. **Gao, L., X. Wang, Y. Tang, S. Huang, C.-A.A. Hu, and Y. Teng**, *FGF19/FGFR4 signaling contributes to the resistance of hepatocellular carcinoma to sorafenib*. Journal of Experimental & Clinical Cancer Research, 2017. 36(1): p. 8.
25. **Gao, L., L. Lang, X. Zhao, C. Shay, A.Y. Shull, and Y. Teng**, *FGF19 amplification reveals an oncogenic dependency upon autocrine FGF19/FGFR4 signaling in head and neck squamous cell carcinoma*. Oncogene, 2019. 38(13): p. 2394-2404.
26. **Sawey, E.T., M. Chanrion, C. Cai, G. Wu, J. Zhang, L. Zender, A. Zhao, R.W. Busuttil, H. Yee, and L. Stein**, *Identification of a therapeutic strategy targeting amplified FGF19 in liver cancer by Oncogenomic screening*. Cancer cell, 2011. 19(3): p. 347-358.
27. **Lang, L., A.Y. Shull, and Y. Teng**, *Interrupting the FGF19-FGFR4 Axis to Therapeutically Disrupt Cancer Progression*. Current cancer drug targets, 2019. 19(1): p. 17-25.
28. **Repana, D. and P. Ross**, *Targeting FGF19/FGFR4 pathway: a novel therapeutic strategy for hepatocellular carcinoma*. Diseases, 2015. 3(4): p. 294-305.
29. **Luo, H., T. Zhang, P. Cheng, D. Li, O. Ogorodniitchouk, C. Lahmamssi, G. Wang, and M. Lan**, *Therapeutic implications of fibroblast growth factor receptor inhibitors in a combination regimen for solid tumors*. Oncology Letters, 2020. 20(3): p. 2525-2536.
30. **Turkington, R., D. Longley, W. Allen, L. Stevenson, K. McLaughlin, P. Dunne, J. Blayney, M. Salto-Tellez, S. Van Schaeybroeck, and P. Johnston**, *Fibroblast growth factor receptor 4 (FGFR4): a targetable regulator of drug resistance in colorectal cancer*. Cell death & disease, 2014. 5(2): p. e1046-e1046.

31. **Ahmed, M.A., E. Selzer, W. Dörr, G. Jomrich, F. Harpain, G.R. Silberhumer, L. Müllauer, K. Holzmann, B. Grasl-Kraupp, and M. Grusch,** *Correction: Fibroblast growth factor receptor 4 induced resistance to radiation therapy in colorectal cancer.* Oncotarget, 2019. 10(51): p. 5385.
32. **Feng, S., L. Shao, P. Castro, I. Coleman, P.S. Nelson, P.D. Smith, B.R. Davies, and M. Ittmann,** *Combination treatment of prostate cancer with FGF receptor and AKT kinase inhibitors.* Oncotarget, 2017. 8(4): p. 6179.
33. **Singleton, K.R., T.K. Hinz, E.K. Kleczko, L.A. Marek, J. Kwak, T. Harp, J. Kim, A.C. Tan, and L.E. Heasley,** *Kinome RNAi screens reveal synergistic targeting of MTOR and FGFR1 pathways for treatment of lung cancer and HNSCC.* Cancer research, 2015. 75(20): p. 4398-4406.
34. **Manchado, E., S. Weissmueller, J.P. Morris, C.-C. Chen, R. Wullenkord, A. Lujambio, E. de Stanchina, J.T. Poirier, J.F. Gainor, and R.B. Corcoran,** *A combinatorial strategy for treating KRAS-mutant lung cancer.* Nature, 2016. 534(7609): p. 647-651.
35. **Wang, J., O. Mikse, R.G. Liao, Y. Li, L. Tan, P.A. Janne, N.S. Gray, K. Wong, and P.S. Hammerman,** *Ligand-associated ERBB2/3 activation confers acquired resistance to FGFR inhibition in FGFR3-dependent cancer cells.* Oncogene, 2015. 34(17): p. 2167-2177.
36. **Herrera-Abreu, M.T., A. Pearson, J. Campbell, S.D. Shnyder, M.A. Knowles, A. Ashworth, and N.C. Turner,** *Parallel RNA interference screens identify EGFR activation as an escape mechanism in FGFR3-mutant cancer.* Cancer discovery, 2013. 3(9): p. 1058-1071.
37. **Issa, A., J.W. Gill, M.R. Heideman, O. Sahin, S. Wiemann, J.H. Dey, and N.E. Hynes,** *Combinatorial targeting of FGF and ErbB receptors blocks growth and metastatic spread of breast cancer models.* Breast Cancer Research, 2013. 15(1).



---

# **CHAPTER 6**

## **CONCLUSIONS AND PERSPECTIVES**

---

## Chapter 6: Conclusions and Perspectives

In the past decade, our knowledge of the FGFR signalling pathway in cancer pathophysiology has advanced considerably [1]. There is increasing evidence that indicates deregulated FGFR signalling contributes to cancer development and progression, across many cancer types including breast cancer [2, 3]. This has highlighted the oncogenic potential of FGFRs and inhibiting the FGFR signalling pathway as a promising treatment strategy, especially for cancers that have few effective targeted treatments. The efficacy of anti-FGFR therapy in clinical studies has been variable [3, 4], although tumours harbouring FGFR genetic alterations such as fusions or mutations often respond to FGFR inhibitor treatment [5]. Therefore, the implementation of screening for FGFR alterations should be essential to provide accurate therapeutics at diagnosis and periodic screening during treatment to assess arising resistance mechanisms. In this chapter, the main findings are summarised, followed by the challenges in FGFR targeting in the clinical setting and potential improvement strategies.

FGFR aberrations that markedly enhance signalling are often oncogenic drivers and tumours exhibiting such alterations appear more likely to respond to FGFR inhibitors [6, 7]. Though FGFR fusions are relatively rare genetic alterations, reports on FGFR fusions are increasing [2]. With FGFR as the 5' fusion gene, the extracellular, transmembrane and kinase domain remain intact, while the 3' fusion partner provides specific domains that favour receptor dimerisation [8, 9]. In this thesis, two FGFR fusions in a TNBC cell line and a TNBC PDX, FGFR3-TACC3 and FGFR2-SKI respectively, were characterised as the oncogenic driver. These FGFR fusions have fusion partners that contain dimerisation-promoting domains and the expressing cells and PDX demonstrated extreme sensitivity to selective FGFR inhibition. These results are consistent with studies that showed FGFR fusions are constitutively activated due to dimerisation driven by the fusion partner [10-12] and activate canonical FGFR signalling [13, 14]. In Chapter 3, the oncogenic effect of FGFR3-TACC3 fusion was only demonstrated in the high-FGFR3 SUM185PE cell line that harboured the FGFR3-TACC3 fusion. To confirm that the oncogenic effect is due to the presence of the FGFR3-TACC3

fusion and not by other kinase alteration, low-FGFR3 cell lines should also be transfected with the FGFR3-TACC3 fusion and observe the changes on cellular function such as proliferation.

However, the non-canonical effects of FGFR fusions are still unknown and a detailed investigation is required. For example, the spatial and temporal localisation of FGFR fusions is unclear, whether they remain cytosolic and at the cell membrane, or are able to localise to other cellular compartments depending on the fusion partner. In this thesis, the vast majority of FGFR3-TACC3 fusion in the SUM185PE TNBC cell line was localised to the cytoplasm and plasma membrane, consistent with data from HeLa cells [11]. However, in glioblastoma, the FGFR3-TACC3 fusion reportedly localised to the mitotic spindle poles, which was also observed in the SUM185PE cells at low frequency. This indicates that the localisation of FGFR3-TACC3 fusion into the nucleus represents a potential mechanism contributing to tumour progression, such as by promoting aneuploidy in cells [10].

The localisation of the novel FGFR2-SKI fusion in the TNBC PDX should also be investigated, given the nuclear localisation signals of SKI and its ability to form an inhibitory complex with SMAD proteins on TGF- $\beta$  target gene promoters [15]. In particular, SKI protein levels fluctuate throughout the cell cycle, with highest expression during mitosis, and SKI can localise at the centrosomes and mitotic spindles [16]. To characterise the role of the FGFR2-SKI fusion, immunofluorescence staining at different stages of the cell cycle, and immunoprecipitation of the fusion protein followed by blotting for candidate partners or unbiased MS analysis may shed light on its localisation and its binding complexes, respectively. With regard to the latter approach, the Daly Laboratory identified tyrosine phosphorylated TACC3-interacting proteins in SUM185PE cells that were not detected in other TNBC cell lines using MS-based analysis. The same approach can be applied to detect nuclear phosphorylated proteins specific to the FGFR2-SKI fusion in this PDX. MS can also be used to compare the phosphorylated protein signatures of the FGFR2-overexpressing TNBC cell line, MFM223, and the PDX harbouring the FGFR2-SKI fusion. Since FGFR fusions may also exhibit distinctive negative feedback signalling or contrasting substrate recruitment due to loss of FGFR domains at the 3' terminus, this may identify other ways in which they differ from the wildtype receptor.

Successful pre-clinical studies have demonstrated effective FGFR targeting using small molecule inhibitors, which led to the evaluation of such approaches in human clinical trials. Consequently, Erdafitinib has received FDA-approval for treatment of locally advanced or metastatic FGFR3-, or FGFR2-positive urothelial carcinoma [17]. This success story supports the investigation of Erdafitinib treatment in other cancers and encourages other FGFR inhibitors to undergo evaluation as single agent treatment or in combination with other therapies. However, dose-limiting toxicity of non-selective FGFR inhibitors is a challenge that decreases drug efficacy [4, 18]. Hence, selective FGFR inhibitors with a narrower toxicity profiles have since been developed and are preferred for effective FGFR targeting without adverse side effects that stem from inhibition of multiple RTKs. Though selective FGFR inhibitors are more tolerable, FGFR inhibition disrupts phosphate homeostasis physiologically maintained by the FGF23 ligand, in which elevated levels induced by FGFR inhibition leads to hyperphosphatemia [3, 19]. Other commonly observed toxicities of selective FGFR inhibitors include stomatitis, fatigue, hand-foot syndrome and nausea [3, 20], all of which complicates patient management.

The majority of tyrosine kinase inhibitors directly target the receptor through competitive ATP inhibition by binding to the catalytic binding site of the kinase domain. Mutations that block the accessibility of the inhibitor to the ATP-binding site on the receptor kinase domain, termed gatekeeper mutations, are a clinical challenge [2]. Gatekeeper mutations are reportedly found across many cancers, for example, in multiple myeloma cell lines, the FGFR3 V555M gatekeeper mutation is involved in resistance to selective FGFR inhibitors, AZD4547 and PD173074 [21]. In hepatocellular carcinoma (HCC), FGFR4 gatekeeper mutation V550M was identified upon disease progression in patients treated with Fisogatinib, which was confirmed to mediate resistance *in vitro* and *in vivo* [22]. In addition, secondary FGFR2 kinase domain mutations were reported in three FGFR fusion-positive cholangiocarcinoma patients after anti-FGFR therapy [23]. These mutations were located in the kinase domain and included a gatekeeper change. In other RTKs, the EGFR gatekeeper T790M mutation to a larger residue negates the inhibitory activity of EGFR inhibitors, Gefitinib and Erlotinib [24, 25].

The occurrence of gatekeeper mutations was implicated as the primary form of resistance to anti-FGFR therapy [22], hence it is important to develop small-molecule compounds that overcome this mechanism. Osimertinib is an FDA-approved EGFR inhibitor, for the treatment of metastatic non-small cell lung cancer (NSCLC) patients that are EGFR T790M mutation-positive [26]. The development of Osimertinib was initiated as a solution for NSCLC patients that disease progressed after developing resistance to first and second-generation EGFR inhibitor therapies due to gatekeeper mutation [26]. In view of the successful advancement against gatekeeper mutations, other kinase inhibitors following suit of Osimertinib include the selective ALK inhibitor, CH5424802, that is capable of inhibiting cell growth driven by the L1196M gatekeeper mutation that confers resistance to kinase inhibitors in NSCLC [27]. Given the known occurrence of gatekeeper mutations in particular FGFRs following patient treatment with selective FGFR inhibitors, the generation of new drugs that target FGFRs with such changes will be an important area for future study.

Resistance to targeted therapy is presented through various mechanisms, and a common example is the selection of tumour cells that have specific mutations, rendering drugs incapable of their intended role. This mechanism is demonstrated by the accumulation of truncated HER2 receptor, p95-HER2, upon Trastuzumab treatment. This is found in approximately 30% of HER2-amplified breast cancer, and lacks the Trastuzumab binding site [28]. Patients expressing p95-HER2 exhibit shorter disease-free survival [29]. Furthermore, resistance to Trastuzumab has been associated with somatic alterations that result in the deregulation of the PI3K signalling pathway. Mutations that inhibit the PTEN tumour suppressor gene and activate the PIK3CA oncogene are frequently reported in breast cancers [30]. Specifically, the loss of PTEN and PIK3CA mutations were reported across various cancers, including gastric cancer and HER2-positive breast cancer [31-33]. In HER2-amplified breast cancer, the loss of PTEN may be sufficient to induce a regulatory effect on PI3K signalling pathway activation and gene expression associated with the cell cycle [31, 34]. Additionally, the PIK3CA gene encodes the p110 $\alpha$  subunit of PI3K, which is constitutively activated by “hot-spot” mutations in the PIK3CA gene (e.g., activating mutation Q546R), found in ~20% of HER2-positive breast cancers. This confers resistance to Trastuzumab *in vitro* and *in vivo* [23, 35]. In contrast, in colorectal cancer, KRAS mutations confer resistance to EGFR monoclonal antibodies, hence

an alternate treatment approach is implemented for patients harbouring KRAS mutations in the clinic [36]. Given that the PI3K-AKT and MAPK-ERK signalling pathway are downstream of FGFRs, these biomarkers may assist in identifying and predicting patients that are less likely to respond to FGFR inhibition. Therefore, investigating both PI3K-AKT and MAPK-ERK pathway changes as combined predictive biomarkers [37] of FGFR resistance may be sufficient to predict diminished response to anti-FGFR therapy. Identification of additional genetic alterations in molecules involved in the FGFR signalling pathway will also be fundamental for predicting response to targeted therapy. Aside from the mentioned mechanisms, potential resistance mechanisms that should be clinically validated include increased expression and function of drug efflux transporters, and/or extracellular sequestration of drug molecules that could hamper effective concentration at target sites [38, 39].

The PI3K-AKT pathway and MAPK-ERK pathway can be activated by other receptor kinases through network rewiring and crosstalk mechanisms, mediating drug resistance and limiting drug response. This was demonstrated in the “bounce-back” of AKT and ERK in the short-term FGFR4 inhibitor-treated MDA-MB-453 (TNBC) and Hep3B (HCC) cell lines respectively, which provided insights into how the FGFR4 signalling pathway is rewired, leading to resistance to FGFR4 blockade. The upregulation of alternative RTKs can mediate drug resistance, as demonstrated by the upregulation of ErbB2 in the long-term BLU9931-treated MDA-MB-453 cells. Similarly, receptor switching of FGFR3-dependent bladder cancer cell lines to HER2- or HER3-driven pathways enabled cells to avoid effects of FGFR inhibition [40]. In AZD4547-resistant FGFR1-amplified lung cancer cells, activation of ErbB3 was upregulated due to Met amplification, and the subsequent combination treatment of FGFR inhibitor with Met inhibitor synergistically inhibited cell proliferation [41, 42]. Ultimately, a comprehensive analysis of how the FGFR signalling network is rewired following drug treatment can lead to rational design of combination treatments to combat resistance to FGFR-targeted therapy [43]. As demonstrated in Chapter 5 of this thesis, combining FGFR4 inhibitors with ErbB inhibitors (ErbB2 or pan-ErbB inhibitors), or FGFR4 inhibitors with AKT inhibitors should improve treatment efficacy. Therefore, the effect of these combinations could be further explored in animal models.

To improve drug response, the use of a multi-omics approach to comprehensively profile FGFs and FGFRs in cancer allows the characterisation of aberrant FGFR signalling for potential targeting. For example, differential expression and phosphorylation of FGFRs in the breast cancer PDXs allowed selection for inhibitor treatment. However, only one out of three PDXs showed sensitivity to FGFR inhibition. This indicates that a magnitude or threshold is required to impart drug sensitivity, and this represents a potential predictive biomarker. The type of FGFR alteration (e.g. mutation, fusion, amplification) may also be indicative of patient response or prognosis, exemplified by demonstration of FGFR1 amplification as an independent negative prognostic factor in TNBC [44]. This approach can be expanded to include gene expression profiling of the FGF ligands and determine if they also play a role in response to drug sensitivity. Pre-clinical evidence suggests tumours with higher FGFR copy number are more likely to respond to FGFR inhibition [1], highlighting an additional predictive biomarker for drug response.

Another approach to predict drug response is utilising computational simulations and modelling to predict alternate signalling pathways that the tumour is likely to utilise to escape drug inhibition. This allows other possible inhibition approaches, such as combination treatment, to block cancer bypass mechanisms, ultimately leading to new treatment strategies. Specifically, predictive computational models can be built based on specific signalling networks in breast cancer using a recently developed Synergistic Drug Combination Discovery (SynDISCO) framework [45]. This system interrogates network nodes to compare co-inhibition effects of possible combinations, based on established quantitative drug synergy metrics. Then, priority drug combinations can be investigated and confirmed in pre-clinical cancer models, thereby accelerating therapeutic strategies for drug development. Drug-induced perturbations of the FGFR signalling network and FGFR signalling dynamics would be included in the computational modelling to predict drug response.

Overall, this thesis supports FGFRs as targets for precision treatment in cancer, while further investigation is required and necessary to reveal well-defined predictive biomarkers for patient response and unravel the resistance mechanisms for optimal FGFR targeting.

## References

1. **Pearson, A., E. Smyth, I.S. Babina, M.T. Herrera-Abreu, N. Tarazona, C. Peckitt, E. Kilgour, N.R. Smith, C. Geh, C. Rooney, R. Cutts, J. Campbell, J. Ning, K. Fenwick, A. Swain, G. Brown, S. Chua, A. Thomas, S.R.D. Johnston, M. Ajaz, K. Sumpter, A. Gillbanks, D. Watkins, I. Chau, S. Popat, D. Cunningham, and N.C. Turner**, *High-level clonal FGFR amplification and response to FGFR inhibition in a translational clinical trial*. *Cancer Discovery*, 2016. 6(8): p. 838-851.
2. **Babina, I.S. and N.C. Turner**, *Advances and challenges in targeting FGFR signalling in cancer*. *Nature Reviews Cancer*, 2017. 17(5): p. 318-332.
3. **Facchinetti, F., A. Hollebecque, R. Bahleda, Y. Loriot, K.A. Olaussen, C. Massard, and L. Friboulet**, *Facts and new hopes on selective FGFR inhibitors in solid tumors*. *Clinical Cancer Research*, 2020. 26(4): p. 764-774.
4. **Touat, M., E. Ileana, S. Postel-Vinay, F. André, and J.C. Soria**, *Targeting FGFR signaling in cancer*. *Clinical Cancer Research*, 2015. 21(12): p. 2684-2694.
5. **De Luca, A., R. Esposito Abate, A.M. Rachiglio, M.R. Maiello, C. Esposito, C. Schettino, F. Izzo, G. Nasti, and N. Normanno**, *FGFR Fusions in Cancer: From Diagnostic Approaches to Therapeutic Intervention*. *International Journal of Molecular Sciences*, 2020. 21(18): p. 6856.
6. **André, F., T. Bachelot, M. Campone, F. Dalenc, J.M. Perez-Garcia, S.A. Hurvitz, N. Turner, H. Rugo, J.W. Smith, S. Deudon, M. Shi, Y. Zhang, A. Kay, D.G. Porta, A. Yovine, and J. Baselga**, *Targeting FGFR with dovitinib (TKI258): Preclinical and clinical data in breast cancer*. *Clinical Cancer Research*, 2013. 19(13): p. 3693-3702.
7. **Shiang, C.Y., Y. Qi, B. Wang, V. Lazar, J. Wang, W.F. Symmans, G.N. Hortobagyi, F. Andre, and L. Pusztai**, *Amplification of fibroblast growth factor receptor-1 in breast cancer and the effects of brivanib alaninate*. *Breast Cancer Research and Treatment*, 2010. 123(3): p. 747-755.



8. **Gallo, L.H., K.N. Nelson, A.N. Meyer, and D.J. Donoghue**, *Functions of Fibroblast Growth Factor Receptors in cancer defined by novel translocations and mutations*. Cytokine and Growth Factor Reviews, 2015. 26(4): p. 425-449.
9. **Parker, B.C., M. Engels, M. Annala, and W. Zhang**, *Emergence of FGFR family gene fusions as therapeutic targets in a wide spectrum of solid tumours*. Journal of Pathology, 2014. 232(1): p. 4-15.
10. **Singh, D., J.M. Chan, P. Zoppoli, F. Niola, R. Sullivan, A. Castano, E.M. Liu, J. Reichel, P. Porraati, S. Pellegatta, K. Qiu, Z. Gao, M. Ceccarelli, R. Riccardi, D.J. Brat, A. Guha, K. Aldape, J.G. Golfinos, D. Zagzag, T. Mikkelsen, G. Finocchiaro, A. Lasorella, R. Rabadan, and A. Iavarone**, *Transforming fusions of FGFR and TACC genes in human glioblastoma*. Science, 2012. 337(6099): p. 1231-1235.
11. **Sarkar, S., E. Ryan, and S. Royle**, *FGFR3-TACC3 cancer gene fusions cause mitotic defects by removal of endogenous TACC3 from the mitotic spindle*. Open Biology, 2017. 7.
12. **Wu, Y.M., F. Su, S. Kalyana-Sundaram, N. Khazanov, B. Ateeq, X. Cao, R.J. Lonigro, P. Vats, R. Wang, S.F. Lin, A.J. Cheng, L.P. Kunju, J. Siddiqui, S.A. Tomlins, P. Wyngaard, S. Sadis, S. Roychowdhury, M.H. Hussain, F.Y. Feng, M.M. Zalupski, M. Talpaz, K.J. Pienta, D.R. Rhodes, D.R. Robinson, and A.M. Chinnaiyan**, *Identification of targetable FGFR gene fusions in diverse cancers*. Cancer Discovery, 2013. 3(6): p. 636-647.
13. **Sia, D., B. Losic, A. Moeini, L. Cabellos, K. Hao, K. Revill, D. Bonal, O. Miltiadous, Z. Zhang, Y. Hoshida, H. Cornella, M. Castillo-Martin, R. Pinyol, Y. Kasai, S. Roayaie, S.N. Thung, J. Fuster, M.E. Schwartz, S. Waxman, C. Cordon-Cardo, E. Schadt, V. Mazzaferro, and J.M. Llovet**, *Massive parallel sequencing uncovers actionable FGFR2-PPHLN1 fusion and ARAF mutations in intrahepatic cholangiocarcinoma*. Nature Communications, 2015. 6(1): p. 6087.
14. **Tanizaki, J., D. Ercan, M. Capelletti, M. Dodge, C. Xu, M. Bahcall, E.M. Tricker, M. Butaney, A. Calles, and L.M. Sholl**, *Identification of oncogenic and drug-*

- sensitizing mutations in the extracellular domain of FGFR2*. Cancer research, 2015. 75(15): p. 3139-3146.
15. **Tecalco-Cruz, A.C., D.G. Ríos-López, G. Vázquez-Victorio, R.E. Rosales-Alvarez, and M. Macías-Silva**, *Transcriptional cofactors Ski and SnoN are major regulators of the TGF- $\beta$ /Smad signaling pathway in health and disease*. Signal Transduction and Targeted Therapy, 2018. 3(1): p. 1-15.
  16. **Marcelain, K. and M.J. Hayman**, *The Ski oncoprotein is upregulated and localized at the centrosomes and mitotic spindle during mitosis*. Oncogene, 2005. 24(27): p. 4321-4329.
  17. **Markham, A.**, *Erdafitinib: first global approval*. Drugs, 2019. 79(9): p. 1017-1021.
  18. **Packer, L.M. and P.M. Pollock**, *Paralog-specific kinase inhibition of FGFR4: Adding to the arsenal of anti-FGFR agents*. Cancer Discovery, 2015. 5(4): p. 355-357.
  19. **Yanochko, G.M., A. Vitsky, J.R. Heyen, B. Hirakawa, J.L. Lam, J. May, T. Nichols, F. Sace, D. Trajkovic, and E. Blasi**, *Pan-FGFR inhibition leads to blockade of FGF23 signaling, soft tissue mineralization, and cardiovascular dysfunction*. toxicological sciences, 2013. 135(2): p. 451-464.
  20. **Chae, Y.K., K. Ranganath, P.S. Hammerman, C. Vaklavas, N. Mohindra, A. Kalyan, M. Matsangou, R. Costa, B. Carneiro, and V.M. Villafior**, *Inhibition of the fibroblast growth factor receptor (FGFR) pathway: the current landscape and barriers to clinical application*. Oncotarget, 2017. 8(9): p. 16052.
  21. **Chell, V., K. Balmanno, A.S. Little, M. Wilson, S. Andrews, L. Blockley, M. Hampson, P.R. Gavine, and S.J. Cook**, *Tumour cell responses to new fibroblast growth factor receptor tyrosine kinase inhibitors and identification of a gatekeeper mutation in FGFR3 as a mechanism of acquired resistance*. Oncogene, 2013. 32(25): p. 3059-3070.
  22. **Hatlen, M.A., O. Schmidt-Kittler, C.A. Sherwin, E. Rozsahegyi, N. Rubin, M.P. Sheets, J.L. Kim, C. Miduturu, N. Bifulco, N. Brooijmans, H. Shi, T. Guzi, A. Boral, C. Lengauer, M. Dorsch, R.D. Kim, Y.K. Kang, B.B. Wolf, and K.P.**

- Hoeflich**, *Acquired on-target clinical resistance validates fgfr4 as a driver of hepatocellular carcinoma*. *Cancer Discovery*, 2019. 9(12): p. 1686-1695.
23. **Goyal, L., S.K. Saha, L.Y. Liu, G. Siravegna, I. Leshchiner, L.G. Ahronian, J.K. Lennerz, P. Vu, V. Deshpande, and A. Kambadakone**, *Polyclonal secondary FGFR2 mutations drive acquired resistance to FGFR inhibition in patients with FGFR2 fusion-positive cholangiocarcinoma*. *Cancer discovery*, 2017. 7(3): p. 252-263.
  24. **Blencke, S., A. Ullrich, and H. Daub**, *Mutation of threonine 766 in the epidermal growth factor receptor reveals a hotspot for resistance formation against selective tyrosine kinase inhibitors*. *Journal of Biological Chemistry*, 2003. 278(17): p. 15435-15440.
  25. **Miller, V.A., V. Hirsh, J. Cadranel, Y.-M. Chen, K. Park, S.-W. Kim, C. Zhou, W.-C. Su, M. Wang, and Y. Sun**, *Afatinib versus placebo for patients with advanced, metastatic non-small-cell lung cancer after failure of erlotinib, gefitinib, or both, and one or two lines of chemotherapy (LUX-Lung 1): a phase 2b/3 randomised trial*. *The lancet oncology*, 2012. 13(5): p. 528-538.
  26. **Greig, S.L.**, *Osimertinib: first global approval*. *Drugs*, 2016. 76(2): p. 263-273.
  27. **Sakamoto, H., T. Tsukaguchi, S. Hiroshima, T. Kodama, T. Kobayashi, T.A. Fukami, N. Oikawa, T. Tsukuda, N. Ishii, and Y. Aoki**, *CH5424802, a selective ALK inhibitor capable of blocking the resistant gatekeeper mutant*. *Cancer cell*, 2011. 19(5): p. 679-690.
  28. **Scaltriti, M., F. Rojo, A. Ocaña, J. Anido, M. Guzman, J. Cortes, S. Di Cosimo, X. Matias-Guiu, S. Ramon y Cajal, and J. Arribas**, *Expression of p95HER2, a truncated form of the HER2 receptor, and response to anti-HER2 therapies in breast cancer*. *Journal of the National Cancer Institute*, 2007. 99(8): p. 628-638.
  29. **Sáez, R., M.A. Molina, E.E. Ramsey, F. Rojo, E.J. Keenan, J. Albanell, A. Lluch, J. García-Conde, J. Baselga, and G.M. Clinton**, *p95HER-2 predicts worse outcome*

- in patients with HER-2-positive breast cancer*. Clinical cancer research, 2006. 12(2): p. 424-431.
30. **Duman, B., B. Şahin, A. Açıklın, M. Ergin, and S. Zorludemir**, *PTEN, Akt, MAPK, p53 and p95 expression to predict trastuzumab resistance in HER2 positive breast cancer*. 2013.
31. **Rimawi, M.F., C. De Angelis, A. Contreras, F. Pareja, F.C. Geyer, K.A. Burke, S. Herrera, T. Wang, I.A. Mayer, and A. Forero**, *Low PTEN levels and PIK3CA mutations predict resistance to neoadjuvant lapatinib and trastuzumab without chemotherapy in patients with HER2 over-expressing breast cancer*. Breast cancer research and treatment, 2018. 167(3): p. 731-740.
32. **Nagata, Y., K.-H. Lan, X. Zhou, M. Tan, F.J. Esteva, A.A. Sahin, K.S. Klos, P. Li, B.P. Monia, and N.T. Nguyen**, *PTEN activation contributes to tumor inhibition by trastuzumab, and loss of PTEN predicts trastuzumab resistance in patients*. Cancer cell, 2004. 6(2): p. 117-127.
33. **Black, J.D., S. Lopez, E. Cocco, S. Bellone, G. Altwerger, C.L. Schwab, D.P. English, E. Bonazzoli, F. Predolini, and F. Ferrari**, *PIK3CA oncogenic mutations represent a major mechanism of resistance to trastuzumab in HER2/neu overexpressing uterine serous carcinomas*. British journal of cancer, 2015. 113(7): p. 1020-1026.
34. **Fu, X., C.J. Creighton, N.C. Biswal, V. Kumar, M. Shea, S. Herrera, A. Contreras, C. Gutierrez, T. Wang, and S. Nanda**, *Overcoming endocrine resistance due to reduced PTEN levels in estrogen receptor-positive breast cancer by co-targeting mammalian target of rapamycin, protein kinase B, or mitogen-activated protein kinase kinase*. Breast Cancer Research, 2014. 16(5): p. 1-17.
35. **Berns, K., H.M. Horlings, B.T. Hennesy, M. Madiredjo, E.M. Hijmans, K. Beelen, S.C. Linn, A.M. Gonzalez-Angulo, K. Stemke-Hale, and M. Hauptmann**, *A functional genetic approach identifies the PI3K pathway as a major determinant of trastuzumab resistance in breast cancer*. Cancer cell, 2007. 12(4): p. 395-402.

36. **Misale, S., R. Yaeger, S. Hobor, E. Scala, M. Janakiraman, D. Liska, E. Valtorta, R. Schiavo, M. Buscarino, and G. Siravegna,** *Emergence of KRAS mutations and acquired resistance to anti-EGFR therapy in colorectal cancer.* Nature, 2012. 486(7404): p. 532-536.
37. **Esteva, F.J., H. Guo, S. Zhang, C. Santa-Maria, S. Stone, J.S. Lanchbury, A.A. Sahin, G.N. Hortobagyi, and D. Yu,** *PTEN, PIK3CA, p-AKT, and p-p70S6K status: association with trastuzumab response and survival in patients with HER2-positive metastatic breast cancer.* The American journal of pathology, 2010. 177(4): p. 1647-1656.
38. **Burger, H., T. Alexander, S. Segeletz, A.W. Boersma, P. de Bruijn, M. Debiec-Rychter, T. Taguchi, S. Sleijfer, A. Sparreboom, and R.H. Mathijssen,** *Lysosomal sequestration determines intracellular imatinib levels.* Molecular pharmacology, 2015. 88(3): p. 477-487.
39. **Maacha, S., A.A. Bhat, L. Jimenez, A. Raza, M. Haris, S. Uddin, and J.-C. Grivel,** *Extracellular vesicles-mediated intercellular communication: roles in the tumor microenvironment and anti-cancer drug resistance.* Molecular cancer, 2019. 18(1): p. 55.
40. **Wang, J., O. Mikse, R.G. Liao, Y. Li, L. Tan, P.A. Janne, N.S. Gray, K. Wong, and P.S. Hammerman,** *Ligand-associated ERBB2/3 activation confers acquired resistance to FGFR inhibition in FGFR3-dependent cancer cells.* Oncogene, 2015. 34(17): p. 2167-2177.
41. **Kim, H.R., D.J. Kim, D.R. Kang, J.G. Lee, S.M. Lim, C.Y. Lee, S.Y. Rha, M.K. Bae, Y.J. Lee, S.H. Kim, S.J. Ha, R.A. Soo, K.Y. Chung, J.H. Kim, J.H. Lee, H.S. Shim, and B.C. Cho,** *Fibroblast growth factor receptor 1 gene amplification is associated with poor survival and cigarette smoking dosage in patients with resected squamous cell lung cancer.* Journal of Clinical Oncology, 2013. 31(6): p. 731-737.
42. **Kim, S., H. Kim, M. Yun, H. Kang, K. Pyo, H. Park, J. Lee, H. Choi, P. Ellinghaus, and M. Ocker,** *Activation of the Met kinase confers acquired drug resistance in FGFR-targeted lung cancer therapy.* Oncogenesis, 2016. 5(7): p. e241-e241.

43. **Luo, H., T. Zhang, P. Cheng, D. Li, O. Ogorodniitchouk, C. Lahmamssi, G. Wang, and M. Lan,** *Therapeutic implications of fibroblast growth factor receptor inhibitors in a combination regimen for solid tumors.* Oncology Letters, 2020. 20(3): p. 2525-2536.
44. **Cheng, C.L., A.A. Thike, S.Y.J. Tan, P.J. Chua, B.H. Bay, and P.H. Tan,** *Expression of FGFR1 is an independent prognostic factor in triple-negative breast cancer.* Breast Cancer Research and Treatment, 2015. 151(1): p. 99-111.
45. **Shin, S.-Y., A.-K. Müller, N. Verma, S. Lev, and L.K. Nguyen,** *Systems modelling of the EGFR-PYK2-c-Met interaction network predicts and prioritizes synergistic drug combinations for triple-negative breast cancer.* PLoS computational biology, 2018. 14(6): p. e1006192.

---

# APPENDIX

## PUBLICATION IN ORIGINAL FORMAT

---

**THIS PAGE HAS BEEN INTENTIONALLY LEFT BLANK**




RESEARCH

Open Access



# FGFR3 signaling and function in triple negative breast cancer

Nicole J. Chew<sup>1,2</sup>, Elizabeth V. Nguyen<sup>1,2</sup>, Shih-Ping Su<sup>1,2</sup>, Karel Novy<sup>1,2</sup>, Howard C. Chan<sup>1,2</sup>, Lan K. Nguyen<sup>1,2</sup>, Jennii Luu<sup>3,4</sup>, Kaylene J. Simpson<sup>3,4</sup>, Rachel S. Lee<sup>1,2†</sup> and Roger J. Daly<sup>1,2\*†</sup> 

## Abstract

**Background:** Triple negative breast cancer (TNBC) accounts for 16% of breast cancers and represents an aggressive subtype that lacks targeted therapeutic options. In this study, mass spectrometry (MS)-based tyrosine phosphorylation profiling identified aberrant FGFR3 activation in a subset of TNBC cell lines. This kinase was therefore evaluated as a potential therapeutic target.

**Methods:** MS-based tyrosine phosphorylation profiling was undertaken across a panel of 24 TNBC cell lines. Immunoprecipitation and Western blot were used to further characterize FGFR3 phosphorylation. Indirect immunofluorescence and confocal microscopy were used to determine FGFR3 localization. The selective FGFR1–3 inhibitor, PD173074 and siRNA knockdowns were used to characterize the functional role of FGFR3 in vitro. The TCGA and Metabric breast cancer datasets were interrogated to identify FGFR3 alterations and how they relate to breast cancer subtype and overall patient survival.

**Results:** High FGFR3 expression and phosphorylation were detected in SUM185PE cells, which harbor a FGFR3-TACC3 gene fusion. Low FGFR3 phosphorylation was detected in CAL51, MFM-223 and MDA-MB-231 cells. In SUM185PE cells, the FGFR3-TACC3 fusion protein contributed the majority of phosphorylated FGFR3, and largely localized to the cytoplasm and plasma membrane, with staining at the mitotic spindle in a small subset of cells. Knockdown of the FGFR3-TACC3 fusion and wildtype FGFR3 in SUM185PE cells decreased FRS2, AKT and ERK phosphorylation, and induced cell death. Knockdown of wildtype FGFR3 resulted in only a trend for decreased proliferation. PD173074 significantly decreased FRS2, AKT and ERK activation, and reduced SUM185PE cell proliferation. Cyclin A and pRb were also decreased in the presence of PD173074, while cleaved PARP was increased, indicating cell cycle arrest in G1 phase and apoptosis. Knockdown of FGFR3 in CAL51, MFM-223 and MDA-MB-231 cells had no significant effect on cell proliferation. Interrogation of public datasets revealed that increased FGFR3 expression in breast cancer was significantly associated with reduced overall survival, and that potentially oncogenic FGFR3 alterations (eg mutation and amplification) occur in the TNBC/basal, luminal A and luminal B subtypes, but are rare.

**Conclusions:** These results indicate that targeting FGFR3 may represent a therapeutic option for TNBC, but only for patients with oncogenic FGFR3 alterations, such as the FGFR3-TACC3 fusion.

**Keywords:** Receptor tyrosine kinase, Fibroblast growth factor receptor, Oncogene, Targeted therapy, Signal transduction

\* Correspondence: [roger.daly@monash.edu](mailto:roger.daly@monash.edu)

<sup>†</sup>Rachel S. Lee and Roger J. Daly contributed equally to this work.

<sup>1</sup>Cancer Program, Biomedicine Discovery Institute, Monash University, Melbourne, VIC 3800, Australia

<sup>2</sup>Department of Biochemistry and Molecular Biology, Monash University, Melbourne, VIC 3800, Australia

Full list of author information is available at the end of the article



© The Author(s). 2020 **Open Access** This article is distributed under the terms of the Creative Commons Attribution 4.0 International License (<http://creativecommons.org/licenses/by/4.0/>), which permits unrestricted use, distribution, and reproduction in any medium, provided you give appropriate credit to the original author(s) and the source, provide a link to the Creative Commons license, and indicate if changes were made. The Creative Commons Public Domain Dedication waiver (<http://creativecommons.org/publicdomain/zero/1.0/>) applies to the data made available in this article, unless otherwise stated.

## Background

Breast cancer accounts for 25% of all cancer and ranks as the second most common cancer in the world [1]. Triple negative breast cancer (TNBC) is the most aggressive subtype that represents approximately 10–20% of breast cancers and its oncogenic drivers are poorly understood [2, 3]. TNBC lacks expression of estrogen receptor (ER), progesterone receptor (PR) and human epidermal growth factor receptor-2 (HER-2) resulting in clinical resistance to endocrine and trastuzumab therapy [4]. Chemotherapy remains the only treatment option since targeted treatment strategies are lacking [5]. TNBC is associated with higher tumor grade, larger tumor size, higher metastasis rate, lymph node involvement and a median survival of 13 months after relapse [6–8]. To improve patient outcomes, we need to identify new therapeutic targets to build a platform for personalized treatment strategies.

Fibroblast growth factor receptors (FGFRs) are a family of four highly conserved transmembrane receptor tyrosine kinases (RTKs), comprising of FGFR1, FGFR2, FGFR3 and FGFR4 [9]. Activated FGFRs initiate intracellular signaling cascades involved in regulating a wide range of physiological processes such as cellular differentiation, proliferation, survival and migration, embryonic development and angiogenesis [10]. Aberrant FGFR signaling has been reported in many human cancers including breast cancer, colorectal carcinoma and endometrial carcinoma, and contributes to oncogenesis, tumor progression and resistance to anticancer therapies [11–13]. FGFR alterations have been reported in approximately 7.1% of cancers (most commonly in urothelial and breast cancer), with gene amplification being the most frequent FGFR aberration (66%), followed by mutation (26%) and rearrangement (8%) [14]. Given the oncogenic potential of FGFRs and their ‘druggability’, there has been considerable interest in developing targeted cancer therapies directed towards these receptors. Dovitinib, a multi-tyrosine kinase inhibitor with FGFR-inhibiting activity, induced tumor regression in patient-derived xenograft models exhibiting gene sets related to the FGFR signaling pathway, highlighting the latter as potential predictors for Dovitinib sensitivity [15]. Dovitinib is currently in phase 2 clinical trials and has demonstrated modest efficacy against lung squamous cell carcinomas harboring FGFR1 amplification [16]. BGJ398, a highly potent and selective pan-FGFR kinase inhibitor in clinical trials, has demonstrated antitumor activity in advanced cholangiocarcinoma patients with FGFR2 alterations [17] and promoted tumor reductions in FGFR1-amplified breast cancer patients [18]. Erdafitinib, an inhibitor of FGFR1–4, resulted in tumor shrinkage in an adrenal carcinoma patient with the FGFR3-TACC3 fusion [19]. Pemigatinib is another

selective FGFR inhibitor that is currently under evaluation for its efficacy and safety in patients with urothelial carcinoma (NCT03011372).

FGFRs represent potential therapeutic targets in many human malignancies including breast cancer [20]. FGFR1 amplification on chromosome 8p11–12 is the most common FGFR1 alteration [21, 22], occurring in 14% of breast cancers and 16–27% of luminal B breast cancer, where it is associated with poor prognosis, shorter overall survival and resistance to endocrine therapies [23–25]. FGFR1 amplification is also an independent negative prognostic factor in gastric cancer, lung squamous cell carcinoma and TNBC [26–28]. Knock-down of FGFR1 expression in a FGFR1-overexpressing TNBC cell line MDA-MB-231 significantly reduced cell migration [28] and knock-out of FGFR1 reduced primary tumor growth and metastasis in a mouse mammary tumor model [29]. FGFR2 amplification is also a common FGFR aberration, occurring in 5–10% of breast cancers and 4% of TNBCs, and FGFR2 signaling drives resistance to Tamoxifen in ER+ disease [30, 31]. Knock-down of FGFR2 significantly reduced cell survival in the TNBC cell line MFM223 and this cell line also showed substantial sensitivity to the FGFR inhibitor PD173074 [30]. In breast cancer, high FGFR2 expression is significantly associated with tumor size and metastasis, shorter overall survival and lower disease-free survival rates [32]. Expression of autocrine FGF2 is associated with the basal/TNBC subtype of breast cancer cell lines and primary breast cancers, and in the former, confers sensitivity to PD173074 [33].

While the roles of FGFR1 and FGFR2 in breast cancer have been studied in considerable detail, FGFR3 remains poorly characterized in this setting. Molecular screening via segmental transcript analysis identified a FGFR3-TACC3 fusion in a primary TNBC specimen and TNBC cell line, SUM185PE [34]. In this fusion, the FGFR3 kinase domain is fused to the upstream region of the coiled-coil domain of transforming acidic coiled-coil 3 (TACC3) protein [34, 35]. FGFR3-TACC3 fusions also occur in other cancers, such as glioblastoma (3 out of 97 tumors examined, 3.1%), bladder cancer (2 of 43 bladder cancer cell lines, 4.7%) and nasopharyngeal carcinoma (4 out of 159 patients, 2.5%) [35–37]. The presence of the coiled-coil domain of TACC3 enhances dimerization of the fusion protein, thus activating the FGFR3 tyrosine kinase [38]. The presence of the FGFR3-TACC3 fusion increases cell proliferation and tumor formation in vivo [35], but confers sensitivity to specific FGFR inhibitors, indicating an oncogenic addiction to the fusion [37, 39, 40].

Previously, we utilized MS to compare the tyrosine phosphorylation profiles of luminal breast cancer and TNBC cell lines. This identified a prominent Src family

kinase signaling network in TNBC and highlighted multiple kinases for further evaluation as therapeutic targets and biomarkers [41]. In this study, we applied this approach to a large panel of TNBC cell lines to interrogate this disease subtype in more detail and identify targets for personalized treatment. One potential target that emerged was FGFR3, and this was characterized in detail in this study.

## Materials and Methods

### Cell lines, cell culture and reagents

The BT549, BT20, DU4475, HCC38, HCC70, HCC1500, HCC1569, HCC1954, HCC1806, HCC1143, HCC1937, HS578T, MDA-MB-157, MDA-MB-436, MDA-MB-453, MDA-MB-231 and MDA-MB-468 cell lines were purchased from the American Type Culture Collection (ATCC; Manassas, VA, USA). CAL51, CAL148 and CAL851 cells were obtained from Deutsche Sammlung von Mikroorganismen und Zellkulturen (DSMZ) and CAL120 cells were a gift from Professor Elgene Lim from the Garvan Institute of Medical Research, Darlinghurst, NSW 2010, Australia. MFM223 cells were purchased from Sigma Aldrich. SUM185PE and SUM149PT cells were purchased from Asterand Bioscience. Cells were cultured in RPMI 1640 (Gibco) supplemented with 10% (v/v) FBS, 10 µg/mL insulin and 20 mM HEPES.

### Tyrosine phosphorylation profiling by mass spectrometry

To harvest proteins for mass spectrometry (MS) analysis, TNBC cell lines were cultured until 80% confluent, washed twice with ice cold phosphate-buffered saline (PBS), and lysed directly in the dish with lysis buffer (6 M guanidine hydrochloride, 50 mM Tris-HCl, 1 mM sodium orthovanadate, 2.5 mM sodium pyrophosphate, 1 mM b-glycerophosphate). Approximately 20 mg of lysate protein was reduced with 5 mM TCEP at 37 °C for 1 h and alkylated with iodoacetamide in the dark for 1 h. The samples were then diluted 1:4 with ammonium bicarbonate (25 mM) before digestion with a 1:200 LysC (Worthington) at room temperature (RT) for 4 h. Samples were further diluted 10x from the original volume before digested with a 1:100 trypsin (Promega) at 37 °C for 18 h. Tryptic digests were acidified with 10%TFA to pH 3 before desalting on a C18 column (Thermo Fisher Scientific) and elution with 0.1% TFA/40% ACN. Peptides were dried in a SpeedVac and reconstituted in 1.8 ml of IAP wash buffer (1% n-octyl-β-D-glucopyranoside, 50 mM Tris-HCl, 150 mM NaCl, pH 7.4). 50 µg each of P-Tyr-1000 (Cell Signaling Technology, 8954), P-Tyr-100 (Cell Signaling Technology, 9411), and P-Tyr-20 (BD Biosciences, 610,000) antibodies were coupled to 60 µL of sepharose beads slurry (Rec-Protein G, Zymed) and incubated overnight with peptide samples at 4 °C with gentle shaking. Immobilized antibody beads were

washed three times with IAP buffer and further washed three times with water before elution with 110 µL of 0.15% TFA. Samples were then desalted on a C18 column (as described above) and evaporated to dryness in a SpeedVac. The dried peptides were reconstituted in 2% ACN/0.5% FA.

### Mass spectrometry analysis

Samples were analyzed on an UltiMate 3000 RSLC nano LC system (Thermo Fisher Scientific) coupled to an LTQ-Orbitrap mass spectrometer (LTQ-Orbitrap, Thermo Fisher Scientific). Peptides were loaded via an Acclaim PepMap 100 trap column (100 µm × 2 cm, nanoViper, C18, 5 µm, 100 Å, Thermo Fisher Scientific) and subsequent peptide separation was on an Acclaim PepMap RSLC analytical column (75 µm × 50 cm, nanoViper, C18, 2 µm, 100 Å, Thermo Fisher Scientific). For each liquid chromatography-tandem mass spectrometry (LC-MS/MS) analysis, 1 µg of peptides as measured by a nanodrop 1000 spectrophotometer (Thermo Fisher Scientific) was loaded on the pre-column with microliter pickup. Peptides were eluted using a 2 h linear gradient of 80% ACN/0.1% FA at a flow rate of 250 nL/min using a mobile phase gradient of 2.5–42.5% ACN. The eluting peptides were interrogated with an Orbitrap mass spectrometer. The HRM DIA method consisted of a survey scan (MS1) at 35,000 resolution (automatic gain control target 5e6 and maximum injection time of 120 ms) from 400 to 1220 m/z followed by tandem MS/MS scans (MS2) through 19 overlapping DIA windows increasing from 30 to 222 Da. MS/MS scans were acquired at 35,000 resolution (automatic gain control target 3e6 and auto for injection time). Stepped collision energy was 22.5, 25, 27.5% and a 30 m/z isolation window. The spectra were recorded in profile type.

### HRM-DIA data analysis

The DIA data were analyzed with Spectronaut 8, a mass spectrometer vendor-independent software from Biognosys. The default settings were used for the Spectronaut search. Retention time prediction type was set to dynamic indexed Retention Time (iRT; correction factor for window 1). Decoy generation was set to scrambled (no decoy limit). Interference correction on MS2 level was enabled. The false discovery rate (FDR) was set to 1% at peptide level. A peptide identification required at least 3 transitions in quantification. Quantification was based on the top 3 proteotypic peptides for each protein, normalized with the default settings, and exported as an excel file with Spectronaut 8 software [42]. For generation of the spectral libraries, DDA measurements of each sample were performed. The DDA spectra were analyzed with the MaxQuant Version 1.5.2.8 analysis software using default settings. Enzyme specificity was

set to Trypsin/P, minimal peptide length of 6, and up to 3 missed cleavages were allowed. Search criteria included carbamidomethylation of cysteine as a fixed modification; oxidation of methionine; acetyl (protein N terminus); and phosphorylation of serine, threonine, and tyrosine as variable modifications. The mass tolerance for the precursor was 4.5 ppm and for the fragment ions was 20 ppm. The DDA files were searched against the human UniProt fasta database (v2015–08, 20,210 entries) and the Biognosys HRM calibration peptides. The identifications were filtered to satisfy FDR of 1% on peptide and protein level. The spectral library was generated in Spectronaut and normalized to iRT peptides.

### Cell lysis

Cells at 80% confluency were washed twice with ice cold 1x PBS then lysed with RIPA buffer (0.5% (w/v) sodium deoxycholate, 150 mM NaCl, 1% (v/v) NP40, 50 mM Tris HCl pH 8.0, 0.1% (w/v) sodium dodecyl sulfate (SDS), 10% (v/v) glycerol, 5 mM EDTA and 20 mM NaF), supplemented with 10 µg/mL aprotinin, 1 mM phenylmethane sulfonyl fluoride (PMSF), 10 µg/mL leupeptin, 1 mM sodium orthovanadate, 2.5 mM sodium pyrophosphate and 2.5 mM β-glycerophosphate prior to use. Lysed cells were collected and clarified by centrifugation at 21130 x *g* at 4 °C for 10 min, then the protein concentration was determined using a Pierce BCA protein assay kit (Thermoscientific) according to the manufacturer's protocol.

### Western blotting

Protein lysates were subjected to Western blot analysis with antibodies. The following antibodies were purchased from Cell Signaling Technology: FGFR1 (9740), wildtype FGFR3 (4574), pan-phosFGFR (Y653, Y654) (3471), TACC3 (8069), AKT (4685), ERK (4695), pAKT (S473) (4058), pERK (T202, Y204) (4370), pFRS2 (Y436) (3861), PARP (9546), Rb (9313) and pRb (S780) (3590). The following antibodies were purchased from Santa Cruz Biotechnology: FGFR2 (sc-6930), FW FGFR3 (sc-13,121), FGFR4 (sc-136,988), pFGFR3 (Y724) (sc-33,041), FRS2 (sc-17,841), cyclin A (sc-53,227) and β-actin (sc-69,879). Two α-tubulin antibodies were purchased from Sigma-Aldrich (T5168) and from Abcam (ab6046).

### Immunoprecipitation

Protein lysates (2.5 mg) were incubated with 10 µg of the indicated antibodies overnight at 4 °C with gentle rotation. 40 µL of recombinant protein G-Sepharose 4B conjugate beads (Life Technologies, 101,242) was equilibrated in RIPA buffer were added to samples and incubated for 3 h at 4 °C with gentle rotation. Samples were centrifuged at 500 x *g* for 1 min at 4 °C and the unbound fraction transferred to a fresh microfuge tube. Beads

were washed thrice with RIPA buffer and centrifuged for 1 min at 500 x *g* at 4 °C and the supernatant removed. Immunoprecipitated proteins were then eluted using 2x sample loading buffer.

### Immunofluorescence and cell synchronization

SUM185PE cells seeded onto coverslips were fixed and permeabilized with PTEMF buffer (20 mM PIPES pH 6.8, 0.2% (v/v) Triton X 100, 10 mM EGTA, 1 mM MgCl<sub>2</sub>, 4% (v/v) PFA) 24 h post seeding for 20 mins. The samples were then blocked with 1% (w/v) bovine serum albumin for 1 h then immunostained with the indicated primary antibodies for 2 h followed by either anti-mouse Alexa Fluor 488 (Life Technologies, A21202) or anti-rabbit Alexa Fluor 555 (Life Technologies, A21428) for 1 h. All antibody incubations were performed at RT. Coverslips were mounted onto microscope slides with ProLong Gold Antifade Mountant with DAPI (Invitrogen). Cells were imaged 48 h later by immunofluorescence using a Nikon inverted confocal microscope. For cell synchronization, SUM185PE cells were synchronized at G1/S phase by 3 mM thymidine block for 18 h then released into media for 9 h. Next, the cells were then subjected to 3 mM thymidine block for another 15 h, released into media for 45 h and imaging was undertaken as above. Mitotic spindles were visualized by staining with rabbit anti-α-tubulin (Abcam, 6046) or mouse anti-α-tubulin (Sigma-Aldrich, T5168).

### Cell viability assays

For assays with siRNAs knockdown, SUM185PE cells were seeded into 96 well plates and cultured for 6 days, while CAL51, MFM223 and MDA-MB-231 were cultured for 4 days, with an 80% end point confluence for all the cell lines. Cell viability was determined using CellTiter96 Aqueous One Solution Cell Proliferation Assay (Promega) according to the manufacturer's protocol. Absorbance was determined using the PHERAstar microplate reader (BMG LABTECH).

For assays with PD173074 treatment, SUM185PE cells and MDA-MB-468 cells were seeded into 6 well plates and cultured for 7 days with an 80% end point confluence. Cell numbers were obtained via direct cell counting. Cells were washed with 1x PBS then trypsinized at 37 °C in a 5% CO<sub>2</sub> atmosphere until detachment. Trypsinized cells were then resuspended thoroughly in complete media to inhibit trypsin. Cells were stained with Trypan blue (EVS-1000, NanoTek), then transferred to an EVE cell counting slide (EVS-1000, NanoTek) and counted with the EVE automatic cell counter (EVE-MC-DEMO, NanoTek) according to the manufacturer's protocol.



### PD173074 treatment

The selective small molecule inhibitor of FGFR1–3, PD173074 (Apex Biotech), was reconstituted in DMSO. For Western blotting, cells were treated with 5–1000 nM PD173074 for the indicated time before lysing in RIPA buffer. For viability assays, cells were treated with PD173074 24 h post seeding and viability determined at the indicated days.

### siRNA knockdown

In 96 well plate format, 7000 SUM185PE cells were reverse transfected with 0.15  $\mu$ L of DharmaFECT1 (Dharmacon RNAi Technologies, Horizon Discovery). Media were changed 24 h later, replaced again at 96 h and the experiment ended at 144 h post transfection. 8000 CAL51 cells were reverse transfected with 0.1  $\mu$ L of lipofectamine 3000 (ThermoFisher Scientific), 5000 MDA-MB-231 cells with 0.1  $\mu$ L of DharmaFECT4 (Dharmacon RNAi Technologies, Horizon Discovery) and 10,000 MFM223 cells with 0.1  $\mu$ L of DharmaFECT3 (Dharmacon RNAi Technologies, Horizon Discovery). Media were changed 24 h later and the experiment ended at 96 h post transfection. In 6 well plate format, 360,000 SUM185PE cells, 300,000 CAL51 cells, 300,000 MFM223 cells and 90,000 MDA-MB-231 cells were reverse transfected with 3  $\mu$ L of the corresponding lipid as previously mentioned. Media were changed 24 h later and the experiment ended at 72 h post transfection.

The FGFR3-TACC3 fusion and wildtype FGFR3 were knocked down together using ON-TARGETplus human FGFR3 set of 4 individual siRNAs labelled as FW 1–4 (Dharmacon RNAi Technologies, Horizon Discovery, Q-003133-00). Wildtype FGFR3 expression was knocked down using 3 individual custom FGFR3 siRNAs from Bioneer with the following sequence: GAGGAAAGG CUGGUACAA (W1), CACAUGUCCAGCACCUUGU (W2) and GAUGCUGUGUAUAUGGUUAU (W3). The ON-TARGETplus non-targeting SMARTpool (siOTP-NT) was used as the control (Dharmacon RNAi Technologies, Horizon Discovery, D-001810-10). All siRNAs were used at a final concentration of 20 nM.

### Quantification and statistical analysis

Quantification by densitometry was performed using ImageLab version 5.2.1 (Bio-Rad) and statistical *t*-tests were performed using GraphPad Prism 8 and Microsoft-Excel.

## Results

### Expression and phosphorylation of FGFRs and FGFR3-TACC3 fusion protein in TNBC cell lines

To identify potential therapeutic targets in TNBC, global MS-based phosphotyrosine profiling was undertaken. First, a data-dependent acquisition (DDA) workflow was

used to generate a spectral library, with 2287 phosphotyrosine sites identified across the 24 TNBC cell lines. Then a hyper-reaction monitoring data-independent acquisition (HRM-DIA) workflow was utilized to quantitatively profile tyrosine phosphorylation patterns across this panel. Since FGFRs are implicated in cancer, including breast cancer, and represent candidate therapeutic targets, we extracted data for specific FGFR phosphorylation sites from this dataset (Fig. 1a, Additional file 2: Table S1). In addition, a panel of 11 TNBC cell lines was selected and subjected to Western blot analysis using selective FGFR antibodies (Fig. 1b). FGFRs resolve as a doublet (FGFR2 and FGFR4) or a triplet (FGFR1 and FGFR3) upon SDS-PAGE due to post-translational modifications (Fig. 1b). Overall, the results revealed high activation and expression of specific FGFRs, highlighting them as potential oncogenic drivers and therapeutic targets in TNBC.

Moderate FGFR1 phosphorylation was observed in BT549, CAL51, HS578T and MFM223 cells, and low phosphorylation in an additional 5 cell lines (Fig. 1a). High FGFR1 expression was detected by Western blotting in CAL120 cells and low to moderate levels in a further 6 cell lines (Fig. 1b). The results for the CAL120 cell line indicate that high FGFR1 expression may not be accompanied by detectable tyrosine phosphorylation (Fig. 1-1a-b).

High FGFR2 phosphorylation was detected in MFM223 cells, moderate phosphorylation in BT549 and low phosphorylation in an additional 9 cell lines (Fig. 1a). High FGFR2 expression was detected in MFM223 cells, and low expression detected in 3 cell lines (Fig. 1b). The results indicate that high FGFR2 phosphorylation correlates with high FGFR2 expression in MFM223 cells (Fig. 1-1a-b).

Moderate FGFR4 phosphorylation was detected in MDA-MB-453 and MFM223 cells (Fig. 1a), and low phosphorylation in SUM185PE cells (Fig. 1a). High and moderate FGFR4 expression was detected in the first two cell lines, respectively (Fig. 1b).

High FGFR3 expression and phosphorylation was detected in SUM185PE cells. In addition, moderate phosphorylation was detected in CAL51 cells and low phosphorylation in an additional 3 cell lines (Fig. 1-1a-b). The SUM185PE cell line harbors a FGFR3-TACC3 fusion [34], and interrogation of our phosphoproteomic dataset revealed that SUM185PE cells were the only TNBC cell line to exhibit tyrosine phosphorylation of TACC3, likely reflecting autophosphorylation of the fusion protein, and the TACC3 interactor CKAP5 (Additional file 2: Table S2 and Figure 1). To distinguish between the FGFR3-TACC3 fusion and the wildtype FGFR3, two antibodies were used (Fig. 1c). FW FGFR3 detects the region of FGFR3 between amino acid 25–

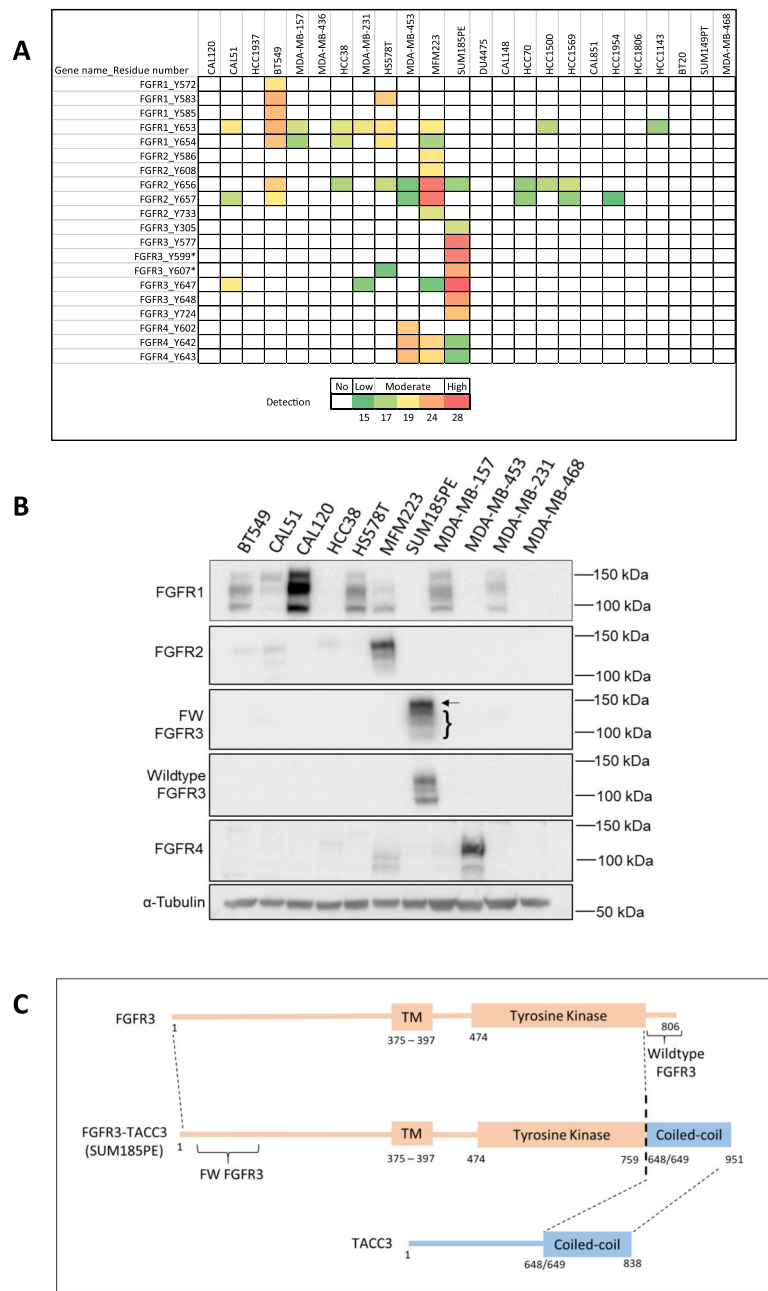


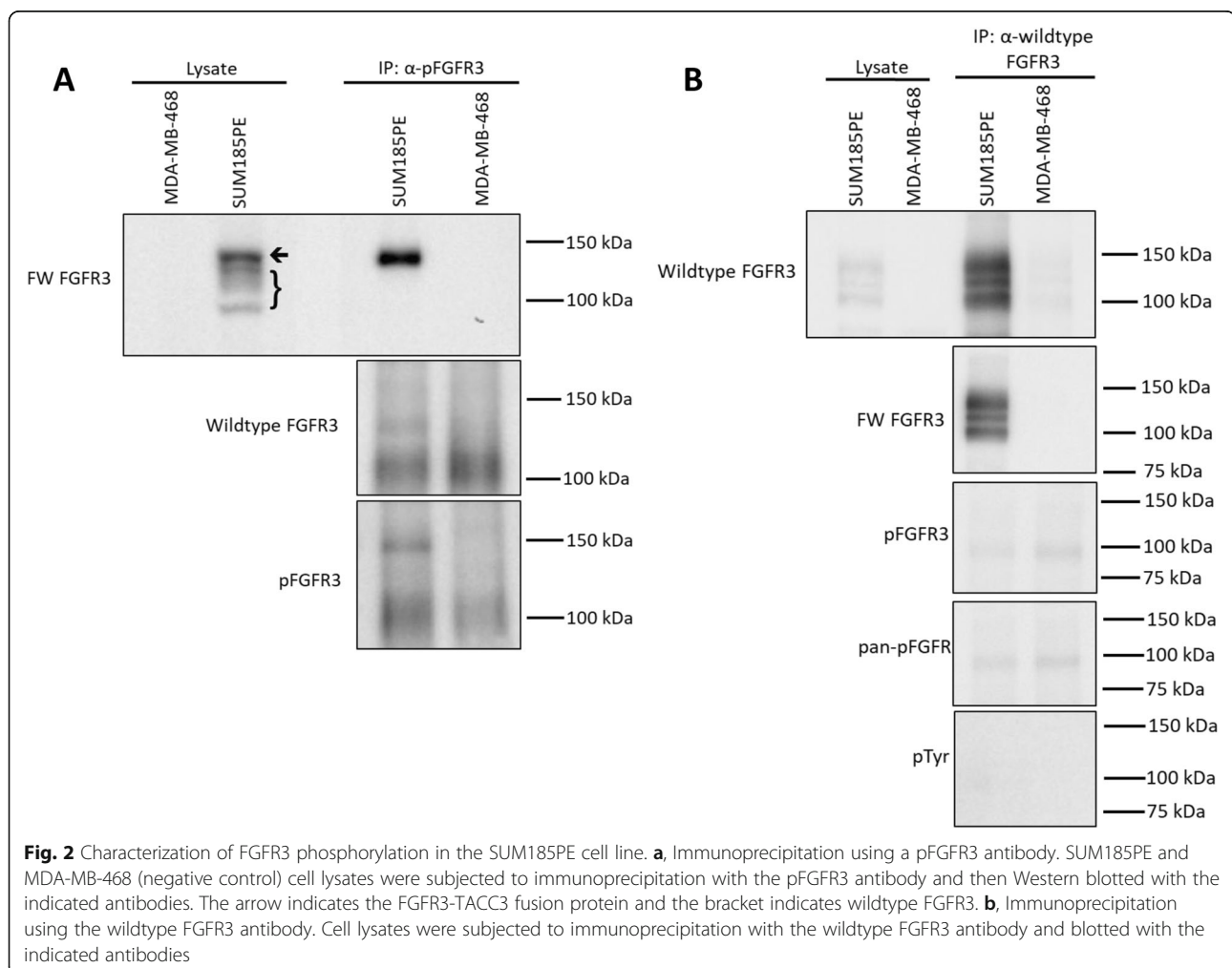
**Fig. 1** FGFR expression and phosphorylation signature in TNBC cell lines as determined by MS-based tyrosine phosphorylation profiling. **a**, Relative normalized abundance of FGFR1–4 phosphorylated tyrosine (pY) residues based on z-score across a panel of 24 TNBC cell lines. The z-scores of detectable tyrosine-phosphosites were obtained by subtracting the mean of all pY sites across the 24 TNBC cell line panel from the value for the pY site, and then dividing by the standard deviation of all 24 TNBC cell lines. The white box represents a non-detectable pY site. The asterisks indicate that FGFR3\_Y599 is identical to FGFR1 (Y605) while FGFR3\_Y607 is identical to FGFR2 (Y616), but the FGFR3 assignment is more likely given relative receptor expression levels. **b**, Characterization of FGFR1–4 expression in a panel of 11 TNBC cell lines. Cell lysates were Western blotted as indicated. Arrow indicates FGFR3-TACC3 fusion protein, bracket indicates wildtype FGFR3. **c**, Schematic of FGFR3-TACC3 fusion protein adapted from Shaver et al. (2016). The protein structure of wildtype FGFR3 is shown in pink and wildtype TACC3 is shown in blue. The grey dotted lines highlight the junction between FGFR3 and TACC3, which forms the FGFR3-TACC3 fusion protein in the SUM185PE cell line. FW FGFR3 antibody detects the region of FGFR3 between amino acids 25–124, recognising both wildtype FGFR3 and the FGFR3-TACC3 fusion protein. Wildtype FGFR3 antibody detects FGFR3 at the C-terminal region, only recognising wildtype FGFR3. TM = transmembrane

124, thereby recognising both wildtype FGFR3 and the FGFR3-TACC3 fusion protein (detected as a slower migrating band above the wildtype FGFR3) (Fig. 1-1b-c). The wildtype-FGFR3 antibody is selective for this form of the receptor as the epitope localizes at the C-terminal region (Fig. 1-1b-c). The results indicate that SUM185PE cells express high levels of wildtype FGFR3 as well as the FGFR3-TACC3 fusion (Fig. 1b). The presence of both wildtype FGFR3 and an oncogenic form, FGFR3-TACC3 fusion in SUM185PE cells, apparent FGFR3 activation in other TNBC cell lines, and the lack of information regarding FGFR3 signaling and function in TNBC, led us to focus on this receptor.

#### Tyrosine phosphorylation of wildtype FGFR3 and the FGFR3-TACC3 fusion in SUM185PE cells

Since the SUM185PE cell line demonstrated high expression of both wildtype FGFR3 and the FGFR3-TACC3 fusion (Fig. 1b), accompanied by high FGFR3 phosphorylation (Fig. 1a), it was necessary to determine the contribution of the two receptor forms to this

phosphorylation pattern. Tyrosine phosphorylated FGFR3 was enriched by immunoprecipitation using a selective antibody then blotted for FGFR3 using the two discriminatory antibodies (Fig. 2a). In this study, the MDA-MB-468 cell line with undetectable FGFR expression and phosphorylation (Fig. 1-1a-b) was used as a negative control. In the SUM185PE lysate enriched for tyrosine phosphorylated FGFR3, a band of the same mobility as the FGFR3-TACC3 fusion was readily detected when immunoblotted with the FW-FGFR3 antibody (Fig. 2a). A faint band was detected with the wildtype FGFR3 antibody (Fig. 2a). However, using this approach, wildtype FGFR3 may be co-purified in the pFGFR3 fraction, but not be directly tyrosine phosphorylated. To confirm the faint band detected in the wildtype FGFR3 blot in Fig. 2a, wildtype FGFR3 was enriched and blotted for phosphorylation using pFGFR3, pan-pFGFR and pTyr antibodies (Fig. 2b). No additional bands were observed in these blots compared to the negative control, indicating phosphorylation of wildtype FGFR3 was undetectable by this approach (Fig. 2b). These results



indicate that the FGFR3-TACC3 fusion must contribute to the majority of phosphorylated FGFR3 in SUM185PE cells.

#### The FGFR3-TACC3 fusion predominantly localizes to the cytoplasm and plasma membrane

TACC3 is a microtubule-associated protein that regulates mitotic spindle organization and stabilization, with the C-terminal coiled-coil domain of TACC3

mediating localization to the mitotic spindle [38, 43]. In glioblastoma, the FGFR3-TACC3 fusion was demonstrated to localize at the mitotic spindle poles in dividing cells, causing chromosomal segregation defects and triggering aneuploidy [35]. Furthermore, fractionation studies in MCF7 cells showed strong FGFR3-TACC3 fusion localisation to the nucleus [44]. However, a later study demonstrated that entry into the secretory pathway or plasma membrane localization was essential for cell

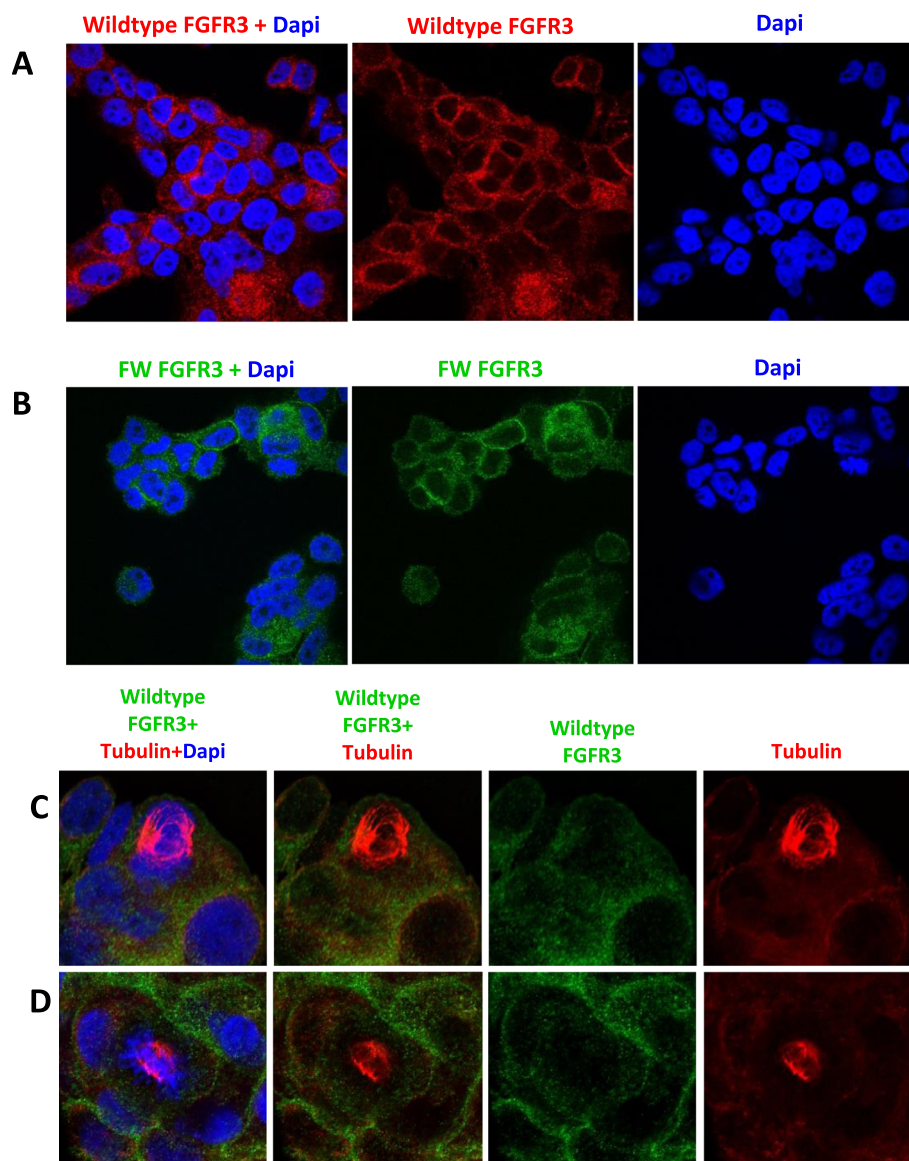


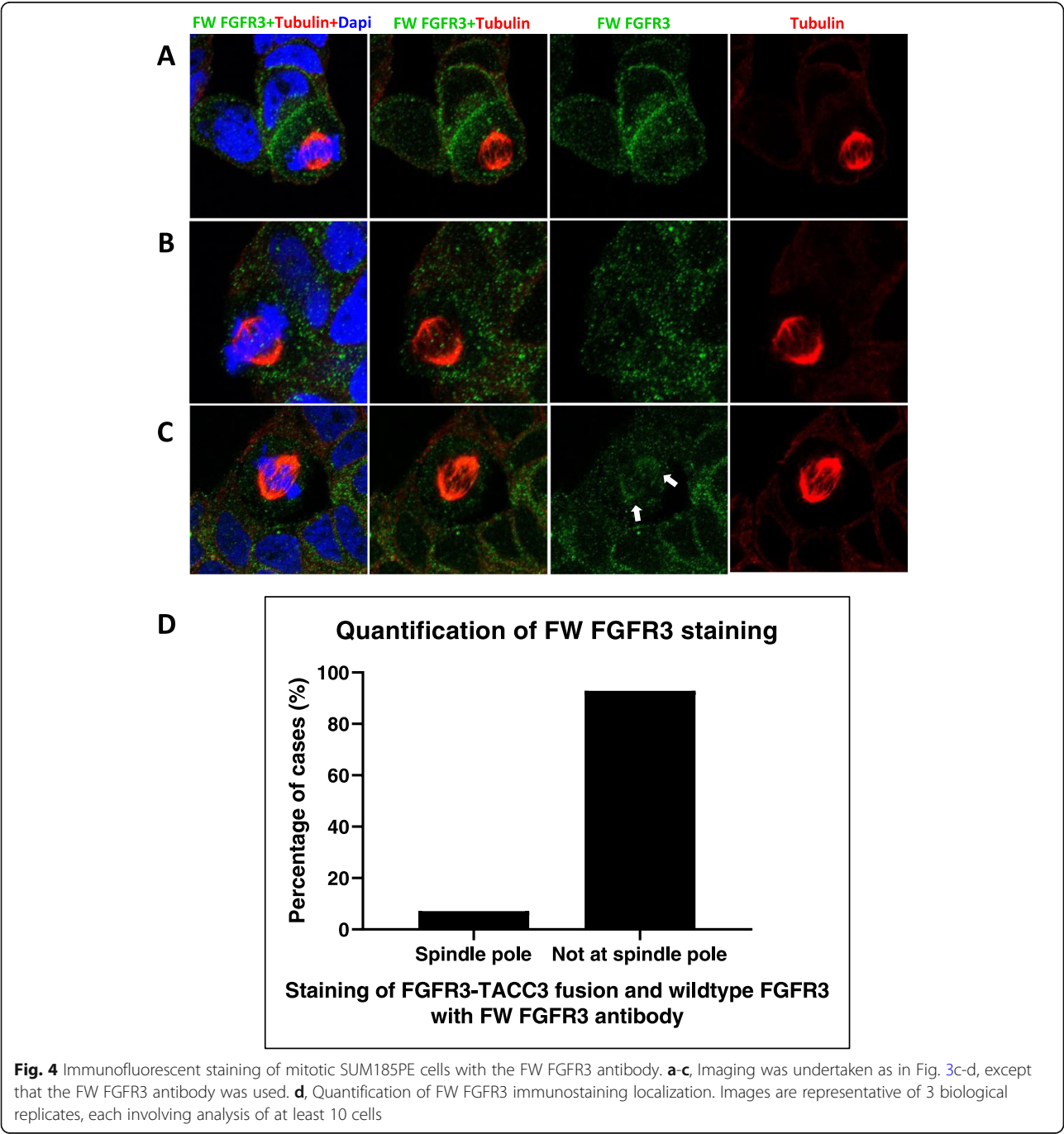
**Fig. 3** Localization of FGFR3-TACC3 fusion and wildtype FGFR3 by immunofluorescent staining in SUM185PE cells. SUM185PE cells were fixed and permeabilised then immunostained with **a**, wildtype FGFR3 antibody or **b**, FW FGFR3 antibody detecting both FGFR3-TACC3 fusion and wildtype FGFR3. Dapi was used to stain DNA of the cells. Images were obtained by confocal microscopy and are representative of 3 biological replicates, each involving analysis of at least 10 cells. **c** and **d**, representative images for immunostaining with the wildtype FGFR3 antibody in mitotic SUM185PE cells. For spindle visualisation, SUM185PE cells were treated with 3 mM of thymidine to halt cell cycle progression at the G1/S phase, and then released into complete media to allow cells to undergo mitosis. Tubulin immunostaining was used to visualize the mitotic spindle



transformation by the FGFR3-TACC3 fusion [45]. Furthermore, in HeLa cells, the FGFR3-TACC3 fusion was found to localize outside the spindle region in membrane vesicles, causing mitotic defects by removing wildtype TACC3 from the mitotic spindle [38]. These findings indicate that the localization and mechanism of FGFR3-TACC3 fusion may vary according to cancer type and cellular context. Consequently, it was important to address the subcellular

localization of the FGFR3-TACC3 fusion in SUM185PE TNBC cells.

Use of the wildtype FGFR3 and FW FGFR3 antibodies for indirect immunofluorescent imaging revealed immunoreactivity in the cytoplasm and plasma membrane (Fig. 3-3a-b). In addition, SUM185PE cells undergoing mitosis were co-stained with tubulin antibodies and the wildtype FGFR3 or FW FGFR3 antibodies (Fig. 3-3, 4-4c-d, a-c). SUM185PE cells stained with the wildtype



FGFR3 antibody only showed localization at the cell membrane and in the cytoplasm (Fig. 3-3c-d). However, upon use of the FW FGFR3 antibody, while the vast majority of dividing SUM185PE cells exhibited immunostaining at the cell membrane and in the cytoplasm (Fig. 4-4, 4a-b, d), 2 out of 28 cells examined (7%) exhibited additional localization at the mitotic spindle (Fig. 4-4c-d). Given the data obtained using the wildtype FGFR3 antibody (Fig. 3-3c-d), this indicates that the additional staining must arise from the FGFR3-TACC3 fusion. Overall, these data indicate that the previously reported localization of FGFR3-TACC3 to the mitotic spindle

[35] occurs, but is not a common event in this TNBC model.

Wildtype FGFR3 and the FGFR3-TACC3 fusion exhibit contrasting functional roles in SUM185PE cells

To characterize the contribution of wildtype FGFR3 and the FGFR3-TACC3 fusion, knockdowns were undertaken with siRNAs that target both the FGFR3-TACC3 fusion and wildtype FGFR3 (FW FGFR3) or only wildtype FGFR3. Knockdown of both FGFR3-TACC3 fusion and wildtype FGFR3 expression decreased phosphorylation of the downstream signaling proteins FRS2, AKT

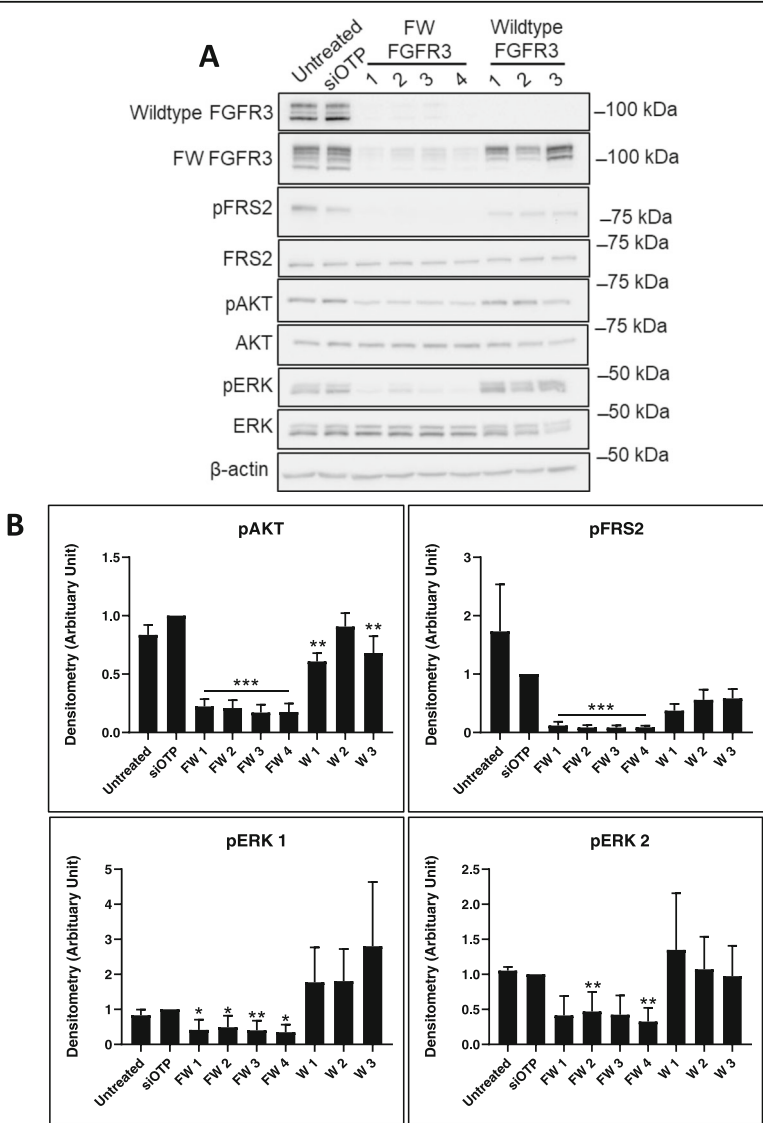


**Fig. 5** Effect of FGFR3 knockdown on downstream signaling in SUM185PE cells. **a**, SUM185PE cells were reverse transfected with 20 nM of individual siRNAs targeting FGFR3-TACC3 fusion and wildtype FGFR3 (FW FGFR3 1–4), or wildtype FGFR3 only (W1–3), and the indicated downstream signaling proteins analysed by Western blot. **b**, Quantification by densitometry of (A). Data were first normalized relative to the β-actin loading control, then phosphorylated proteins were normalized relative to total protein, then data were expressed relative to the siOTP control which was arbitrarily set at 1.0. Error bars: mean ± standard error, of three biological replicates. \* indicates *p*-value of < 0.05, \*\* < 0.01, \*\*\* < 0.001

and ERK, and induced cell death in SUM185PE cells (Figs. 5–6). In contrast, knockdown of wildtype FGFR3 reduced activation of AKT, but not FRS2 and ERK, and resulted in a trend for decreased cell proliferation (Figs. 5–6).

In order to further evaluate these forms of FGFR3 as potential therapeutic targets, we also determined the effects of the small molecule inhibitor PD173074 on signaling and proliferation. This is an ATP-competitive and type-I inhibitor, which targets FGFR1–3 and to a lesser extent, VEGFR2. It has a similar binding mode to other FGFR inhibitors that are in clinical trials (e.g. Erdafitinib, BGJ398, Pemigatinib and Dovitinib). Its selectivity for FGFR1–3 is similar to that of BGJ398 and Pemigatinib, but is much greater than that of Dovitinib, which is a multikinase inhibitor that also targets VEGFRs, PDGFR- $\beta$ , c-kit and FLT3 and is likely to elicit differing biological effects [46, 47]. Treatment of SUM185PE cells with 5–75 nM PD173074 for 1 h led to a significant reduction in the phosphorylation of AKT, ERK1/2 and FRS2, with AKT phosphorylation being the most sensitive to drug treatment (Fig. 7).

In addition, administration of PD173074 for 24–72 h resulted in decreased expression of Cyclin A and pRb, and detection of cleaved PARP (Fig. 8a). Treatment with PD173074 also decreased SUM185PE cell proliferation

in a dose-dependent manner, while no effect was observed in the negative control cell line MDA-MB-468 (Fig. 8b). Overall, these data indicate that the FGFR3-TACC3 fusion, and not wildtype FGFR3, is the main oncogenic driver in SUM185PE cells, and that targeting this oncoprotein leads to cell cycle arrest in the G1 phase of the cell cycle and also apoptosis.

#### Functional role of FGFR3 in TNBC cell lines with low to moderate levels of FGFR3 phosphorylation

Three cell lines exhibited low to moderate FGFR3 phosphorylation in the phosphoproteomic dataset on sites specific to FGFR3: MDA-MB-231, MFM223 and CAL51 (Fig. 1a). Since FGFR3 was undetectable in these cells by direct Western blot (Fig. 1b, Fig. 9a), lysates were subjected to immunoprecipitation to enrich for FGFR3 and the receptor detected by Western blot using the FW FGFR3 antibody (Fig. 9a). This confirmed that each of these cell lines indeed expresses FGFR3, with the identity of the receptor validated by siRNA knockdown (Fig. 9b). However, FGFR3 knockdown did not significantly affect cell proliferation in any of the cell lines (Fig. 9c), indicating that the oncogenic role of FGFR3 in TNBC is likely limited to contexts where it is hyperactivated due to mutation or gene translocation events.

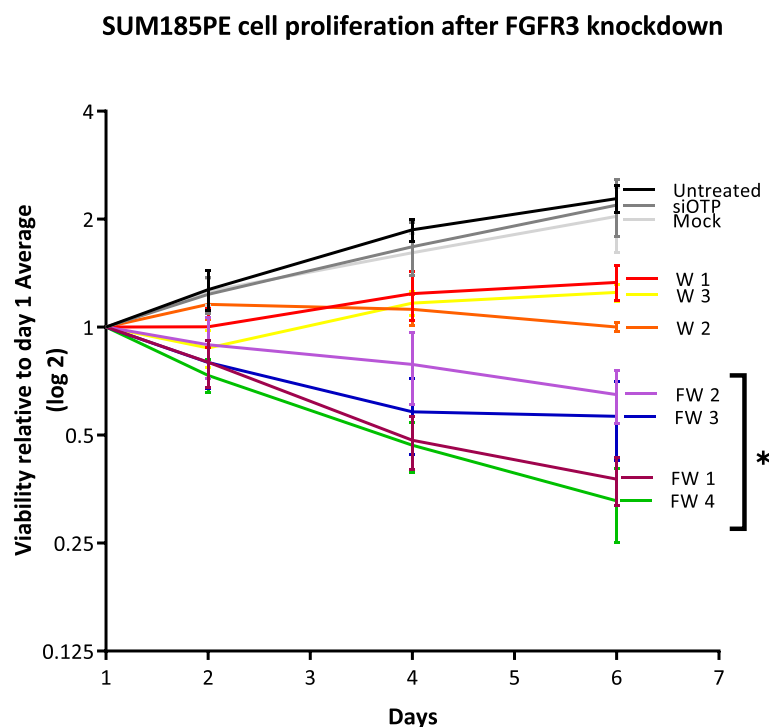


**Fig. 6** Effect of FGFR3 knockdown on SUM185PE cell proliferation. SUM185PE cells were reverse transfected with 20 nM of individual siRNAs targeting FGFR3-TACC3 fusion and wildtype FGFR3 (FW 1–4), or wildtype FGFR3 only (W1–3) and cell proliferation indirectly assayed via MTS absorbance. Error bars: mean  $\pm$  standard error, of three biological replicates. W1, W2 and W3 were associated with  $p$ -values of 0.17, 0.07, and 0.13, respectively. \* indicates  $p$ -value of  $< 0.05$

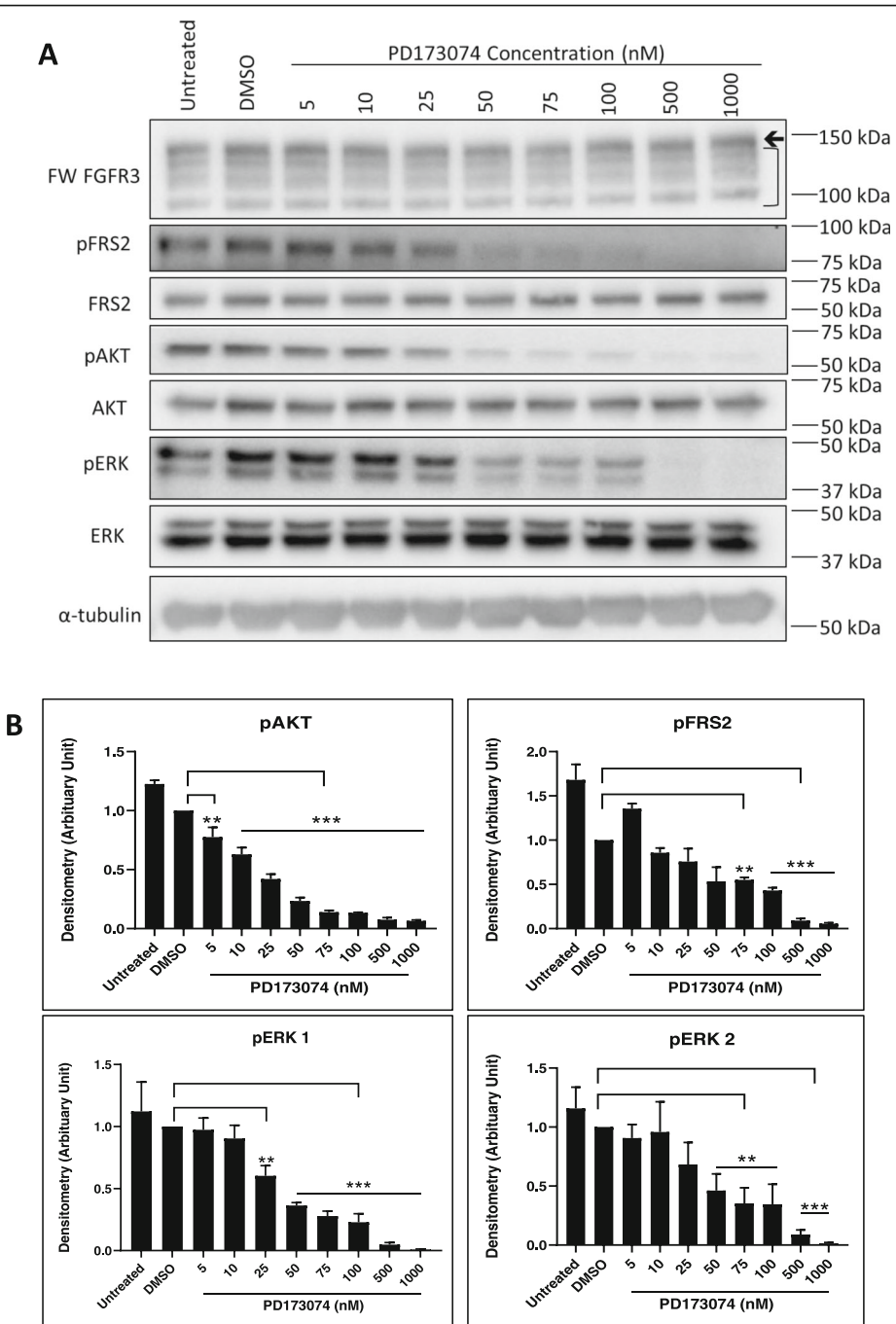


**Fig. 7** Dose dependent effect of the FGFR inhibitor PD173074 on FGFR3 downstream signaling pathways in the SUM185PE cell line. **a**, Expression/activation of downstream signaling proteins 1 h post-treatment with the indicated doses of PD173074. Arrow indicates FGFR3-TACC3 fusion protein, bracket indicates wildtype FGFR3. **b**, Quantification by densitometry of (A). Data were first normalized relative to the tubulin control, then phosphorylated proteins were normalized to total protein, finally data were expressed relative to the DMSO control which was arbitrarily set at 1.0. Error bars: mean  $\pm$  standard error, of three biological replicates. \*\* indicates  $p$ -value of  $< 0.01$ , \*\*\*  $< 0.001$

**Evaluation of FGFR3 alterations in breast cancer patients using public datasets**

The TCGA and the Metabric datasets were analyzed using cBioportal to determine the frequency of FGFR3 alterations in terms of overexpression, mutation,

amplification and deletion in different breast cancer subtypes. In the TCGA and Metabric datasets, 43 out of 994 (4%) and 56 out of 1904 (3%) of breast cancer patients have FGFR3 alterations, respectively (Fig. 10a-b). FGFR3 amplification, which affected 5 breast

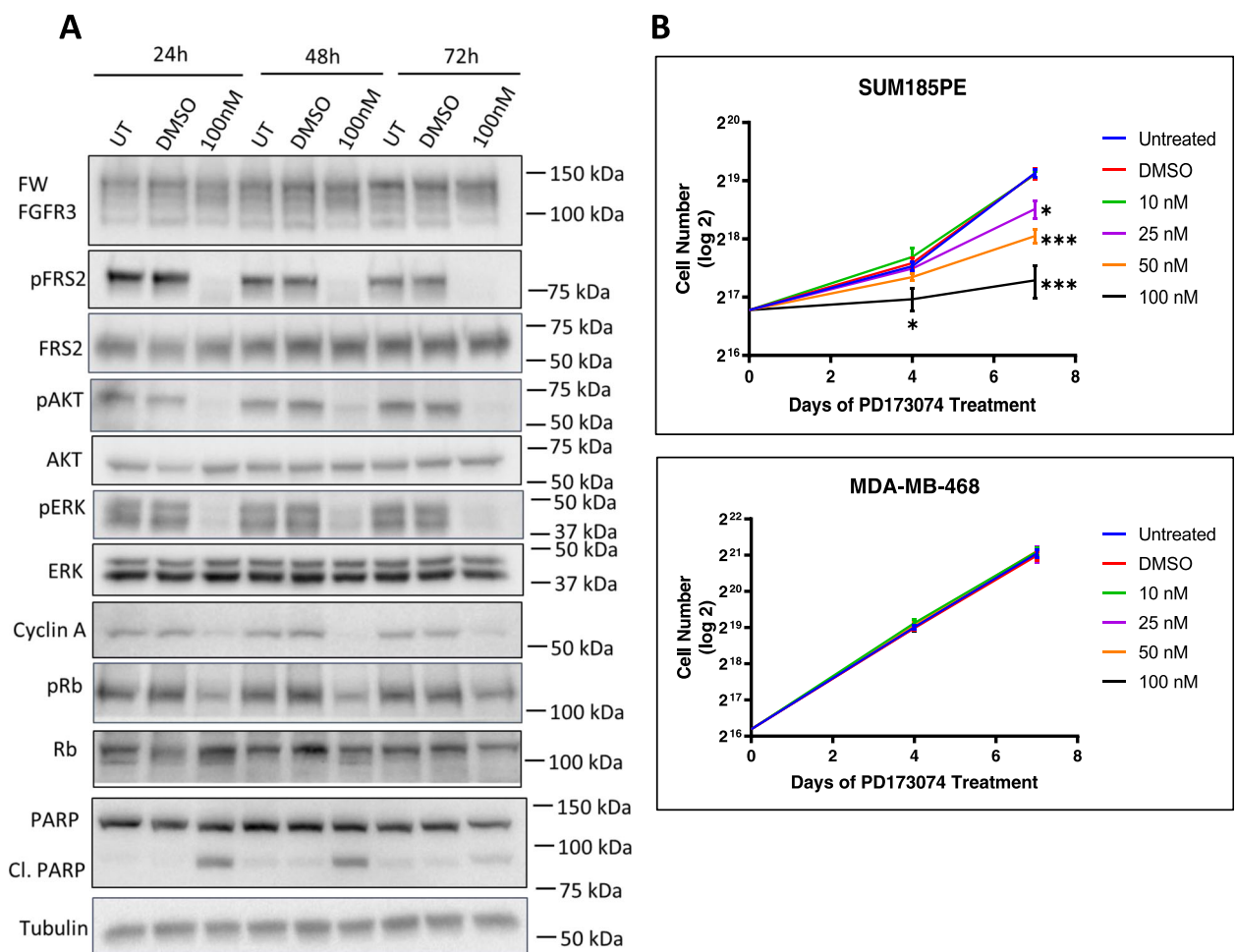


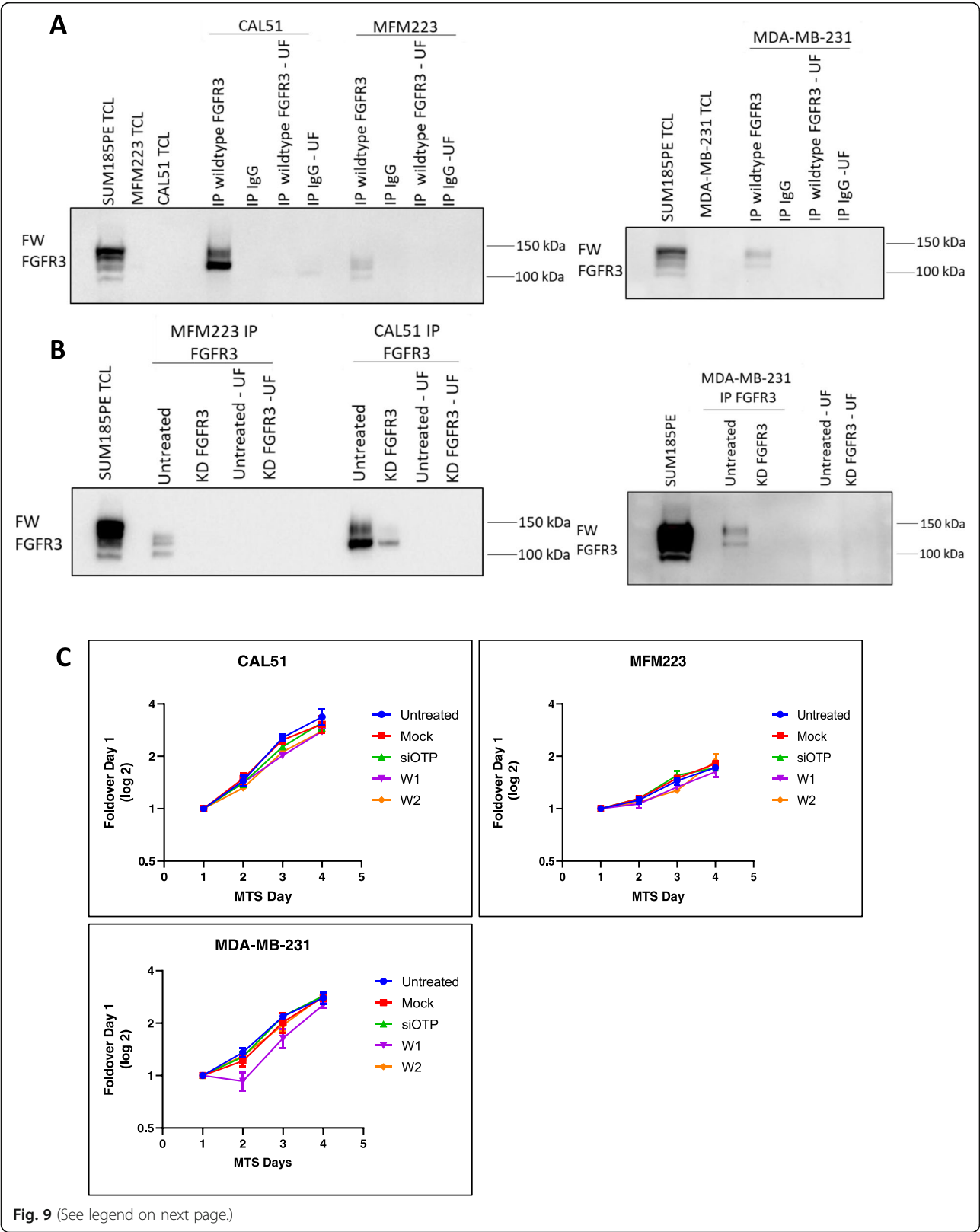
**Fig. 8** Effect of PD173074 on proliferation and apoptosis in SUM185PE cells. **a**, Effect on cell cycle and apoptosis markers. SUM185PE cells were treated with PD173074 for 24 h, 48 h and 72 h and the effect on the indicated proteins analysed by Western blotting. UT indicates 'untreated group' as a control for DMSO addition, in order to monitor any effect of DMSO on cell cycle regulators. **b**, Effect of PD173074 on proliferation of SUM185PE and MDA-MB-468 cells. Cell proliferation was determined by direct cell counting. Error bars: mean  $\pm$  standard error, of three biological replicates \* indicates  $p$ -value of  $< 0.05$ , \*\*\*  $< 0.001$

cancer patients (0.5%) and 9 cases (0.5%) in the TCGA and Metabric datasets respectively, was observed in the TNBC/basal, luminal A and luminal B subtypes, with FGFR3 deep deletion mostly detected in the TNBC/basal or HER2+ subtypes (Fig. 10-10a-b). FGFR3 overexpression was more common in luminal subtypes than TNBC/basal. In the Metabric dataset, breast cancer patients with amplified and/or overexpressed FGFR3 (46 out of 1903, 2%) have a significant ( $p$ -value of 0.0204) worse overall survival compared to breast cancer patients without FGFR3 alterations (Fig. 10c). These data confirm that potentially oncogenic FGFR3 alterations do occur in TNBC, as well as other breast cancer subtypes, albeit at low frequency.

## Discussion

FGFR signaling has many biological roles in normal physiology, including regulation of cell proliferation, migration and survival, however in breast cancer progression, FGFR signaling is often deregulated [24, 33]. FGFR1 amplification is the most common aberration, followed by FGFR2 amplification, and the roles of these receptors have been characterized in detail [23, 28, 30]. To date, our work is the most detailed study on FGFR3, describing its activation, expression and function in TNBC.

Our characterization of FGFR3 function in TNBC cell lines exhibiting differing levels of receptor activation demonstrated that only the aberrantly activated FGFR3-TACC3 fusion in SUM185PE cells functioned as an





(See figure on previous page.)

**Fig. 9** Expression and function of FGFR3 in TNBC cell lines exhibiting low-moderate FGFR3 phosphorylation. **a**, FGFR3 expression analysed by immunoprecipitation and Western blot. Lysates from CAL51, MFM223 and MDA-MB-231 cells were subjected to immunoprecipitation of wildtype FGFR3, which was then detected by Western blotting using the FW FGFR3 antibody. IgG was used as a negative control for immunoprecipitation. TCL = total cell lysate. UF = unbound fraction. **b**, Confirmation of FGFR3 expression by knockdown. Cell lines from (A) were subjected to FGFR3 knockdown prior to immunoprecipitation and Western blot analysis. KD = knockdown. **c**, Effect of FGFR3 knockdown on cell proliferation. Cells were transfected with 20 nM of individual siRNAs targeting wildtype FGFR3 (W1–2) and cell proliferation indirectly assayed via a MTS absorbance assay. Error bars: mean  $\pm$  standard error, of three biological replicates

oncogenic driver, at least in vitro. This fusion is constitutively activated due to dimerization driven by the TACC3 region [35, 38].

Knockdown of wildtype FGFR3 in SUM185PE cells resulted in modest effects on AKT activation and cell proliferation, while having no effect on MFM223, CAL51 and MDA-MB-231 cell proliferation. Since expression of wildtype FGFR3 is higher in SUM185PE cells than the other cell lines, this suggests that a threshold level of expression/activation is required for detectable effects on signaling and proliferation. However, other factors that likely limit the biological role of FGFR3 in TNBC cell lines are the genetic background of the cells, and production of autocrine ligands. MFM223 cells exhibit FGFR2 amplification, which may make FGFR3 redundant. CAL51 cells express detectable FGFR1 and FGFR2

as well as autocrine FGF2 and are sensitive to PD173074 [33]. Therefore, these data and our phosphoproteomic and functional analyses, indicate that FGFR1 and FGFR2 must play a more important functional role in these cells, rather than FGFR3. However, MDA-MB-231 cells are resistant to PD173074 and express very low levels of FGF2 [33] that will limit activation of expressed FGFRs. In light of the latter finding, it remains possible that the oncogenic potential of FGFR3 may be different in vivo, where cancer cells are exposed to paracrine FGFs from the stroma.

This report is the first study of FGFR3-TACC3 signaling and localization in the context of breast cancer. Consistent with previous studies on head and neck malignancies [37] and glioblastoma [35, 48], attenuation of FGFR3-TACC3 activation decreased phosphorylation of

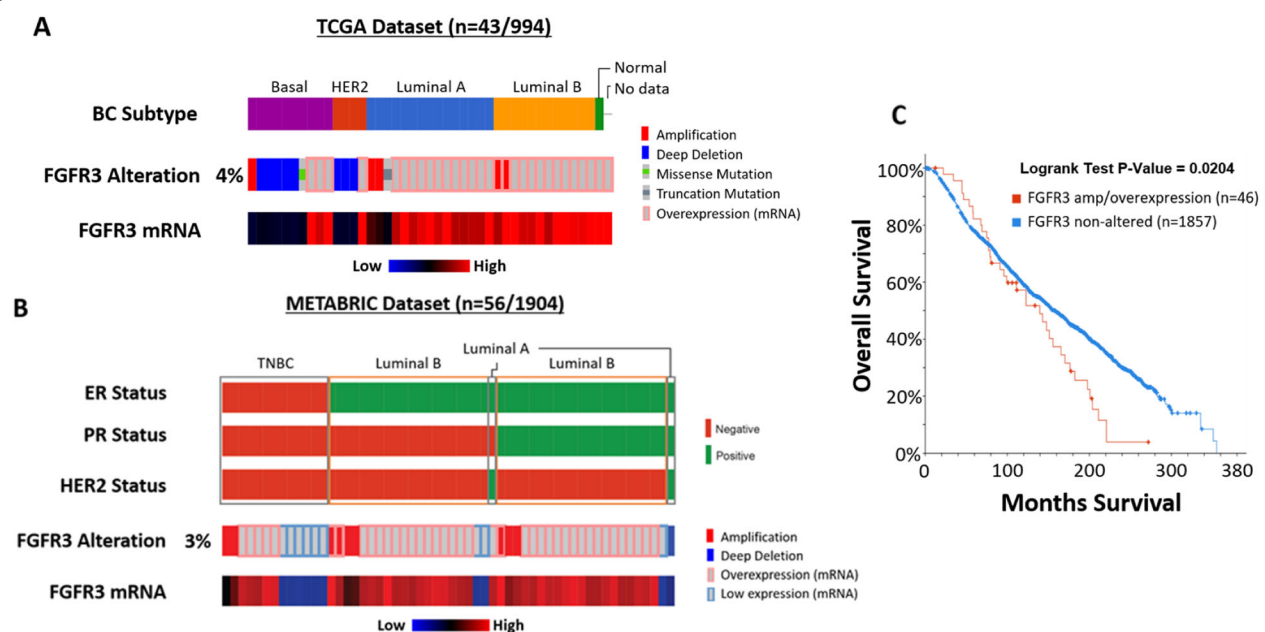


**Fig. 10** FGFR3 alterations in human breast cancer. Frequency of FGFR3 alterations in breast cancer patients analysed using two breast cancer patient datasets, **a**, Pan-cancer Atlas dataset from TCGA and **b**, METABRIC dataset, using cBioportal (note that no mutation data are available for the METABRIC dataset). Only patients with FGFR3 alterations are displayed for brevity. For both cohorts, the breast cancer subtypes based on ER/PR and HER2 receptor status are displayed. **c**, A Kaplan–Meier plot showing patients with amplification and/or overexpression of FGFR3 ( $n = 46$ ) are significantly associated with worse overall survival compared to those without these alterations ( $n = 1857$ ) in the METABRIC dataset. A Logrank test was used,  $P$ -value = 0.0204 ( $P$ -value < 0.05 considered significant). Survival data for the two patient groups were extracted and downloaded from cBioportal, and survival analysis performed using in-house Matlab script

FRS2, AKT and ERK. However, while in glioblastoma, the FGFR3-TACC3 fusion reportedly localizes to the mitotic spindle poles [35], we observed that the vast majority of FGFR3-TACC3 fusion and all of wildtype FGFR3 localized to the cytoplasm and plasma membrane, consistent with data from HeLa cells [38], the requirement for entry into the secretory pathway or localization to the plasma membrane for FGFR3-TACC3 oncogenic function [45] and coupling of FGFR3-TACC3 to canonical downstream signaling pathways usually activated at the plasma membrane. That said, the occasional detection of FGFR3-TACC3 at the spindle poles indicates that this still represents a potential mechanism whereby this oncoprotein may contribute to tumor progression, for example by promoting aneuploidy in a small subpopulation of cells [35].

In the TCGA and Metabric datasets, FGFR3 alterations are observed in a total of 99 out of 2898 breast cancer patients (3.4%), with 16 out of 2898 (0.6%) cases reflecting FGFR3 amplification or mutation (Fig. 10-10a-b). Other studies support the presence, albeit at low frequency, of FGFR3 alterations in breast cancer. In a study of 182 ER+ breast cancer patients, FGFR3 was mutated in 3 out of 126 (2.4%) primary samples and 1 out of 57 (1.8%) metastatic samples [49]. In addition, a FGFR3-TACC3 fusion was detected in 1 out of 253 TNBC tumors (0.4%) [34]. Despite low frequencies, therapeutic targeting of FGFR3 represents a potential option for cancers exhibiting oncogenic forms of FGFR3, supported by our data regarding the efficacy of PD173074 in SUM185PE cells.

In addition to FGFR3 amplification, deep deletions of FGFR3 occur (Fig. 10-10a-b). This has also been observed in inflammatory breast cancer, where 10 out of 156 (6.4%) cases had FGFR3 deletion [50]. The loss of FGFR3 is significantly associated with higher grade urothelial bladder tumors [51] and also leads to chondroma-like lesion formation by downregulating ERK signaling whilst upregulating Hedgehog signaling, suggesting tumor suppressive roles of FGFR3 [52]. Furthermore in pancreatic cancer, where FGFR3 expression is downregulated, FGFR3 functions as a tumor suppressor in cancer cells of epithelial phenotype and an oncogene in cells of mesenchymal phenotype, highlighting context-dependent functional roles [53]. Despite the presence of FGFR3 deletions in a subset of breast cancer patients, amplification and/or overexpression of FGFR3 is associated with poor prognosis in the Metabric dataset, and an immunohistochemical study in breast cancer also identified FGFR3 as a negative prognostic factor [54]. Consequently, while the presence of FGFR3 deletions raises the possibility of context-dependent tumor suppressor roles in a subset of breast cancers, strong evidence also exists for a positive role for this receptor in breast cancer progression.

## Conclusions

Increased expression and activation of FGFR3 occurs in TNBC but an oncogenic role could only be demonstrated for a rare example of a FGFR3-TACC3 fusion. These results indicate that targeting FGFR3 may represent a therapeutic option for TNBC, but only for a select group of patients with oncogenic FGFR3 alterations.

## Supplementary information

**Supplementary information** accompanies this paper at <https://doi.org/10.1186/s12964-019-0486-4>.

**Additional file 1: Figure S1.** Interactions of proteins exhibiting tyrosine phosphorylation specific to SUM185PE cell line using STRING software

**Additional file 2: Table S1.** Quantifiable FGFR tyrosine phosphorylated peptide expression (log2) identified across 24 TNBC cell lines **Table S2.** Quantifiable tyrosine phosphorylated peptide expression (log2) specific to SUM185PE cell line. Tyrosine phosphorylation of TACC3 (highlighted in pink) only occurs in SUM185PE

## Abbreviations

DDA: Data-dependent acquisition; ER: Estrogen receptor; FDR: False discovery rate; FGFR3: Fibroblast growth factor receptor 3; FRS2: Fibroblast growth factor receptor substrate 2; HER-2: Human epidermal growth factor receptor-2; HRM-DIA: Hyper-reaction monitoring data-independent acquisition; iRT: Indexed Retention Time; LC-MS/MS: Liquid chromatography-tandem mass spectrometry; MS: Mass-spectrometry; PR: Progesterone receptor; RTK: Receptor tyrosine kinase; TACC3: Transforming acidic coiled-coil protein 3; TCGA: The cancer genome atlas; TNBC: Triple negative breast cancer

## Acknowledgments

This manuscript has been read and approved by all the authors for publication and has not been submitted and is not under consideration for publication elsewhere. The authors acknowledge the Monash Biomedical Proteomics Facility, Monash University, for the provision of mass spectrometry instrumentation, training and technical support.

## Author's contribution

Conception and design: RD, RL. Development of methodology: NC, EN, SS, KN, LN, JL, KS, RL, RD. Acquisition of data: NC, EN, SS, KN, HC, LN, JL, KS, RL. Analysis and interpretation of data (e.g., statistical analysis, biostatistics, computational analysis): NC, EN, KN, LN, JL, KS, RL, RD. Writing, review, and/or revision of the manuscript: NC, EN, RL, RD. Study supervision: RD, RL. All authors read and approved the final manuscript.

## Funding

RJD was supported by a NHMRC Fellowship (1058540). This work was supported by a Venture Grant from Cancer Council Victoria. The Victorian Centre for Functional Genomics (K.J.S.) is funded by the Australian Cancer Research Foundation (ACRF), the Australian Phenomics Network (APN) through funding from the Australian Government's National Collaborative Research Infrastructure Strategy (NCRIS) program and the Peter MacCallum Cancer Centre Foundation.

## Availability of data and materials

All data generated or analysed during this study are included in this published article and its supplementary information files. The original data supporting these findings are available at any time upon request to the corresponding author.

## Competing interests

The authors declare that they have no competing interests.

## Author details

<sup>1</sup>Cancer Program, Biomedicine Discovery Institute, Monash University, Melbourne, VIC 3800, Australia. <sup>2</sup>Department of Biochemistry and Molecular Biology, Monash University, Melbourne, VIC 3800, Australia. <sup>3</sup>Sir Peter



MacCallum Department of Oncology, The University of Melbourne, Melbourne, VIC 3010, Australia. <sup>4</sup>Victorian Centre for Functional Genomics, Peter MacCallum Cancer Centre, Melbourne, VIC 3000, Australia.

Received: 10 October 2019 Accepted: 22 November 2019

## References

1. Ferlay J, et al. Cancer incidence and mortality worldwide: Sources, methods and major patterns in GLOBOCAN 2012. *Int J Cancer*. 2015;136(5):E359–86.
2. Reis-Filho JS, Tutt ANJ. Triple negative tumours: A critical review. *Histopathology*. 2008;52(1):108–18.
3. Schneider BP, et al. Triple-negative breast cancer: Risk factors to potential targets. *Clin Cancer Res*. 2008;14(24):8010–8.
4. Liedtke C, Rody A. New treatment strategies for patients with triple-negative breast cancer. *Curr Opin Obstet Gynecol*. 2015;27(1):77–84.
5. Mayer IA, et al. New strategies for triple-negative breast cancer-deciphering the heterogeneity. *Clin Cancer Res*. 2014;20(4):782–90.
6. van Roozendaal LM, et al. Risk of regional recurrence in triple-negative breast cancer patients: a Dutch cohort study. *Breast Cancer Res Treat*. 2016;156(3):465–72.
7. Lehmann BD, et al. Identification of human triple-negative breast cancer subtypes and preclinical models for selection of targeted therapies. *J Clin Invest*. 2011;121(7):2750–67.
8. Burstein MD, et al. Comprehensive genomic analysis identifies novel subtypes and targets of triple-negative breast cancer. *Clin Cancer Res*. 2015;21(7):1688–98.
9. Perez-Garcia J, et al. Targeting FGFR pathway in breast cancer. *Breast*. 2018;37:126–33.
10. Haugsten EM, et al. Roles of fibroblast growth factor receptors in carcinogenesis. *Mol Cancer Res*. 2010;8(11):1439–52.
11. Turner N, Grose R. Fibroblast growth factor signalling: From development to cancer. *Nat Rev Cancer*. 2010;10(2):116–29.
12. Dienstmann R, et al. Genomic aberrations in the FGFR pathway: Opportunities for targeted therapies in solid tumors. *Ann Oncol*. 2014;25(3):552–63.
13. Brooks AN, Kilgour E, Smith PD. Molecular pathways: Fibroblast growth factor signaling: A new therapeutic opportunity in cancer. *Clin Cancer Res*. 2012;18(7):1855–62.
14. Helsten T, et al. The FGFR landscape in cancer: Analysis of 4,853 tumors by next-generation sequencing. *Clin Cancer Res*. 2016;22(1):259–67.
15. Kim HR, et al. Co-clinical trials demonstrate predictive biomarkers for dolutinib, an FGFR inhibitor, in lung squamous cell carcinoma. *Ann Oncol*. 2017;28(6):1250–9.
16. Lim SH, et al. Efficacy and safety of dolutinib in pretreated patients with advanced squamous non-small cell lung cancer with FGFR1 amplification: A single-arm, phase 2 study. *Cancer*. 2016;122(19):3027–31.
17. Javle M, et al. Phase II study of BGJ398 in patients with FGFR-Altered advanced cholangiocarcinoma. *J Clin Oncol*. 2018;36(3):276–82.
18. Reis-Filho JS, et al. FGFR1 emerges as a potential therapeutic target for lobular breast carcinomas. *Clin Cancer Res*. 2006;12(22):6652–62.
19. Taberner J, et al. Phase I dose-escalation study of JNJ-42756493, an oral pan-fibroblast growth factor receptor inhibitor, in patients with advanced solid tumors. *J Clin Oncol*. 2015;33(30):3401–8.
20. Roidl A, et al. The FGFR4 Y367C mutant is a dominant oncogene in MDA-MB453 breast cancer cells. *Oncogene*. 2010;29(10):1543–52.
21. Penault-Llorca F, et al. Expression of FGF and FGF receptor genes in human breast cancer. *Int J Cancer*. 1995;61(2):170–6.
22. Neve RM, et al. A collection of breast cancer cell lines for the study of functionally distinct cancer subtypes. *Cancer Cell*. 2006;10(6):515–27.
23. Turner N, et al. FGFR1 amplification drives endocrine therapy resistance and is a therapeutic target in breast cancer. *Cancer Res*. 2010;70(5):2085–94.
24. André F, Cortés J. Rationale for targeting fibroblast growth factor receptor signaling in breast cancer. *Breast Cancer Res Treat*. 2015;150(1):1–8.
25. Elbauomy Elsheikh S, et al. FGFR1 amplification in breast carcinomas: a chromogenic in situ hybridisation analysis. *BCR*. 2007;9(2).
26. Chang J, et al. Prognostic value of FGFR gene amplification in patients with different types of cancer: A systematic review and meta-analysis. *PLoS One*. 2014;9(8).
27. Kim HR, et al. Fibroblast growth factor receptor 1 gene amplification is associated with poor survival and cigarette smoking dosage in patients with resected squamous cell lung cancer. *J Clin Oncol*. 2013;31(6):731–7.
28. Cheng CL, et al. Expression of FGFR1 is an independent prognostic factor in triple-negative breast cancer. *Breast Cancer Res Treat*. 2015;151(1):99–111.
29. Wang W, et al. A Versatile Tumor Gene Deletion System Reveals a Crucial Role for FGFR1 in Breast Cancer Metastasis. *Neoplasia (United States)*. 2017;19(5):421–8.
30. Turner N, et al. Integrative molecular profiling of triple negative breast cancers identifies amplicon drivers and potential therapeutic targets. *Oncogene*. 2010;29(14):2013–23.
31. Turczyk L, et al. FGFR2-Driven Signaling Counteracts Tamoxifen Effect on ERα-Positive Breast Cancer Cells. *Neoplasia (United States)*. 2017;19(10):791–804.
32. Sun S, et al. Increased expression of fibroblastic growth factor receptor 2 is correlated with poor prognosis in patients with breast cancer. *J Surg Oncol*. 2012;105(8):773–9.
33. Sharpe R, et al. FGFR signaling promotes the growth of triple-negative and basal-like breast cancer cell lines both in vitro and in vivo. *Clin Cancer Res*. 2011;17(16):5275–86.
34. Shaver TM, et al. Diverse, biologically relevant, and targetable gene rearrangements in triple-negative breast cancer and other malignancies. *Cancer Res*. 2016;76(16):4850–60.
35. Singh D, et al. Transforming fusions of FGFR and TACC genes in human glioblastoma. *Science*. 2012;337(6099):1231–5.
36. Williams SV, Hurst CD, Knowles MA. Oncogenic FGFR3 gene fusions in bladder cancer. *Hum Mol Genet*. 2013;22(4):795–803.
37. Yuan L, et al. Recurrent FGFR3-TACC3 fusion gene in nasopharyngeal carcinoma. *Cancer Biol Ther*. 2014;15(12):1613–21.
38. Sarkar S, Ryan E, Royle S. FGFR3-TACC3 cancer gene fusions cause mitotic defects by removal of endogenous TACC3 from the mitotic spindle. *Open Biol*. 2017;7.
39. Wu YM, et al. Identification of targetable FGFR gene fusions in diverse cancers. *Cancer Discovery*. 2013;3(6):636–47.
40. Di Stefano AL, et al. Detection, characterization, and inhibition of FGFR-TACC fusions in IDH wild-type glioma. *Clin Cancer Res*. 2015;21(14):3307–17.
41. Hochgräfe F, et al. Tyrosine phosphorylation profiling reveals the signaling network characteristics of basal breast cancer cells. *Cancer Res*. 2010;70(22):9391–401.
42. Bruderer R, et al. Extending the limits of quantitative proteome profiling with data-independent acquisition and application to acetaminophen-treated three-dimensional liver microtissues. *Mol Cell Proteomics*. 2015;14(5):1400–10.
43. Hood FE, Royle SJ. Pulling it together: The mitotic function of TACC3. *BioArchitecture*. 2011;1(3):105–9.
44. Nelson KN, et al. Oncogenic gene fusion FGFR3-TACC3 is regulated by tyrosine phosphorylation. *Mol Cancer Res*. 2016;14(5):458–69.
45. Nelson KN, et al. Oncogenic driver FGFR3-TACC3 is dependent on membrane trafficking and ERK signaling. *Oncotarget*. 2018;9(76):34306–19.
46. Dai S, et al. Fibroblast Growth Factor Receptors (FGFRs): Structures and Small Molecular Inhibitors. *Cells*. 2019;8(6):614.
47. Ghedini GC, et al. Future applications of FGF/FGFR inhibitors in cancer. *Expert Rev Anticancer Ther*. 2018;18(9):861–72.
48. Daly C, et al. FGFR3-TACC3 fusion proteins act as naturally occurring drivers of tumor resistance by functionally substituting for EGFR/ERK signaling. *Oncogene*. 2017;36(4):471–81.
49. Fumagalli D, et al. Somatic mutation, copy number and transcriptomic profiles of primary and matched metastatic estrogen receptor-positive breast cancers. *Ann Oncol*. 2016;27(10):1860–6.
50. Liang X, et al. Targeted next-generation sequencing identifies clinically relevant somatic mutations in a large cohort of inflammatory breast cancer. *Breast Cancer Res*. 2018;20(1).
51. Mhawech-Fauceglia P, et al. FGFR3 and p53 protein expressions in patients with pTa and pT1 urothelial bladder cancer. *Eur J Surg Oncol*. 2006;32(2):231–7.
52. Zhou S, et al. FGFR3 Deficiency Causes Multiple Chondroma-like Lesions by Upregulating Hedgehog Signaling. *PLoS Genet*. 2015;11(6).
53. Lafitte M, et al. FGFR3 has tumor suppressor properties in cells with epithelial phenotype. *Mol Cancer*. 2013;12(1).
54. Kuroso K, et al. Immunohistochemical detection of fibroblast growth factor receptor 3 in human breast cancer: Correlation with clinicopathological/molecular parameters and prognosis. *Pathobiology*. 2010;77(5):231–40.

## Publisher's Note

Springer Nature remains neutral with regard to jurisdictional claims in published maps and institutional affiliations.